SAPIENZA
UNIVERSITÀ DI ROMA

DOTTORATO DI RICERCA IN BIOLOGIA AMBIENTALE ED EVOLUZIONISTICA
XXXII CICLO

MODELING HABITAT SUITABILITY ACCOUNTING FOR FOREST STRUCTURE AND DYNAMICS: APENNINE BROWN BEAR AS CASE STUDY

PHD CANDIDATE: MATTEO FALCO

TUTOR: PROF. PAOLO CIUCCI
CO-TUTOR: PROF. LUIGI MAIORANO

FACOLTÀ DI SCIENZE MATEMATICHE, FISICHE E NATURALI
DIPARTIMENTO DI BIOLOGIA E BIOTECNOLOGIE "CHARLES DARWIN"
ANNO ACCADEMICO 2016-2019

Tables of contents

Introduction

Globally, human encroachment is recognized as the major risk for wildlife persistence (Di Marco and Santini 2015), particularly for those animals able to cover a large distances, needed wide home ranges, and characterized by low reproductive rates such as large carnivores. Accordingly, the coexistence between human and large carnivore populations is becoming one of the major wildlife conservation challenges, especially in highly human dominated landscapes, like the European continent (Chapron et al. 2014). In this context, as large carnivore populations increase, also overlap and conflicts between animals and human population are likely to increase (Ordiz et al. 2014). Despite many studies suggest that large carnivores can modify their behaviors as a response to human daily and seasonal habits (e.g. Mace et al. 1996; Dickson et al. 2005; Abrahms et al. 2016), their fitness is affected by direct (e.g., road kills, poaching) and indirect (e.g., barriers for dispersal, habitat fragmentation and loss) effects of human activities that can lead to the extinction of local populations. As other large carnivores living in Europe (i.e., wolf, lynx and wolverine), brown bears (*Ursus arctos*) need wide spaces, large distances for dispersing and high permeability landscape matrix. Despite the high level of urbanization, Europe maintains a few tens of uncontaminated natural areas that host several large and stable bear populations (i.e., Carpathian, Scandinavian, Dynairc-Pindus and Karenian populations), but also endemic (i.e., Apennines population) and reintroduced (i.e., Alps and Pyrenean populations) populations with a few tens of individuals (Chapron et al. 2014). Apennines brown bears (*Ursus arctos marsicanus*; Altobello 1921), isolated from the other European bear populations for at least 1500 years (Benazzo et al. 2017), are critically endangered and confined to a restricted range (Abruzzo-Lazio-Molise National Park, PNALM, and surrounding areas) in Italy. In light of the persistent small size of the Apennine brown bear population (Ciucci and Boitani 2008, Ciucci et al. 2015, Gervasi et al. 2017) and its high human-caused mortality rates reported during the past decades (Zunino and Herrero 1972, Boscagli 1987, Lorenzini et al. 2004), a renewed effort for conservation of this population is critically and urgently needed. Its long-term isolation from other brown bear populations also makes brown bear a unique evolutionary and conservation unit, based on genetic (Randi et al. 1994, Lorenzini et al. 2004, Benazzo et al. 2017), morphological (Loy et al. 2008, Colangelo et al. 2012) and perhaps behavioral traits. Although many studies on brown bear's food habits (Ciucci et al. 2014), demography and dynamics (Ciucci et al. 2015, Gervasi et al. 2017, Tosoni et al. 2017) have been carried out, a formal investigation on factors limiting population growth within the core of the Apennine bear population range (Ciucci and Boitani 2008) has not yet been conducted. In addition, whereas previous habitat selection studies focused on predicting the potential species distribution to evaluate the effectiveness of the national and regional networks of protected areas (Posillico et al. 2004), and the detection of ecological traps (Falcucci et al. 2009) and structural connectivity linking the critical habitat patches at landscape scale (Maiorano et al. 2019), in this thesis I performed fine scale analysis to develop habitat management schemes that enhance the conservation of this unique brown bear population. Specifically, I investigated all those environmental and ecological drivers that can affect resource selection by bears, accounting for the hierarchical nature of resource selection (i.e., landscape, home range, and single forest patch scales), and the behavioral responses related to seasonal and circadian effects. Moreover, in collaboration with national (i.e., Forest Service of Abruzzo-Lazio-Molise National Park, PNALM, and Forest Service of the "Unità territoriale per la Biodiversità", UTB, of Castel di Sangro) and international (i.e., Swiss Federal Research Institute WSL, and Forest Research and Management Institute, ICAS, Romania) partners, I also investigated the impact of climate change and forest harvesting management, forecasting future forest species composition and tridimensional structure to quantify changes in habitat suitability for bears, in the next 100 years.

Aims of the Thesis

To conduct my research, I focused on the following three research questions:

1. Which environmental and ecological drivers affect resource selection by bears?

2. How does forest structure affect habitat selection by bears?
3. How natural succession and human-driven habitat changes will affect habitat suitability for bears in the future?

Using a modelling approach closely linked to the biological requirements of the species and explicitly incorporating the landscape structure as perceived by the animals, the main purposes of this PhD project can be represented by four main points: (*i*) modeling landscape habitat selection patterns by bears at different spatial and temporal scales (Chapter I), (*ii*) modeling forest structure combining remote sensing techniques and forest field-data inventory (Chapter II), (*iii*) modeling habitat selection patterns accounting for the horizontal and tridimensional structure of the forest habitat (Chapter III), and (*iv*) simulating future dynamic forest scenarios to evaluate the effects of climate change and human forest management on bear's habitat suitability (Chapter IV).

Executive Summary

Chapter I – Unveiling differences in scale-dependent habitat selection of the Apennine brown bear using multi-grain, multi-order resource selection functions

Habitat selection is a dynamic, scale-sensitive process responding to the spatial and temporal scales of the environment (Levin 1992, Mayor et al. 2009, McGarigal et al. 2016). Detecting the most informative scale(s) of analysis is therefore critical to correctly understand habitat selection and provide ecologically based management strategies in wildlife conservation policy. Resource selection functions (RSFs; Manly et al. 2002) are commonly used to support conservation decision making, focusing on the animal responses to habitat features, and testing which is the best explicative model for animal resource selection (i.e., proportional to the probability of use of a certain resource unit). In this study, I used Global Positioning System (GPS) locations recorded from 11 adult female bears (*Ursus arctos marsicanus*; 2006-2010) to unveil differences in habitat selection according to different scale domains, investigating which environmental drivers affect bear's resource selection. I compared habitat features within bears' home range and the study area (i.e., second-order of selection; *sensu* Johnson 1980), and the habitat features at bear GPS locations and seasonal home ranges (i.e., third-order of selection; Johnson 1980). At both orders of selection, I used mixed-effects logistic regression models (Generalized Linear Mixed Models, GLMMs), using the 'lme4' R package (Bates et al. 2015), treating individual bears as random intercepts, to take into account differences in sample size among individuals and autocorrelation of data within individual bears (Gillies et al. 2006). Finally, to investigate the circadian effects on seasonal habitat selection at the home range scale (third-order selection), I carried out direct comparisons of habitat resources use between two groups of interest (i.e., day *vs* night), producing quantifiable measurements of the relationships' strength (i.e., Latent Selection Differences, LSD; Czetwertynski et al. 2007). At the landscape scale (second-order of selection), I detected relevant seasonal and circadian effects in habitat selection by adult female bears at the home range extent; consistently across seasons, adult female bears selected proxies of food and cover (agriculture and forest cover) or of inaccessibility by humans (i.e., steeper slopes, rough terrain, and greater distance from dirt roads), while avoiding less exposed sites. At the contrary, at the individual level, adult female bears expectedly showed high variability in their third-order, seasonal habitat selection; specifically, selection patterns shared by all or most adult female bears consistently reflected (a) avoidance of areas closer to dirt roads (spring and late-summer), and (b) selection for forest cover (spring and early-summer), agricultural fields (early-summer, late-summer and autumn), shrub lands (late-summer), steeper slopes (spring and late-summer), rough terrain (late-summer), and sites less exposed to sunlight (spring). I also detected functional responses by adult female bears toward anthropogenic features at the third-order selection, in particular paved and unpaved roads, both in spring and late-summer, and settlements in autumn.

Chapter II – Combining forest inventory data and remote sensing to map forest structure using an ensemble modelling approach

Forest inventories are the raw material providing structural information at the level of the forest plots being investigated, and subsequently data can be summarized to the stand (or higher) level using standard statistical procedures (Brosofske et al. 2014). National forest inventories (NFIs) are designed to acquire information about nationwide forest resources, with the aim of supporting national-level strategic planning and policy development (White et al. 2016). However, given detailed knowledge on forest structure can be also useful to investigate habitat selection by animals deeply related to forest habitat, such as brown bear (*Ursus arctos*). In this chapter, I aimed to outline a novel and feasible framework to produce spatially explicit forest structural maps, by modeling NFIs stands information, and using time series vegetation indices (i.e., Landsat 5/7 TM/ETM+ satellite images) and environmental characteristic as model predictors. Specifically, I carried out a multi-scale modelling design, accounting for different temporal and spatial scale, under an ensemble modeling approach (Elith and Leathwick 2009, Thuiller et al. 2009). In this framework, I used different statistical algorithms, such as generalize linear model (GLM), generalized additive model (GAM), boosted regression trees (GBM), and random forest (RF), to model trees' basal area (G; m^2/ha) and number of stems (N; trees/ha), for two target species which dominate the forest in the study area, beech (*Fagus sylvatica*) and oak (*Quercus* spp.). Although passive remote sensing images (e.g., Landsat) are generally considered to be poor predictors for tridimensional structure measurements (e.g., Foody et al. 2001) compared to active remote sensing (e.g., LiDAR) images, in this chapter I we described a novel modeling framework that account for multiple scales (spatial and temporal) of analysis to spatially predict tridimensional forest structure with good level of predictive performance, by using easy-to-acquire remote sensing and point-based inventory data.

Chapter III **– The importance of forest management strategies in wildlife conservation: Apennine brown bear's habitat selection**

Forest structural composition largely determines habitat quality for animals, because they may influence the availability and accessibility of resources under many aspects, like selection for rest sites and food (e.g., Hayes and Loeb 2007), exposure to predators (e.g., Baxter et al. 2006) and microclimatic conditions (e.g., Chen et al. 1999). For instance, mature forests characterized by old trees (i.e., higher log's diameter or basal area) likely provide more resources of food (e.g., hard mast), compared to younger forest characterized instead by smaller trees (i.e., lower log's diameter and basal area); otherwise, the number of trees (i.e., tree density) of the forest can profoundly affects animal movement (e.g., Caras and Korine 2009), which is especially important not only for flying animals such as birds and bats, but also for larger animals like ungulates (e.g., deer, moose, and wild boars) and carnivores (e.g., wolves, bears and lynxes), which may prefer different forest structures depending on their daily and seasonal activities (i.e., foraging, sheltering, moving to escape from predation or defend the territory). In this chapter, I considered forest horizontal and vertical structure (obtained in Chapter 2) to investigate bear's space use patterns at two order of selection (Johnson

1980), home range (third-order selection) and single forest patch level (fourth-order selection), testing different spatial (i.e., multi-grain analysis; Laforge et al. 2015) and temporal (i.e., seasonal and circadian) scales. At both orders of selection, I used mixed effects logistic regression models (Generalized Linear Mixed Models, GLMMs), treating individual bears as random intercepts, to consider differences in sample size among individuals and autocorrelation of data within individual bears (Gillies et al. 2006). This study confirmed that brown bear is a species related to the forest ecosystem and not limited only to the forest. Looking at the main results, at the home range scale (third-order of selection) the results confirmed the importance of forest like fundamental resource for this brown bear population, related to two main causes: (*i*) covering by anthropogenic disturbance, highlighted by the selection of continuous forest patch, especially during daily hours in summer (early-summer and late-summer), and (*ii*) foraging within the forest, highlighted by the increasingly selection for these continuous forested areas mainly in autumn, when there is the peak of hard mast production in the forests. At the single forest patch scale (fourth-order of selection), more evident circadian effects highlight that oak forest selection respect to the beech forest is mainly nocturnal and never diurnal, and this may suggest a trophic rather than covering effect, probably linked to a higher diversity and availability of food.

Chapter IV – Forecasting habitat suitability for Apennine brown bear under climate change and alternative forest management scenarios

Forest landscape dynamics result from the complex interaction of driving forces and ecological processes operating on various scales, including large-scale natural disturbances (e.g., wildfires, windthrow), forest management (e.g., trees harvesting), physical environment (e.g., temperature, precipitation and soil), and stand-scale succession and competition processes (e.g., growth, reproduction, seed dispersal and death of the trees). Dynamic landscape-scale models enable us to investigate these complex systems in a quantitative and structured manner (Mladenoff and Baker

1999). In this chapter, I investigate how climate change and human forest management can influence the habitat quality and bears-forest habitat relationship. I simulated forest succession dynamics under climate change conditions using spatially explicit landscape-scale vegetation models (i.e., LandClim software; Schumacher et al. 2004; Schumacher and Bugmann 2006) over 50,686-ha study landscape (i.e., Abruzzo-Lazio-Molise National Park, PNALM), using 5 alternatives forest harvesting scenarios. These scenarios were obtained by the combination of different harvesting strategies, and forest-edge treatments, namely *S0*, *S1a*, *S1b*, *S2a*, and *S2b*. To forecast future habitat suitability by bears, I used the coefficients estimated in the current habitat selection models at both home range and forest patch-level scales (third and fourth order of Johnson; Chapter 3) in combination with the respective tridimensional structure, composition, and spatial configuration of forest predicted by LandClim's after 100 years of simulations. In the PNALM, these results suggested that climate change have a substantial impact on forest vegetation: in the next 100 years, LandClim simulations evidenced substantial changes related to the biomass and species composition distribution along altitudinal range, with a gradually conversion of beech dominated forest to oaks domination in all scenarios evaluated. At both orders of selection, I evidenced a general increase of habitat suitability in all the scenarios contemplated compared to the current levels of bear's habitat suitability. Specifically, at the home range scale (third-order of selection), climate change had a considerable impact on forest species composition compared to the effects of forest harvesting strategies adopted; this trend changes at the forest patch scale (fourth-order of selection), where the different forest strategy adopted increase (or decrease) bear's habitat suitability.

REFERENCES

Abrahms, B., N. R. Jordan, K. A. Golabek, J. W. McNutt, A. M. Wilson, and J. S. Brashares. 2016. Lessons from integrating behaviour and resource selection: Activity-specific responses of African wild dogs to roads. Animal Conservation 19:247–255.

Bates, D., M. Mächler, B. Bolker, and S. Walker. 2015. Fitting linear mixed-effects models using lme4. Journal of Statistical Software 67:1–48.

Baxter, D. J. M., J. M. Psyllakis, M. P. Gillingham, and E. L. O'Brien. 2006. Behavioural response of bats to perceived predation risk while foraging. Ethology 112:977–983.

Benazzo, A., E. Trucchi, J. A. Cahill, P. M. Delser, S. Mona, M. Fumagalli, L. Bunnefeld, L. Cornetti, S. Ghirotto, M. Girardi, L. Ometto, A. Panziera, O. Rota-Stabelli, E. Zanetti, A. Karamanlidis, C. Groff, L. Paule, L. Gentile, C. Vilà, S. Vicario, L. Boitani, L. Orlando, S. Fuselli, C. Vernesi, B. Shapiro, P. Ciucci, and G. Bertorelle. 2017. Survival and divergence in a small group: The extraordinary genomic history of the endangered Apennine brown bear stragglers. Proceedings of the National Academy of Sciences of the United States of America 114:E9589–E9597.

Boscagli, G. 1987. Brown bear mortality in central Italy from 1970 to 1984. International Conference Research and Management 7:97–98.

Brosofske, K. D., R. E. Froese, M. J. Falkowski, and A. Banskota. 2014. A review of methods for mapping and prediction of inventory attributes for operational forest management. Forest Science 60:733–756.

Caras, T., and C. Korine. 2009. Effect of vegetation density on the use of trails by bats in a secondary tropical rain forest. Journal of Tropical Ecology 25:97–101.

Chapron, G., P. Kaczensky, J. D. C. Linnell, M. von Arx, D. Huber, H. Andrén, J. V. López-Bao, M. Adamec, F. Álvares, O. Anders, L. Balčiauskas, V. Balys, P. Bedő, F. Bego, J. C. Blanco, U. Breitenmoser, H. Brøseth, L. Bufka, R. Bunikyte, P. Ciucci, A. Dutsov, T. Engleder, C. Fuxjäger, C. Groff, K. Holmala, B. Hoxha, Y. Iliopoulos, O. Ionescu, J. Jeremić, K. Jerina, G. Kluth, F. Knauer, I. Kojola, I. Kos, M. Krofel, J. Kubala, S. Kunovac, J. Kusak, M. Kutal, O. Liberg, A. Majić, P. Männil, R. Manz, E. Marboutin, F. Marucco, D. Melovski, K. Mersini, Y. Mertzanis, R. W. Mysłajek, S. Nowak, J. Odden, J. Ozolins, G. Palomero, M. Paunović, J. Persson, H. Potočnik, P.-Y. Quenette, G. Rauer, I. Reinhardt, R. Rigg, A. Ryser, V. Salvatori, T. Skrbinšek, A. Stojanov, J. E. Swenson, L. Szemethy, A. Trajçe, E. Tsingarska-Sedefcheva, M. Váňa, R. Veeroja, P. Wabakken, M. Wölfl, S. Wölfl, F. Zimmermann, D. Zlatanova, and L. Boitani. 2014. Recovery of large carnivores in Europe's modern human-dominated landscapes. Science 346:1517–1519.

Chen, J., S. C. Saunders, K. D. Brosofske, G. D. Mroz, T. R. Crow, R. J. Naiman, J. F. Franklin, and B. L. Brookshire. 1999. Microclimate in forest ecosystem and landscape ecology: Variations in local climate can be used to monitor and compare the effects of different management regimes. BioScience 49:288–297.

Ciucci, P., and L. Boitani. 2008. The Apennine brown bear: A critical review of its status and conservation problems. Ursus 19:130–145.

Ciucci, P., V. Gervasi, L. Boitani, J. Boulanger, D. Paetkau, R. Prive, and E. Tosoni. 2015. Estimating abundance of the remnant Apennine brown bear population using multiple non invasive genetic data sources. Journal of Mammalogy 96:206–220.

Ciucci, P., E. Tosoni, G. Di Domenico, F. Quattrociocchi, and L. Boitani. 2014. Seasonal and annual variation in the food habits of Apennine brown bears, central Italy. Journal of Mammalogy 95:572–586.

Colangelo, P., A. Loy, D. Huber, T. Gomerčić, A. Vigna Taglianti, and P. Ciucci. 2012. Cranial distinctiveness in the Apennine brown bear: Genetic drift effect or ecophenotypic adaptation? Biological Journal of the Linnean Society 107:15–26.

Czetwertynski, S. M., M. S. Boyce, and F. K. Schmiegelow. 2007. Effects of hunting on demographic parameters of American black bears. Ursus 18:1–18.

Dickson, B. G., J. S. Jenness, and P. Beier. 2005. Influence of vegetation, topography, and roads on cougar movement in southern California. Journal of Wildlife Management 69:264–276.

Elith, J., and J. R. Leathwick. 2009. Species distribution models: ecological explanation and prediction across space and time. Annual Review of Ecology, Evolution, and Systematics 40:677–697.

Falcucci, A., P. Ciucci, L. Maiorano, L. Gentile, and L. Boitani. 2009. Assessing habitat quality for conservation using an integrated occurrence-mortality model. Journal of Applied Ecology 46:600–609.

Foody, G. M., M. E. Cutler, J. McMorrow, D. Pelz, H. Tangki, D. S. Boyd, and I. Douglas. 2001. Mapping the biomass of Bornean tropical rain forest from remotely sensed data. Global Ecology and Biogeography 10:379–387.

Gervasi, V., L. Boitani, D. Paetkau, M. Posillico, E. Randi, and P. Ciucci. 2017. Estimating survival in the Apennine brown bear accounting for uncertainty in age classification. Population Ecology 59:119–130. Springer Japan.

Gillies, C. S., M. Hebblewhite, S. E. Nielsen, M. A. Krawchuk, C. L. Aldridge, J. L. Frair, D. J. Saher, C. E. Stevens, and C. L. Jerde. 2006. Application of random effects to the study of resource selection by animals. Journal of Animal Ecology 75:887–898.

Hayes, J. P., and S. C. Loeb. 2007. The influences of forest management on bats in North America. Pages 207–236 in. Bats in Forests: Conservation and Management. eds M.J. L. John Hopkins University Press, Baltimore, MD.

Johnson, D. H. 1980. The comparison of usage and availability measurements for evaluating resource preference. Ecology 61:65–71.

Laforge, M. P., E. Vander Wal, R. K. Brook, E. M. Bayne, and P. D. McLoughlin. 2015. Process-focussed, multi-grain resource selection functions. Ecological Modelling 305:10–21.

Levin, S. A. 1992. The problem of pattern and scale in ecology: The Robert H. MacArthur award lecture. Ecology 73:1943–1967.

Lorenzini, R., M. Posillico, S. Lovari, and A. Petrella. 2004. Non-invasive genotyping of the endangered Apennine brown bear: A case study not to let one's hair down. Animal Conservation 7:199–209.

Loy, A., P. Genov, M. Galfo, M. G. Jacobone, A. V. Taglianti, P. Genov, M. Galfo, M. G. Jacobone, and A. V. Taglianti. 2008. Cranial morphometrics of the Apennine brown bear (*Ursus arctos marsicanus*) and preliminary notes on the relationships with other southern European populations. Italian Journal of Zoology 75:67–75.

Mace, R. D., J. S. Waller, T. L. Manley, L. J. Lyon, and H. Zuuring. 1996. Relationships among grizzly bears, roads and habitat in the Swan Mountains Montana. The Journal of Applied Ecology 33:1395–1404.

Maiorano, L., L. Chiaverini, M. Falco, and P. Ciucci. 2019. Combining multi-state species distribution models, mortality estimates, and landscape connectivity to model potential species distribution for endangered species in human dominated landscapes. Biological Conservation 237:19–27.

Manly, B. F. J., L. Mcdonald, D. Thomas, T. L. McDonald, and W. P. Erickson. 2002. Resource selection by animals: Statistical design and analysis for field studies. 2nd ed. Volume 1. Kluwer Academic Publishers, Dordrecht, Netherlands. Merkle.

Di Marco, M., and L. Santini. 2015. Human pressures predict species' geographic range size better than biological traits. Global Change Biology 21:2169–2178.

Mayor, S. J., D. C. Schneider, J. A. Schaefer, and S. P. Mahoney. 2009. Habitat selection at multiple scales. Écoscience 16:238–247.

McGarigal, K., H. Y. Wan, K. A. Zeller, B. C. Timm, and S. A. Cushman. 2016. Multi-scale habitat selection modeling: A review and outlook. Landscape Ecology 31:1161–1175.

Mladenoff, D. J., and W. L. Baker. 1999. Development of forest and landscape modeling approaches. Pages 1–13 in. Mladenoff, D.J., Baker, W.L. (Eds.), Spatial Modeling of Forest Landscape Change: Approaches and Applications. Cambridge University Press, Cambridge, UK.

Ordiz, A., J. Kindberg, S. Sæbø, J. E. Swenson, and O. G. Støen. 2014. Brown bear circadian behavior reveals human environmental encroachment. Biological Conservation 173:1–9.

Posillico, M., A. Meriggi, E. Pagnin, S. Lovari, and L. Russo. 2004. A habitat model for brown bear conservation and land use planning in the central Apennines. Biological Conservation 118:141–150.

Randi, E., L. Gentile, G. Boscagli, D. Huber, and H. U. Roth. 1994. Mitochondrial DNA sequence divergence among some west European brown bear (*Ursus arctos* L.) populations. Lessons for conservation. Heredity 73:480–489.

Schumacher, S., and H. Bugmann. 2006. The relative importance of climatic effects, wildfires and management for future forest landscape dynamics in the Swiss Alps. Global Change Biology 12:1435–1450.

Schumacher, S., H. Bugmann, and D. J. Mladenoff. 2004. Improving the formulation of tree growth and succession in a spatially explicit landscape model. Ecological Modelling 180:175–194.

Thuiller, W., B. Lafourcade, R. Engler, and M. B. Araújo. 2009. BIOMOD - a platform for ensemble forecasting of species distributions. Ecography 32:369–373.

Tosoni, E., L. Boitani, L. Gentile, V. Gervasi, R. Latini, and P. Ciucci. 2017. Assessment of key reproductive traits in the Apennine brown bear population. Ursus 28:105–116.

White, J. C., N. C. Coops, M. A. Wulder, M. Vastaranta, T. Hilker, and P. Tompalski. 2016. Remote sensing technologies for enhancing forest inventories: A review. Canadian Journal of Remote Sensing 42:619–641.

Zunino, F., and S. Herrero. 1972. The status of the brown bear (*Ursus arctos*) in Abruzzo National Park, Italy, 1971. Biological Conservation 4:263–272.

Chapter I

Unveiling differences in scale-dependent habitat selection of the Apennine brown bear using multi-grain, multi-order resource selection functions

Matteo Falco, Luigi Maiorano, and Paolo Ciucci

Sapienza University of Rome, Dept. of Biology and Biotechnology "Charles Darwin", Viale dell'Università 32, Roma 00185, Italy

INTRODUCTION

Habitat selection is a dynamic process that depends on the different spatial and temporal scales of the environment in which the species live (Levin 1992; Mayor et al. 2009; McGarigal et al. 2016). Habitat is characterized by a multidimensional structure in which species perceive and respond to their surroundings across a range of spatial scales, also defined as scales of domain (Wiens 1989, Kotliar and Wiens 1990, Levin 1992). Identifying the scale of domain at which habitat selection operates is therefore fundamental to understand unambiguously the relative risk or rewards animals obtain by selecting a given resource at an adequate scale of investigation (Roland and Taylor 1997; Holland et al. 2004). In this context, multiscale habitat analysis provides important theoretical insight into ecological patterns and processes, and facilitates effective conservation and management (Benítez-López et al. 2017; Pimenta et al. 2018). The concept of scale in ecology has been widely used to describe a variety of related concepts (Wiens 1989, Levin 1992, Schneider 2001, McGarigal et al. 2016*b*), among which both extent and grain are of particular operational value (Levin 1992, Hall et al. 1997, Morrison and Hall 2002, Mayor et al. 2009, McGarigal et al. 2016*b*). While the former refers to the geographic and temporal constraint in which resources are effectively available to animals, the latter refers to the resolution at which an animal responds to the environmental heterogeneity, generally measured as the radius within which animals perceive and respond to environmental predictors [also referred as ‘grain response’ or ‘characteristic scale’ (Addicott et al. 1987; Holland et al. 2004)]. Nevertheless, even though habitat selection is increasingly recognized as a multi-scale process (Holland et al. 2004, Mayor et al. 2009, Laforge et al. 2015, McGarigal et al. 2016*a*), habitat selection studies still very often consider a single extent and a fixed grain (Mayor et al. 2009), thereby failing to identify changes in habitat selection across ecological domains (Wiens 1989). A multi-scale approach involves the explicit consideration of explanatory variables measured at more than one spatial and/or temporal scale, with variations on how to choose and analyze relationships across scales (McGarigal et al. 2016*a*). In this context, Johnson's (1980) hierarchical framework to investigate habitat selection, though potentially confused with a multi-scale approach

(Wheatley and Johnson 2009), can been conveniently adopted to define given spatial and temporal extents when adopting use vs availability study designs to assess habitat selection (Mayor et al. 2009, Gaillard et al. 2010). In some circumstances, temporal scale may be more important than spatial scale (Fahrig 1992), because differences between seasonal and daily decisions can affect spatial decisions in choosing the home range within landscape (i.e., second-order of selection; Johnson 1980), and high-suitable patches within home range (i.e., third-order of selection; Johnson 1980).

There are numerous analytical approaches and statistical modelling methods available for developing multiscale habitat selection modeling. In this sense, RSFs framework can be easily adapted for modeling different spatial scales both in terms of extent and grain, and temporal scales (i.e., the duration and resolution of observations in time). Similar to other statistical methods, such as species distribution models (SDMs; Guisan and Zimmermann 2000) and Ecological Niche factor Analysis (ENFA; Hirzel et al. 2002), RSFs have been widely used in studies of wildlife habitat selection (Boyce and McDonald 1999, Manly et al. 2002), and they serve an applied role of converting ecological niche relationships in environmental space into gradients of predicted habitat suitability across geographic space (Hirzel and Le Lay 2008).

Large carnivores with their wide movement ranges and large spatial requirements are a good model for understanding how scales influence resources selection and space use of animal populations, particularly in human dominated landscapes. A large carnivore species recognized for its remarkable plasticity to persist in human-altered landscapes is brown bear (*Ursus arctos*) (Cozzi et al. 2016). Brown bear distribution encompass the majority habitats of the Holarctic region (North America and Eurasia), but its optimal habitat is considered to be human-less areas with a mosaic of early-seral staged forests and natural openings in proximity to forest stands that provide day beds and hiding cover (Herrero 1972, Blanchard 1983, Hamer and Herrero 1987) located in dense vegetation and steeper terrain (Moe et al. 2007, Elfström et al. 2008, Ordiz et al. 2011). Nonetheless, different factors could influence spatial or temporal habitat segregation among bears, such as innate sexual differences, age classes, and individual temperament (Martin and Réale 2008, Ellenberg et al. 2009);

for instance, female bears with small cubs mast prioritize offspring security and frequently select lower-quality habitat characterized by a more human dominated landscapes in order to avoid males (Elfström et al. 2014*b*, Lamb et al. 2016). This bear's capacity to adapt its spatiotemporal niche to human presence becomes a fundamental trait for its persistence in human dominated environments, and knowledge on such adaptations is essential for effective and long-term conservation planning (Ordiz et al. 2012).

Living surrounded by a very high human-dominated landscape in central Italy, Apennine brown bear (*Ursus arctos marsicanus*; Altobello 1921) represent the last remnant of an autochthonous population, isolated from other European bear populations for at least 1,500 years (Benazzo et al. 2017). Most of the current core distribution of Apennine brown bear is constituted by the Abruzzo-Lazio-Molise National Park (PNALM), which comprises relatively ideal habitat conditions for bears compared to other regions of Italy. Human infrastructures, including settlements and roads, have been historically present in the area at low densities, and multiple use practices (e.g. tourism, livestock husbandry, silvicultural activities) have been traditionally allowed in the park (Mancinelli et al. 2019). This bear population is facing serious risks of extinction due to its persistent small size and reduced genetic variability (Ciucci et al. 2015, Benazzo et al. 2017, Gervasi and Ciucci 2018), and needed immediate proactive conservation measures (Ciucci and Boitani 2008).

To achieve this goal, previous habitat-modelling applications were conducted at landscape scale to evaluate, for instance, the effectiveness of the national and regional networks of protected areas (Posillico et al. 2004), potential ecological traps (Falcucci et al. 2009) and corridors linking the core distribution (i.e., distribution range of female bears producing cubs; Ciucci et al. 2017) with the other surrounding suitable areas within its historical distribution range (Maiorano et al. 2019). Nonetheless, habitat selection analysis developed using a multi-scale approach to evidence bears-habitat relationships within its core distribution is not yet conducted. Assessing new ecological information over this population accounting for multiple spatial and temporal scales become critical for achieving evidenced-base habitat management schemes, and enhancing conservation efforts for the demographic expansion of this unique brown bear population.

In this study, I used Global Positioning System (GPS) locations recorded from 11 adult females (2006-2010) to model bears' habitat selection based on multi-grain resource selection functions (MRSF) study design. My objectives are to model the home range space-use pattern by bears associated to available resources at landscape scale (e.g. second-order of selection; Johnson 1980) and within home range (e.g. third-order of selection; Johnson 1980), contemplating a set of environmental and anthropogenic predictors, and investigate bears' behavioral responses to seasonal and circadian effects, at both population and individual level. My working hypotheses are that (*i*) resource selection by female bears is related to factors describing human inaccessible habitats, and (or) attraction of foods available in the forest ecosystem. In addition, (*ii*) habitat selection by female bears could be spatial scale-dependent, and changes in habitat selection across ecological domains (Wiens 1989) may be revealed by accounting for multiple observational scales (including extent and grain; Wheatley and Johnson 2009); accordingly, I expect that human-risk perceived by female bears is greater in choosing home ranges in the landscape (second-order), compared to patch-level habitat selection within home range (third-order); nonetheless, at the third-order, temporal scale may highlight differences in anthropogenic features response, similar to the seasonal and circadian human avoidance pattern found by Mancinelli et al. (2019) for wolves in the same study area. Finally, (*iii*) habitat selection at population level may hide a high-variability in selection pattern among individuals (Gill et al. 2001, Elfström et al. 2014*b*), and spatiotemporal variation in the selection pattern for anthropogenic features may be in part explained by functional responses, occurring when individuals change their preference as a function of the availability of particular habitat features (Mysterud and Ims 1998, Hebblewhite and Merrill 2008).

METHODS

Study area

I defined the study area as the area encompassed within a 10 km buffer (see Model development below) around the composite 100% MCP calculated using all Global Positioning System (GPS) locations of radio-collared female bears included in the analysis (Fig. 1). The 656.8 km^2 study area comprises the range of reproductive Apennine female bears in the Abruzzo Lazio and Molise National Park (PNALM) and adjacent areas (Ciucci et al. 2017). Altitude ranges from 145 to 2278 m. a. s. l., progressing from gentle slopes dominated by cultivated lands and human settlements to typically mountainous terrain, mainly covered by forests interspersed with pastures, meadows, and alpine prairies. Forests cover 68.6% of the study area, mainly beech (*Fagus sylvatica*) and oak (mainly *Quercus cerris* and *Q. pubescens*), followed by open fields and shrublands. Agriculture is scarce and highly localized along valley bottoms and close to human settlements. The study area features a relatively low paved road density (45.3 km/100 km^2) and a few, scattered villages (Table 1). Human presence (27.1±16.7 inhabitants/km^2) and activities markedly increase during summer, mostly due to tourism and livestock grazing (Mancinelli et al. 2018).

Data collection

From 2005 to 2010, I live-trapped bears and deployed Global Positioning System (GPS) collars (Televilt Tellus GSM-VHF, and Vectronic GPS Plus) on 19 adult (≥ 4 years) bears (8 males and 11 females). I focused the habitat analysis on adult female bears only due to their critical demographic role (Knight and Eberhardt 1985, Wiegand et al. 1998, Boyce et al. 2001, Nielsen et al. 2006). Stationary collars posted at fixed points (n = 100) within the study area had an average location error of 24.7m (±16.3m SD) (Mancinelli et al. 2019). Collars deployed on bears were programmed to acquire one location every hour (i.e., 24 relocations/day) for 10 days a month, followed by one location every 4–6 hours for the rest of the month. For the scope of the analysis, I subsampled all locations at an equal rate of 4 locations/day. I limited the analyses to locations collected during the active period, defined according to the median dates of den exit and entrance of adult females in this bear population (7 Mar and 23 Nov, respectively; Ciucci et al. 2012). Observed acquisition rates of GPS locations ranged 73.1–98.6% for individual bear ($\bar{x}$ =86.7±9.2%; Supplementary Table S1). To enhance the quality of GPS locations used in the analyses (Lewis et al. 2007), I retained all GPS locations acquired with: (*i*) 3 satellites, but with horizontal dilution of precision (HDOP) < 8 (location error: $\bar{x}$=23.3±33.8 m), and (*ii*) ≥ 4 satellites (Supplementary Table S2 and Fig. S1). At the third order of selection, to account for seasonal variation in habitat selection I considered 4 periods according to the local seasonality in bear key foods (Ciucci et al. 2014): spring (March–May), early-summer (June–July), late-summer (August–September), and fall (October–23 November). If a bear had been tracked for more than one year, I did not include seasonal duplicates but selected the season with the highest number of acquired locations. The final dataset comprised a total of 9,380 GPS locations for 11 adult female bears (38 bear-seasons; Supplementary Table S1).

Habitat variables

To account for resource selection by adult female bears, I considered a set of 11 environmental, topographic and anthropogenic variables in a GIS environment (ArcMap v. 10.2; Environmental Systems Research Institute, ESRI, Redlands, CA, USA). I obtained land cover layers from the regional Corine Land Cover (CLC) V level and forest type vector maps, at 1:10,000 scale, from Regional administrations (http://geoportale.regione.abruzzo.it/; https://geoportale.regione.lazio.it/; http://www.geo.regione.molise.it/). I combined the original land cover categories into four classes: forests (including broadleaf and coniferous forest), open fields (including pastures, meadows, and alpine prairies), shrublands, and cultivated lands, the latter mostly characterized in the study area by non-intensive agriculture. To account for topographic variables, I used a digital elevation model (DEM; 10x10 m cell-size) obtained by the Italian Military Geographic Institute (IGM), from which I computed hillshade, slope and its standard deviation (Spatial Analyst Tool; ArcMap v. 10.2, ESRI). Hillshade is a orographic measure of solar exposition indicating the average amount of shade at any pixel (ranging from 0 to 255; Ciarniello et al. 2005), whereas the standard deviation of the slope is a measure of terrain roughness (Maiorano et al. 2015).

Anthropogenic variables included the Euclidean distance to the closest road and settlement edge. The former was derived combining the De Agostini-GeoNext and TeleAtlas databases (updated to 2003), the latter by the National Institute of Statistics (ISTAT 2011). I classified roads as either paved roads or unpaved roads, both accessible by vehicles; although I lacked measures of traffic volumes, I expected a markedly lower vehicle traffic on unpaved roads. Furthermore, to eliminate all road segments really inaccessible by vehicles, I integrated the available road network GIS-layer with the trails network collected by the Forest service, during the LIFE-project ARCTOS (http://www.parcoabruzzo.it/pagina.php?id=201), within the same study area. All variables were calculated or re-sampled (i.e., DEM) with a common origin and 20x20 m cell size resolution. For each variable, I used the focal statistics tool in ArcGIS (ESRI) to ran a map-algebra focal function over the entire study area; to this aim, and to allow a multi-grain approach, I used moving windows of different radii to model alternative grain sizes (see Optimized multi-grain analysis).

Multi-grain Resource Selection Functions

Based on an use-availability design (Manly et al. 2002), I developed two multi-grain resource selection functions (MRSFs; Laforge et al. 2015), one contrasting habitat features at the landscape (study area) extent with those within the bears' annual home ranges (i.e., second-order selection, *sensu* Johnson 1980), and one contrasting habitat features at bears' GPS locations with those within their corresponding seasonal home ranges (i.e., third-order selection; Johnson 1980). At both orders of selection, I fitted a mixed-effects logistic regression model (Generalized Linear Mixed Models, GLMMs) using the 'lme4' R package (Bates et al. 2015). I treated individual bears as random intercepts, to take into account differences in sample size among individuals and autocorrelation of data within individual bears (Gillies et al. 2006). I standardized each variable by subtracting the mean value from each observation and dividing by its standard deviation to allow comparison of covariates' effects and to improve model convergence (Zuur et al. 2009). I then calibrated GLMMs including all combinations of variables (*dredge* function in 'MuMIn' R package; Barton 2018), and performed model selection using the sample-size corrected Akaike's Information Criterion (AIC_c; Burnham and Anderson 2002). I averaged estimates based on model weights ('MuMIn' R package; Barton 2018) limited to models whose AIC_c value was ≤ 2 from the most supported model (Burnham and Anderson

2002). Finally, I estimated unconditional standard errors and 95% confidence intervals for averaged coefficients, the latter considered significant when they did not include the 0 value. I also determined the relative importance of each covariate by summing the AIC$_c$ weights of all models including a given covariate (Burnham and Anderson 2002). As few candidate models receive Akaike weights > 0, I did not incur the risk of spurious results from averaging parameter estimates of too many models with low weight (Grueber et al. 2011). Finally, using 'MuMIn' R package (Barton 2018), I quantified the proportion of variance explained by the averaged models, calculating the coefficient of determination (R^2; Nakagawa et al. 2017), distinguishing between the variance explained by the fixed effects (i.e., marginal, $R^2_{(m)}$) and the variance explained by both fixed and random effects (i.e., conditional form, $R^2_{(c)}$). Because these analysis was based on a relatively small sample size, I accounted for overfitting problems (Anderson 2008) by considering models with low complexity and a limited number of covariates, and by reducing the number of models to be compared. In addition, the aim of these models was not to make predictions of habitat use by bears outside the study area, further reducing the negative effects of potential overfitting (Zellner et al. 2001, Anderson 2008).

To assess the calibration power of the final model (i.e., how much model predictions differed from a random expectation; Vaughan and Ormerod 2005), I used k-fold cross-validation (k=10) randomly splitting the dataset into 10 bins. By removing 1 bin at time, successively used as a validation set, I used the remaining data (training set) to estimate the MRSF coefficients, and I repeated the procedure for all the remaining bins. For each training set, instead of using fixed classes, I partitioned the predicted MRSF values into continuous bins calculated through a moving window of width W (W = 1/10 of the highest predicted value) (Hirzel et al. 2006). For each continuous bin, I first calculated the frequency of evaluation points falling in each class respect the total number of points (*predicted frequency*), and then the frequency of the predicted values of each class compared to the total amount of training points (*expected frequency*). Finally, I computed the Spearman rank correlation coefficient, also called "continuous Boyce index" (hereafter Boyce index, $B_{cont(W)}$; Hirzel et al. 2006), over the predicted-expected frequencies of all classes. The Boyce index ranges from -1 to 1, where positive values indicate both high predictive model's performance and deviation from randomness (i.e., values close to zero), while negative values indicate an incorrect model. The whole validation procedure was repeated for 100 times.

At the third-order selection, to investigate circadian effects on seasonal selection patterns basis I distinguished between daily and night GPS locations using the *solarpos* function ('maptools' R package; Bivand et al. 2016).

Optimized multi-grain analysis

To identify the optimal grain size for each environmental variable, I used the grain optimization procedure developed by Laforge et al. (2015). Within a resource selection function framework, this procedure involves assessing the most parsimonious grain size of a given variable by changing the grain size of one variable at the time, conditionally on the other covariates. Specifically, for one variable at the time, I compared the model with and without the focal variable measured at a given grain size using AIC_c; that is (Laforge et al. 2015):

$$\Delta AIC_c variable(x) = AIC_{c\,global\,model} - AIC_{c\,global\,model-variable(x)}$$

Using the 'MuMin' R package (Barton 2018), and by repeating the procedure above for different grain sizes, I then plotted ΔAIC_c versus grain size for each variable to identify the most parsimonious (i.e., minimum ΔAIC_c values) grain for a given variable (see Laforge et al. 2015 for more details). As this procedures potentially allows to detect different selection patterns for a given variable at different grain sizes (i.e., coefficients of different sign; Ciucci et al., 2018; Laforge et al., 2015), in these cases I included the variable twice in the in the final, multi-grain model using both grain sizes, provided these were not correlated (see below). To identify the values and range of grain sizes to be assessed for each variable, I followed Zeller et al. (2014) by first fitting a Pareto function to the adult female bears' step-length distribution, and then by dividing this function into quintiles ('POT' and 'adehabitatLT' R packages; Calenge 2006, Ribatet and Dutang 2016) (see Supplementary material for further details). The entire grain-size optimization procedure was repeated to develop MRSF models both at the second and the third order of selection (Supplementary Fig. S2-S11).

Habitat selection at the landscape scale (second-order selection)

To model resource selection at the landscape extent I followed a design II (Thomas and Taylor 2006) by quantifying habitat use of each adult female bear by randomly sampling its annual home range (100% Minimum Convex Polygon, MCP) at a density of 100 points/km^2, and measuring availability at the population level by randomly sampling 10,000 points within the study area, defined as the overall MCP of all adult female bears GPS locations and including a 10-km external buffer, (i.e., the upper limit of the 95% confidence interval of each adult female bear's annual MCP diameter). After checking for collinearity among covariates, including those entered in the model with >1 grain size, I discarded first altitude and distance from paved roads as these were correlated with distance from settlements ($r>0.7$; Supplementary Table S3), and then open field to reduce multicollinearity (VIF<3; Supplementary Table S4). I therefore retained a total of 8 uncorrelated variables in the final model.

Habitat selection within the home range (third-order selection)

To model seasonal resource selection at the home range extent, I followed a design III (Thomas and Taylor 2006) by using adult female bear's seasonal GPS locations to represent use and randomly sampling locations within their seasonal home ranges (100% MCP) at a density of 100 points/km^2 to measure availability. After checking for collinearity among covariates, including entered in the model with >1 grain size, I discarded open fields and altitude as these were correlated with forest and distance from settlements ($VIF>3$; Supplementary Table S9). I therefore retained a total of 8 uncorrelated variables in the final models.

To test my hypothesis of a circadian effect on seasonal habitat selection at the third-order, I used Latent Selection Differences (LSD) functions (Czetwertynski et al. 2007). Similar to an RSF approach, this method allows a direct comparisons of habitat selection between two groups of interest (in my case, day *vs* night), producing quantifiable measurements of the relationships' strength (Czetwertynski et al. 2007, Latham et al. 2011). A fundamental assumption of LSD is that all habitat-types should be equally available to both groups of interest, an assumption that reasonably holds on a seasonal basis in my case.

Functional response in habitat selection

To investigate functional responses toward anthropogenic features, the relatively small sample size of adult female bears ($9 \leq n \leq 10$) did not allow us to contemplate models including individual ID both as an intercept and a random coefficient (e.g., Gillies et al. 2006). Instead, following the procedure described above, I used generalized linear models (GLMs; R Development Core Team, 2019) to develop individual, seasonal MRSFs at the third order selection for each adult female bear. Successively, I used generalized additive models (GAMs; ‘mgcv’ R package; Wood 2011), to assess individual responses by fitting individual MRSFs coefficients of anthropogenic features as a function of their availability within each adult female’s the home range. I then used an information-theoretic approach to perform model selection, comparing each model calibrated (i.e., anthropogenic model) with the respective intercept-only model (i.e., null-model); comparing AIC_c values of the two models, I assessed statistical significance of the functional response when the AIC_c value of the former (anthropogenic model) is lower than the latter (null-model). Finally, I calculated the variance explained by the model (R^2) as a measures of the strength of the relationship between model and the dependent variable (Zuur et al. 2009).

RESULTS

Habitat selection at the landscape scale

At the study area extent, the most parsimonious grain for all variables was the maximum I modelled, except for the variables mean slope and roughness (47 m and 666 m, respectively; Table 2). I averaged the global model without slope (w_i=0.59) and the global model (w_i=0.35), and the averaged model fitted the data reasonably well ($B_{cont(W)}$=0.90±0.06). The variance explained by both fixed and random effect ($R^2_{(c)} = 0.50$) was higher than the variance explained by the fixed effects alone ($R^2_{(m)} = 0.40$).

When locating their home ranges at the landscape scale, adult female bears selected areas with higher forest cover but avoided cultivated lands, shrubland, areas closer to human settlements and less exposed sites. They also selected areas closer to unpaved roads and for relatively even terrain at a small grain (Table 3).

Habitat selection within the home range

Within the home range, the most parsimonious grain size varied across covariates, ranging from 47 m (forest, shrubland) to 1531 m (roughness) and, on average, was consistently small across seasons, with few exceptions (e.g., shrubland in early summer; Table 2). The global model was the most supported in early-summer ($B_{cont(W)}$ = 0.82±0.07), late-summer ($B_{cont(W)}$ = 0.83±0.07), and autumn ($B_{cont(W)}$ = 0.74±0.21); in spring, however, the model without settlements was similarly plausible and was averaged with the global model ($B_{cont(W)}$ = 0.73±0.09). Whereas the variance explained by the global models varied among seasons, within each season the variance explained by both fixed and random effect ($0.15 \leq R^2_{(c)} \leq 0.28$) was consistently higher than the variance explained by the fixed effect alone ($0.07 \leq R^2_{(m)} \leq 0.19$).

I detected relevant seasonal (Table 4) and circadian (Table 5) effects in habitat selection by adult female bears at the home range extent. Consistently across seasons, adult female bears selected proxies of food and cover (agriculture and forest cover) or of inaccessibility by humans (i.e., steeper slopes, rough terrain, and greater distance from dirt roads), while avoiding less exposed sites (Table 4). However, consistently across seasons, forest cover was exceedingly selected during daylight hours compared to the night, whereas agricultural fields were increasingly selected during the night in spring and fall (Table 5). Areas further from dirt roads were especially selected during daylight hours, and so were steeper slopes in three out of four seasons (Table 5). Shrub lands were avoided by adult female bears in spring but were selected in the other seasons (Table 4), with a greater use during daylight hours in early and late summer (Table 5). Areas closer to main paved roads were avoided in early and late summer but increasingly used in spring and fall, whereas areas closer to human settlements were increasingly used during early and late summer (Table 4), both without apparent circadian effects (Table 5).

Functional responses towards anthropogenic features

At the individual level, adult female bears expectedly showed high variability in their third-order, seasonal habitat selection (Supplementary Tables S11−S14 and Fig. S12). Most parsimonious MRSF models at the individual level had R^2 values largely differing across individuals and seasons (spring: $0.15 \leq R^2 \leq 0.68$, n=9; early-summer: $0.05 \leq R^2 \leq 0.63$, n=9; late-summer: $0.21 \leq R^2 \leq 0.33$, n=10; autumn: $0.11 \leq R^2 \leq 0.57$; n=10). However, selection patterns shared by all or most adult female bears consistently reflected (a) avoidance of areas closer to dirt roads (spring and late summer), and (b) selection for forest cover (spring and early summer), agricultural fields (early summer, late summer and fall), shrub lands (late summer), steeper slopes (spring and late summer), rough terrain (late summer), and sites less exposed to sunlight (spring) (Supplementary Fig. S12).

Based on individual, seasonal MRSFs, I detected functional responses by adult female bears toward anthropogenic features at the third-order selection, in particular paved (Fig. 2A-B) and unpaved (Fig. 3A-B) roads, both in spring and late summer, and settlements in autumn (Fig. 4). I failed to detect a functional response towards the same anthropogenic features in the other seasons (i.e., $\mathrm{AIC_c}$(*null model*) > $\mathrm{AIC_c}$(*anthropogenic model*); $3.64\% \leq R^2 \leq 29.8\%$). During spring, adult female bears showed strong avoidance (i.e., positive βs) of areas closer to paved roads at high road densities (i.e., low average distance from roads within the home range), but avoidance waned at intermediate and low road densities (R^2_{sp}=0.42; Fig. 2A); similarly, during summer, avoidance of areas closer to paved roads was highest at intermediate road densities and waned as road density decreased (R^2_{ls}=0.87; Fig. 2B). Contrarily, adult female bears increasingly avoided areas closer to unpaved roads at decreasing road densities within their home range, consistently in spring and late summer (R^2_{sp}=0.52 and R^2_{ls}=0.49, respectively), even they never selected for areas close to unpaved roads also where these occurred at higher densities (Fig. 3A-B). Finally, limited to the autumn, adult female bears selected for areas closer to settlements where these occurred at higher density (i.e., a lower mean distance from settlements within the home range), but selection rapidly waned at decreasing settlement density (R^2_{au}=0.79, Fig. 4).

DISCUSSION

My findings revealed a hierarchical and scale-sensitive process, according to the spatial (i.e., extent and grain) and temporal (i.e., seasons and circadian effect) scales investigated. Whereas land cover and anthropogenic variables are key-factors determining habitat selection by female bears at the landscape scale (i.e., second-order), orographic characteristics become crucial in the habitat selection at the patch-level (i.e., third-order). Compared to the landscape, I found that habitat selection at the home range scale by adult female bears indicates plausible changes in ecological domains. The heavily selection for further distances from human settlements and agricultural fields (i.e., second-order), particularly during the night (i.e., third-order), may indicate a trade-off between the risk of frequenting human-associated land covers and the attraction of foods available at lower altitudes, following phenology of grasses and forbs whose consumption by Apennine bears is highest in spring and fall (Ciucci et al. 2014). Because of the more accessible vegetable foods that can be forage, and according to seasonal food availability, bears commonly utilize human-derived foods near settlements (Elfström et al. 2014; Zarzo-Arias et al. 2018) and cultivate lands (Swenson et al. 1999, Große et al. 2003, Roever et al. 2008*a*, *b*). For bears living in densely populated countries, this might correspond to understanding the main sources of human-caused mortality or compromised fitness, and accordingly assess their spatial variation across scales. Actually, the ‘scale’ factor has been little considered in the previous Apennine brown bear’s habitat selection studies. For instance, Posillico et al. (2004) tempt to capture bear-habitat relationship at landscape scale accounting for one single-coarse grain resolution (5x5km grid-cell), while in following studies (Falcucci et al. 2009, Maiorano et al. 2015, 2019) habitat selection models were performed by using a smaller grain size (i.e., 400 m) and accounting for a larger set of predictor variables. Overall, brown bear’s presence in the central Apennine has been positive associated with elevation and steeper areas rich in broadleaf forests, while negative associated to roads (both paved and unpaved), human density, shrubs, and cultivated fields.

Despite there were an increasingly use of more sophisticated analysis through the time, going from ENFA analysis (Falcucci et al. 2009) to SDMs (Maiorano et al. 2015, 2019), as well as the use of ever more high-resolution variables, these findings partially explain the occurring bears-habitat relationships that instead emerge when resource selection is investigated by accounting for multiple observational scales.

Although limited by a relatively small number of GPS-collared female bears, my study represents the first investigation to describe bear's responses to habitat resources accounting for a multi-grain, multi-order habitat selection approach within their core distribution area. Even though there is widespread recognition of the importance of multi-scale analyses for modeling habitat relationships, a large majority of published habitat ecology papers still do not explicitly consider scale (McGarigal et al. 2016*b*), and scale optimization is rarely done. According to MRSF results, I revealed differences in the characteristic scale (*sensu* Addicott et al. 1987) used in the analysis among different order of selections; at home range scale, the grain responses were consistently smaller than grains selected at landscape scale, indicating that neglecting the hierarchical and multi-scalar nature of resource selection may lead to misleading predictions of their potential habitat suitability at the landscape extent.

At landscape extent, adult female bears aversion for cultivated lands and human settlements reflects their tendency to reduce risk associated to human disturbance. This is in line with previous findings, according to which bears avoid land use and features associated to human disturbance when selecting their home range in human dominated landscape (Güthlin et al. 2011, Peters et al. 2015), even though the low or non-significant selection for orographic features is not crucial as I expected. In fact, I found that terrain slope and roughness had a scarce impact in predicting female bear presence (Güthlin et al. 2011, Peters et al. 2015). This pattern can be explained by the fact that, in more pristine ecosystems of North America where anthropogenic effects are less apparent, terrain roughness, elevation, and forest management interventions (i.e., wood harvesting) are among the features most selected by bears when selecting home range within the landscape (Nielsen et al. 2006, Cristescu et al. 2016). In contrast with bears' resource selection pattern revealed at the patch-level, at landscape scale this selection pattern reflect a high human-induced risk of mortality by female bears, which prefer areas with low-level of human disturbance (i.e., human settlements and paved roads, the latter high-correlated with the former), high-cover of forest, and high-presence of low-traffic roads (i.e., dirt roads).

At the home range extent, I detected relevant seasonal and circadian effects in habitat selection by adult female bears, likely indicating that bears selected proxies of food and cover (agriculture, forest and shrub cover) or of inaccessibility by humans (i.e., steeper slopes, rough terrain, and greater distance from dirt roads). Among seasons, forest cover was exceedingly selected during daylight hours compared to the night, whereas agricultural fields were increasingly selected during the night in spring and fall. Agriculture is scarce in the study area, and agricultural fields are often associated to natural open areas, mainly close to human infrastructures, but well integrated within the Apennine's forest ecosystem. Similar to forest, shrublands are selected during all year, excepted in spring season which may increasingly interesting for bears due to the enhanced availability of food (e.g., ants, fruits) and cover function (poor in spring due to absence of leaves); however, the greater use of such resource during daylight hours in early- and late-summer may indicate also the role of shrubs cover in addition to food (e.g., Cristescu et al. 2016). Indeed, shrubland associated to young regenerating forest may be important not only in terms of shelter (e.g., daybed site selection; Skuban and Find'o 2018), but also in terms of matrix permeability and habitat continuity, because it may provide both complementary (or even supplementary) foraging resources and linkage areas through which bears can move between other forest habitat patches (Mateo Sánchez et al. 2013). In line with previous findings, human settlements may indicate attraction for food although a few bears did so, and it (i.e., positive selection) possibly accounts for the relatively small number of villages in the study area. Nonetheless, female bears needed of inaccessible areas by humans (i.e., steeper slopes, rough terrain, and greater distance from dirt roads), while avoiding more exposed sites. Bears commonly use imperviousness areas that offering a higher relative security (Nielsen et al. 2004, Martin et al. 2010), and Apennine female bears seem to be not an exception. While the use of steeper slopes by female bears can be related to the need of refuge areas, the consistently selection for less sun-exposed sites can be linked to their thermoregulatory needs. Thermoregulation played a critical role in many female brown bear populations in North America (Pigeon et al. 2016*a*, *b*) and Europe (Ordiz et al. 2011). As also observed in many other species (e.g., du Plessis et al. 2012, van Beest et al. 2012), bears effectively may reduce the risks of hyperthermia by pushing them into more thermally suitable habitats (e.g., thermal shelter; Pigeon et al. 2016*a*) while foraging in warm habitats, like Mediterranean forest ecosystem that can reach higher temperatures compare to other northern brown bear populations.

Differently by land use and orographic selection pattern, paved roads represent a double-edged blade for female brown bear, particularly avoided in early and late-summer but increasingly used in spring and fall. Female bears' rewards derived from anthropogenic features seems to be higher during low human activity seasons, even if this always occur in specific safety environmental conditions, like high forest cover, steeper slope and roughness. Spatiotemporal avoidance of humans linear features during daytime is commonly reported in some European countries with high-human density, such as in Scandinavia (Moe et al. 2007, Ordiz et al. 2014) and Balkan (Kaczensky et al. 2006), where bears activities are higher in the nocturnal and twilight hours respect during the day in areas with higher road density, compared to roadless areas. In North America, Mace and John (1997) suggested that grizzly bears can persist in areas with roads, but spatial avoidance will increase and survival will decrease as traffic levels, road densities, and human settlement increases; moreover, grizzly bears living in areas less populated by humans are most active during the day (Boyce et al. 2010) showed no daily pattern to their use of roads (Roever et al. 2010), even though they may avoid roads in function of increasing volume traffic, attributed to a disproportionate use of roads during the night in areas more densely populated by humans (McLellan and Shackleton 1988, Waller and Servheen 2005, Northrup et al. 2012). In line with this pattern, behavioral responses to roads may indicate a trade-off between attraction for food at valley bottom and nearby roads (e.g., forbs and ants) and traffic perceived risk; when the human-use of paved roads increase (e.g., summer season), female bears avoid roads (possibly attracted elsewhere, e.g. *Rhamnus*), but when food elsewhere is not as attractive, and vehicular volume tourism-dependent decreases significantly (i.e., spring and autumn seasons), ecotones along roads may provide fruiting species which attract bears. In the same study area, Mancinelli et al. (2019) highlighted that wolves also avoids anthropogenic features during daylight hours (i.e. periods of higher), compared to the night (i.e. periods of lower human activity), even though this tendency was strongly affected by other factors, including season (i.e., mostly in summer). Similar to wolf, female bears may be affected by the human peak of summer activities (e.g., cattle, forestry practice) and flow of tourists (http://www.parcoabruzzo.it/dettaglio.php?xml:id=11151), associated to the change in direction for the paved roads selection occurring in summer season (i.e., avoidance of paved roads), especially during the period that range from August to September (i.e., late-summer), and the selection of areas further from dirt roads, especially during the daylight hours. However, this spatiotemporal discrimination of human derived risk is linked to the individual capacity of bear to adapt their behavior to daily and seasonal human activities. From the results, female bears showed a high individual variability in habitat selection (Roever et al. 2008*b*, Martin et al. 2010, Northrup et al. 2012), and may better respond to the local conditions in which individuals find themselves. Comparing individual and population results, I found that anthropogenic features show the greater variability in bears' habitat selection. Furthermore, part of space-use pattern variability among individual female bears can be explained by a discovered functional response according to the increase or decrease of anthropogenic features availability, and this evidenced plasticity towards human features could be the following result of a flexible co-habitation dynamics between bears and humans locally persisting for centuries. Nonetheless, for few seasons and variables, I found that female bears' selection pattern at the individual level reflect the results evidenced in the MRSF at the population level, like the positive selection for forest cover in spring and early-summer, and the avoidance for unpaved roads in spring and late-summer. The fact that both approaches indicated the same direction in habitat selection underly that these response patterns exceed the inter-individual variability, resulting fundamental for this population.

In conclusion, multi-scale habitat selection I examined reveals a habitat-mediated coexistence strategy where resources are used according to spatiotemporal patterns that minimize disturbance by humans and risk of human-induced mortality, thereby revealing trade-offs in multiple scales resource selection decisions (Thompson and McGarigal 2002; Leblond et al. 2011). Human perceived risk become more evident by the daily preference of forest cover (i.e., shelter), and in the avoidance of main roads (i.e., paved roads) during the peak of tourism in late-summer, also corresponding to the bear's early-hyperphagia. During late-summer, fleshy fruits are predominated in bear's diet with a preference for buckthorn (*Rhamnus* spp.) (Ciucci et al. 2014), which grow in open fields at high altitudes and are a vital food during this period, likely explaining why, at the home range (and individual) level, beta coefficient of forest cover (negative correlated with open fields) are lower compared to the other seasons.

Although forest remains a fundamental positive-selected resource independently from the ecological domain investigated, and as I could not contemplate forest structure and hard must productivity in the habitat selection models, I caution that these results ignore the relative effect of these factors as drivers of forest selection by bears. Indeed, structural proprieties of forests likely provide an excellent measure of shelter (e.g., tree density and understory) and of hard must productivity (e.g., diameter and basal area of the tree), both relevant to bears. How forests' structure and productivity affect habitat selection by Apennine bears deserves further and more in depth investigation, especially in the light of the important implications this knowledge may have to design proactive forestry practices to sustain and maintain in the long term the structural value and the productivity of forest ecosystems to bears.

Since I may observe and interpret biological processes differently at different scales, the more appropriate scale to address management decisions depends on the management question (Boyce et al. 2003, Hobbs 2003, Boyce 2006). If the objective is to delineate brown bear conservation priority, then the landscape extent will reflect the broad resource selection of female bears throughout the reproductive core area. However, when management questions become more specific, such as managing for human access in particular periods of the year for reducing bear's disturbance, then accounting for patch-level responses is the best choice at home range scale. From these findings, early- (i.e., June–July) and, mostly, late-summer (i.e., August–September) appear to be the seasons with the highest negatively responses to anthropogenic factors associated with the increased hazards posed by human activities. My suggestions are to address management efforts to critical areas where human activities (e.g., hiking, cattle browsing, and forest cutting) could alter habitat perceived risk by bears, change their resource selection, and reduce their fitness. In this sense, habitat suitability maps derived by projected models (Supplementary Fig. S13-14) can provide useful spatially indications: for instance, at landscape scale, habitat suitability maps can be used by the Park's Authority as supporting tool to provide spatially explicit information, and prioritize critical areas within the Park's boundaries, including and, consequently, protecting new suitable areas currently outside the Park.

REFERENCES

Addicott, J. F., J. M. Aho, M. F. Antolin, D. K. Padilla, J. S. Richardson, and D. A. Soluk. 1987. Ecological neighborhoods: Scaling environmental patterns. Oikos 49:340–346.

Anderson, D. R. 2008. Model based inference in the life sciences: a primer on evidence. U. Springer, New York, New York, editor.

Barton, K. 2018. Package "MuMIn" Title Multi-Model Inference. Cran-R.

Bates, D., M. Mächler, B. Bolker, and S. Walker. 2015. Fitting linear mixed-effects models using lme4. Journal of Statistical Software 67:1–48.

van Beest, F. M., B. Van Moorter, and J. M. Milner. 2012. Temperature-mediated habitat use and selection by a heat-sensitive northern ungulate. Animal Behaviour 84:723–735.

Benazzo, A., E. Trucchi, J. A. Cahill, P. M. Delser, S. Mona, M. Fumagalli, L. Bunnefeld, L. Cornetti, S. Ghirotto, M. Girardi, L. Ometto, A. Panziera, O. Rota-Stabelli, E. Zanetti, A. Karamanlidis, C. Groff, L. Paule, L. Gentile, C. Vilà, S. Vicario, L. Boitani, L. Orlando, S. Fuselli, C. Vernesi, B. Shapiro, P. Ciucci, and G. Bertorelle. 2017. Survival and divergence in a small group: The extraordinary genomic history of the endangered Apennine brown bear stragglers. Proceedings of the National Academy of Sciences of the United States of America 114:E9589–E9597.

Benítez-López, A., J. Viñuela, F. Mougeot, and J. T. García. 2017. A multi-scale approach for identifying conservation needs of two threatened sympatric steppe birds. Biodiversity and Conservation 26:63–83.

Bivand, R., N. Lewin-Koh, E. Pebesma, E. Archer, A. Baddeley, N. Bearman, H.-J. Bibiko, S. Brey, J. Callahan, G. Carrillo, S. Dray, D. Forrest, M. Friendly, P. Giraudoux, D. Golicher, V. G. Rubio, P. Hausmann, K. O. Hufthammer, T. Jagger, K. Johnson, S. Luque, D. MacQueen, A. Niccolai, E. Pebesma, O. P. Lamigueiro, T. Short, G. Snow, B. Stabler, M. Stokely, and R. Turner. 2016. Tools for Reading and Handling Spatial Objects: Package "maptools." R Documentation.

Blanchard, B. M. 1983. Grizzly Bear: Habitat Relationships in the Yellowstone Area. Bears: Their Biology and Management 5:118–123.

Boyce, M. S. 2006. Scale for resource selection functions. Diversity and Distributions 12:269–276.

Boyce, M. S., B. M. Blanchard, R. R. Knight, and C. Servheen. 2001. Population viability for grizzly bears: a critical review. International Association of Bear Research and Management 1–39.

Boyce, M. S., J. S. Mao, E. H. Merrill, D. Fortin, M. G. Turner, J. Fryxell, and P. Turchin. 2003. Scale and heterogeneity in habitat selection by elk in Yellowstone National Park. Ecoscience 10:421–431.

Boyce, M. S., and L. L. McDonald. 1999. Relating populations to habitats using resource selection functions. Trends in Ecology and Evolution 14:268–272.

Boyce, M. S., J. Pitt, J. M. Northrup, A. T. Morehouse, K. H. Knopff, B. Cristescu, and G. B. Stenhouse. 2010. Temporal autocorrelation functions for movement rates from global positioning system radiotelemetry data. Philosophical Transactions of the Royal Society B: Biological Sciences 365:2213–2219.

Burnham, K. P., and D. R. Anderson. 2002. Model selection and multimodel inference: A practical information-theoretic approach. Ecological Modelling. 2nd edition. Springer-Verlag, New York, New York, USA.

Calenge, C. 2006. The package “adehabitat” for the R software: A tool for the analysis of space and habitat use by animals. Ecological Modelling.

Ciarniello, L. M., M. S. Boyce, D. C. Heard, and D. R. Seip. 2005. Denning behavior and den site selection of grizzly bears along the Parsnip River, British Columbia, Canada. Ursus 16:47–58.

Ciucci, P., T. Altea, A. Antonucci, L. Chiaverini, A. Di Croce, F. Mauro, P. Forconi, R. Latini, L. Maiorano, A. Monaco, P. Morini, F. Ricci, L. Sammarone, F. Striglioni, E. Tosoni, L. Carotenuto, I. Pizzol, M. C. Saltari, D. Serafini, M. Caporioni, L. Tarquini, S. Donfrancesco, I. Guj, A. Lecce, G. Di Clemente, and E. Peria. 2017. Distribution of the brown bear (*Ursus arctos marsicanus*) in the central Apennines, Italy, 2005–2014. Hystrix 28:1–6.

Ciucci, P., and L. Boitani. 2008. The Apennine brown bear: A critical review of its status and conservation problems. Ursus 19:130–145.

Ciucci, P., L. Boitani, M. Falco, and L. Maiorano. 2018. Hierarchical, multi-grain rendezvous site selection by wolves in southern Italy. The Journal of Wildlife Management 82:1049–1061.

Ciucci, P., V. Gervasi, L. Boitani, J. Boulanger, D. Paetkau, R. Prive, and E. Tosoni. 2015. Estimating abundance of the remnant Apennine brown bear population using multiple non invasive genetic data sources. Journal of Mammalogy 96:206–220.

Ciucci, P., E. Tosoni, G. Di Domenico, F. Quattrociocchi, and L. Boitani. 2014. Seasonal and annual variation in the food habits of Apennine brown bears, central Italy. Journal of Mammalogy 95:572–586.

Ciucci, P., E. Tosoni, L. Maiorano, L. Gentile, C. Sulli, and L. Boitani. 2012. Denning in the Apennine brown bear (*Ursus arctos marsicanus*) and potential conflict areas: Toward proactive conservation measures. VIII Congresso Italiano di Teriologia. Hystrix, It. J. Mamm. (N.S.) 64.

Cozzi, G., M. Chynoweth, J. Kusak, E. Çoban, A. Çoban, A. Ozgul, and H. Şekercioğlu. 2016. Anthropogenic food resources foster the coexistence of distinct life history strategies: year-round sedentary and migratory brown bears. Journal of Zoology 300:142–150.

Cristescu, B., G. B. Stenhouse, M. Symbaluk, S. E. Nielsen, and M. S. Boyce. 2016. Wildlife habitat selection on landscapes with industrial disturbance. Environmental Conservation 43:327–336.

Czetwertynski, S. M., M. S. Boyce, and F. K. Schmiegelow. 2007. Effects of hunting on demographic parameters of American black bears. Ursus 18:1–18.

Elfström, M., J. E. Swenson, and J. P. Ball. 2008. Selection of denning habitats by Scandinavian brown bears Ursus arctos. Wildlife Biology 14:176–187.

Elfström, M., A. Zedrosser, K. Jerina, O. G. Støen, J. Kindberg, L. Budic, M. Jonozovič, and J. E. Swenson. 2014a. Does despotic behavior or food search explain the occurrence of problem brown bears in Europe? Journal of Wildlife Management 78:881–893.

Elfström, M., A. Zedrosser, O. G. Støen, and J. E. Swenson. 2014b. Ultimate and proximate mechanisms underlying the occurrence of bears close to human settlements: Review and management implications. Mammal Review 44:5–18.

Ellenberg, U., T. Mattern, and P. J. Seddon. 2009. Habituation potential of yellow-eyed penguins depends on sex, character and previous experience with humans. Animal Behaviour 77:289–296.

Fahrig, L. 1992. Relative importance of spatial and temporal scales in a patchy environment. Theoretical Population Biology 41:300–314.

Falcucci, A., P. Ciucci, L. Maiorano, L. Gentile, and L. Boitani. 2009. Assessing habitat quality for conservation using an integrated occurrence-mortality model. Journal of Applied Ecology 46:600–609.

Gaillard, J. M., M. Hebblewhite, A. Loison, M. Fuller, R. Powell, M. Basille, and B. Van Moorter. 2010. Habitat-performance relationships: Finding the right metric at a given spatial scale. Philosophical Transactions of the Royal Society B: Biological Sciences 365:2255–2265.

Gervasi, V., and P. Ciucci. 2018. Demographic projections of the Apennine brown bear population *Ursus arctos marsicanus* (Mammalia: Ursidae) under alternative management scenarios. The European Zoological Journal 85:242–252.

Gill, J. A., K. Norris, and W. J. Sutherland. 2001. Why behavioural responses may not reflect the population consequences of human disturbance. Biological Conservation 97:265–268.

Gillies, C. S., M. Hebblewhite, S. E. Nielsen, M. A. Krawchuk, C. L. Aldridge, J. L. Frair, D. J. Saher, C. E. Stevens, and C. L. Jerde. 2006. Application of random effects to the study of resource selection by animals. Journal of Animal Ecology 75:887–898.

Große, C., P. Kaczensky, and F. Knauer. 2003. Ants: A food source sought by Slovenian brown bears (*Ursus arctos*)? Canadian Journal of Zoology 81:1996–2005.

Grueber, C. E., S. Nakagawa, R. J. Laws, and I. G. Jamieson. 2011. Multimodel inference in ecology and evolution: Challenges and solutions. Journal of Evolutionary Biology 24:699–711.

Guisan, A., and N. E. Zimmermann. 2000. Predictive habitat distribution models in ecology. Ecological Modelling 135:147–186.

Güthlin, D., F. Knauer, T. Kneib, H. Küchenhoff, P. Kaczensky, G. Rauer, M. Jonozovič, A. Mustoni, and K. Jerina. 2011. Estimating habitat suitability and potential population size for brown bears in the Eastern Alps. Biological Conservation 144:1733–1741.

Hall, L. S., P. R. Krausman, M. L. Morrison, L. S. Hall, P. R. Krausman, and M. L. Morrison. 1997. The habitat concept and a plea for standard terminology. Wildlife Society Bulletin 25:173–182.

Hamer, D., and S. Herrero. 1987. Grizzly bear food and habitat in the front ranges of Banff National Park, Alberta. Bears: Their Biology and Management. A Selection of Papers from the Seventh International Conference on Bear Research and Management, Williamsburg, Virginia, USA, and Plitvice Lakes, Yugoslavia 7:199–213.

Hebblewhite, M., and E. Merrill. 2008. Modelling wildlife-human relationships for social species with mixed-effects resource selection models. Journal of Applied Ecology 45:834–844.

Herrero, S. 1972. Aspects of Evolution and Adaptation in American Black Bears (*Ursus americanus* Pallas) and Brown and Grizzly Bears (*U. arctos* Linné.) of North America. Bears: Their Biology and Management 2:221–231.

Hirzel, A. H., J. Hausser, D. Chessel, and N. Perrin. 2002. Ecological-niche factor analysis: How to compute habitat-suitability maps without absence data? Ecology 83:2027–2036.

Hirzel, A. H., and G. Le Lay. 2008. Habitat suitability modelling and niche theory. Journal of Applied Ecology 45:1372–1381.

Hirzel, A. H., G. Le Lay, V. Helfer, C. Randin, and A. Guisan. 2006. Evaluating the ability of habitat suitability models to predict species presences. Ecological Modelling 199:142–152.

Hobbs, N. T. 2003. Challenges and opportunities in integrating ecological knowledge across scales. Forest Ecology and Management 181:223–238.

Holland, J. E. Y. D., D. G. Bert, and L. Fahrig. 2004. Determine spatial scale of species' response to habitat. BioScience 54:227–233.

Johnson, D. H. 1980. The comparison of usage and availability measurements for evaluating resource preference. Ecology 61:65–71.

Kaczensky, P., D. Huber, F. Knauer, H. Roth, A. Wagner, and J. Kusak. 2006. Activity patterns of brown bears (*Ursus arctos*) in Slovenia and Croatia. Journal of Zoology 269:474–485.

Knight, R. R., and L. L. Eberhardt. 1985. Population dynamics of Yellowstone grizzly bears. Ecology 66:323–334.

Kotliar, N. B., and J. A. Wiens. 1990. Multiple scales of patchiness and patch Structure: A hierarchical framework for the Study of Heterogeneity. Oikos 59:253–260.

Laforge, M. P., E. Vander Wal, R. K. Brook, E. M. Bayne, and P. D. McLoughlin. 2015. Process-focussed, multi-grain resource selection functions. Ecological Modelling 305:10–21.

Lamb, C. T., G. Mowat, B. N. McLellan, S. E. Nielsen, and S. Boutin. 2016. Forbidden fruit: human settlement and abundant fruit create an ecological trap for an apex omnivore. Journal of Animal Ecology 86:55–65.

Latham, A. D. M., M. C. Latham, and M. S. Boyce. 2011. Habitat selection and spatial relationships of black bears (*Ursus americanus*) with woodland caribou (*Rangifer tarandus caribou*) in northeastern Alberta. Canadian Journal of Zoology 89:267–277.

Leblond, M., J. Frair, D. Fortin, C. Dussault, J. P. Ouellet, and R. Courtois. 2011. Assessing the influence of resource covariates at multiple spatial scales: An application to forest-dwelling caribou faced with intensive human activity. Landscape Ecology 26:1433–1446.

Levin, S. A. 1992. The problem of pattern and scale in ecology: The Robert H. MacArthur award lecture. Ecology 73:1943–1967.

Lewis, J. S., J. L. Rachlow, E. O. Garton, and L. A. Vierling. 2007. Effects of habitat on GPS collar performance: Using data screening to reduce location error. Journal of Applied Ecology 44:663–671.

Mace, R. D., and W. S. John. 1997. Spatial and temporal interaction of male and female grizzly bears in Northwestern Montana. Journal of Wildlife Management 61:39–52.

Maiorano, L., L. Boitani, A. Monaco, E. Tosoni, and P. Ciucci. 2015. Modeling the distribution of

Apennine brown bears during hyperphagia to reduce the impact of wild boar hunting. European Journal of Wildlife Research 61:241–253.

Maiorano, L., L. Chiaverini, M. Falco, and P. Ciucci. 2019. Combining multi-state species distribution models, mortality estimates, and landscape connectivity to model potential species distribution for endangered species in human dominated landscapes. Biological Conservation 237:19–27.

Mancinelli, S., L. Boitani, and P. Ciucci. 2018. Determinants of home range size and space use patterns in a protected wolf (*Canis lupus*) population in the central Apennines, Italy. Canadian Journal of Zoology 96:828–838.

Mancinelli, S., M. Falco, L. Boitani, and P. Ciucci. 2019. Social, behavioural and temporal components of wolf (*Canis lupus*) responses to anthropogenic landscape features in the central Apennines, Italy. Journal of Zoology 309:114–124.

Manly, B. F. J., L. Mcdonald, D. Thomas, T. L. McDonald, and W. P. Erickson. 2002. Resource selection by animals: Statistical design and analysis for field studies. 2nd ed. Volume 1. Kluwer Academic Publishers, Dordrecht, Netherlands. Merkle.

Martin, J., M. Basille, B. van Moorter, J. Kindberg, D. Allainé, and J. E. Swenson. 2010. Coping with human disturbance: Spatial and temporal tactics of the brown bear (*Ursus arctos*). Canadian Journal of Zoology 88:875–883.

Martin, J. G. A., and D. Réale. 2008. Animal temperament and human disturbance: Implications for the response of wildlife to tourism. Behavioural Processes 77:66–72.

Mateo Sánchez, M. C., S. A. Cushman, and S. Saura. 2013. Scale dependence in habitat selection: the case of the endangered brown bear (*Ursus arctos*) in the Cantabrian Range (NW Spain). International Journal of Geographical Information Science 28:1531–1546.

Mayor, S. J., D. C. Schneider, J. A. Schaefer, and S. P. Mahoney. 2009. Habitat selection at multiple scales. Écoscience 16:238–247.

McGarigal, K., H. Y. Wan, K. A. Zeller, B. C. Timm, and S. A. Cushman. 2016a. Multi-scale habitat selection modeling: A review and outlook. Landscape Ecology 31:1161–1175.

McGarigal, K., K. A. Zeller, and S. A. Cushman. 2016b. Multi-scale habitat selection modeling: Introduction to the special issue. Landscape Ecology 31:1157–1160.

McLellan, B. N., and D. M. Shackleton. 1988. Grizzly bears and resource-extraction industries: Effects of roads on behaviour, habitat use and demography. The Journal of Applied Ecology 25:451–460.

Moe, T. F., J. Kindberg, I. Jansson, and J. E. Swenson. 2007. Importance of diel behaviour when studying habitat selection: Examples from female Scandinavian brown bears (*Ursus arctos*). Canadian Journal of Zoology 85:518–525.

Morrison, M. L., and S. Hall. 2002. Standard Terminology: Toward a common language to advance ecological understanding and applications. Pages in 43-52, J. M. Scott, P. J. Heglund, and M. L. Morrison, editors. Symposium on predicting species occurrences: issues of scale and accuracy. Island Press, Covelo, California, USA.

Mysterud, A., and R. A. Ims. 1998. Functional responses in habitat use: Availability influences relative use in trade-off situations. Ecology.

Nakagawa, S., P. C. D. Johnson, and H. Schielzeth. 2017. The coefficient of determination R2 and intra-class correlation coefficient from generalized linear mixed-effects models revisited and expanded. Journal of the Royal Society Interface 14:20170213.

Nielsen, S. E., R. H. M. Munro, E. L. Bainbridge, G. B. Stenhouse, and M. S. Boyce. 2004. Grizzly bears and forestry: II. Distribution of grizzly bear foods in clearcuts of west-central Alberta, Canada. Forest Ecology and Management 199:67–82.

Nielsen, S. E., G. B. Stenhouse, and M. S. Boyce. 2006. A habitat-based framework for grizzly bear conservation in Alberta. Biological Conservation 130:217–229.

Northrup, J. M., J. Pitt, T. B. Muhly, G. B. Stenhouse, M. Musiani, and M. S. Boyce. 2012. Vehicle traffic shapes grizzly bear behaviour on a multiple-use landscape. Journal of Applied Ecology 49:1159–1167.

Ordiz, A., J. Kindberg, S. Sæbø, J. E. Swenson, and O. G. Støen. 2014. Brown bear circadian behavior reveals human environmental encroachment. Biological Conservation 173:1–9.

Ordiz, A., O. G. Støen, M. Delibes, and J. E. Swenson. 2011. Predators or prey? Spatio-temporal discrimination of human-derived risk by brown bears. Oecologia 166:59–67.

Ordiz, A., O. G. Støen, S. Sæbø, J. Kindberg, M. Delibes, and J. E. Swenson. 2012. Do bears know they are being hunted? Biological Conservation 152:21–28.

Peters, W., M. Hebblewhite, M. Cavedon, L. Pedrotti, A. Mustoni, F. Zibordi, C. Groff, M. Zanin, and F. Cagnacci. 2015. Resource selection and connectivity reveal conservation challenges for reintroduced brown bears in the Italian Alps. Biological Conservation 186:123–133.

Pigeon, K. E., E. Cardinal, G. B. Stenhouse, and S. D. Côté. 2016a. Staying cool in a changing landscape: the influence of maximum daily ambient temperature on grizzly bear habitat selection. Oecologia 181:1101–1116.

Pigeon, K. E., S. D. Côté, and G. B. Stenhouse. 2016b. Assessing den selection and den characteristics of grizzly bears. Journal of Wildlife Management 80:884–893.

Pimenta, N. C., A. L. S. Gonçalves, G. H. Shepard, V. W. Macedo, and A. P. A. Barnett. 2018. The return of giant otter to the Baniwa Landscape: A multi-scale approach to species recovery in the middle Içana River, Northwest Amazonia, Brazil. Biological Conservation 224:318–326.

du Plessis, K. L., R. O. Martin, P. A. R. Hockey, S. J. Cunningham, and A. R. Ridley. 2012. The costs of keeping cool in a warming world: Implications of high temperatures for foraging, thermoregulation and body condition of an arid-zone bird. Global Change Biology 18:3063–3070.

Posillico, M., A. Meriggi, E. Pagnin, S. Lovari, and L. Russo. 2004. A habitat model for brown bear conservation and land use planning in the central Apennines. Biological Conservation 118:141–150.

Ribatet, M., and C. Dutang. 2016. POT: Generalized pareto distribution and peaks over threshold.

Roever, C. L., M. S. Boyce, and G. B. Stenhouse. 2008a. Grizzly bears and forestry I: Road vegetation and placement as an attractant to grizzly bears. Forest Ecology and Management 256:1253–1261.

Roever, C. L., M. S. Boyce, and G. B. Stenhouse. 2008b. Grizzly bears and forestry II: Grizzly bear habitat selection and conflicts with road placement. Forest Ecology and Management 256:1262–1269.

Roever, C. L., M. S. Boyce, and G. B. Stenhouse. 2010. Grizzly bear movements relative to roads: Application of step selection functions. Ecography 33:1113–1122.

Roland, J., and P. D. Taylor. 1997. Insect parasitoid species respond to forest structure at different spatial scales. Nature 386:710–713.

Schneider, D. C. 2001. The Rise of the Concept of Scale in Ecology. BioScience 51:545–553.

Skuban, M., and S. Find'o. 2018. Bears napping nearby: Daybed selection by brown bears (*Ursus arctos*) in a human-dominated landscape. Canadian Journal of Zoology 96:1–11.

Swenson, J. E., A. Jansson, R. Riig, and F. Sandegren. 1999. Bears and ants: Myrmecophagy by brown bears in central Scandinavia. Canadian Journal of Zoology 77:551–561.

Team, R. C. 2019. R: A language and environment for statistical computing. Vienna, Austria.

Thomas, D. L., and E. J. Taylor. 2006. Study designs and tests for comparing resource use and availability. The Journal of Wildlife Management 54:322.

Thompson, C. M., and K. McGarigal. 2002. The influence of research scale on bald eagle habitat selection along the lower Hudson River, New York (USA). Landscape Ecology 17:569–586.

Vaughan, I. P., and S. J. Ormerod. 2005. The continuing challenges of testing species distribution models. Journal of Applied Ecology 42:720–730.

Waller, J. S., and C. Servheen. 2005. Effects of transportation infrastructure on grizzly bears in Norternwestern Montana. Journal of Wildlife Management 69:985–1000.

Wheatley, M., and C. Johnson. 2009. Factors limiting our understanding of ecological scale. Ecological Complexity 6:150–159.

Wiegand, T., J. Naves, T. Stephan, and A. Fernandez. 1998. Assessing the risk of extinction for the brown bear (*Ursus arctos*) in the Cordillera Cantabrica, Spain. Ecological Monographs 68:539–570.

Wiens, J. A. 1989. Spatial scaling in ecology. Functional Ecology 3:385–397.

Wood, S. N. 2011. Fast stable restricted maximum likelihood and marginal likelihood estimation of semiparametric generalized linear models. Journal of the Royal Statistical Society. Series B: Statistical Methodology 73:3–36.

Zarzo-Arias, A., M. del M. Delgado, A. Ordiz, J. García Díaz, D. Cañedo, M. A. González, C. Romo, P. Vázquez García, G. Bombieri, C. Bettega, L. F. Russo, P. Cabral, R. García González, J. Martínez-Padilla, and V. Penteriani. 2018. Brown bear behaviour in human-modified landscapes: The case of the endangered Cantabrian population, NW Spain. Global Ecology and Conservation 16:e00499.

Zeller, K. A., K. McGarigal, P. Beier, S. A. Cushman, T. W. Vickers, and W. M. Boyce. 2014.

Sensitivity of landscape resistance estimates based on point selection functions to scale and behavioral state: Pumas as a case study. Landscape Ecology 29:541–557.

Zellner, A., H. A. Keuzenkamp, and M. McAleer. 2001. Simplicity, inference, and modeling. U. K. Cambridge University Press, Cambridge, editor.

Zuur, A. F., E. N. Ieno, N. J. Walker, A. A. Saveliev, G. M. Smith, Z. I. Walker, and S. Smith. 2009. Mixed effects models and extensions in ecology with R. Ecology. Springer-Verlag, New York, New York, USA.

TABLES AND FIGURES

Table 1. Covariates contemplated to develop multi-grain resource selection functions to investigate second- and third-order habitat selection by Apennine brown bears in the Abruzzo, Lazio, and Molise National Park central Italy, 2005–2010. Because of collinearity, not all covariates were retained in the final models.

Variable				Study area		Home range	
Type	**Description**	**Source**	**Code**	$\bar{\chi}$	**SD**	$\bar{\chi}$	**SD**
Environmental	Agricultural areas (%)	Regional CLC V level	Agri	16.4	-	2.2	2.7
	Forests (%)	Regional CLC V level	For	58.4	-	69.1	8.6
	Shrublands (%)	Regional CLC V level	Shrub	4.6	-	4.2	3.4
	Open areas (%) [a]	Regional CLC V level	Open	20.6	-	24.6	9.7
Anthropogenic	Paved roads (km/100 km^2) [b]	De Agostini-GeoNext and TeleAtlas databases	DisRoad1	45.3	-	20.3	17.3
	Unpaved roads (km/100 km^2) [c]	De Agostini-GeoNext and TeleAtlas databases	DisRoad2	97.0	-	88.0	34.7
	Settlements (km^2/100 km^2)	ISTAT	DisSettl	0.2	-	0.7	0.7
Orographic	Altitude (m. a. s. l.)	IGM	DEM	1100	473.1	1421.9	334.0
	Hillshade [d]	IGM	Hill	165.7	42.4	163.1	45.4
	Slope (°)	IGM	SlpM	18.2	12.0	21.2	11. 5
			SlpSD	22.23	-	19.80	1.80

[a]: Including meadows, pastures, alpine prairies, and clearings. Not included in the final model due to collinearity with other variables

[b]: Including primary roads connecting the main human settlements. I reported measures of densities rather than distances (used in the analysis) for a more immediate picture of the human-modified landscape.

[c]: Including secondary roads connecting primary roads and human settlements with wilderness surrounding areas. I reported measures of densities rather than distances (used in the analysis) for a more immediate picture of the human-modified landscape.

[d]: Hillshade (Spatial Analyst Tool; ArcMap v. 10.2, ESRI) indicates the average annual amount of shading, ranging from 0 to 255, (0= completed shaded sites, 255= most sun-exposed sites)

Table 2. Most parsimonious AICc-selected, multi-grain, mixed effects logistic regression model to assess habitat selection by Apennine brown bears when establishing a territory (second-order selection), and within their home ranges (third-order selection). Habitat use has been investigated by means of GPS locations collected on 11 adult female bears in the Abruzzo, Lazio, and Molise National Park, central Italy (2005−2010). Model selection occurred through model dredging. Only candidate models with ΔAIC$_c$≤2 are shown. K = number of model's parameters; logLik = loglikelihood; AIC$_c$ = Akaike's Information Criterion adjusted for small sample size; ΔAIC$_c$ = AIC$_c$ difference between each candidate model and the most parsimonious model; w_i = Akaike weights.

Extent	Season	Model description [a]	K	logLik	AIC$_c$	ΔAIC$_c$	w_i
Study area	Annual	For$_{1531}$ + Agri$_{1531}$ + Shrub$_{1531}$ + DisSettl + Hill$_{1531}$ + DisRoad2 + SlpSD$_{666}$	9	-26275.92	52569.80	0.00	0.59
(2nd order)		For$_{1531}$ + Agri$_{1531}$ + Shrub$_{1531}$ + DisSettl + Hill$_{1531}$ + DisRoad2 + SlpM$_{47}$ + SlpSD$_{666}$	10	-26275.42	52570.90	1.01	0.35
Home range	Spring	For$_{47}$ + Agri$_{198}$ + Shrub$_{140}$ + DisSettl + Hill$_{140}$ + DisRoad1 + DisRoad2 + SlpM$_{116}$ + SlpSD$_{236}$	11	-7661.00	15344.00	0.00	0.50
(3rd order)		For$_{47}$ + Agri$_{198}$ + Shrub$_{140}$ + Hill$_{140}$ + DisRoad1 + DisRoad2 + SlpM$_{116}$ + SlpSD$_{236}$	10	-7661.99	15344.00	0.01	0.50
	Early-summer	For$_{47}$ + Agri$_{925}$ + Shrub$_{1531}$ + DisSettl + Hill$_{666}$ + DisRoad1 + DisRoad2 + SlpM$_{281}$ + SlpSD$_{1531}$	11	-9157.24	18336.50	0.00	0.98
	Late-summer	For$_{47}$ + Agri$_{236}$ + Shrub$_{47}$ + DisSettl + Hill$_{1531}$ + DisRoad1 + DisRoad2 + SlpM$_{116}$ + SlpSD$_{1531}$	11	-10944.93	21911.90	0.00	0.76
	Autumn	For$_{47}$ + Agri$_{96}$ + Shrub$_{47}$ + DisSettl + Hill$_{925}$ + DisRoad1 + DisRoad2 + SlpM$_{236}$ + SlpSD$_{1531}$	11	-8692.28	17406.60	0.00	0.75

[a]: for variables names see Table 1.

Table 3. Coefficients of multi-grain resource selection functions to investigate habitat selection by adult female bears when establishing their annual home ranges (second-order selection) in the Abruzzo, Lazio, and Molise National Park, central Italy (2006–2010).

Variable [a]	Grain (m) [b]	β	SE	95% CI	
				Lower	Upper
(Intercept)	-	-2.31	0.25	-2.79	-1.83
Agri	1531	-1.37	0.04	-1.46	-1.29
Shrub	1531	-0.07	0.01	-0.09	-0.05
For	1531	0.14	0.01	0.11	0.17
Hill	1531	-0.06	0.01	-0.08	-0.04
DisRoad2	-	-0.15	0.01	-0.18	-0.13
SlpM	666	0.00	0.01	-0.01	0.02
SlpSD	47	-0.05	0.02	-0.08	-0.02
DisSettl	-	0.30	0.01	0.28	0.33

[a]: for variables names see Table 1. All variable relative importance equals 1, excepted for SlpM = 0.38.

[b]: most parsimonious grain size based on single variable grain analysis.

Table 4. Coefficients of seasonal multi-grain resource selection functions to investigate within-home range habitat selection (third-order) by adult female bears in the Abruzzo Lazio and Molise National Park, central Italy (2006–2010).

	Spring					Early-summer					Late-summer					Autumn				
Variable [a]	Grain (m) [b]	β	SE	95% CI		Grain (m) [b]	β	SE	95% CI		Grain (m) [b]	β	SE	95% CI		Grain (m) [b]	β	SE	95% CI	
				Lower	Upper				Lower	Upper				Lower	Upper				Lower	Upper
(Intercept)	-	-3.42	0.22	-3.86	-2.99	-	-3.30	0.17	-3.66	-2.94	-	-3.30	0.16	-3.47	-2.69	-	-3.29	0.15	-4.13	-3.01
Agri	198	0.29	0.03	0.23	0.35	925	0.36	0.03	0.31	0.42	236	0.05	0.02	0.00	0.10	96	0.26	0.02	0.22	0.29
Shrub	140	-0.16	0.04	-0.23	-0.08	1531	0.22	0.03	0.17	0.28	47	0.10	0.02	0.06	0.14	47	0.09	0.03	0.03	0.15
For	47	0.44	0.04	0.37	0.51	47	0.37	0.03	0.32	0.43	47	0.15	0.02	0.10	0.19	47	0.34	0.03	0.28	0.41
Hill	140	-0.13	0.02	-0.18	-0.09	666	-0.15	0.02	-0.19	-0.10	1531	-0.10	0.03	-0.15	-0.04	925	-0.08	0.03	-0.14	-0.03
DisRoad1	-	-0.39	0.04	-0.47	-0.30	-	0.19	0.05	0.10	0.28	-	0.31	0.04	0.23	0.38	-	-0.11	0.05	-0.20	-0.01
DisRoad2	-	0.22	0.03	0.16	0.28	-	0.08	0.03	0.03	0.13	-	0.24	0.02	0.20	0.28	-	0.18	0.03	0.13	0.23
SlpM	116	0.49	0.03	0.43	0.55	281	0.29	0.03	0.24	0.34	116	0.12	0.02	0.08	0.17	236	0.09	0.03	0.04	0.15
SlpSD	236	0.25	0.03	0.19	0.30	1531	0.22	0.03	0.17	0.28	1531	0.16	0.03	0.11	0.21	1531	0.18	0.03	0.12	0.23
DisSettl	-	-0.03	0.04	-0.14	0.02	-	-0.25	0.04	-0.33	-0.16	-	-0.21	0.04	-0.29	-0.14	-	-0.24	0.04	-0.33	-0.16

[a]: for variables names see Table 1. All variable relative importance equals 1, excepted for DisSettl=0.5.

[b]: most parsimonious grain size based on single variable grain analysis.

Table 5. Circadian effects in seasonal third-order habitat selection by adult female Apennine bears (Abruzzo Lazio and Molise National Park, central Italy, 2006–2010) through Latent Selection Differences models (see Methods). For each season and variable, coefficients represent the differences in habitat selection between daylight (reference value) and night.

Variable [a]	Spring				Early summer				Late summer				Autumn			
	β	SE	95% CI		β	SE	95% CI		β	SE	95% CI		β	SE	95% CI	
			Lower	Upper			Lower	Upper			Lower	Upper			Lower	Upper
(Intercept)	-0.14	0.09	-0.31	0.03	-0.49	0.08	-0.65	-0.33	0.30	0.11	0.08	0.51	0.53	0.22	0.10	0.95
Agri	0.23	0.08	0.07	0.39	0.00	0.02	-0.05	0.04	-0.02	0.05	-0.12	0.09	0.18	0.08	0.03	0.03
Shrub	0.00	0.00	-0.04	0.04	-0.22	0.07	-0.37	-0.08	-0.15	0.05	-0.24	-0.06	-0.02	0.05	-0.11	0.08
For	-0.25	0.09	-0.38	-0.11	-0.45	0.06	-0.57	-0.33	-1.12	0.06	-1.24	-1.01	-0.80	0.08	-0.96	-0.64
Hill	-0.03	0.04	-0.11	0.05	0.00	0.03	-0.05	0.05	0.00	0.03	-0.05	0.05	0.00	0.03	-0.05	0.05
DisRoad1	-0.05	0.08	-0.20	0.10	0.01	0.03	-0.05	0.06	-0.06	0.08	-0.21	0.09	0.00	0.03	-0.06	0.05
DisRoad2	-0.14	0.06	-0.25	-0.02	-0.26	0.06	-0.37	-0.14	-0.23	0.05	-0.33	-0.12	-0.25	0.07	-0.39	-0.12
SlpM	-0.12	0.06	-0.23	-0.01	-0.43	0.05	-0.53	-0.32	-0.51	0.05	-0.62	-0.41	-0.65	0.06	-0.77	-0.53
SlpSD	0.01	0.05	-0.04	0.05	0.18	0.05	0.08	0.29	0.15	0.06	0.03	0.27	0.38	0.07	0.24	0.53
DisSettl	-0.17	0.09	-0.35	0.00	0.00	0.02	-0.04	0.04	-0.02	0.05	-0.13	0.08	-0.01	0.04	-0.09	0.06

[a]: for variables names see Table 1.

Figure 1. The study area (grey area) used to assess multi-scale habitat selection by adult females Apennine brown bears (Abruzzo Lazio and Molise National Park, central Apennines, 2006–2010). The study area is comprised within a 10-km buffer beyond the composite Minimum Convex Polygon (100% MCP), calculated using all GPS locations of all-female bears included in the analysis (dots).

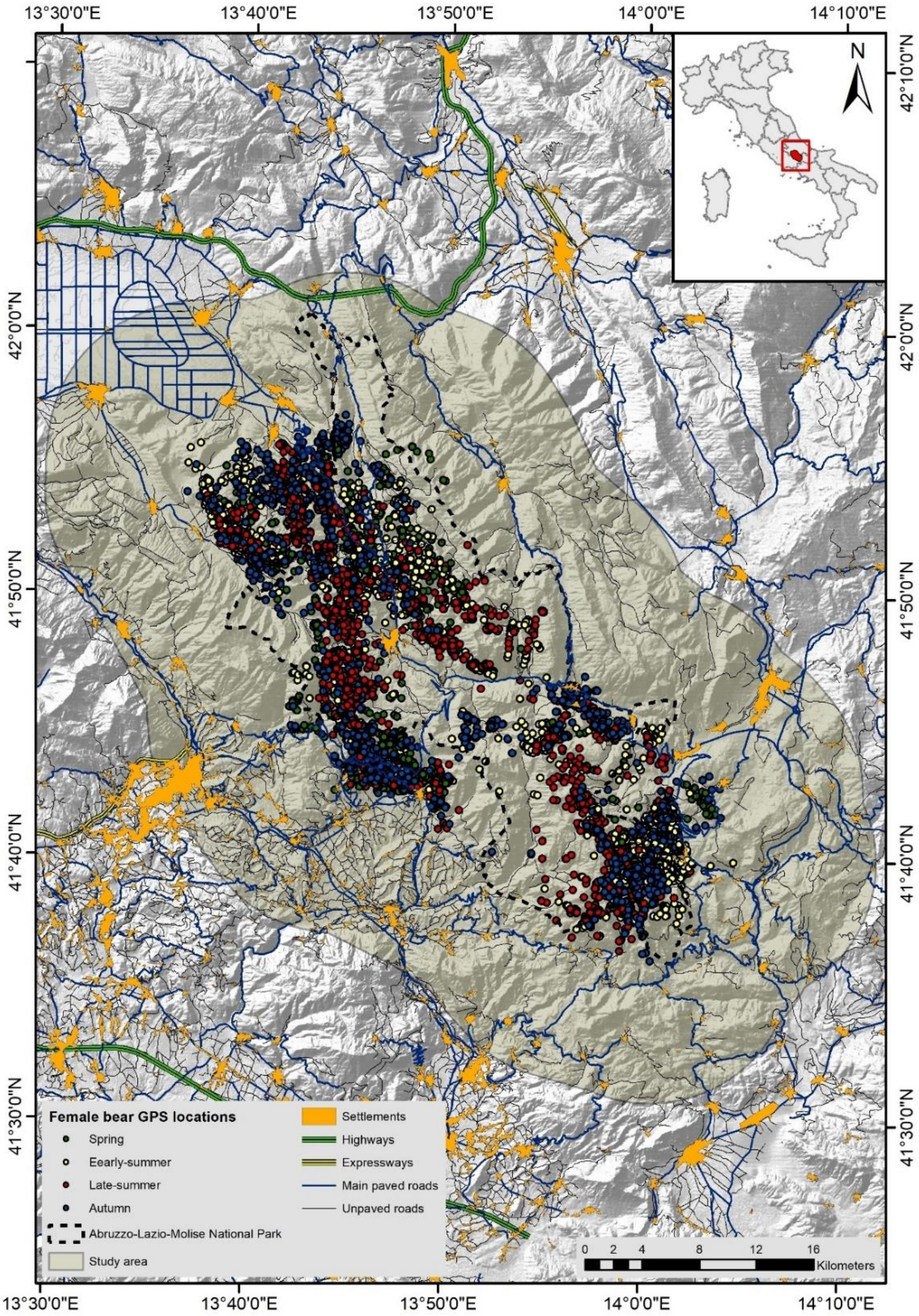

Figure 2. Functional response at the third-order selection towards paved roads by 9 adult female Apennine brown bears (Abruzzo, Lazio, and Molise National Park, central Italy, 2006-2010) in spring (A) and late summer (B). Gray areas represent predicted 95% confidence intervals.

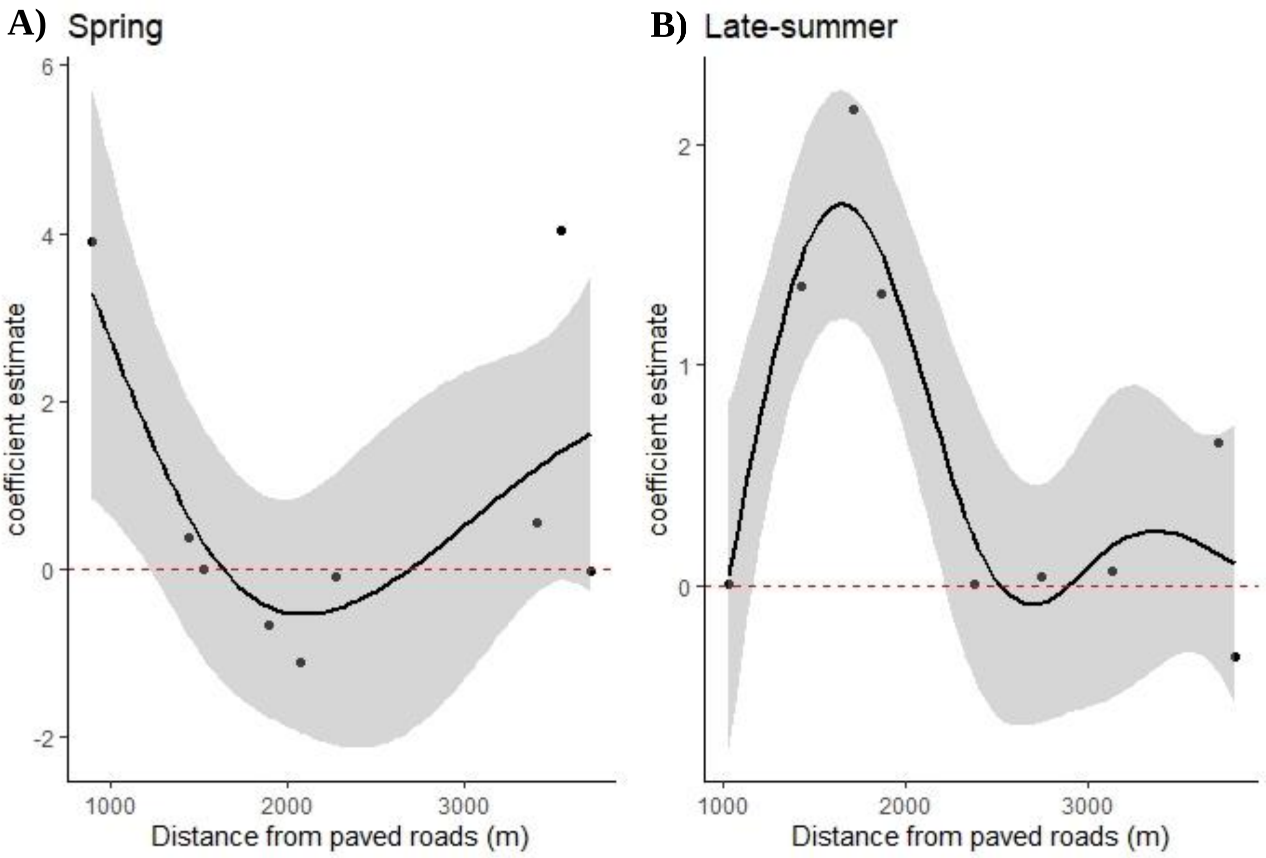

Figure 3. Functional response at the third-order selection towards unpaved roads by 9 adult female Apennine brown bears (Abruzzo, Lazio, and Molise National Park, central Italy, 2006-2010) in spring (A) and late summer (B). Gray areas represent predicted 95% confidence intervals.

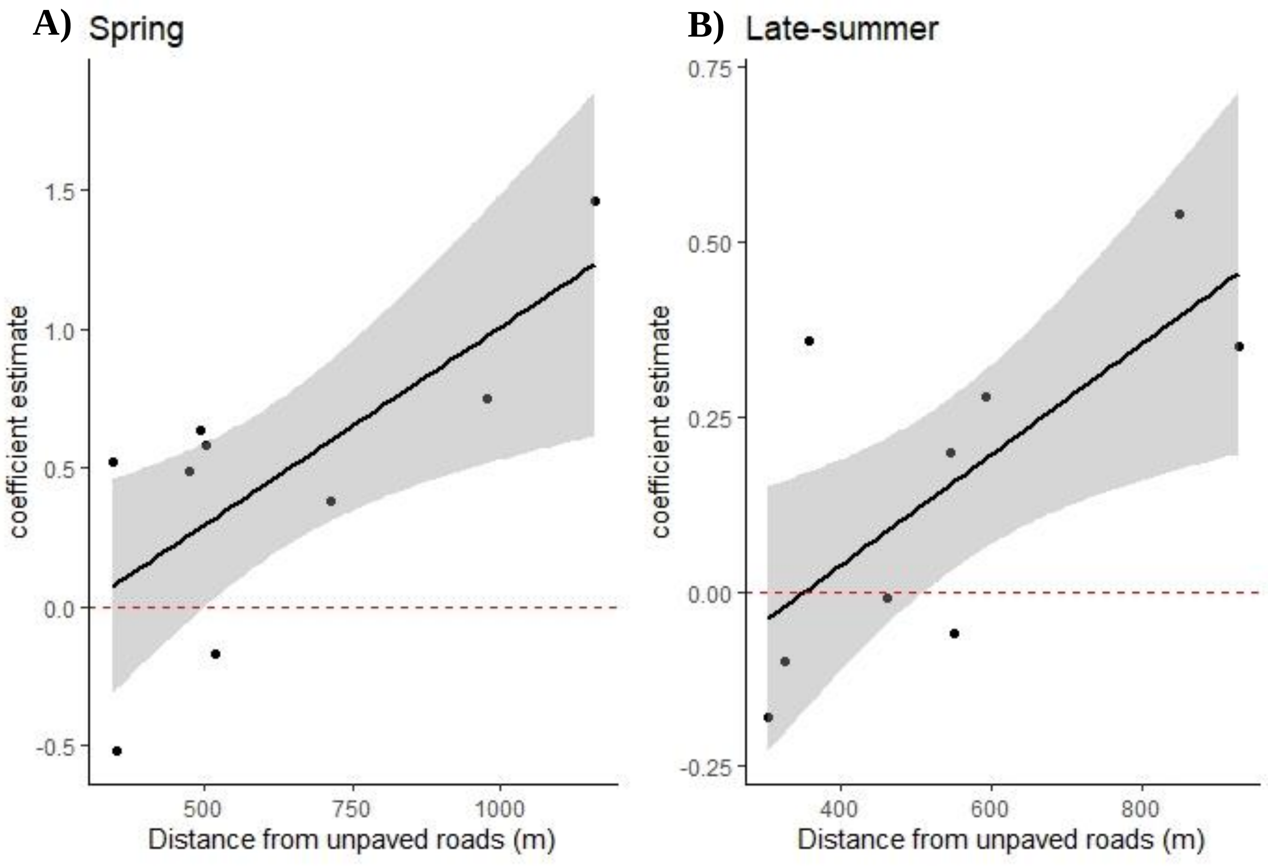

Figure 4. Functional response at the third-order selection towards settlements by 9 adult female Apennine brown bears (Abruzzo, Lazio, and Molise National Park, central Italy, 2006-2010) in autumn. Gray areas represent predicted 95% confidence intervals.

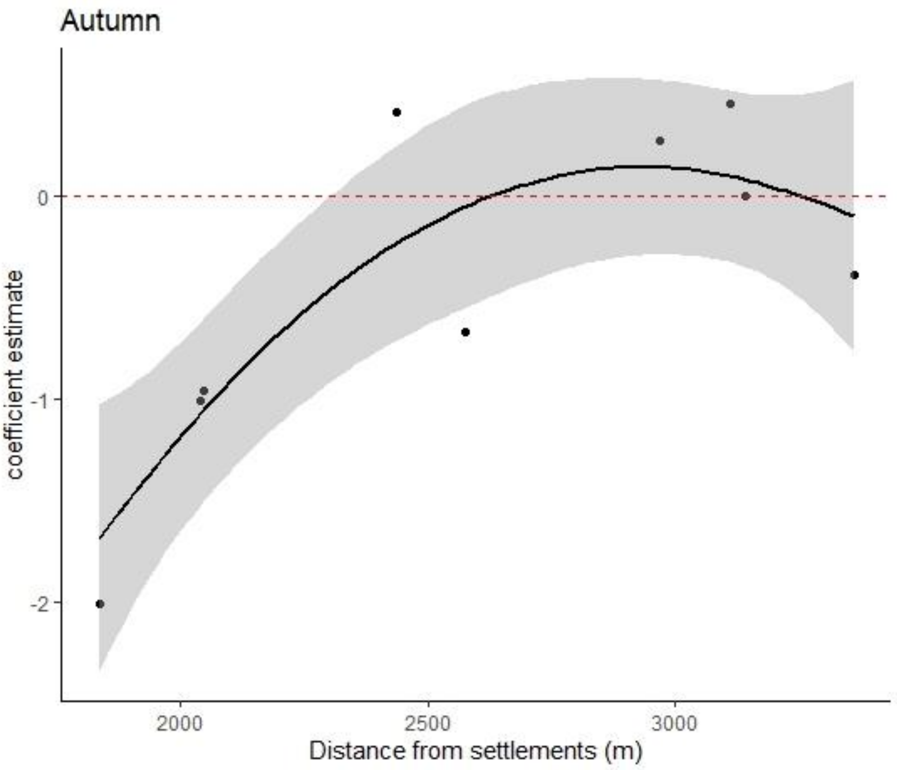

SUPPLEMENTARY MATERIAL

Table S1. Tracking period, acquisition rate and total locations recorded from 11 GPS-collared adult female Apennine bears during the active period (March-November 23; Abruzzo Lazio and Molise National Park, central Italy, 2005–2010). For each bear, I reported tracking time, number of GPS-locations for each year sampled, fix rate acquisition (%; percentage of fixes acquired respect to the expected), and season(s) in which GPS-locations are included in the final models. SP: spring; ES: early-summer; LS: late-summer; AU: autumn.

ID-bear	Tracking time	Seasons	GPS-locations	Fix rate (%)
F01	19 May – 19 Nov 2006	SP-ES-LS-AU	965	78.86
F02	28 Oct – 4 Dec 2005	-	208	82.25
	22 Mar – 9 Nov 2006	SP-ES-LS-AU	1234	78.43
F03	11 Jul – 24 Nov 2006	ES-LS-AU	700	90.91
	31 Mar – 6 May 2007	SP	124	79.23
F04	25 Jul – 11 Sep 2006	ES-LS	178	73.92
F05	5 Sep – 2 Nov 2006	LS-AU	214	76.92
	1 Apr – 19 Jul 2007	SP-ES	404	78.28
F06	8 – 28 Nov 2006	AU	91	78.26
	16 Mar – 26 May 2007	SP	318	73.09
F07	21 May – 10 Dec 2007	-	713	74.41
	26 May – 12 Nov 2008	SP-ES-LS-AU	982	95.99
	7 – 10 Mar 2009	-	19	95.00
F08	20 Oct – 9 Dec 2008	-	278	88.20
	17 Mar – 11 Dec 2009	SP-ES-LS-AU	1321	91.92
	4 Apr – 24 May 2010	-	281	94.61
F09	2 Sep – 21 Oct 2009	LS-AU	293	98.17
F10	25 Oct – 22 Nov 2008	-	167	98.58
	11 Apr – 11 Nov 2009	-	532	91.20
	4 Apr – 12 Nov 2010	SP-ES-LS-AU	1287	96.81
F13	14 Oct – 11 Nov 2009	-	161	97.42
	4 Apr – 17 Nov 2010	SP-ES-LS-AU	1269	94.34

Table S2. Performance of the 98 stationary GPS-collars evaluated in the Abruzzo Lazio and Molise National Park according to a stratified sampling in bear habitat (Molinari 2007). Values of HDOP below the horizontal dashed line have been used to filter out 2-D GPS fixes (i.e., acquired with 3 satellites) from the analysis, corresponding to the first HDOP class with discontinuity in median, mean, and 75%ile value of the location error distribution; at the contrary, I included all 3-D GPS fixes (i.e., acquired with >3 satellites) in the analysis (Lewis et al. 2007).

HDOP	**Location error (m)**		
(min – max)	**median**	**mean**	**75%ile**
$0 \leq x \leq 2$	10	18.41	20
$2 < x < 3$	14	24.79	27
$3 \leq x < 4$	17	28.13	31
$4 \leq x < 5$	20.5	36.27	45
$5 \leq x < 6$	20	28.54	38
$6 \leq x < 7$	23	41.54	48
$7 \leq x < 8$	37.5	40.53	49.25
$8 \leq x < 9$	50	62.79	96
$9 \leq x < 10$	37	100.3	54
$10 \leq x < 11$	29	44.18	42.5
$11 \leq x \leq 13$	46.5	60	79.5
$13 \leq x < 15$	30	62.8	94

Table S3. Pair-wise correlation (Pearson's *r*) between variables at the second-order of selection calculated for each variable and reported as mean (white) and standard deviation (grey box) calculated at each grain size (i.e., from 47m to 1531m). Agri = cultivated land cover; DisRoad1 = distance to paved roads; DisRoad2 = distance to unpaved roads; DisSettl = distance to human settlements; For = forest cover; Hill = hillshade; Shrub = shrubland cover; SlpM = average slope; SlpSD = slope standard deviation.

	Agri	Open	Shrub	For	DEM	SlpSD	SlpM	Hill	DisSettl	DisRoad1	DisRoad2
Agri	-	-0.25	-0.12	-0.51	-0.57	-0.47	-0.63	0.17	-0.39	-0.39	-0.05
Open	0.04	-	-0.03	-0.55	0.45	0.08	0.02	-0.03	0.29	0.27	0.18
Shrub	0.02	0.04	-	-0.20	0.12	0.04	0.10	-0.06	0.03	0.05	0.08
For	0.04	0.03	0.04	-	0.10	0.29	0.44	-0.09	0.14	0.13	-0.10
DEM	0.05	0.06	0.03	0.03	-	0.23	0.44	-0.11	**0.76**	0.66	0.27
SlpSD	0.05	0.03	0.02	0.01	0.03	-	0.55	-0.16	0.17	0.20	0.00
SlpM	0.07	0.06	0.05	0.03	0.05	0.02	-	-0.33	0.29	0.35	0.16
Hill	0.06	0.02	0.02	0.05	0.03	0.04	0.07	-	-0.04	-0.07	-0.10
DisSettl	0.03	0.05	0.01	0.02	0.00	0.04	0.04	0.02	-	**0.74**	0.25
DisRoad1	0.03	0.04	0.01	0.02	0.00	0.03	0.05	0.02	0.00	-	0.23
DisRoad2	0.01	0.03	0.02	0.02	0.01	0.05	0.01	0.02	0.00	0.00	-

Table S4. Variance Inflation Factors (VIF) at the second-order of selection calculated for each variable and reported as mean and standard deviation (in parentheses) calculated at each grain size (i.e., from 47m to 1531m). I excluded from the analysis open fields, altitude, and distance from paved roads (VIF>3).

Variables[a]	**VIF**	
	1st round	**2nd round**
For	7.96 (±2.35)	1.63 (±0.10)
Open	6.20 (±1.75)	-
DEM	3.82 (±0.50)	-
Agri	6.39 (±2.94)	2.29 (±0.45)
DisSettl	3.37 (±0.12)	1.28 (±0.06)
DisRoad1	3.17 (±0.03)	-
Shrub	1.79 (±0.05)	1.15 (±0.01)
SlpSD	1.56 (±0.06)	1.53 (±0.05)
SlpM	2.48 (±0.43)	2.33 (±0.39)
Hill	1.16 (±0.10)	1.16 (±0.09)
DisRoad2	2.42 (±0.02)	1.15 (±0.03)

[a]: for variables names see Table S3.

Table S5. Pair-wise correlation (Pearson's *r*) between variables at the third-order of selection during spring (March–May) calculated for each variable and reported as mean (white) and standard deviation (grey box) calculated at each grain size (i.e., from 47m to 1531m). I excluded from the analysis open fields, as this variable was correlated with forest cover (*r* = -0.81). For variables names see Table S3.

	Agri	Open	Shrub	For	DEM	SlpSD	SlpM	Hill	DisSettl	DisRoad1	DisRoad2
Agri	-	-0.10	-0.05	-0.26	-0.48	-0.25	-0.30	0.03	-0.32	-0.24	-0.16
Open	0.04	-	-0.09	**-0.81**	0.45	0.13	-0.06	-0.02	0.30	0.36	0.38
Shrub	0.01	0.04	-	-0.22	0.07	-0.06	0.00	0.00	-0.06	-0.05	0.06
For	0.06	0.02	0.02	-	-0.17	0.00	0.13	0.04	-0.03	-0.13	-0.30
DEM	0.08	0.02	0.05	0.03	-	0.24	0.29	-0.02	**0.71**[a]	0.66	0.46
SlpSD	0.06	0.01	0.03	0.01	0.09	-	0.38	-0.10	0.21	0.27	0.17
SlpM	0.03	0.08	0.01	0.06	0.02	0.09	-	-0.30	0.11	0.16	0.34
Hill	0.05	0.04	0.09	0.02	0.04	0.08	0.07	-	0.05	0.01	-0.19
DisSettl	0.05	0.02	0.00	0.03	0.02	0.06	0.01	0.03	-	**0.70**[a]	0.21
DisRoad1	0.04	0.01	0.01	0.03	0.01	0.04	0.02	0.01	0.00	-	0.32
DisRoad2	0.01	0.05	0.03	0.03	0.02	0.03	0.04	0.04	0.00	0.00	-

[a]: I decided to maintain both distance to settlements and distance to paved roads to check their multivariate correlation (see VIF analysis below), despite pair-wise correlation is higher than threshold value (i.e., *r* = 0.7).

Table S6. Pair-wise correlation (Pearson's *r*) between variables at the third-order of selection during early-summer (June–July) calculated for each variable and reported as mean (white) and standard deviation (grey box) calculated at each grain size (i.e., from 47m to 1531m). I excluded from the analysis open fields, as this variable was correlated with forest cover (*r* = -0.81). For variables names see Table S3.

	Agri	Open	Shrub	For	DEM	SlpSD	SlpM	Hill	DisSettl	DisRoad1	DisRoad2
Agri	-	-0.04	-0.02	-0.26	-0.36	-0.12	-0.25	0.02	-0.30	-0.24	-0.15
Open	0.02	-	-0.03	**-0.81**	0.40	0.08	-0.04	-0.01	0.20	0.25	0.38
Shrub	0.01	0.02	-	-0.27	0.17	-0.11	-0.02	0.00	0.02	0.00	0.10
For	0.03	0.02	0.03	-	-0.23	0.00	0.09	0.02	0.00	-0.07	-0.31
DEM	0.08	0.05	0.03	0.02	-	0.13	0.29	0.01	**0.71**[a]	0.63	0.43
SlpSD	0.10	0.04	0.05	0.03	0.13	-	0.35	-0.14	0.09	0.14	0.15
SlpM	0.03	0.06	0.01	0.05	0.02	0.09	-	-0.35	0.16	0.17	0.35
Hill	0.02	0.03	0.05	0.02	0.02	0.07	0.07	-	0.03	-0.01	-0.17
DisSettl	0.07	0.04	0.00	0.00	0.01	0.09	0.03	0.01	-	**0.70**[a]	0.21
DisRoad1	0.06	0.05	0.01	0.01	0.01	0.06	0.03	0.00	0.00	-	0.29
DisRoad2	0.02	0.06	0.02	0.05	0.02	0.02	0.05	0.04	0.00	0.00	-

[a]: I decided to maintain both distance to settlements and distance to paved roads to check their multivariate correlation (see VIF analysis below), despite pair-wise correlation is higher than threshold value (i.e., *r* = 0.7).

Table S7. Pair-wise correlation (Pearson's *r*) between variables at the third-order of selection during late-summer (July–September) calculated for each variable and reported as mean (white) and standard deviation (grey box) calculated at each grain size (i.e., from 47m to 1531m). I excluded from the analysis open fields, as this variable was correlated with forest cover (*r* = -0.81), and altitude as it was correlated with distance to settlements (*r* = 0.71). For variables names see Table S3.

	Agri	Open	Shrub	For	DEM	SlpSD	SlpM	Hill	DisSettl	DisRoad1	DisRoad2
Agri	-	-0.10	-0.05	-0.26	-0.48	-0.25	-0.30	0.03	-0.32	-0.24	-0.16
Open	0.02	-	-0.09	**-0.81**	0.45	0.13	-0.06	-0.02	0.30	0.36	0.38
Shrub	0.01	0.02	-	-0.22	0.07	-0.06	0.00	0.00	-0.06	-0.05	0.06
For	0.03	0.01	0.06	-	-0.17	0.00	0.13	0.04	-0.03	-0.13	-0.30
DEM	0.06	0.06	0.01	0.01	-	0.24	0.29	-0.02	**0.71**[a]	0.66	0.46
SlpSD	0.07	0.05	0.03	0.04	0.08	-	0.38	-0.10	0.21	0.27	0.17
SlpM	0.03	0.05	0.02	0.04	0.03	0.06	-	-0.30	0.11	0.16	0.34
Hill	0.02	0.03	0.06	0.02	0.00	0.04	0.06	-	0.05	0.01	-0.19
DisSettl	0.04	0.05	0.02	0.01	0.02	0.06	0.03	0.01	-	**0.70**[a]	0.21
DisRoad1	0.03	0.06	0.02	0.03	0.01	0.04	0.04	0.01	0.00	-	0.32
DisRoad2	0.01	0.05	0.01	0.04	0.02	0.02	0.04	0.05	0.00	0.00	-

[a]: I decided to maintain both distance to settlements and distance to paved roads to check their multivariate correlation (see VIF analysis below), despite pair-wise correlation is higher than threshold value (i.e., *r* = 0.7).

Table S8. Pair-wise correlation (Pearson's *r*) between variables at the third-order of selection during autumn (October-November 23) calculated for each variable and reported as mean (white) and standard deviation (grey box) calculated at each grain size (i.e., from 47m to 1531m). I excluded from the analysis open fields, correlated with forest cover (*r* = -0.80). For variables names see Table S3.

	Agri	Open	Shrub	For	DEM	SlpSD	SlpM	Hill	DisSettl	DisRoad1	DisRoad2
Agri	-	-0.09	-0.03	-0.30	-0.46	-0.20	-0.25	0.02	-0.32	-0.24	-0.15
Open	0.02	-	-0.07	**-0.80**	0.46	0.15	0.00	-0.07	0.22	0.25	0.48
Shrub	0.00	0.03	-	-0.21	-0.10	-0.03	-0.12	0.07	-0.14	-0.17	-0.09
For	0.03	0.01	0.05	-	-0.12	-0.02	0.09	0.07	0.06	0.02	-0.34
DEM	0.06	0.06	0.04	0.01	-	0.23	0.26	-0.06	**0.71**[a]	0.60	0.49
SlpSD	0.10	0.06	0.03	0.08	0.07	-	0.34	-0.10	0.17	0.20	0.20
SlpM	0.02	0.08	0.04	0.06	0.03	0.06	-	-0.31	0.14	0.17	0.28
Hill	0.03	0.06	0.09	0.05	0.01	0.06	0.08	-	0.00	-0.03	-0.22
DisSettl	0.04	0.04	0.06	0.01	0.02	0.06	0.03	0.00	-	**0.70**[a]	0.25
DisRoad1	0.03	0.04	0.07	0.01	0.01	0.03	0.04	0.01	0.00	-	0.31
DisRoad2	0.01	0.07	0.03	0.06	0.01	0.03	0.03	0.06	0.00	0.00	-

[a]: I decided to maintain both distance to settlements and paved roads and check multivariate correlation (see VIF analysis below), despite pairwise correlation reach threshold value (i.e., r = 0.7).

Table S9. Variance Inflation Factor (VIF) at the third-order of selection reported on a seasonal basis. For each variable, VIF values are reported as mean and standard deviation calculated at each grain size (i.e., from 47m to 1531m). For variables names see Table S3.

Variables	**VIF**							
	Spring		**Early-summer**		**Late-summer**		**Autumn**	
	1st round	**2nd round**	**1st round**	**2nd round**	**1st round**	**2nd round**	**1st round**	**2nd round**
For	10.00 (±1.81)	1.54 (±0.13)	7.21 (±1.75)	1.41 (±0.07)	8.77 (±2.07)	1.40 (±0.08)	8.52 (±2.45)	1.50 (±0.13)
Open	7.23 (±0.92)	-	6.91 (±2.01)	-	9.35 (±3.04)	-	8.55 (±2.86)	-
DEM	2.96 (±0.63)	-	3.05 (±0.51)	-	3.8 (±0.93)	-	3.17 (±0.56)	-
DisSettl	2.75 (±0.14)	2.18 (±0.06)	3.39 (±0.14)	2.70 (±0.08)	3.29 (±0.12)	2.68 (±0.06)	3.54 (±0.13)	2.88 (±0.05)
DisRoad1	2.20 (±0.04)	2.13 (±0.03)	2.76 (±0.03)	2.72 (±0.02)	2.92 (±0.15)	2.77 (±0.07)	2.95 (±0.09)	2.90 (±0.06)
DisRoad2	1.40 (±0.06)	1.33 (±0.08)	1.53 (±0.11)	1.45 (±0.12)	1.58 (±0.08)	1.44 (±0.10)	1.66 (±0.12)	1.52 (±0.15)
Agri	2.16 (±0.53)	1.34 (±0.15)	1.82 (±0.41)	1.30 (±0.12)	2.41 (±0.73)	1.39 (±0.12)	2.47 (±0.87)	1.40 (±0.14)
Shrub	3.38 (±0.37)	1.35 (±0.07)	1.78 (±0.07)	1.12 (±0.00)	1.90 (±0.06)	1.10 (±0.02)	1.63 (±0.08)	1.16 (±0.08)
Hill	1.24 (±0.23)	1.21 (±0.23)	1.21 (±0.16)	1.19 (±0.14)	1.15 (±0.11)	1.15 (±0.11)	1.19 (±0.18)	1.18 (±0.18)
SlpM	1.63 (±0.10)	1.51 (±0.08)	1.69 (±0.15)	1.54 (±0.07)	1.66 (±0.13)	1.52 (±0.06)	1.49 (±0.10)	1.40 (±0.07)
SlpSD	1.14 (±0.05)	1.21 (±0.05)	1.22 (±0.05)	1.21 (±0.06)	1.32 (±0.02)	1.29 (±0.05)	1.22 (±0.03)	1.21 (±0.04)

Table S10. Variance inflation factor (VIF) at the second and the third orders of selection recalculated after grain size for each variable has been determined through multigrain analysis. For variables names see Table S3.

Variables	Second-order		Third-order							
	Annual		Spring		Early-summer		Late-summer		Autumn	
	Grain (m)	VIF	Grain (m)	VIF	Grain (m)	VIF	Grain (m)	VIF	Grain (m)	VIF
For	1531	1.81	47	1.32	47	1.20	47	1.33	47	1.32
Shrub	1531	1.15	140	1.12	1531	1.09	47	1.13	47	1.13
Agri	1531	2.79	198	1.28	925	1.31	236	1.27	96	1.24
Hill	1531	1.23	140	1.10	666	1.24	1531	1.31	925	1.21
SlpM	47	1.54	116	1.37	281	1.35	116	1.30	236	1.35
SlpSD	666	1.47	236	1.19	1531	1.12	1531	1.15	1531	1.10
DisSettl	-	1.41	-	2.60	-	2.73	-	2.67	-	2.65
DisRoad1	-	-	-	2.62	-	2.66	-	2.66	-	2.66
DisRoad2	-	1.19	-	1.31	-	1.38	-	1.38	-	1.37

Table S11. Coefficients of individual resource selection functions at the third order of selection by Apennine adult female bears during spring (March-May; Abruzzo Lazio and Molise National Park, central Italy, 2005–2010). Significance level: * p<0.05; ** p<0.01; *** p<0.001. For variables names see Table S3.

Bear ID	**Spring**																	
	Agri		**For**		**Shrub**		**Hill**		**DisRoad1**		**DisRoad2**		**DisSettl**		**SlpM**		**SlpSD**	
	β	**p-value**	**β**	**p-value**	**β**	**p-value**	**β**	**p-value**	**β**	**p-value**	**β**	**p-value**	**β**	**p-value**	**β**	**p-value**	**β**	**p-value**
F02[a]	-	-	2.05	***	-0.15		-0.41	***	-0.65	***	0.58	***	-	-	-	-	0.20	***
	-	-	-	-	-	-	-	-	-	-	-	-	-	-	-	-	-0.20	*
F03[a]	-	-	1.26	***	-	-	0.02		-0.02		0.38	**	-	-	3.44	***	-0.50	**
	-	-	-	-	-	-	-	-	-	-	-	-	-	-	-	-	0.92	**
F05	0.58	**	1.25	***	-0.02		0.01		-1.11	***	0.64	***	0.34	**	0.59	***	0.67	***
F06[a]	-1.29	***	1.53	***	-	-	-0.23	***	3.90	***	0.75	***	-2.53	***	-		1.55	***
	-0.18		-	-	-	-	-	-	-	-	-	-	-	-	-	-	-	-
F08[a]	-0.49	*	-0.42	***	-0.44	***	-0.65	***	-	-	-0.20	*	-0.05		0.71	***	0.67	***
	1.22	***	0.37	*	-	-	-	-	-	-	-	-	-	-	-	-	-	-
F10	-	-	2.97	***	-0.62	*	-0.03		-0.01		0.52	***	-	-	0.90	***	0.28	***
F13	-	-	0.25	**	0.83	***	-0.39	***	0.38	**	0.49	***	-0.43	***	0.06		0.20	**

[a]: Bear showing an opposite double-grain response to variable(s) (i.e., at small and large grain size, differently by bear ID), derived by the multi-grain analysis.

Table S12. Coefficients of individual resource selection functions at the third order of selection by Apennine adult female bears during early-summer (June-July; Abruzzo Lazio and Molise National Park, central Italy, 2005–2010). Significance level: * p<0.05; ** p<0.01; *** p<0.001. For variables names see Table S3.

Bear ID	**Early-summer**																	
	Agri		**For**		**Shrub**		**Hill**		**DisRoad1**		**DisRoad2**		**DisSettl**		**SlpM**		**SlpSD**	
	β	**p-value**	**β**	**p-value**	**β**	**p-value**	**β**	**p-value**	**β**	**p-value**	**β**	**p-value**	**β**	**p-value**	**β**	**p-value**	**β**	**p-value**
F01	-	-	0.93	***	-0.82	**	0.07		-0.17		0.59	***	-	-	0.54	***	0.06	
F02	-	-	0.51	*	-2.07	*	-0.92	***	-0.30	***	-0.18	*	-	-	-	-	-0.39	***
F03	-	-	0.02		0.97	*	-0.33	**	0.81	***	0.38	*	-	-	-1.13	***	-0.11	
F05	-	-	0.57	***	0.18	*	0.10		0.01		-0.05		-0.32	**	-0.36	*	-0.27	*
F07	1.38	***	0.47	***	0.33	***	-0.43	***	0.26	***	0.60	***	-	-	0.41	***	0.04	
F08	-	-	0.47	***	0.38	***	-0.22	***	0.34	*	-0.35	***	-0.42	***	0.18	*	-0.14	*
F10	-	-	2.54	***	0.00		-0.03		-1.33	***	0.25	*			0.71	***	0.89	***
F13	0.17	***	0.12		-0.49		-0.66	***	0.23		-0.36	***	-0.41	**	0.70	***	0.70	***

Table S13. Coefficients of individual resource selection functions at the third order of selection by Apennine adult female bears during late-summer (August-September; Abruzzo Lazio and Molise National Park, central Italy, 2005–2010). Significance level: * $p<0.05$; ** $p<0.01$; *** $p<0.001$. For variables names see Table S3.

Bear ID	**Late-summer**																	
	Agri		**For**		**Shrub**		**Hill**		**DisRoad1**		**DisRoad2**		**DisSettl**		**SlpM**		**SlpSD**	
	β	**p-value**	**β**	**p-value**	**β**	**p-value**	**β**	**p-value**	**β**	**p-value**	**β**	**p-value**	**β**	**p-value**	**β**	**p-value**	**β**	**p-value**
F01[a]	-	-	0.49	***	0.28	**	0.36	***	-0.33	**	0.35	***	-	-	0.94	***	0.33	***
	-	-	-0.81	***	-0.41	**	-0.44	***	-	-	-	-	-	-	-	-	-	-
F02	-	-	0.43	***	0.08		-0.45	***	0.65	***	0.54	***	-	-	0.49	***	0.44	***
F03	0.21	***	-0.07		0.50	***	-0.23	***	1.36	***	-0.06		-0.08		0.86	***	-0.29	***
F04	-	-	-0.52	***	-	-	0.73	***	1.32	***	-0.18		0.06		0.70	***	-0.01	
F07	1.89	***	0.02		1.17	***	-0.83	***	0.07		0.28	***	-	-	-0.26	***	0.42	***
F08	-2.14	***	0.36	***	0.31	***	0.01		0.01		0.20	*	-0.50	***	-0.84	***	0.64	***
F09	0.27		0.88	**	0.34	***	-	-	0.01		0.36		-0.34		-1.15	***	0.68	***
F10[a]	-	-	-0.86	***	-	***	0.43	***	0.04		-0.10		-	-	0.75	***	0.52	***
	-	-	-	-	-0.82	***	-	-	-	-	-	-	-	-	-	-	-	-
F13	-	-	-0.62	***	-	-	-0.89	***	2.16	***	-0.01		-1.06	***	0.32	***	0.44	***

[a]: Bear showing an opposite double-grain response to variable(s) (i.e., at small and large grain size, differently by bear ID), derived by the multi-grain analysis.

Table S14. Coefficients of individual resource selection functions at the third order of selection by Apennine adult female bears during autumn (October-November 23; Abruzzo Lazio and Molise National Park, central Italy, 2005–2010). Significance level: * p<0.05; ** p<0.01; *** p<0.001. For variables names see Table S3.

Bear ID	**Autumn**																	
	Agri		**For**		**Shrub**		**Hill**		**DisRoad1**		**DisRoad2**		**DisSettl**		**SlpM**		**SlpSD**	
	β	**p-value**	**β**	**p-value**	**β**	**p-value**	**β**	**p-value**	**β**	**p-value**	**β**	**p-value**	**β**	**p-value**	**β**	**p-value**	**β**	**p-value**
F01	-	-	1.21	***	0.50	**	-0.11		0.02		0.73	***	-	-	-	-	-0.27	***
F02	-	-	0.01		-0.68	*	-	-	-0.01		0.00		-	-	0.83	***	-0.80	***
F03	0.21	***	0.32	**	0.70	***	-0.25	*	-0.03		-0.33	**	-	-	-0.10		0.42	***
F05	2.50	***	2.11	***	0.40	***	-0.92	***	-1.01	***	0.04		-0.67	***	0.81	***	-0.04	
F07	0.15	***	-0.22	*	-1.96	***	0.86	***	-0.80	***	-0.47	**	-	-	-0.05		0.46	***
F08	-1.76	***	1.11	***	-1.25	***	0.56	***	0.57	*	1.02	***	-1.01	***	-0.90	***	0.49	***
F09[a]	1.08	***	0.90	***	0.35	**	-	-	-0.90	*	0.71	***	-	-	0.80	***	0.29	**
	-	-	-1.61	***	-	-	-	-	-	-	-	-	-	-	-	-	-0.60	***
F10[a]	-	-	1.04	***	0.49	***	0.01		1.12	***	-0.02		-	-	0.90	***	0.96	***
															-1.40	***		
F13	-	-	-1.07	***	0.17	**	-0.31	***	0.45	**	0.01		-	-	-0.31	***	0.28	*

[a]: Bear showing an opposite double-grain response to variable(s) (i.e., at small and large grain size, differently by bear ID), derived by the multi-grain analysis.

Figure S1. I selected recovered HDOP threshold value for 2-D fixes, based on their location errors (2nd screening option in Lewis et al. 2007). For this scope, from the stationary radio-collar tested data (n=2888), I selected only high rates locations (n=2318) and I subdivided their HDOP values into 10 bin classes (deciles). To find a trade-off between number of 2-D fixes selected and location error, I identified a changing break in the location error distribution (i.e. differences in mean, median, quantiles or IC95%), and, finally, I selected HDOP=8 as threshold values, where the mean and the standard deviation change from 23.30 (± 33.76) to 65.03 (± 90.59). A) scatterplot correlation HDOP and location error (m); B) boxplot relating dimension of GPS-locations (e.g., 2D vs 3D) and location error (m).

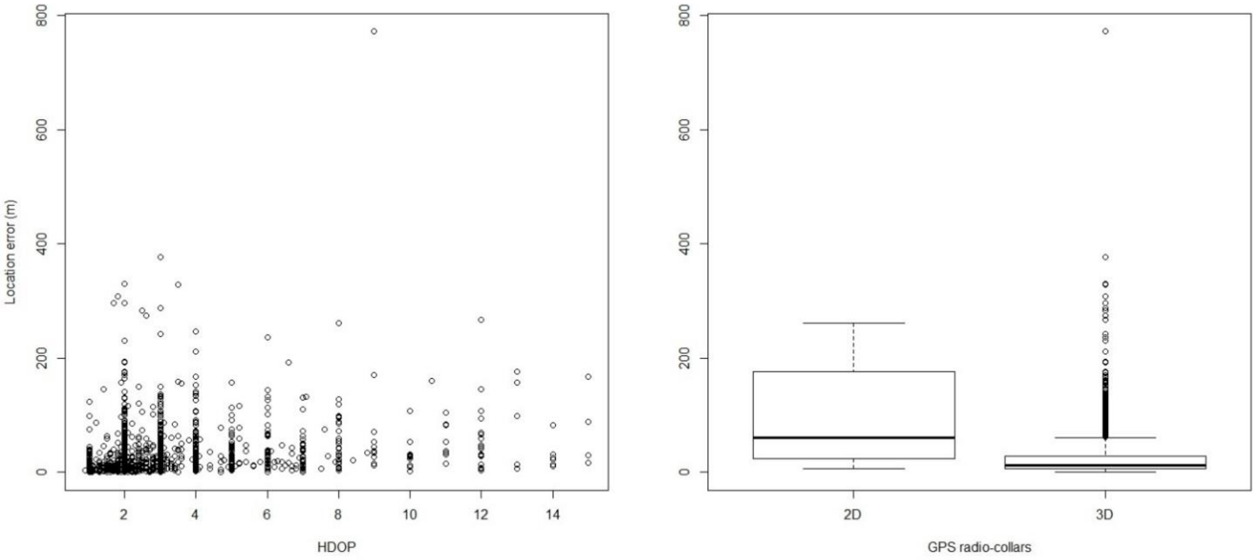

Figure S2. Effect of adding a given variable to the quasi-global resource selection model (*sensu* Laforge et al. 2015) to assess habitat selection at the second-order of selection by adult Apennine female bears ($n = 9$) in the Abruzzo-Lazio-Molise National Park (central Italy, 2005–2010). Effects are assessed at incremental grain sizes, from 47 to 1,531 m, and are measured both in terms of AIC score (ΔAIC_c, top row) and model averaged coefficients (β ± 95% confidence intervals, bottom row) across incremental grain sizes from 47–1,531 m. Following Laforge et al. (2015), I retained the grain size corresponding to the lowest ΔAIC_c for each variable: agriculture, forest, and shrublands.

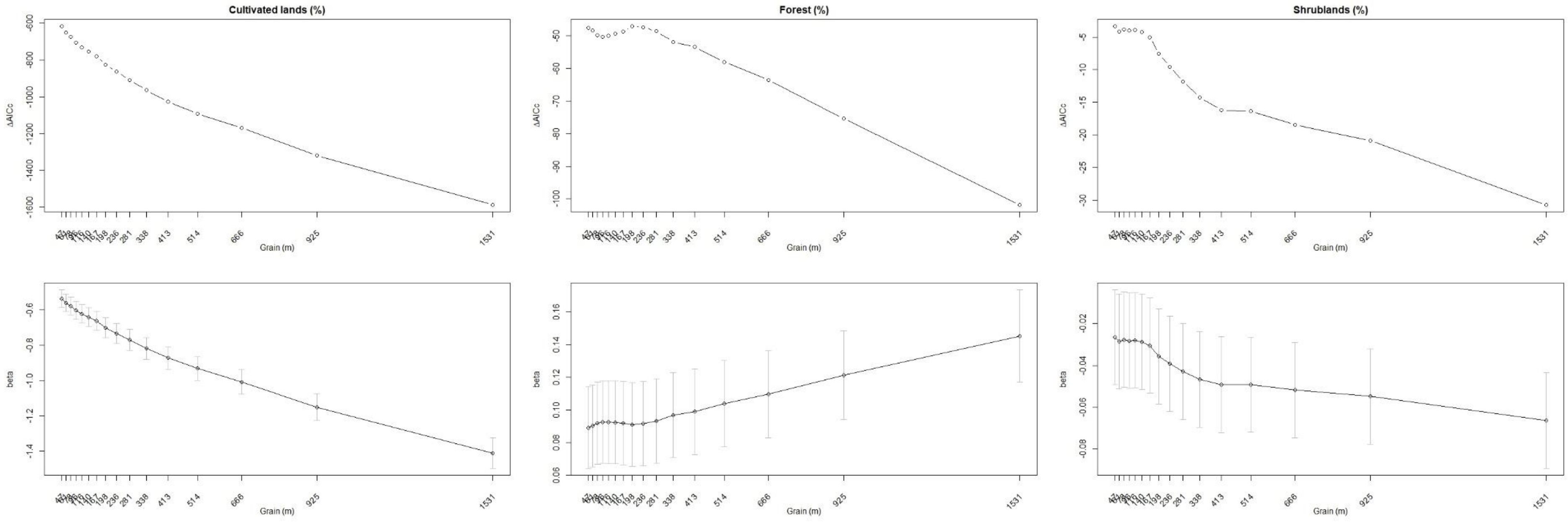

Figure S3. Effect of adding a given variable to the quasi-global resource selection model (*sensu* Laforge et al. 2015) to assess habitat selection at the second-order of selection by adult Apennine female bears ($n = 9$) in the Abruzzo-Lazio-Molise National Park (central Italy, 2005–2010). Effects are assessed at incremental grain sizes, from 47 to 1,531 m, and are measured both in terms of AIC score (ΔAIC_c, top row) and model averaged coefficients (β ± 95% confidence intervals, bottom row) across incremental grain sizes from 47–1,531 m. Following Laforge et al. (2015), I retained the grain size corresponding to the lowest ΔAIC_c for each variable: hillshade, mean slope, and standard deviation of slope.

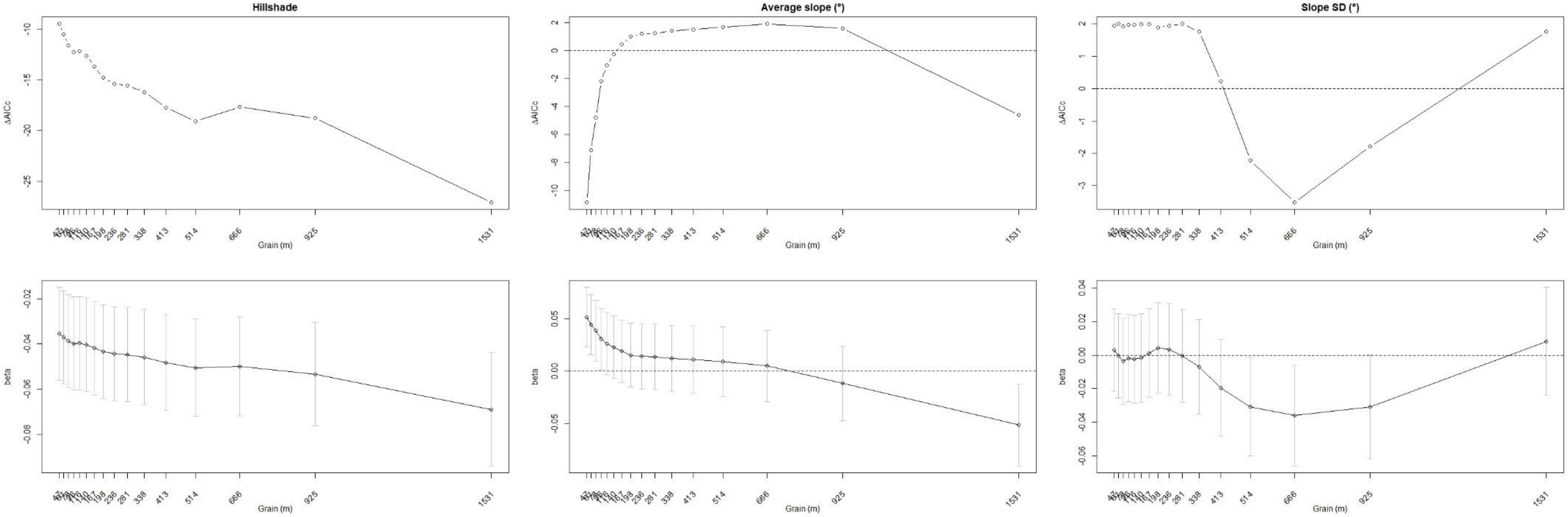

Figure S4. Effect of adding a given variable to the quasi-global resource selection model (*sensu* Laforge et al. 2015) to assess habitat selection at the third-order of selection by adult Apennine female bears (n = 11) during spring (March–May) in the Abruzzo-Lazio-Molise National Park (central Italy, 2005–2010). Effects assessed at incremental grain sizes, from 47 to 1,531 m, and are measured both in terms of AIC score (ΔAIC_c, top row) and model averaged coefficients (β ±95% confidence intervals; bottom row) across incremental grain sizes from 47 to 1,531 m. Following Laforge et al. (2015), I retained the grain size corresponding to the lowest ΔAIC_c for each variable: agriculture, forest, and shrublands.

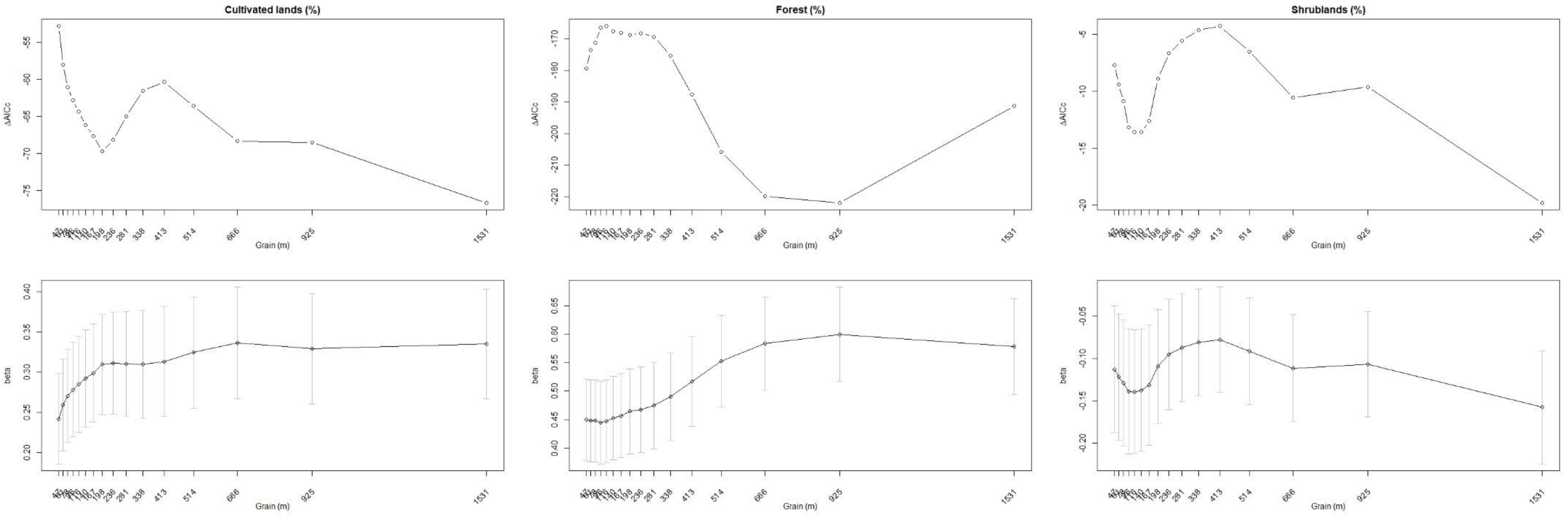

Figure S5. Effect of adding a given variable to the quasi-global resource selection model (*sensu* Laforge et al. 2015) to assess habitat selection at the third-order of selection by adult Apennine female bears (n = 11) during spring (March–May) in the Abruzzo-Lazio-Molise National Park (central Italy, 2005–2010). Effects assessed at incremental grain sizes, from 47 to 1,531 m, and are measured both in terms of AIC score (ΔAIC_c, top row) and model averaged coefficients (β ±95% confidence intervals; bottom row) across incremental grain sizes from 47 to 1,531 m. Following Laforge et al. (2015), I retained the grain size corresponding to the lowest ΔAIC_c for each variable: hillshade, mean slope, and standard deviation of slope.

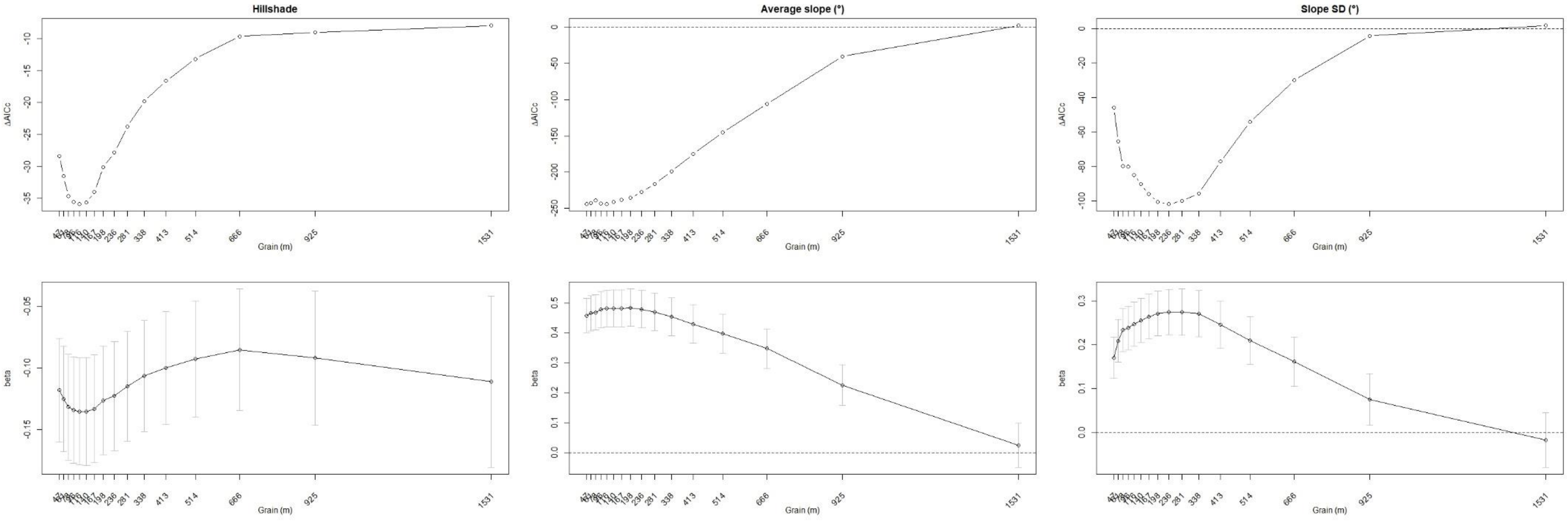

Figure S6. Effect of adding a given variable to the quasi-global resource selection model (*sensu* Laforge et al. 2015) to assess to assess habitat selection at the third-order of selection by adult Apennine female bears (n = 11) during early-summer (June–July) in the Abruzzo-Lazio-Molise National Park (central Italy, 2005–2010). Effects assessed at incremental grain sizes, from 47 to 1,531 m, and are measured both in terms of AIC score (ΔAIC_c, top row) and model averaged coefficients (β ±95% confidence intervals; bottom row) across incremental grain sizes from 47 to 1,531 m. Following Laforge et al. (2015), I retained the grain size corresponding to the lowest ΔAIC_c for each variable: agriculture, forest, and shrublands.

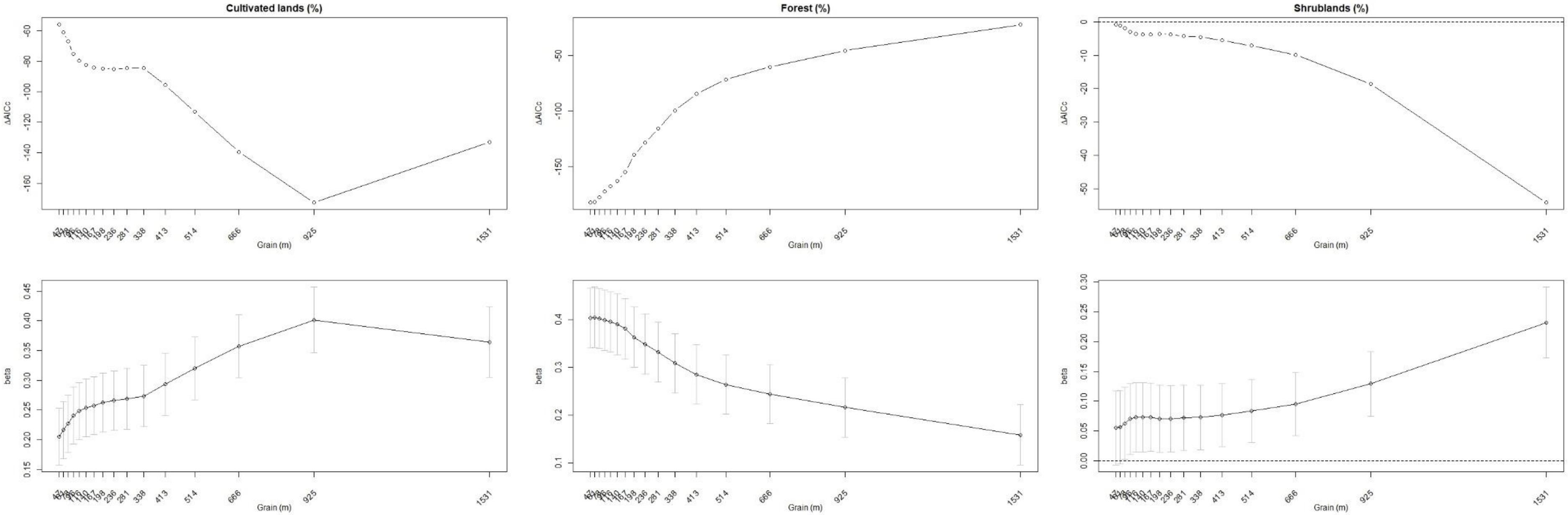

Figure S7. Effect of adding a given variable to the quasi-global resource selection model (*sensu* Laforge et al. 2015) to assess to assess habitat selection at the third-order of selection by adult Apennine female bears (n = 11) during early-summer (June–July) in the Abruzzo-Lazio-Molise National Park (central Italy, 2005–2010). Effects assessed at incremental grain sizes, from 47 to 1,531 m, and are measured both in terms of AIC score (ΔAIC_c, top row) and model averaged coefficients (β ±95% confidence intervals; bottom row) across incremental grain sizes from 47 to 1,531 m. Following Laforge et al. (2015), I retained the grain size corresponding to the lowest ΔAIC_c for each variable: hillshade, mean slope, and standard deviation of slope.

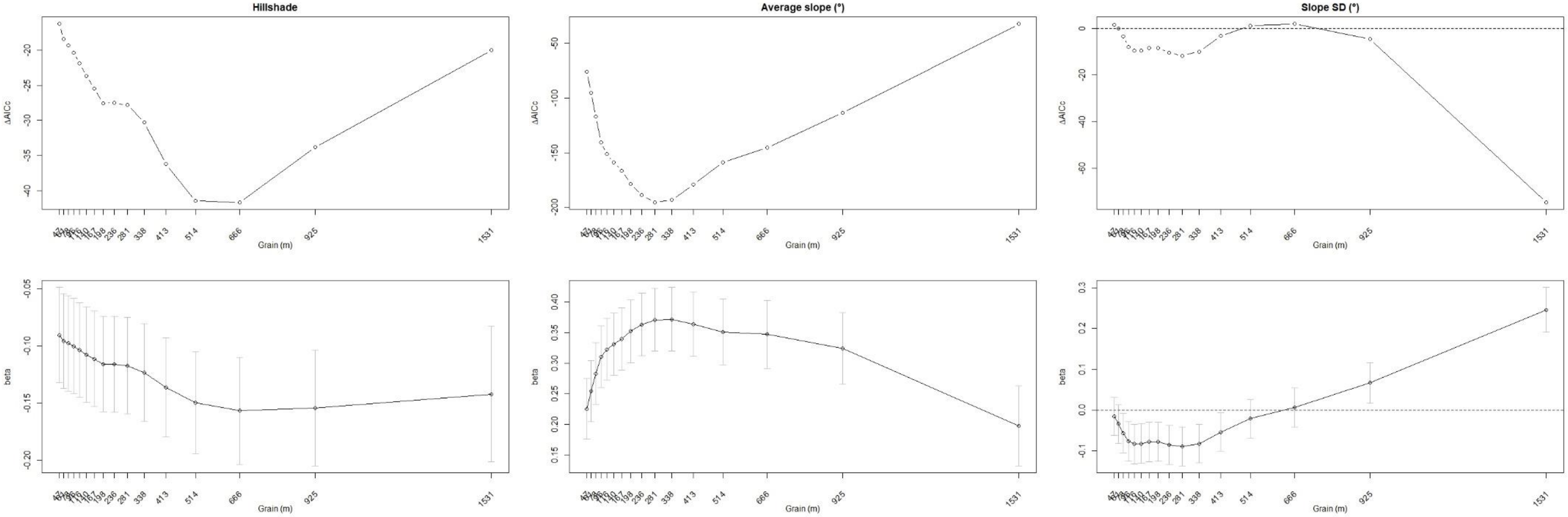

Figure S8. Effect of adding a given variable to the quasi-global resource selection model (*sensu* Laforge et al. 2015) to assess to assess habitat selection at the third-order of selection by adult Apennine female bears (n = 11) during late-summer (August–September) in the Abruzzo-Lazio-Molise National Park (central Italy, 2005–2010). Effects assessed at incremental grain sizes, from 47 to 1,531 m, and are measured both in terms of AIC score (ΔAIC_c, top row) and model averaged coefficients (β ±95% confidence intervals; bottom row) across incremental grain sizes from 47–1,531 m. Following Laforge et al. (2015), I retained the grain size corresponding to the lowest ΔAIC_c for each variable: agriculture, forest, and shrublands.

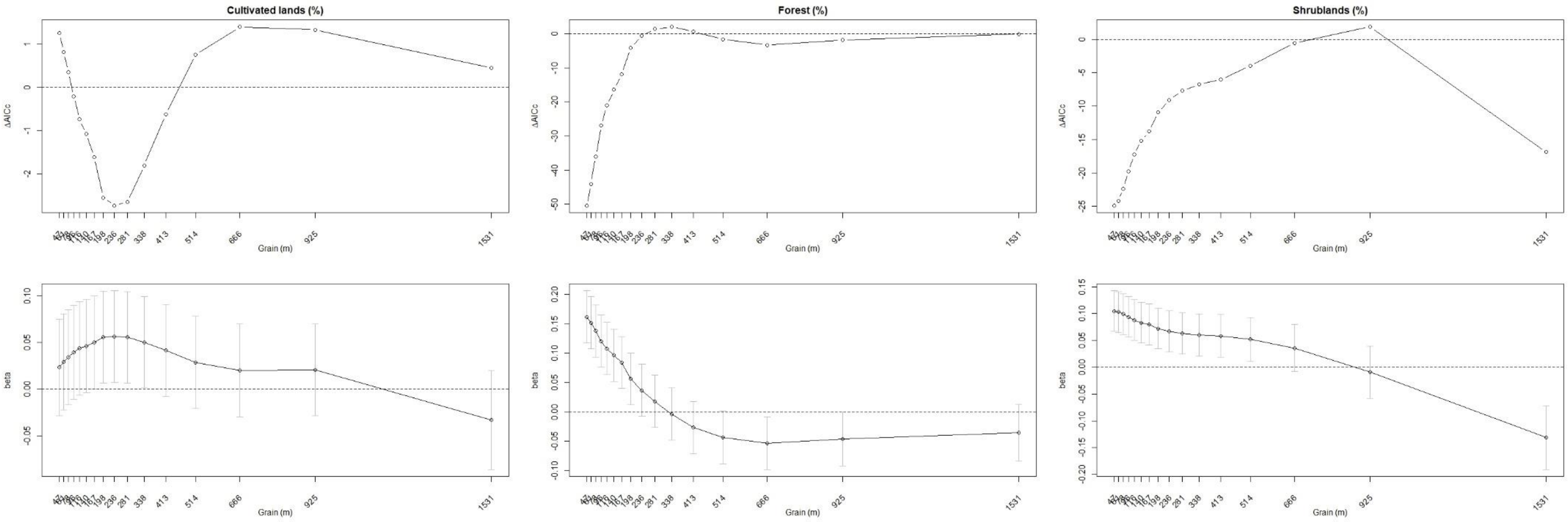
Cultivated lands (%)
Forest (%)
Shrublands (%)
ΔAICc
beta
Grain (m)
198
236
281
338
413
514
666
925
1531
1
0
-1
-2
-10
-20
-30
-40
-50
-5
-15
-20
-25
0.10
0.05
0.00
-0.05
0.20
0.15
-0.10
-0.15
-0.20

Figure S9. Effect of adding a given variable to the quasi-global resource selection model (*sensu* Laforge et al. 2015) to assess to assess habitat selection at the third-order of selection by adult Apennine female bears (n = 11) during late-summer (August–September) in the Abruzzo-Lazio-Molise National Park (central Italy, 2005–2010). Effects assessed at incremental grain sizes, from 47 to 1,531 m, and are measured both in terms of AIC score (ΔAIC_c, top row) and model averaged coefficients (β ±95% confidence intervals; bottom row) across incremental grain sizes from 47–1,531 m. Following Laforge et al. (2015), I retained the grain size corresponding to the lowest ΔAIC_c for each variable: hillshade, mean slope, and standard deviation of slope.

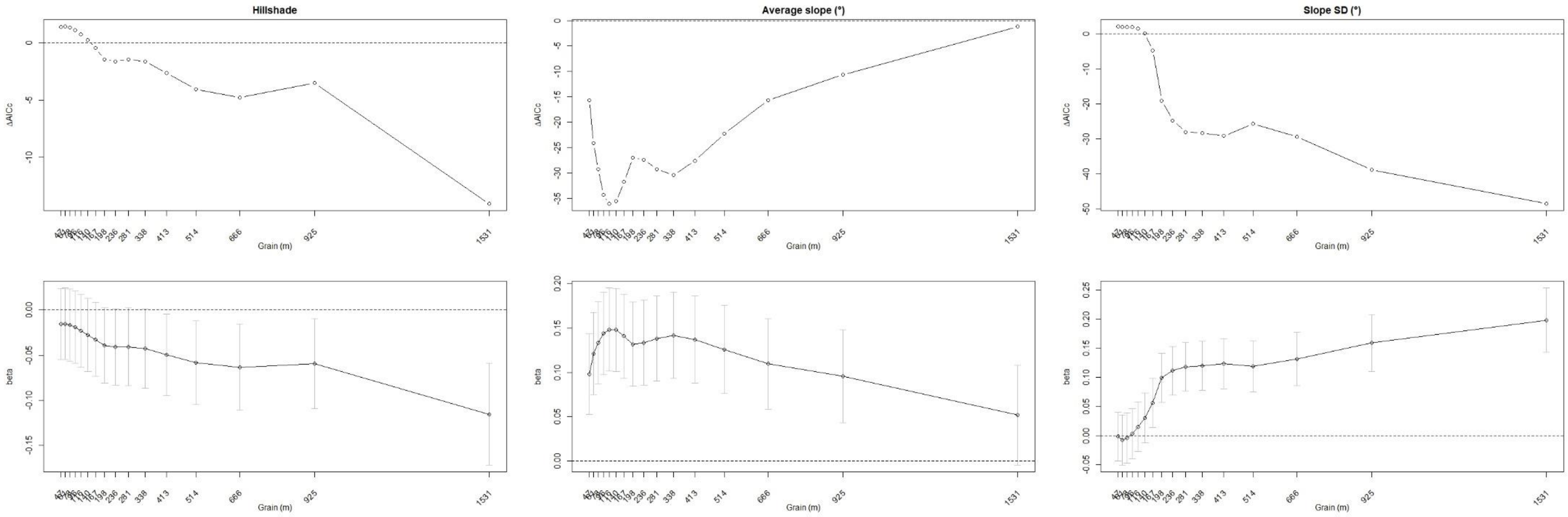
Hillshade
Average slope (°)
Slope SD (°)
ΔAICc
beta
Grain (m)
47
110
167
198
236
281
338
413
514
666
925
1531

Figure S10. Effect of adding a given variable to the quasi-global resource selection model (*sensu* Laforge et al. 2015) to assess to assess habitat selection at the third-order of selection by adult Apennine female bears (*n* = 11) during autumn (October–November 23) in the Abruzzo-Lazio-Molise National Park (central Italy, 2005–2010). Effects assessed at incremental grain sizes, from 47 to 1,531 m, and are measured both in terms of AIC score (ΔAIC_c, top row) and model averaged coefficients (β ±95% confidence intervals; bottom row) across incremental grain sizes from 47–1,531 m. Following Laforge et al. (2015), I retained the grain size corresponding to the lowest $\Delta\text{AIC}_\text{c}$ for each variable: agriculture, forest, and shrublands.

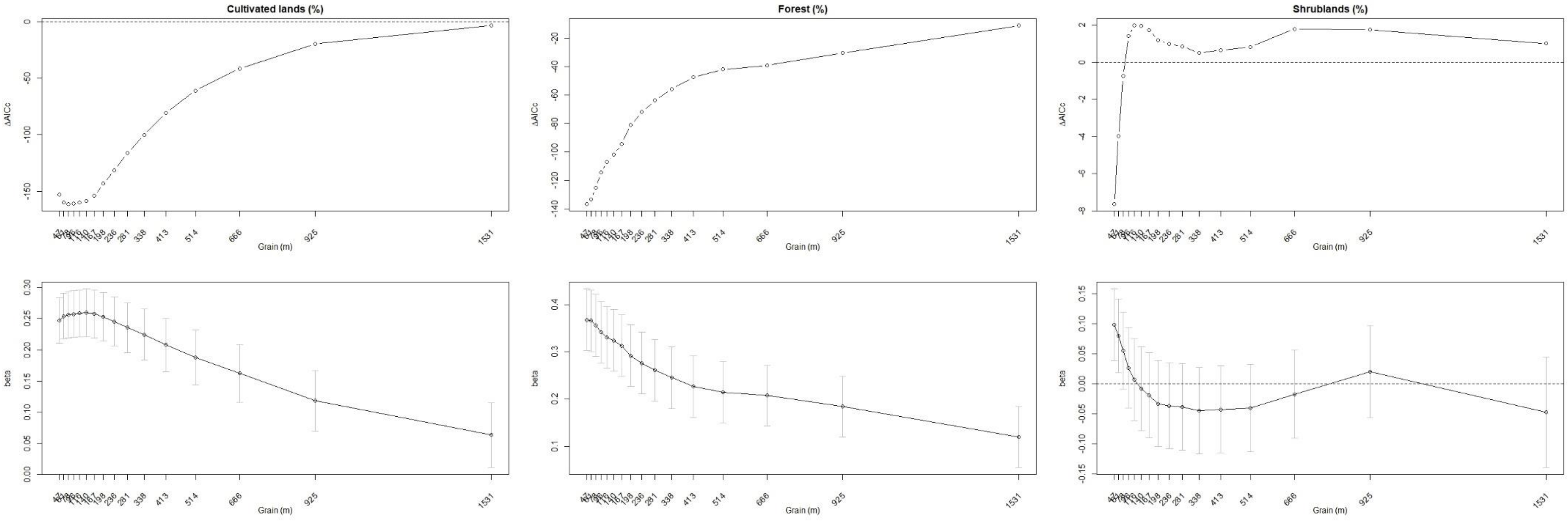

Figure S11. Effect of adding a given variable to the quasi-global resource selection model (*sensu* Laforge et al. 2015) to assess to assess habitat selection at the third-order of selection by adult Apennine female bears (*n* = 11) during autumn (October–November 23) in the Abruzzo-Lazio-Molise National Park (central Italy, 2005–2010). Effects assessed at incremental grain sizes, from 47 to 1,531 m, and are measured both in terms of AIC score (ΔAIC_c, top row) and model averaged coefficients (β ±95% confidence intervals; bottom row) across incremental grain sizes from 47–1,531 m. Following Laforge et al. (2015), I retained the grain size corresponding to the lowest ΔAIC_c for each variable: hillshade, mean slope, and standard deviation of slope.

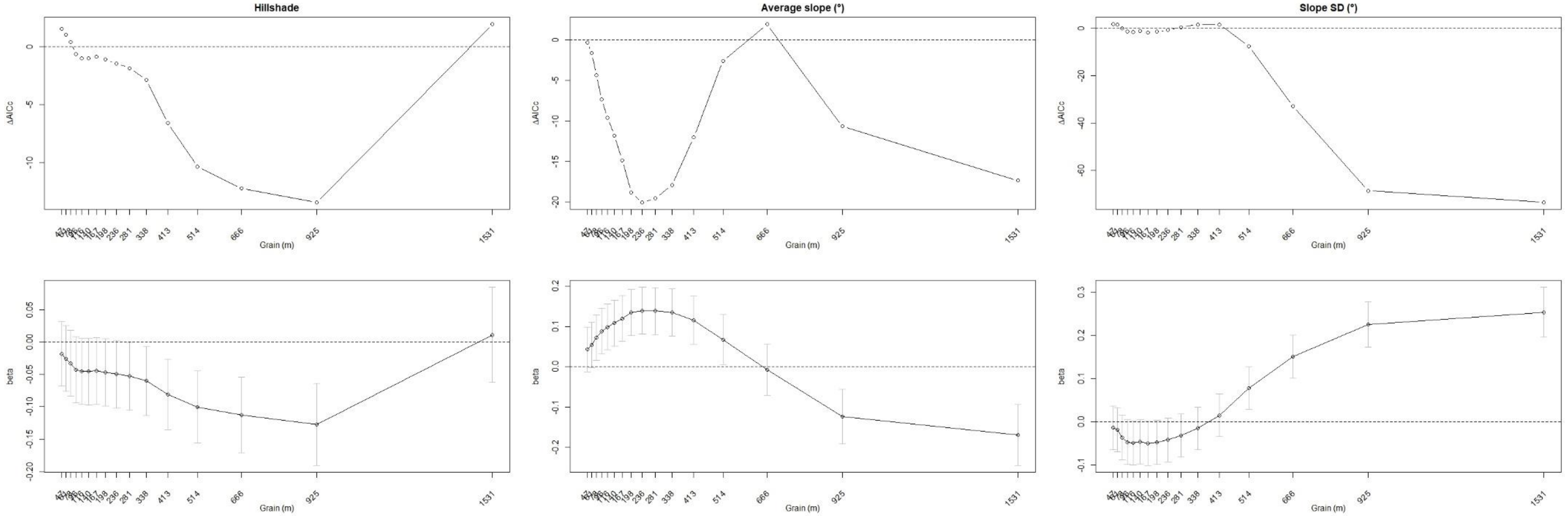

Figure S12. Coefficients (mean ± 95% confidence interval) of individual Resource Selection Functions at the third order of selection by adult Apennine female bears according to season. Different colors represent the different variables (see legend), and symbols of the same color represent different individual bears. For simplicity, are depicted only coefficients whose 95% CI does not include the zero value (see Table S11-14 for betas coefficient values). Agr = cultivated land cover; DisRoad1 = distance to paved roads; DisRoad2 = distance to unpaved roads; DisSettl = distance to human settlements; For = forest cover; Hill = hillshade; Shrub = shrubland cover; SlpM = average slope; SlpSD = slope standard deviation.

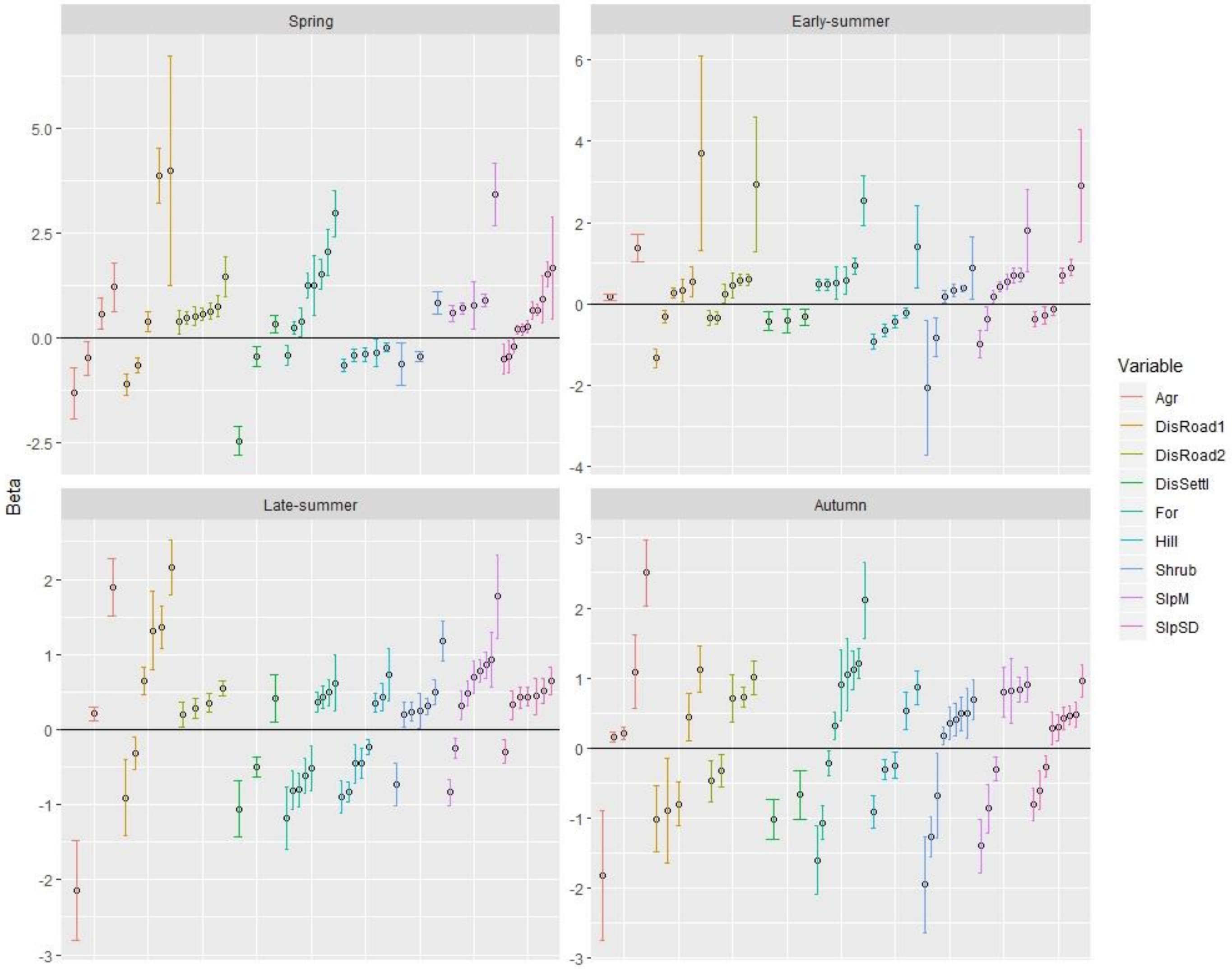

Figure S13. Relative probability of use by adult Apennine female bears in the Abruzzo Lazio and Molise National Park (central Italy, 2005–2010) as from multi-grain resource selection functions (averaged models) at the second order of selection. The continuous map depicts the relative probability of use when bears establish a home range at the landscape (i.e. study area) extent.

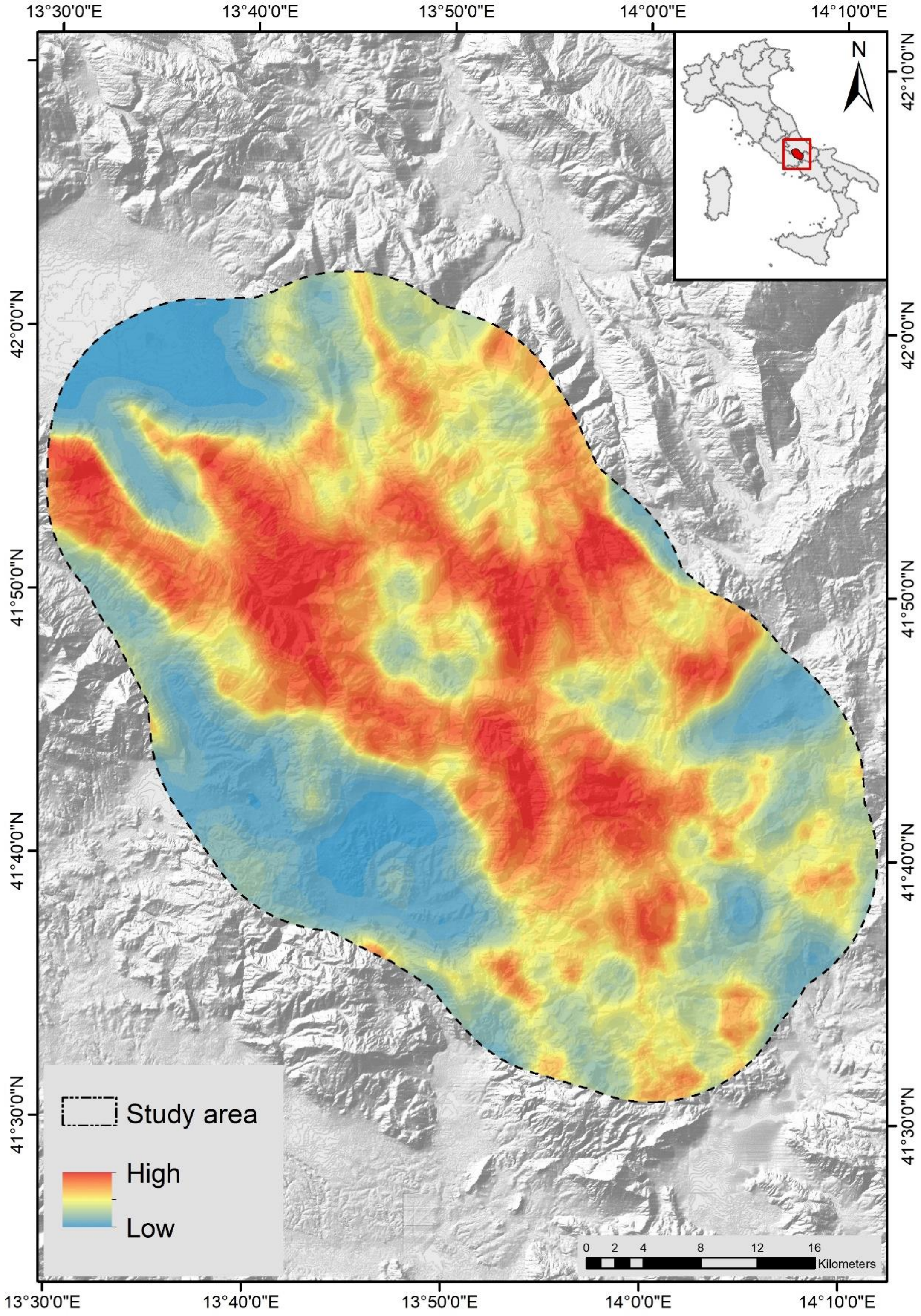

Figure S14. Relative probability of use by adult Apennine female bears in the Abruzzo Lazio and Molise National Park (central Italy, 2005‒2010) as from multi-grain resource selection functions (averaged models) at the third order of selection. A) spring (March‒May), B) early-summer (June‒July), C) late-summer (August‒September), and D) autumn (October‒November 23). The continuous map depicts the relative probability of use when bears select the habitat within the home range. According to a hierarchical habitat selection process, I did not project this map over the entire study area but only where conditions were equal or greater that a minimum threshold of relative probability. I defined this threshold across predicted values at the second-order of selection using the 'PresenceAbsence' R package (function *optimal.thresholds*, option *MaxSens+Spec*; Freeman and Moisen 2008) by minimizing the mean error rate for both positive and negative observations (Ciucci et al. 2018).

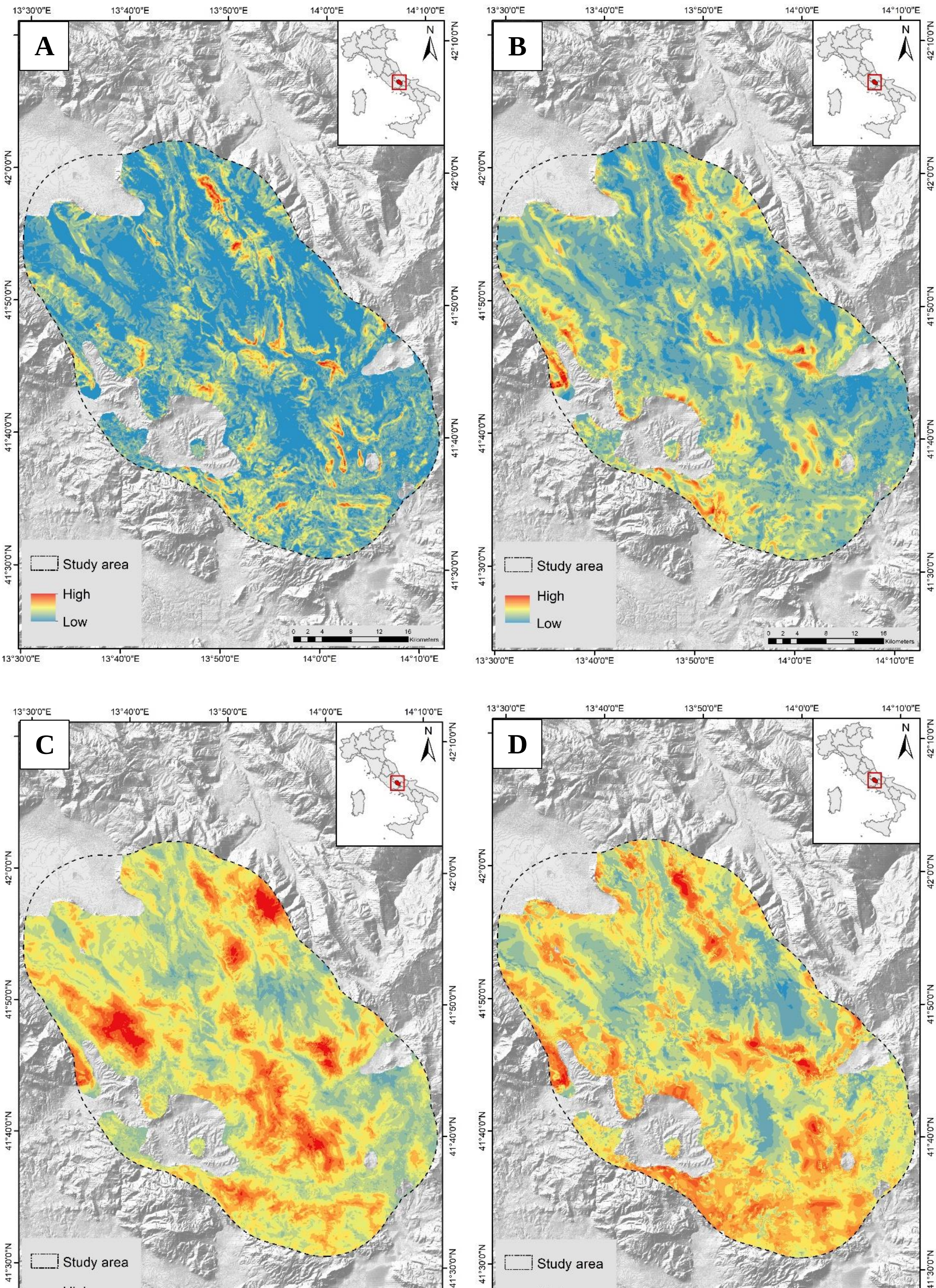
A
B
C
D
N
13°30'0"E
13°40'0"E
13°50'0"E
14°0'0"E
14°10'0"E
42°10'0"N
42°0'0"N
41°50'0"N
41°40'0"N
41°30'0"N
Study area
High
Low
0 2 4 8 12 16
Kilometers

REFERENCES

Ciucci, P., L. Boitani, M. Falco, and L. Maiorano. 2018. Hierarchical, multi-grain rendezvous site selection by wolves in southern Italy. The Journal of Wildlife Management 82:1049–1061.

Freeman, E. A., and G. Moisen. 2008. PresenceAbsence: An R package for PresenceAbsence analysis. Journal of Statistical Software 23:1–31.

Laforge, M. P., E. Vander Wal, R. K. Brook, E. M. Bayne, and P. D. McLoughlin. 2015. Process-focussed, multi-grain resource selection functions. Ecological Modelling 305:10–21.

Lewis, J. S., J. L. Rachlow, E. O. Garton, and L. A. Vierling. 2007. Effects of habitat on GPS collar performance: Using data screening to reduce location error. Journal of Applied Ecology 44:663–671.

Molinari, L. 2007. Analisi delle prestazioni (accuratezza e tasso di acquisizione) del radiocollare a tecnologia satellitare, nel Parco Nazionale d’Abruzzo Lazio e Molise nell’ambito del progetto Grandi Carnivori. Università di Roma “La Sapienza.”

Chapter II

Combining forest inventory data and remote sensing to map forest structure using an ensemble modelling approach

Matteo Falco[1], Paolo Ciucci[1], Luigi Maiorano[1], Mario Posillico[2], Achilleas Psomas[4], Luciano Sammarone[2,3], and Niklaus E. Zimmermann[4]

[1] *Sapienza University of Rome, Dept. of Biology and Biotechnology "Charles Darwin", Viale dell'Università 32, Roma 00185, Italy*

[2] *Corpo Forestale dello Stato, Ufficio Territoriale Biodiversità, Via Sangro 45, 67031 Castel di Sangro (AQ), Italy*

[3] *Parco Nazionale d'Abruzzo, Lazio e Molise, Pescasseroli (AQ), Italy*

[4] *Swiss Federal Research Institute WSL, Zürcherstr 111, Birmensdorf 8903, Switzerland*

INTRODUCTION

Detailed and continuous spatially explicit information on forest composition and structure is needed for achieving different goals, going from silviculture (e.g., Pond et al. 2014), to ecological restoration and risk assessment (e.g., Pierce et al. 2009), from biodiversity and habitat conservation (e.g., Turner et al. 2003; Helmer et al. 2010; Jung et al. 2012), to carbon management and reporting (e.g., Hall et al. 2006; Hoover and Rebain 2011), and to forest health assessment and management (e.g., Solberg et al. 2004; Wolter et al. 2009). Extensive, spatially continuous sampling of large forested areas is practically and economically unfeasible, especially in rough and remote areas, but local and/or national forest inventories are often available (Gillis et al. 2005, Fattorini et al. 2006, Blackard et al. 2008). Therefore, a variety of statistical methods have been used for producing continuous forest structure maps calibrated with a limited sampling effort, and a number of studies have explored the use of different types of data and approaches (e.g., Labrecque et al. 2006; Maselli and Chiesi 2006; Tonolli et al. 2011).

Brosofske et al. (2014) reviewed the analytical methods that can be used for developing geospatial forest inventory models in which individual plots can be extrapolated to continuous surfaces. The authors highlighted that regression is the method commonly used in this context (Hudak et al. 2006, le Maire et al. 2011, Stephens et al. 2012), closely followed by spatial interpolations (e.g., nearest neighbor imputations) and machine-learning algorithms (e.g., random forest), with often more than one method being applied at the same case study (Durbha et al. 2007, Hudak et al. 2008, LeMay et al. 2008, Zhao et al. 2011). Irrespective of the statistical algorithms, most of these models are based on remote sensing data together with other ancillary variables available across the area of interest (Hudak et al. 2008, Gleason and Im 2012, Beaudoin et al. 2014).

In the last years, the availability of ancillary data has been increasing exponentially, including passive and active satellite and airborne remotely sensed data (e.g., optical, radar, and LiDAR). Unlike passive satellite sensors (e.g., Landsat and MODIS), active remote sensing has the advantage to better penetrate vegetation and clouds, but cost and availability still limit its operational feasibility

(Wulder et al. 2008; Wolter et al. 2009). Furthermore, active sensor images can directly provide forest tridimensional structure (Hudak et al. 2006, Falkowski et al. 2009, Helmer et al. 2010, Næsset et al. 2011, Hall et al. 2019, Saukkola et al. 2019), which can be particularly important for specific applications (Turner et al. 2003, Estes et al. 2008, Wulder et al. 2008). Landsat imagery or other passive remote sensing data are traditionally used for characterizing horizontal forest structure (Drake et al. 2002, Lefsky et al. 2002), but they present many drawbacks if the aim is to obtain detailed tridimensional forest attributes (Brosofske et al. 2014).

A few studies investigated the use of both types of remote sensing data (e.g., Watt et al. 2004; Pascual et al. 2010), and typically passive sensors are considered not suited for representing tridimensional forest characteristics. Nevertheless, specific spectral bands obtained through passive sensors, or a combination of them (e.g., vegetation indices), have been used to predict tridimensional forest structural attributes (Fiorella and Ripple 1993, Ingram et al. 2005, Hall et al. 2006). For instance, Fiorella and Ripple (1993) and Hall et al. (2006) found strong negative correlations between Landsat TM and ETM+ spectral bands and two structural stand variables, namely stand height and crown closure. Similarly, Ingram et al. (2005) found that reflectance of Landsat bands 3, 4, 5, and 7 are useful predictors of basal area in tropical forests. However, spectral bands or derived-vegetation indices change over the time (e.g., seasonality), and they are also affected by spatial resolution (e.g., surrounding species and structural composition of wooded patch). This aspect was not deeply investigated, and no studies focused on how these two factors (seasonality and spatial resolution) can influence the power prediction of vegetation indices when they are used for predicting understory tridimensional structure. Furthermore, because there is growing evidence that many natural phenomena have their own characteristic scales (or range of scales; Goodchild and Quattrochi 1997; Peterson and Parker 1998; Holland et al. 2004; Jackson and Fahrig 2015), vegetation indices should be manipulated using several spatial and temporal scales to detect at which scale(s) they better reflect tridimensional understory forest structure.

In this work, may main objective is to propose a novel framework based on freely available satellite images which can be used to produce continuous and spatially explicit structural forest maps starting from inventory data. My modelling framework is based on an ensemble forecasting approach (Araújo and New 2007) used to predict structural forest attributes (basal area, BA, and tree density, TD), using Landsat satellite vegetation indexes (NDVI and EVI) and other ancillary variables. Using independent data, I also validated these models to demonstrate the reliability of the framework when high resolution images from active sensors are not available.

METHODS

Study area and data collection

The study area is located in the Apennine mountains, Italy (Fig. 1). The area, 509.51 km^2, includes all forested areas within the Abruzzo-Lazio-Molise National Park (PNALM) and its external protection area. The landscape of the region is dominated by mountainous forests, with elevation ranging from 145 to 2,278 m above sea level, going from gentle slopes dominated by non-intensive cultivated lands and with few and small human settlements to typically mountainous terrain, mainly covered by forests interspersed with pastures, meadows and alpine prairies. Forest is mainly dominated by beech (*Fagus sylvatica*) and oaks (*Quercus* spp.), followed by hop-hornbeam (*Fraxinus* ssp. and *Carpinus* ssp.), and other mixed broadleaf species (e.g., *Acer* spp.). Coniferous are exceedingly rare in the study area, with *Abies alba* representing a glacial relict species limited to a small area, and *Pinus nigra* occurring in historical silvicultural plantations restricted to few areas near the main human settlements.

Forest monitoring is performed by the Forest Service at the local (Castel di Sangro Territorial Offices, Carabinieri per la Biodiversità, hereafter UTB) and national level (National Forests and Carbon Stock Inventory, INFC). I obtained 301 forest plots, 210 collected by the UTB, and 91 by the INFC (https://www.inventarioforestale.org/). All plots were sampled in 2005 using the same design (Gasparini et al. 2009). Each plot was classified according to the dominant tree species: beech (n=176), oak (n=98), hop-hornbeam (n=18), black pine (n=6), and hygrophilous (n=3) forests. For all plots, I calculated the following two structural variables: sum of trees' basal area (m^2/ha; hereafter BA), and number of trees per hectare (trees/ha; hereafter TD). For the purpose of the analyses, the few plots classified as hop-hornbeam and hygrophilous forests were clumped together with oak forests, considering that most of the former occur within forests patches dominated by oaks (see Supplementary). The forests plots classified as black pine were excluded from the analysis because of the small sample size and because of their artificial origin.

I also obtained independent forest structure data collected by the Park's Forestry service within forest management areas. These areas are used for the management of local silvicultural actions, and for each area it was collected trees structural information associated to the entire forest patch, like the number of stems (i.e., tree density) and the averaged diameter at the breast height (DBH).

Predictor variables

To map BA and TD for the entire study area, I considered a set of predictor variables, including both remote sensing (e.g., vegetation indices) and orographic predictors. I considered both EVI and NDVI (Tucker 1979; Huete et al. 2002) calculated with Landsat 5 TM/7 ETM+ satellite images (30x30m resolution), acquired from the LSDS Science Research and Development (LSRD) (https://espa.cr.usgs.gov/, accessed 1 March 2018) for a period ranging from May to August (2005). I acquired a total of 18 NDVI and EVI layers (1.8 images/month) with cloud cover over forested areas <10%.

I also considered orographic features and distance to forest edges, all of which may affect directly or indirectly the growth of a forest patch and its tridimensional composition. Among orographic variables, I included elevation, slope and solar radiation. The structure of a forest patch, in fact, can be influenced by both elevation and terrain roughness (Clark and Clark 2000; Jucker et al. 2018), and solar radiation, clearly linked locally to orographic features, may be an important factor for tree's productivity and, consequently, for log size. I calculated these variables using a digital elevation model (DEM) with a resolution of 10x10 m (Italian Military Geographic Institute): percent slope and solar radiation (Watt/day) were calculated using the Spatial Analyst Tool in ArcMap (v.

10.2; Environmental Systems Research Institute, ESRI, Redlands, CA, USA). I also included distance to forest edges (negative values inside the forest patch), because the interior of the forest may have different tree density and composition respect to forest occurring close to the edge (e.g., Matlack 1994; López-Barrera et al. 2006). All variables were re-sampled with a common origin and 30x30 m cell size resolution, snapping everything to the available vegetation indices. All analyses and data manipulation were performed using ArcGIS 10.2 (ESRI ©) and the R library 'raster' (Hijmans et al. 2017).

Modeling procedure

My framework includes 3 main steps (Fig. 2): (*i*) multi-scale variables preparation and selection, (*ii*) model calibration and evaluation, and (*iii*) independent spatial evaluation. All analysis described below have been performed for each forest attribute (i.e., TD and BA) and for each dominant tree species (i.e., beech and oak).

Multi-scale variables preparation and selection

For the vegetation indices I tested different spatial and temporal scales to identify which combination better reflects the empirical relationship with tridimensional forest attributes (i.e., BA and TD). We considered 5 temporal windows (including all continuous temporal windows spanning 2 or 3 months) and for each calculated the mean and the standard deviation NDVI and EVI (Fig. 3A-B) using two approaches: the temporal-fist and the spatial-first approach. In the temporal-first approach, we calculated for each pixel of the study area the mean and standard deviation of EVI and NDVI in each temporal window; then, we applied a circular moving window with 10 different radii (from 30 to 300 m with 30 m increments) and calculated the average value (Fig. 3A). In the spatial-first approach, we calculated the mean and standard deviation for both EVI and NDVI within a circular moving window (same approach described above with the same radii) and then we calculated the average value in the temporal window (Fig. 3B).

To select the variables better reflecting the forest structure attributes, I first selected the grain size with the highest correlation score, one for each temporal window and multi-scale approach

(Supplementary Table S1); then, to avoid multicollinearity in the final set of predictor variables (Dormann et al. 2013), I retained all vegetation indices and topographic variables with $r < |0.8|$.

Model calibration and evaluation

I calibrated the models for both BA and TD with four algorithms: generalized linear models (GLM; McCullagh and Nelder 1989), generalized additive models (GAM; Hastie and Tibshirani 1986), boosted regression trees (GBM; Ridgeway 1999), and random forest (RF; Breiman 2001). For GLMs and GAMs, I considered all possible combinations of covariates (*dredge* function in the R package 'MuMIn'; Barton 2018) and calculated the final model as the weighted average using the AIC_c as weights. For GBM and RF I considered multiple decision trees (N=200).

I performed model evaluation using a *k*-fold cross validation (*k*=5). For each run of the cross validation, I calculated the Pearson's correlation between the values predicted by the models and values observed in the leave-out fold. In addition, for each model I also calculated the root mean square error (RMSE). The entire evaluation procedure was repeated 10,000 times for each combination of algorithm (GLM, GAM, GBM, and RF), tree species (beech and oak), and forest attribute measure (BA and TD), for a total of 160,000 predicted models.

The final TD and BA models for beech and oak were calculated as the weighted mean of all models, with each repetition weighted by the respective Pearson score obtained from the evaluation. Models with $r<0.6$ were excluded. To ensure that selected models well discriminate from randomness, I also performed a permutation test to assess the statistical significance of the cut-off threshold selected ($r=0.6$), creating 10,000 random models. The null-hypothesis (H_0) assume that there is no difference between predicted and random models (i.e., IC95% value of the Pearson's *r* random distribution is higher than $r=0.6$), while the alternative hypothesis (H_1) assume that predicted models are statistically different from randomness (i.e., IC95% value of the Pearson's *r* random distribution is lower than $r=0.6$).

Independent spatial evaluation

I projected the ensemble model for both TD and BA and for both beech and oak over the study area, and I used independent field data collected at the scale of the single forest management unit to evaluate the accuracy of maps' spatial prediction. However, whereas the number of trees is collected with the same metric unit in both forest inventory and forest unit management dataset, the log size of trees was collected in two different but comparable measures: basal area, and diameter at breast (DBH). To convert BA forest map into DBH measure, I used the 'map algebra' Spatial Analyst Tool (ArcGIS 10.2, ESRI), and I divided BA and TD maps obtaining the average BA (BA_{avg}); then, to calculate the averaged DBH map (hereafter, namely DBH), I used the inverse of the circle area formula (i.e., $DBH = \sqrt{\frac{BA_{avg}}{\pi}}$). To evaluate the maps prediction accuracy, I calculated the RMSE between the TD and DBH values collected in each forest management units (observed values) with the respective values extracted by the maps (predicted values); moreover, I built the observed-predicted response curves fitting an additive term in the linear regression (GAM; Wood 2011) to account for non-linear pattern responses.

RESULTS

Multi-scale variables selection

For predicting oak forest structure, the most selected temporal window is June-July, followed by June-August, corresponding to the most selected for beech forest (Table 1). This pattern is not influenced by the vegetation index selected. In addition, while correlation between vegetation indices and forest structure is higher in oak using mean statistic, at the contrary I did not find any clear pattern for beech. I also evidenced comparable high correlation between forest structure attributes and orographic variables, mainly in oak's TD (Table 1).

Variables multicollinearity

According to the uncorrelated set of model predictors (Supplementary Table S2-S5), saturated models are composed by the combination of both NDVI and EVI, and both multi-scale approach (temporal- and spatial-first) without any clear pattern of preference, excepted for the standard deviation which is the more used selected in oak respect to beech, mainly in the TD set of model predictors (Table 2).

Models calibration and evaluation

Almost 13% of the models obtained evaluation scores *r*>0.6, without any difference among algorithms (Fig. 4). In general, oak models gave higher evaluation scores compared to beech, also with scores greater than 0.9. I found a similar pattern in the RSME scores calculated among model algorithms, where BA and TD had always a lower prediction error in oak forest compared to the beech (Table 3), with RF that provide a better fit with the data (Supplementary Fig. S1-S4). Ensemble models provides an averaged RMSE respect to the other model algorithms, always lower than regression (GLM and GAM) and higher than machine learning (RF and GBM) models (Table 3).

From the permutation test results, I reject the null hypothesis (H_0: IC95%>0.6), and I confirm that, using *r*>0.6 as threshold in model evaluation, models differ from randomness (H_1: IC95%<0.6), independently by target species and forest structure (Fig. 5).

Independent spatial validation of forest maps

I obtained a good spatial validation of the forest structure maps (Fig. 6-8), where RMSE scores for both TD (RSME=886.72) and DBH (RMSE=8.74) are comparable with those calculated during the ensemble modeling procedure. The response curves confirmed this result, evidencing a positive relationship between the TD (and BA) values predicted by forest maps and the observed values collected on the field (Fig. 9A-B); accordingly, at the increase of the observed value of forest structure follows a linear increase of the predicted value, excepted for a little non-linear inflection in the intermediate DBH values (Fig. 9A).

DISCUSSION

In this study I provided an approach to predict tridimensional forest structure combining forest inventory and passive remote sensing data. Although active sensors (e.g., LIDAR) are more appropriate to model tridimensional forest structure, there may be situations where they are not available or not cost-effective. Commonly considered to be poor predictors of tridimensional structure attributes (Foody et al. 2001), optical remote-sensing products (e.g., Landsat vegetation indices) were used in few studies aimed to predict tridimensional forest structure (Pocewicz et al. 2004, le Maire et al. 2011), while they are commonly used in combination with several other modelling techniques for mapping vegetation and individual trees forest type (Engler et al. 2013), predicting fire susceptibility and disturbance (Hislop et al. 2019, Tehrany et al. 2019), and forest biomass (Blackard et al. 2008). This is the first study that try to capture the relationship between vegetation indices and forest structure accounting for changes in time and space, thanks to a cutting edge multi-scale approach able to select the best predictive set of model predictors for maximizing the power prediction of tridimensional forest structure maps. In addition, the main advantage of the proposed framework is its extremely plasticity, connected to the opportunity of selecting different vegetation indices and ancillary predictor variables (e.g., temperature, precipitation, and soil characteristics) when they are available, model algorithms, and temporal range (window) of time-series images, the latter related to the seasonality of the study area (i.e., bud buster of trees).

The entire modelling framework proposed in this work is based on the availability of forest inventory data, from which I extracted tridimensional information of forest (training dataset). Since become unfeasible to sample the entire study area, inventory data are limited to a small portion of the landscape, and the collected stand information should be representative of the entire variability of forest structure occurring on the field. In this sense, using an ensemble modeling approach that accounting for several model predictions, instead of identifying the ‘best’ model from an ensemble of predictions (Thuiller 2003, Segurado and Araújo 2004), help to overcome the drawback of inventory point-based data. In addition, given that I were less interested to which is the model that better fit the data (i.e., explanatory power), and I wanted to predict adequately outcomes over a different area of projections (i.e., predictive power of model), only the best performing model algorithm (i.e., RF in the case study) was not sufficient to guarantee the predictions of all stand structure variability.

Although few models were selected from thousands of replicates, I evidenced good power of predictions and accuracy of the forest structural maps. This result was confirmed by the comparable RMSE values found during modeling procedure (model selection) and the spatially validation of TD and DBH maps. In the response curves of forest maps, whereas observed-predicted curve of TD shows a clear linear pattern (i.e., predicted values increase at the increase of the expected), the averaged DBH showed a slightly non-linear inflection at the level of the intermediate values. This can be a consequence of the fact that the extreme successional stages of forest (i.e., mature- and early-successional stage) are better represented by predictive models, compared to the intermediate ones. This result may lead to caution about a certain degree of uncertainty about intermediate structural predictions, reflected in the mid-successional stages of the forest.

Continuous forest attributes maps are useful not only for managing silvicultural practices, but also for strategic and operational management of all components of forest ecosystems, including wildlife-habitat relationship. The structural composition of forest stands largely determines habitat quality for animals, because it may influence the availability and accessibility of several resources, such as rest sites and food (Hayes and Loeb 2007), exposure to predators (Baxter et al. 2006), and thermoregulation (Chen et al. 1999). Having continuous and tridimensional structural information of the forest habitat, it could be possible deeply investigating the ecological relationship between animal populations (or community of species) and available resources associated to different stages of forest succession. For instance, I could distinguish in a continuous way mature forest patches (old-growth forest), characterized by large trees occurring at low density, from earlier seral succession (i.e., secondary/pioneer forest), characterized by small trees occurring at highest density. In this sense, tridimensional forest composition become essential for defining what habitat is suitable or not for those animals, which must move and forage within the three-dimensional arrangements of forests and their canopies to fulfil all their biological requirements. In addition, in wilderness areas characterized by high biodiversity but low budget assigned for conservation purposes (e.g., some areas of South-East Asia, South America and central Africa), these continuous layers may become fundamental tools for taking proactive forest management actions, no more focused on the economic value of the forest (e.g., wood harvest), but otherwise focused on the preservation of habitat quality to guarantee the highest biodiversity and the derived ecosystem services (de Groot et al. 2010).

REFERENCES

Araújo, M. B., and M. New. 2007. Ensemble forecasting of species distributions. Trends in Ecology & Evolution 22:42–47.

Barton, K. 2018. Package “MuMIn” Title Multi-Model Inference. Cran-R.

Baxter, D. J. M., J. M. Psyllakis, M. P. Gillingham, and E. L. O’Brien. 2006. Behavioural response of bats to perceived predation risk while foraging. Ethology 112:977–983.

Beaudoin, A., P. Y. Bernier, L. Guindon, P. Villemaire, X. J. Guo, G. Stinson, T. Bergeron, S. Magnussen, and R. J. Hall. 2014. Mapping attributes of Canada’s forests at moderate resolution through kNN and MODIS imagery. Canadian Journal of Forest Research 44:521–532.

Blackard, J. A., M. V. Finco, E. H. Helmer, G. R. Holden, M. L. Hoppus, D. M. Jacobs, A. J. Lister, G. G. Moisen, M. D. Nelson, R. Riemann, B. Ruefenacht, D. Salajanu, D. L. Weyermann, K. C. Winterberger, T. J. Brandeis, R. L. Czaplewski, R. E. McRoberts, P. L. Patterson, and R. P. Tymcio. 2008. Mapping U.S. forest biomass using nationwide forest inventory data and moderate resolution information. Remote Sensing of Environment 112:1658–1677.

Breiman, L. 2001. Random Forrests. Machine learning 45:5–32.

Brosofske, K. D., R. E. Froese, M. J. Falkowski, and A. Banskota. 2014. A review of methods for mapping and prediction of inventory attributes for operational forest management. Forest Science 60:733–756.

Chen, J., S. C. Saunders, K. D. Brosofske, G. D. Mroz, T. R. Crow, R. J. Naiman, J. F. Franklin, and B. L. Brookshire. 1999. Microclimate in forest ecosystem and landscape ecology: Variations in local climate can be used to monitor and compare the effects of different management regimes. BioScience 49:288–297.

Clark, D. B., and D. A. Clark. 2000. Landscape-scale variation in forest structure and biomass in a tropical rain forest. Forest Ecology and Management 137:185–198.

Dormann, C. F., J. Elith, S. Bacher, C. Buchmann, G. Carl, G. Carré, J. R. G. Marquéz, B. Gruber, B. Lafourcade, P. J. Leitão, T. Münkemüller, C. Mcclean, P. E. Osborne, B. Reineking, B. Schröder, A. K. Skidmore, D. Zurell, and S. Lautenbach. 2013. Collinearity: A review of methods to deal with it and a simulation study evaluating their performance. Ecography 36:027–046.

Drake, J. B., R. O. Dubayah, D. B. Clark, R. G. Knox, J. B. Blair, M. A. Hofton, R. L. Chazdon, J. F. Weishampel, and S. Prince. 2002. Estimation of tropical forest structural characteristics, using large-footprint lidar. Remote Sensing of Environment 79:305–319.

Durbha, S. S., R. L. King, and N. H. Younan. 2007. Support vector machines regression for retrieval of leaf area index from multiangle imaging spectroradiometer. Remote Sensing of Environment 107:348–361.

Engler, R., L. T. Waser, N. E. Zimmermann, M. Schaub, S. Berdos, and C. Ginzler. 2013. Forest ecology and management combining ensemble modeling and remote sensing for mapping individual tree species at high spatial resolution. Forest Ecology and Management 310:64–73.

Estes, L. D., G. S. Okin, A. G. Mwangi, and H. H. Shugart. 2008. Habitat selection by a rare forest antelope: A multi-scale approach combining field data and imagery from three sensors. Remote Sensing of Environment 112:2033–2050.

Falkowski, M. J., J. S. Evans, S. Martinuzzi, P. E. Gessler, and A. T. Hudak. 2009. Characterizing forest succession with lidar data: An evaluation for the Inland Northwest, USA. Remote Sensing of Environment 113:946–956.

Fattorini, L., M. Marcheselli, and C. Pisani. 2006. A three-phase sampling strategy for large-scale multiresource forest inventories. Journal of Agricultural, Biological, and Environmental Statistics 11:296–316.

Fiorella, M., and W. H. Ripple. 1993. Analysis of conifer forest regeneration using Landsat Thematic Mapper data. Photogrammetric Engineering and Remote Sensing 59:1383–1388.

Foody, G. M., M. E. Cutler, J. McMorrow, D. Pelz, H. Tangki, D. S. Boyd, and I. Douglas. 2001. Mapping the biomass of Bornean tropical rain forest from remotely sensed data. Global Ecology and Biogeography 10:379–387.

Gasparini, P., R. Bertani, F. De Natale, D. Cosmo, and E. Pompei. 2009. Quality control procedures in the Italian national forest inventory. Journal of Environmental Monitoring 11:761–768.

Gillis, M. D., A. Y. Omule, and T. Brierley. 2005. Monitoring Canada's forests: The national forest inventory. Forestry Chronicle 81:214–221.

Gleason, C. J., and J. Im. 2012. Forest biomass estimation from airborne LiDAR data using machine learning approaches. Remote Sensing of Environment 125:80–91.

Goodchild, M., and D. a Quattrochi. 1997. Scale, Multiscaling, Remote Sensing, and GIS. M.F., editor. Scale in Remote Sensing and GIS.

de Groot, R. S., R. Alkemade, L. Braat, L. Hein, and L. Willemen. 2010. Challenges in integrating the concept of ecosystem services and values in landscape planning, management and decision making. Ecological Complexity 7:260–272.

Hall, R. J., R. S. Skakun, E. J. Arsenault, and B. S. Case. 2006. Modeling forest stand structure attributes using Landsat ETM+ data: Application to mapping of aboveground biomass and stand volume. Forest Ecology and Management 225:378–390.

Hall, R. J., R. S. Skakun, E. J. Arsenault, B. S. Case, J. A. Blackard, M. V. Finco, E. H. Helmer, G. R. Holden, M. L. Hoppus, D. M. Jacobs, A. J. Lister, G. G. Moisen, M. D. Nelson, R. Riemann, B. Ruefenacht, D. Salajanu, D. L. Weyermann, K. C. Winterberger, T. J. Brandeis, R. L. Czaplewski, R. E. McRoberts, P. L. Patterson, R. P. Tymcio, L. D. Estes, G. S. Okin, A. G. Mwangi, H. H. Shugart, G. V. Hilderbrand, T. A. Hanley, C. T. Robbins, C. C. Schwartz, G. Chirici, M. Mura, D. McInerney, N. Py, E. O. Tomppo, L. T. Waser, D. Travaglini, R. E. McRoberts, P. Fatehi, A. Damm, R. Leiterer, M. P. Bavaghar, M. E. Schaepman, M. Kneubühler, S. P. Kearney, N. C. Coops, G. B. Stenhouse, S. E. Nielsen, T. Hermosilla, J. C. White, M. A. Wulder, S. M. Mendia, M. D. Johnson, J. M. Higley, S. E. Nielsen, M. S. Boyce, G. B. Stenhouse, O. J. Schmitz, D. Hawlena, G. C. Trussell, A. Traveset, M. F. Willson, F. Zellweger, F. Morsdorf, R. S. Purves, V. Braunisch, K. Bollmann, E. Zyśk-Gorczyńska, Z. Jakubiec, A. Wuczyński, P. Gasparini, R. Bertani, F. De Natale, D. Cosmo, and E. Pompei.

2019. A meta-analysis and review of the literature on the k-Nearest Neighbors technique for forestry applications that use remotely sensed data. Remote Sensing of Environment 112:761–768.

Hastie, T., and R. Tibshirani. 1986. Generalized additive models. Statistical Science 1:297–318.

Hayes, J. P., and S. C. Loeb. 2007. The influences of forest management on bats in North America. Pages 207–236 in. Bats in Forests: Conservation and Management. eds M.J. L. John Hopkins University Press, Baltimore, MD.

Helmer, E. H., T. S. Ruzycki, J. M. Wunderle, S. Vogesser, B. Ruefenacht, C. Kwit, T. J. Brandeis, and D. N. Ewert. 2010. Mapping tropical dry forest height, foliage height profiles and disturbance type and age with a time series of cloud-cleared Landsat and ALI image mosaics to characterize avian habitat. Remote Sensing of Environment 307:303–312.

Hijmans, R. J., J. van Etter, J. Cheng, M. Mattiuzzi, M. Summer, J. A. Greenberg, O. P. Lamigueiro, A. Bevan, E. B. Racine, A. Shortridge, and A. Ghosh. 2017. Geographic data analysis and modeling [R package raster version 2.9-5]. R CRAN Project.

Hislop, S., S. Jones, M. Soto-Berelov, A. Skidmore, A. Haywood, and T. H. Nguyen. 2019. A fusion approach to forest disturbance mapping using time series ensemble techniques. Remote Sensing of Environment 221:188–197.

Holland, J. E. Y. D., D. G. Bert, and L. Fahrig. 2004. Determine spatial scale of species' response to habitat. BioScience 54:227–233.

Hoover, C. M., and S. A. Rebain. 2011. Forest carbon estimation using the forest vegetation simulator: Seven things you need to know. Gen. Tech. Rep. NRS-77. Newtown Square, PA: U.S. Department of Agriculture, Forest Service, Northern Research Station 1–16.

Hudak, A. T., N. L. Crookston, J. S. Evans, M. J. Falkowski, A. M. S. Smith, P. E. Gessler, and P. Morgan. 2006. Regression modeling and mapping of coniferous forest basal area and tree density from discrete-return lidar and multispectral satellite data. Canadian Journal of Remote Sensing 32:126–138.

Hudak, A. T., N. L. Crookston, J. S. Evans, D. E. Hall, and M. J. Falkowski. 2008. Nearest neighbor imputation of species-level, plot-scale forest structure attributes from LiDAR data. Remote Sensing of Environment 112:2232–2245.

Huete, A., K. Didan, T. Miura, E. P. Rodriguez, X. Gao, and L. G. Ferreira. 2002. Overview of the radiometric and biophysical performance of the MODIS vegetation indices. Remote Sensing of Environment 83:195–213.

Ingram, J. C., T. P. Dawson, and R. J. Whittaker. 2005. Mapping tropical forest structure in southeastern Madagascar using remote sensing and artificial neural networks. Remote Sensing of Environment 94:491–507.

Jackson, H. B., and L. Fahrig. 2015. Are ecologists conducting research at the optimal scale? Global Ecology and Biogeography 24:52–63.

Jucker, T., B. Bongalov, D. F. R. P. Burslem, R. Nilus, M. Dalponte, S. L. Lewis, O. L. Phillips, L. Qie, and D. A. Coomes. 2018. Topography shapes the structure, composition and function of tropical forest landscapes. Ecology Letters 21:989–1000.

Jung, K., S. Kaiser, S. Böhm, J. Nieschulze, and E. K. V Kalko. 2012. Moving in three dimensions: Effects of structural complexity on occurrence and activity of insectivorous bats in managed forest stands. Journal of Applied Ecology 49:523–531.

Labrecque, S., R. A. Fournier, J. E. Luther, and D. Piercey. 2006. A comparison of four methods to map biomass from Landsat-TM and inventory data in western Newfoundland. Forest Ecology and Management 226:129–144.

Lefsky, M. A., W. B. Cohen, G. G. Parker, and D. J. Harding. 2002. Lidar remote sensing for ecosystem studies. BioScience 52:19–30.

LeMay, V., J. Maedel, and N. C. Coops. 2008. Estimating stand structural details using nearest neighbor analyses to link ground data, forest cover maps, and Landsat imagery. Remote Sensing of Environment 112:2578–2591.

López-Barrera, F., R. H. Manson, M. González-Espinosa, and A. C. Newton. 2006. Effects of the type of montane forest edge on oak seedling establishment along forest-edge-exterior gradients. Forest Ecology and Management 225:234–244.

le Maire, G., C. Marsden, Y. Nouvellon, C. Grinand, R. Hakamada, J. L. Stape, and J. P. Laclau. 2011. MODIS NDVI time-series allow the monitoring of Eucalyptus plantation biomass. Remote Sensing of Environment 115:2613–2625.

Maselli, F., and M. Chiesi. 2006. Integration of multi-source NDVI data for the estimation of Mediterranean forest productivity. International Journal of Remote Sensing 27:55–72.

Matlack, G. R. 1994. Vegetation dynamics of the forest edge: trends in space and successional time. Journal of Ecology 82:113–123.

McCullagh, P., and J. A. Nelder. 1989. Generalized Linear Models. 2nd edition. Chapman and Hall/CRC Monographs on Statistics and Applied Probability Series, Chapman & Hall.

Næsset, E., T. Gobakken, S. Solberg, T. G. Gregoire, R. Nelson, G. Ståhl, and D. Weydahl. 2011. Model-assisted regional forest biomass estimation using LiDAR and InSAR as auxiliary data: A case study from a boreal forest area. Remote Sensing of Environment 115:3599–3614.

Pascual, C., A. García-Abril, W. B. Cohen, and S. Martín-Fernández. 2010. Relationship between LiDAR-derived forest canopy height and Landsat images. International Journal of Remote Sensing 31:1261–1280.

Peterson, D. L., and V. T. Parker. 1998. Ecological Scale: Theory and Applications. Columbia University Press, editor. Ecological Economics.

Pierce, K. B., J. L. Ohmann, M. C. Wimberly, M. J. Gregory, and J. S. Fried. 2009. Mapping wildland fuels and forest structure for land management: A comparison of nearest neighbor imputation and other methods. Canadian Journal of Forest Research 39:1901–1916.

Pocewicz, A. L., P. Gessler, and A. P. Robinson. 2004. The relationship between effective plant area index and Landsat spectral response across elevation, solar insolation, and spatial scales in a northern Idaho forest. Canadian Journal of Forest Research 34:465–480.

Pond, N. C., R. E. Froese, and L. M. Nagel. 2014. Sustainability of the selection system in northern hardwood forests. Forest Science 60:374–381.

Ridgeway, G. 1999. The state of boosting. Computing Science and Statistics 31:172–181.

Saukkola, A., T. Melkas, K. Riekki, S. Sirparanta, J. Peuhkurinen, M. Holopainen, J. Hyyppä, and M. Vastaranta. 2019. Predicting forest inventory attributes using airborne laser scanning, aerial imagery, and harvester data. Remote Sensing 11:1–15.

Segurado, P., and M. B. Araújo. 2004. An evaluation of methods for modelling species distributions. Journal of Biogeography 31:1555–1568.

Solberg, S., E. Næsset, H. Lange, and O. M. Bollandås. 2004. Remote Sensing of Forest Health. Pages 161–166 in. ISPRS WG VIII/2 Workshop 'Laser-Scanners for Forest and LandscapeAssessment’. International Archives of Photogrammetry, Remote Sensing andSpatial Information Sciences. Volume 36.

Stephens, P. R., M. O. Kimberley, P. N. Beets, T. S. H. Paul, N. Searles, A. Bell, C. Brack, and J. Broadley. 2012. Airborne scanning LiDAR in a double sampling forest carbon inventory. Remote Sensing of Environment 117:348–357.

Tehrany, M. S., S. Jones, F. Shabani, F. Martínez-Álvarez, and D. Tien Bui. 2019. A novel ensemble modeling approach for the spatial prediction of tropical forest fire susceptibility using LogitBoost machine learning classifier and multi-source geospatial data. Theoretical and Applied Climatology 137:637–653.

Thuiller, W. 2003. BIOMOD - Optimizing predictions of species distributions and projecting potential future shifts under global change. Global Change Biology 9:1353–1362.

Tonolli, S., M. Dalponte, M. Neteler, M. Rodeghiero, L. Vescovo, and D. Gianelle. 2011. Fusion of airborne LiDAR and satellite multispectral data for the estimation of timber volume in the Southern Alps. Remote Sensing of Environment 115:2486–2498.

Tucker, C. J. 1979. Red and photographic infrared linear combinations for monitoring vegetation. Remote Sensing of Environment 8:127–150.

Turner, W., S. Spector, N. Gardiner, M. Fladeland, E. Sterling, and M. Steininger. 2003. Remote sensing for biodiversity science and conservation. Trends in Ecology and Evolution 18:306–314.

Watt, P. J., D. N. M. Donoghue, K. B. McManus, and R. W. Dunford. 2004. Predicting forest height from IKONOS, LANDSAT and LIDAR imagery. ISPRS Arch. XXXVI-8/W2:228–231.

Wolter, P. T., P. A. Townsend, and B. R. Sturtevant. 2009. Estimation of forest structural parameters using 5 and 10 meter SPOT-5 satellite data. Remote Sensing of Environment 113:2019–2036.

Wood, S. N. 2011. Fast stable restricted maximum likelihood and marginal likelihood estimation of semiparametric generalized linear models. Journal of the Royal Statistical Society. Series B: Statistical Methodology 73:3–36.

Wulder, M. A., C. W. Bater, N. C. Coops, T. Hilker, and J. C. White. 2008. The role of LiDAR in sustainable forest management. Forestry Chronicle 84:807–826.

Zhao, K., S. Popescu, X. Meng, Y. Pang, and M. Agca. 2011. Characterizing forest canopy structure with lidar composite metrics and machine learning. Remote Sensing of Environment 115:1978–1996.

TABLES AND FIGURES

Table 1. Univariate pair-wise Pearson’s correlation calculated between vegetation indices (NDVI and EVI) and forest structure measurements (basal area and tree density), according to time-window, statistic metric (mean and standard deviation), and variables’ manipulation approach (i.e., temporal and spatial-first). All correlation values are reported as mean value of the Pearson’s correlation calculated at each grain size, excepted for environmental variables.

Varibales	**Pearson’s correlation coefficients (*r*)**				
	May-June	**May-July**	**June-July**	**June-August**	**No time-window**
F. sylvatica					
Basal area					
EVI[a]	**0.11**	**0.11**	**0.09**	**0.11**	-
Smean	0.12	0.12	0.12	0.13	-
Ssd	-0.20	-0.17	-0.09	-0.13	-
Tmean	0.08	0.07	0.10	0.12	-
Tsd	0.04	0.06	0.04	-0.07	-
NDVI[a]	**0.09**	**0.08**	**0.07**	**0.14**	**-**
Smean	0.06	0.06	0.08	0.14	-
Ssd	-0.20	-0.16	-0.09	-0.12	-
Tmean	0.05	0.05	0.08	0.12	-
Tsd	0.05	0.05	-0.03	-0.17	-
DEM	-	-	-	-	0.07
DistFor	-	-	-	-	-0.08
Slope	-	-	-	-	-0.10
SolRad	-	-	-	-	0.14
Tree density					
EVI[a]	**0.16**	**0.17**	**0.22**	**0.19**	**-**
Smean	-0.23	-0.25	-0.27	-0.20	-
Ssd	0.18	0.19	0.21	0.15	-
Tmean	-0.20	-0.18	-0.27	-0.21	-
Tsd	0.04	0.06	0.14	-0.19	-
NDVI[a]	**0.18**	**0.18**	**0.17**	**0.16**	**-**
Smean	-0.22	-0.22	-0.20	-0.15	-
Ssd	0.23	0.22	0.20	0.17	-
Tmean	-0.19	-0.14	-0.20	-0.15	-
Tsd	0.10	0.12	-0.08	-0.18	-
DEM	-	-	-	-	0.12
DistFor	-	-	-	-	0.05
Slope	-	-	-	-	0.13
SolRad	-	-	-	-	-0.07

[a] expressed as absolute value.

Table 1. (continued) Univariate pair-wise Pearson's correlation calculated between vegetation indices (NDVI and EVI) and forest structure measurements (basal area and tree density), according to time-window, statistic metric (mean and standard deviation), and variables' manipulation approach (i.e., temporal and spatial-first). All correlation values are reported as mean value of the Pearson's correlation calculated at each grain size, excepted for environmental variables.

Varibales	**Pearson's correlation coefficients (*r*)**				
	May-June	**May-July**	**June-July**	**June-August**	**No time-window**
***Quercus* spp.**					
Basal area					
EVI^a	**0.21**	**0.23**	**0.28**	**0.24**	**-**
Smean	0.23	0.25	0.32	0.30	-
Ssd	-0.17	-0.20	-0.20	-0.20	-
Tmean	0.24	0.26	0.33	0.31	-
Tsd	0.20	0.20	-0.28	-0.14	-
NDVI^a	**0.21**	**0.23**	**0.32**	**0.29**	**-**
Smean	0.27	0.29	0.39	0.37	-
Ssd	-0.26	-0.27	-0.25	-0.23	-
Tmean	0.28	0.31	0.41	0.38	-
Tsd	0.04	0.04	-0.23	-0.17	-
DEM	-	-	-	-	0.12
DistFor	-	-	-	-	-0.22
Slope	-	-	-	-	-0.03
SolRad	-	-	-	-	0.18
Tree density					
EVI^a	**0.12**	**0.13**	**0.17**	**0.15**	**-**
Smean	0.16	0.19	0.20	0.18	-
Ssd	0.11	0.07	-0.10	-0.08	-
Tmean	0.15	0.18	0.20	0.18	-
Tsd	-0.06	-0.08	-0.17	-0.17	-
NDVI^a	**0.15**	**0.17**	**0.22**	**0.22**	**-**
Smean	0.21	0.24	0.26	0.27	-
Ssd	-0.09	-0.10	-0.14	-0.12	-
Tmean	0.20	0.22	0.26	0.27	-
Tsd	-0.10	-0.12	-0.19	-0.20	-
DEM	-	-	-	-	-0.18
DistFor	-	-	-	-	-0.27
Slope	-	-	-	-	0.40
SolRad	-	-	-	-	-0.31

[a]: expressed as absolute value.

Table 2. Covariates composing full models used to develop forest structure models. I contrasted the full model with models developed using all possible combinations of covariates and several model algorithms (GLM, GAM, RF, and GBM) in an ensemble modeling procedure to predict stand structure attributes (tree density and basal area) for each tree species (beech and oak).

Dominant Species	**Response variable**[a]	**Model algorithm**[b]	***K***[c]	**Full model**[d]
Beech	BA	GLMs GAMs RFs GBMs	10	Savg-NDVI-30$_{(JunAug)}$ + Ssd-NDVI-300$_{(MayJun)}$ + Savg-EVI-210$_{(MayJul)}$ + Savg-EVI-270$_{(JunAug)}$ + Ssd-EVI-300$_{(MayJun)}$ + Ssd-EVI-300$_{(JunAug)}$ + DEM + Slp + DistFor + SolRad$_{(JunAug)}$
	TD	GLMs GAMs RFs GBMs	11	Tavg-EVI-60$_{(MayJun)}$ + Savg-EVI-210$_{(MayJul)}$ + Tavg-EVI-60$_{(JunJul)}$ + Ssd-EVI-210$_{(JunJul)}$ + Savg-NDVI-60$_{(JunJul)}$ + Ssd-NDVI-30$_{(MayJul)}$ + Ssd-NDVI-90$_{(JunAug)}$ + Slp + DEM + DistFor + SolRad$_{(JunJul)}$
Oak	BA	GLMs GAMs RFs GBMs	14	Ssd-EVI-300$_{(MayJun)}$ + Tsd-EVI-240$_{(MayJun)}$ + Ssd-EVI-300$_{(JunJul)}$ + Tsd-EVI-30$_{(JunJul)}$ + Tsd-EVI-30$_{(JunAug)}$ + Tavg-NDVI-30$_{(JunJul)}$ + Ssd-NDVI-270$_{(MayJul)}$ + Ssd-NDVI-30$_{(JunJuly)}$ + Tsd-NDVI-30$_{(JunJul)}$ + Tsd-NDVI-30$_{(JunAug)}$ + DEM + Slp + DistFor + SolRad$_{(JunJul)}$
	TD	GLMs GAMs RFs GBMs	14	Ssd-EVI-180$_{(MayJun)}$ + Tsd-EVI-240$_{(JunJul)}$ + Tsd-EVI-240$_{(JunAug)}$ + Savg-NDVI-30$_{(MayJul)}$ + Savg-NDVI-30$_{(JunAug)}$ + Ssd-NDVI-240$_{(MayJul)}$ + Tsd-NDVI-300$_{(MayJul)}$ + Ssd-NDVI-30$_{(JunJul)}$ + Tsd-NDVI-210$_{(JunJul)}$ + Tsd-NDVI-240$_{(JunAug)}$ + DEM + Slp + DistFor + SolRad$_{(JunJul)}$

[a]: BA = basal area; TD = tree density.

[b]: GLMs = generalized linear models; GAMs = generalized additive models; RFs = random forest models; GBMs = generalized boosted regression models

[c]: number of explanatory variables.

[d]: Savg = “spatial-first” approach, using mean statistic; Ssd = “spatial-first” approach, using standard deviation statistic; Tavg = “temporal-first” approach, using mean statistic; Tsd = “temporal-first” approach, using standard deviation statistic; DEM = altitude; Slp = slope; DisFor = distance to forest edge; SolRad = solar radiation. Time windows: MayJun = from May to June; MayJul = from May to July; JunJul = from June to July; JunAug = from June to August.

Table 3. Root mean square error (RMSE) calculated by the weighted mean of all models obtained from the model evaluation procedure (i.e. Pearson's *r*>0.6). For each algorithm (GLM, GAM, GBM, and RF), I reported RSME values as mean and standard deviation (in parentheses), and the RMSE calculated from the ensemble model calculated as the weighted average (i.e., single Pearson's *r* score) among all retained models. GLM: generalize linear model; GAM: generalized additive model; GBM: generalized boosted regression model; RF: random forest.

Dominant tree species	**Forest structural attributes**	**RSME**				
		GLM	**GAM**	**GBM**	**RF**	**Ensemble**
Beech	BA	17.82 (±00.7)	17.87 (±0.07)	13.43 (±0.30)	9.88 (±0.51)	14.39
Oak	BA	10.57 (±0.04)	10.75 (±0.08)	7.05 (±0.25)	5.75 (±0.42)	8.14
Beech	TD	992.24 (±3.28)	993.98 (±6.64)	757.36 (±18.88)	530.69 (±45.49)	977.36
Oak	TD	955.67 (±6.82)	993.59 (±15.19)	698.97 (±34.97)	548.01 (±20.53)	807.92

Figure 1. Study area (black polygon) encompass the wooded areas (green color) within the composite Minimum Convex Polygon (100%MCP) calculated using all national forest inventory (NFI; red stars) and local forest inventory (Forest Service of Unione Territoriale di Castel di Sangro, UTB; yellow stars) plots included in the analysis, and collected within the Abruzzo Lazio and Molise National park (PNALM) and its external areas.

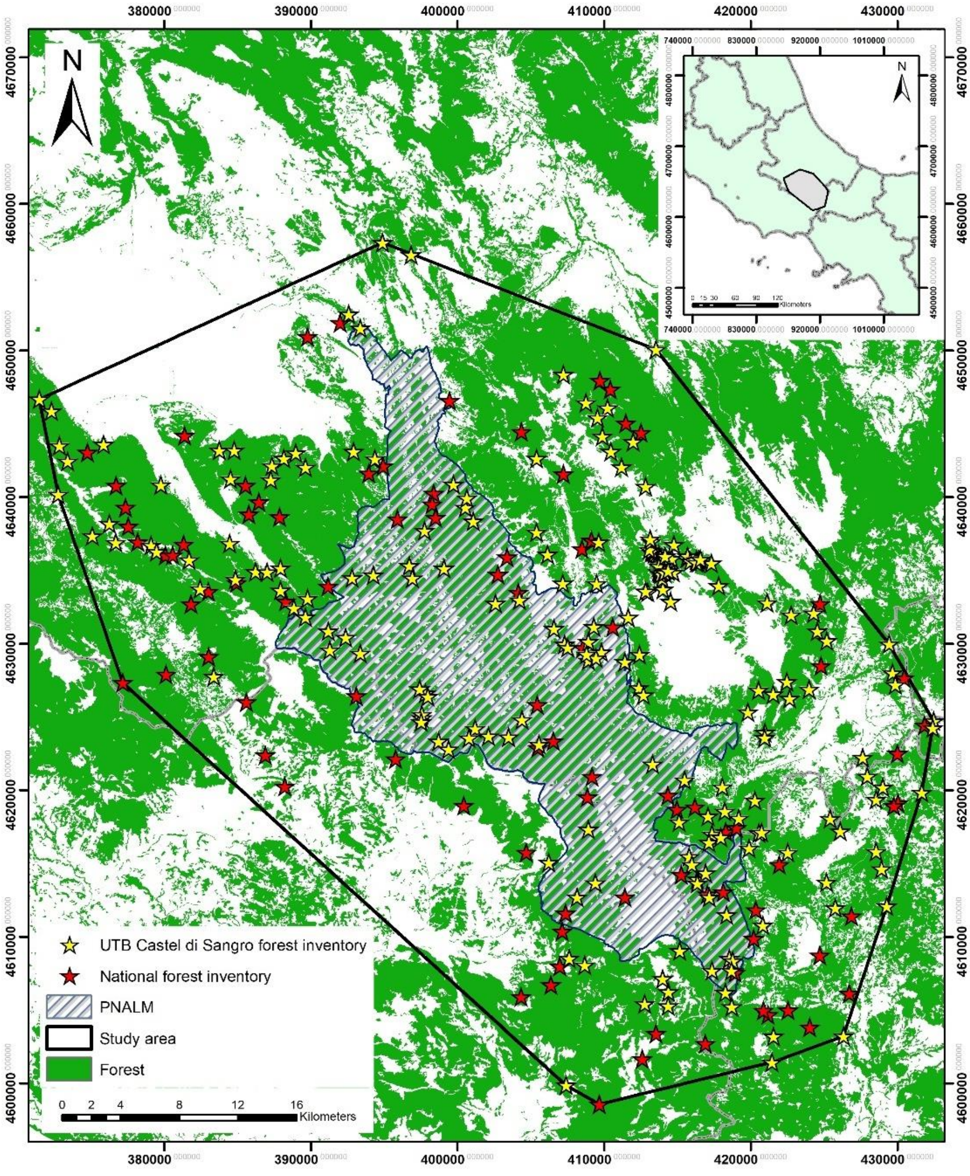

Figure 2. Modelling workflow design: starting from NDVI and EVI images derived by Landsat ETM+/TM remote sensing (RS) data ("RS images" in the figure), I divided all images into time-windows (2-3 months temporal resolution; "Time-window division"); next, I manipulated over the time and space the vegetation indices using mean and standard deviation as algebra statistics in GIS environment ("Spatial and temporal manipulation"); then, I tested the variables multicollinearity ("Multicollinearity"), and I retained all uncorrelated variables ($r<0.8$) used to predict forest strcuture models (i.e., tree density and basal area) in an ensemble modeling procedure. Vegetation indices (1) = NDVI and EVI divided by time-window (i.e., May-June, May-July, June-July, June-August); Vegetation indices (2) = NDVI and EVI calculated using mean and standard deviation as algebra statistics within both "spatial-first" and "temporal-first" variables manipulation approach (for more details see Fig.3); Vegetation indices (3) = set of the best predictive (i.e., higher Pearson's correlation coefficient) varibales after grain-sizes selection, i.e. one grain for each time-window.

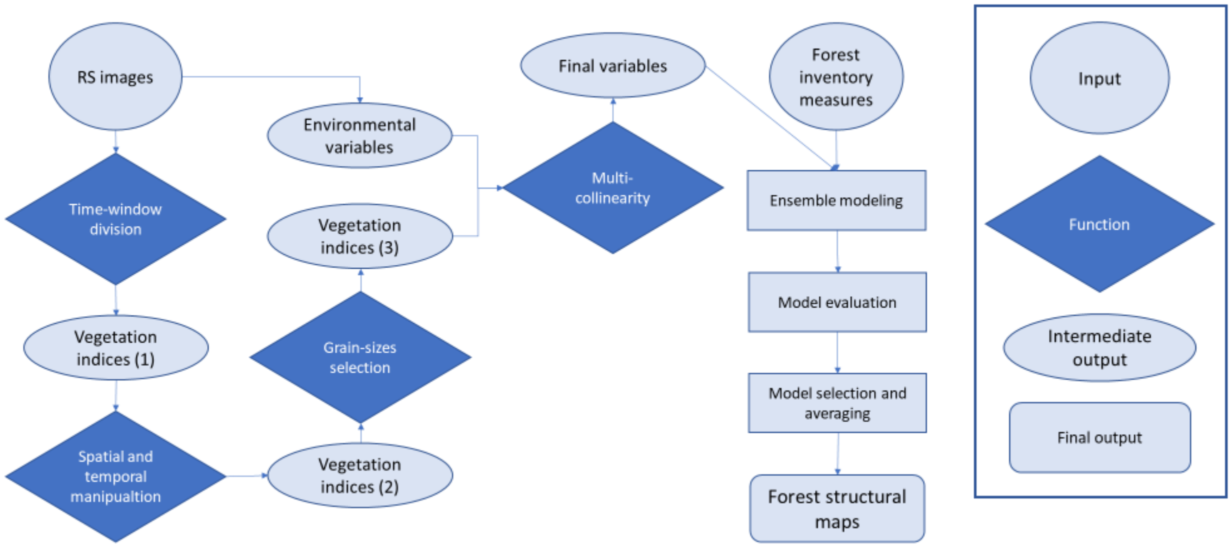

Figure 3. Spatial and temporal manipulation of the vegetational indices (i.e., NDVI and EVI). (A) Using the "temporal-first" approach vegetational indices are firstly combined over the time (i.e., each pixel have the mean or standard deviation of all combined satellite images), and then, I averaged over the space using differen spatial grains (i.e., from 30 to 300 m, by 30 m); B) using the "spatial-first" approach (B) vegetational indices are first spatially combined over the space (i.e., each pixel is the mean or standard deviation extracted around a buffer, calculated by using different grain sizes), and then averaged over the time (i.e., using all images within each time-window). Specifically, in the "temporal-first" manipulation approach, I first calculated the mean and standard deviation value for each pixel using all images grouped in each time-window (i.e., temporal-mean and temporal-standard deviation), and then, the average value within a circular buffer for each spatial grain; at the contrary, using the "spatial-first" manipulation approach, for each pixel in each image I first calculated the mean and standard deviation value using different spatial grains (i.e., spatial-mean and spatial-standard deviation), and then, for each time-window and grain size I extracted the average value by each pixel.

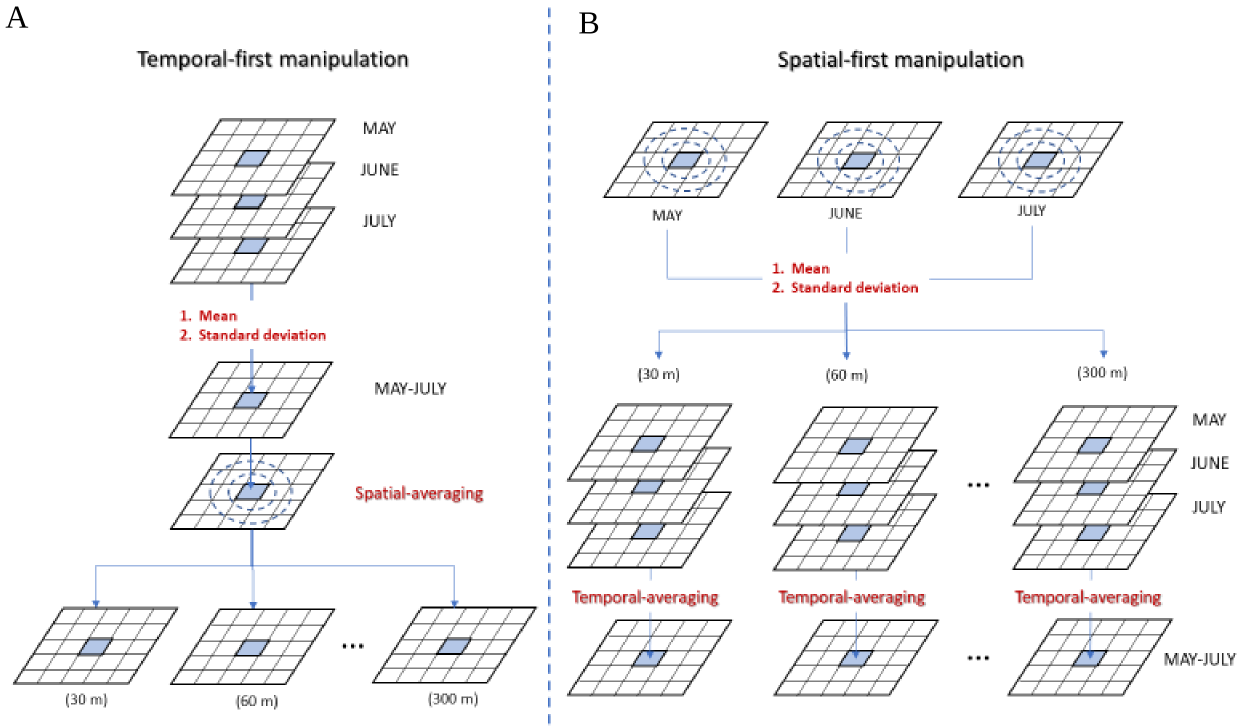

Figure 4. Violin boxplot representing the Person's correlation (*r*) scores distribution (y-axis) derived by each model selected from the model evaluation (*r*>0.6) grouped by forest dominated species (beech and oak) and stand structure attribute (tree density and basal area), and separated by model algorithm (x-axis): generalized linear model (GLM), generalized additive model (GAM), generalized boosted regression model (GBM), and random forest (RF). For each algorithm, species, and forest structure I also reported the average Pearson's score (red color).

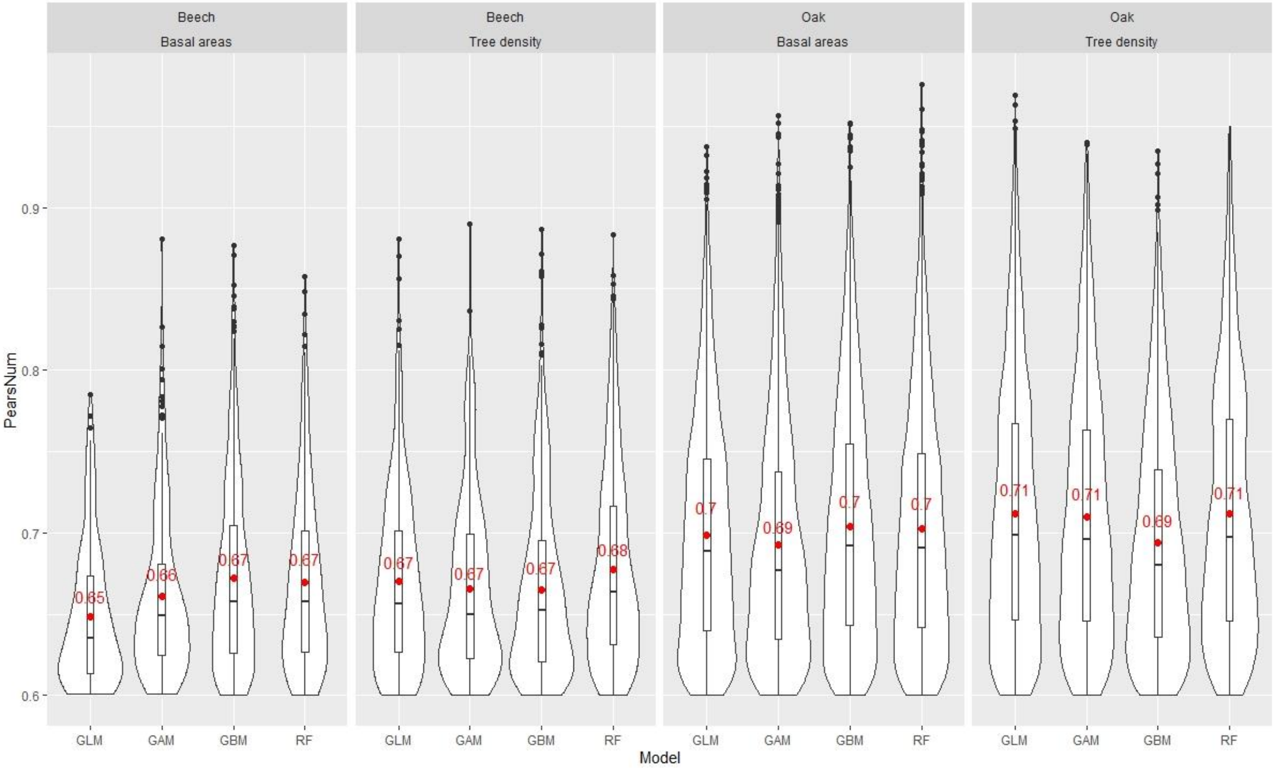

Figure 5. Pearson's correlation (*r*) distribution derived by the permutation test performed by modeling 10,000 random models for each stand structure measure and tree species: (A) beech's basal area, (B) beech's tree density, (C) oak's basal area, and (D) oak's tree density. I compared the value used as cut-off threshold value (*r*=0.6) in the model evaluation (dotted line) with the value derived by the confidence interval calculated at the 95%ile of the random distribution (95%CI; solid line). The null-hypothesis (H_0) assume that there is no difference between predicted and random models (i.e., IC95% > 0.6), while the alternative hypothesis (H_1) propose that predicted models are statistically different from randomness (i.e., IC95% < 0.6). In all situations described above, I reject H_0 and accept H_1 (IC95%<0.6).

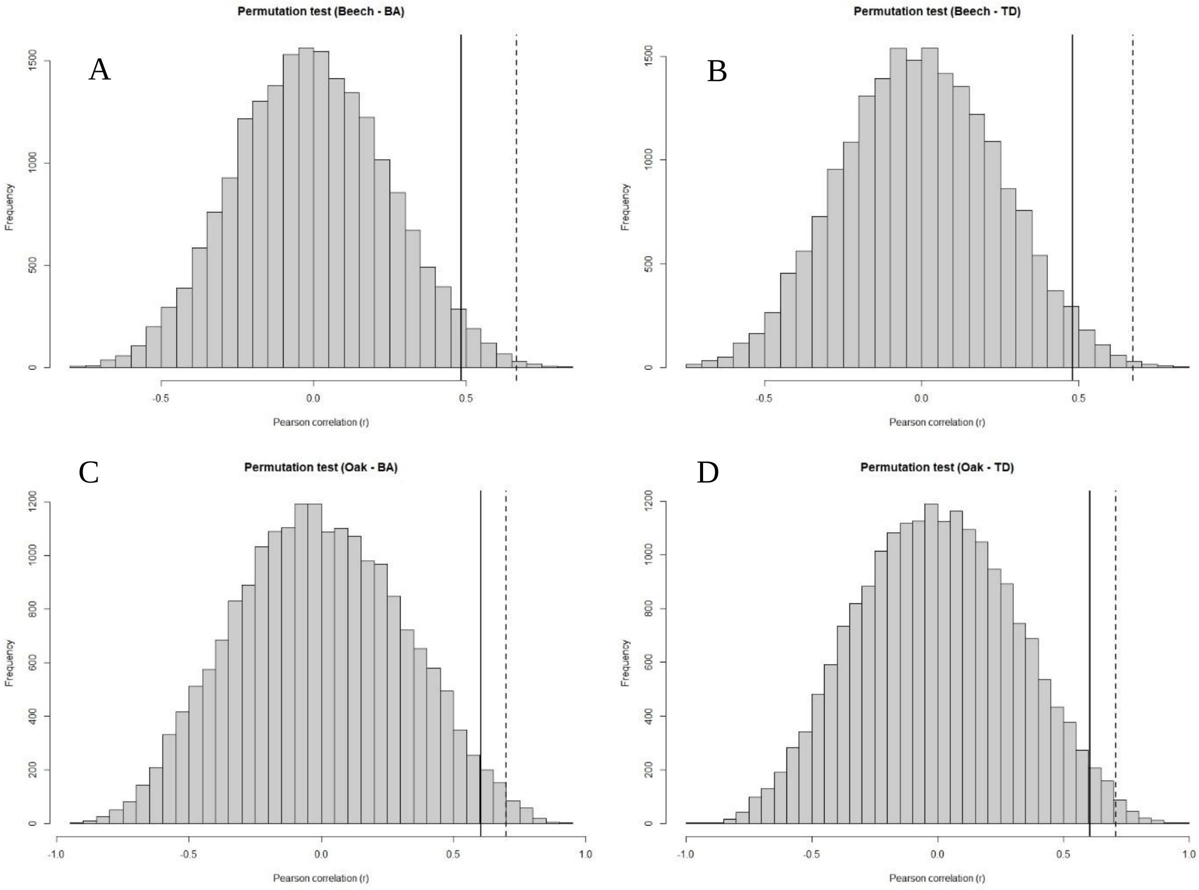

Figure 6. Basal area predicted values derived by the combination of beech and oak basal area predicted values (averaged models) and developed by an ensemble modeling procedure. Continuous values indicate forest patches with higher (dark green) and lower (light green) tree's basal area (m^2/ha).

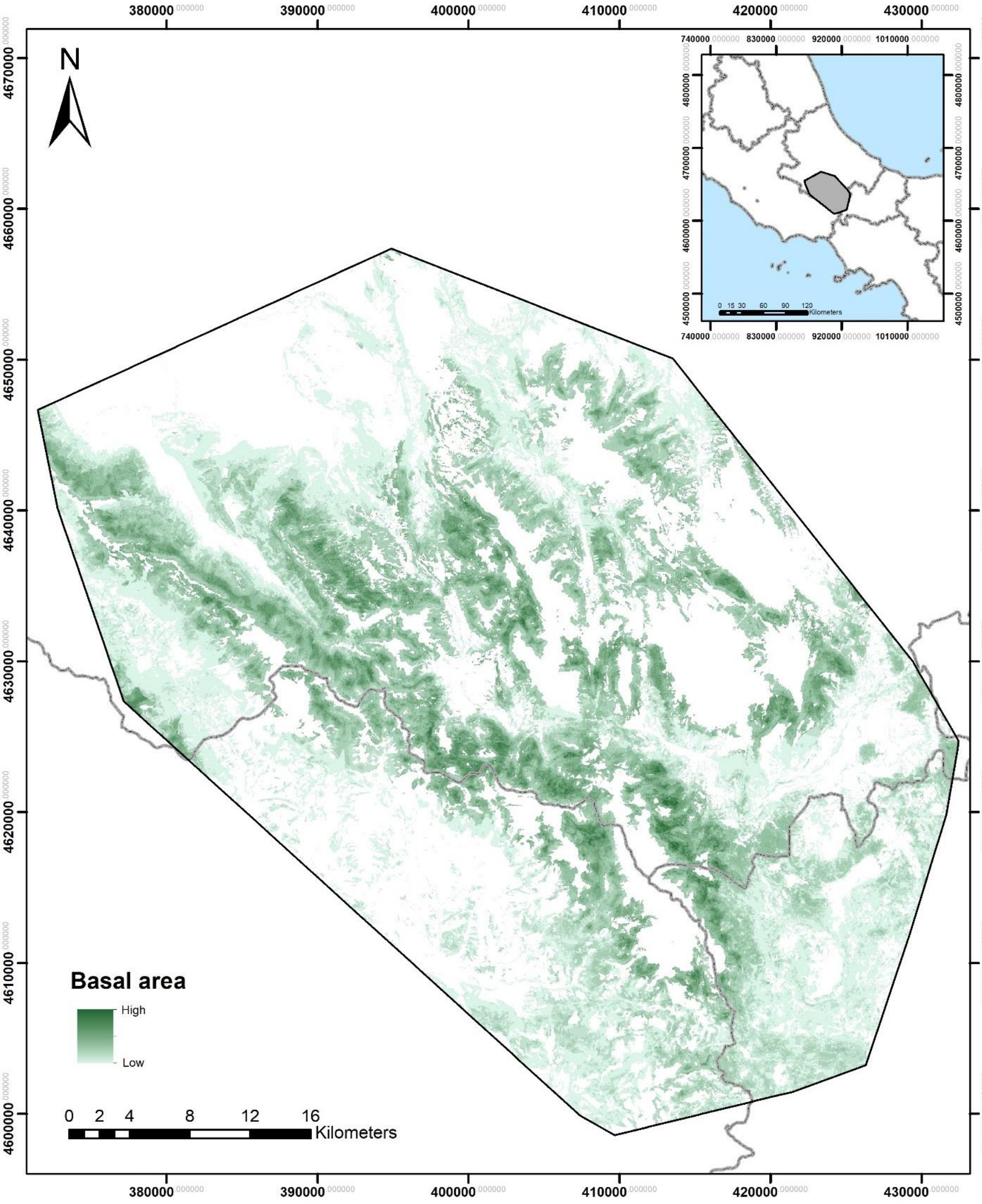

Figure 7. Tree density predicted values derived by the combination of beech and oak tree density predicted values (averaged models) and developed by an ensemble modeling procedure. Continuous values indicate forest patches with higher (dark green) and lower (light green) tree density (N/ha).

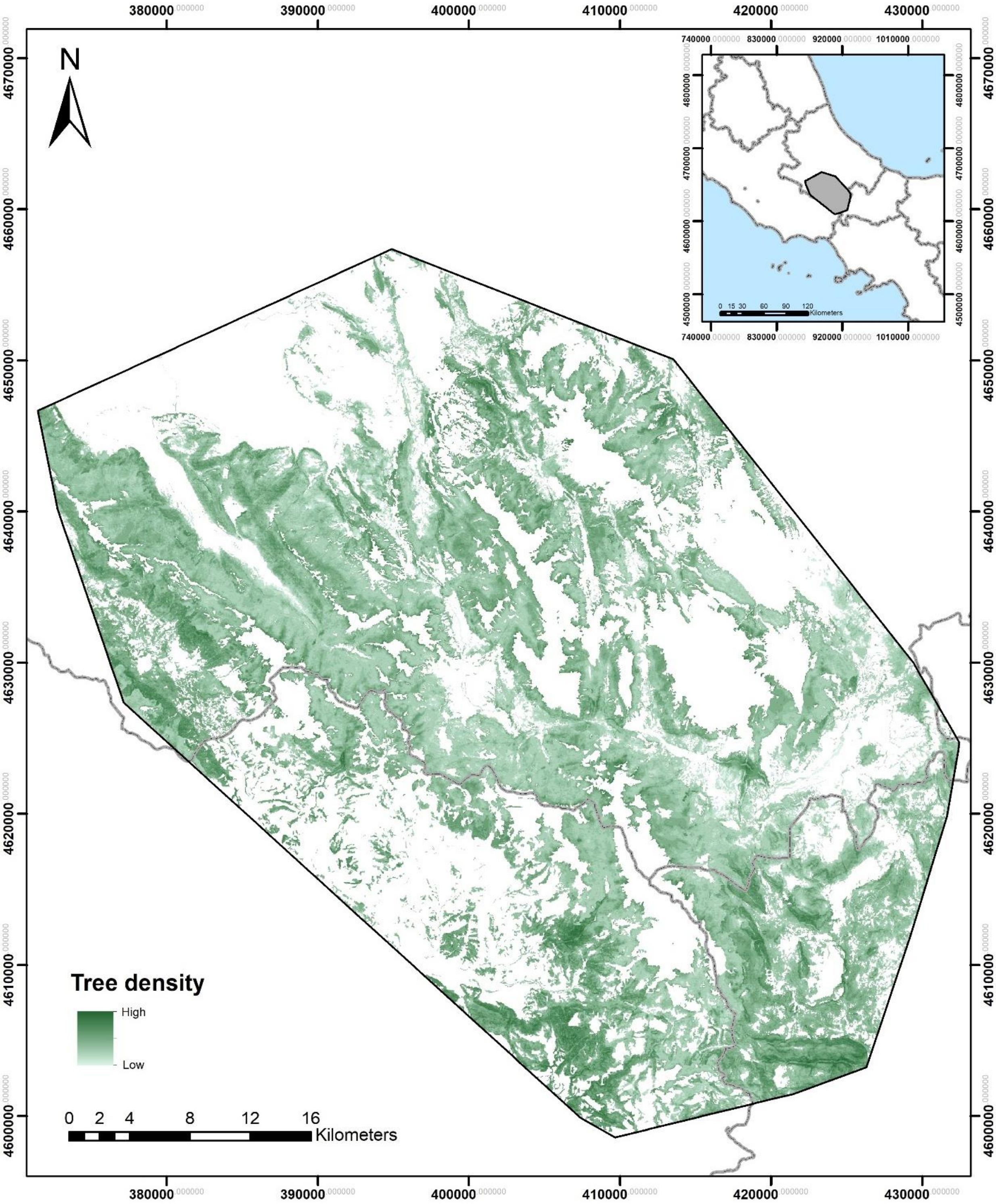

Figure 8. Averaged basal area (and DBH) predicted values derived by the division between basal area (and DBH) and tree density forest maps. Continuous values indicate forest patches with higher (dark green) and lower (light green) BA (and DBH).

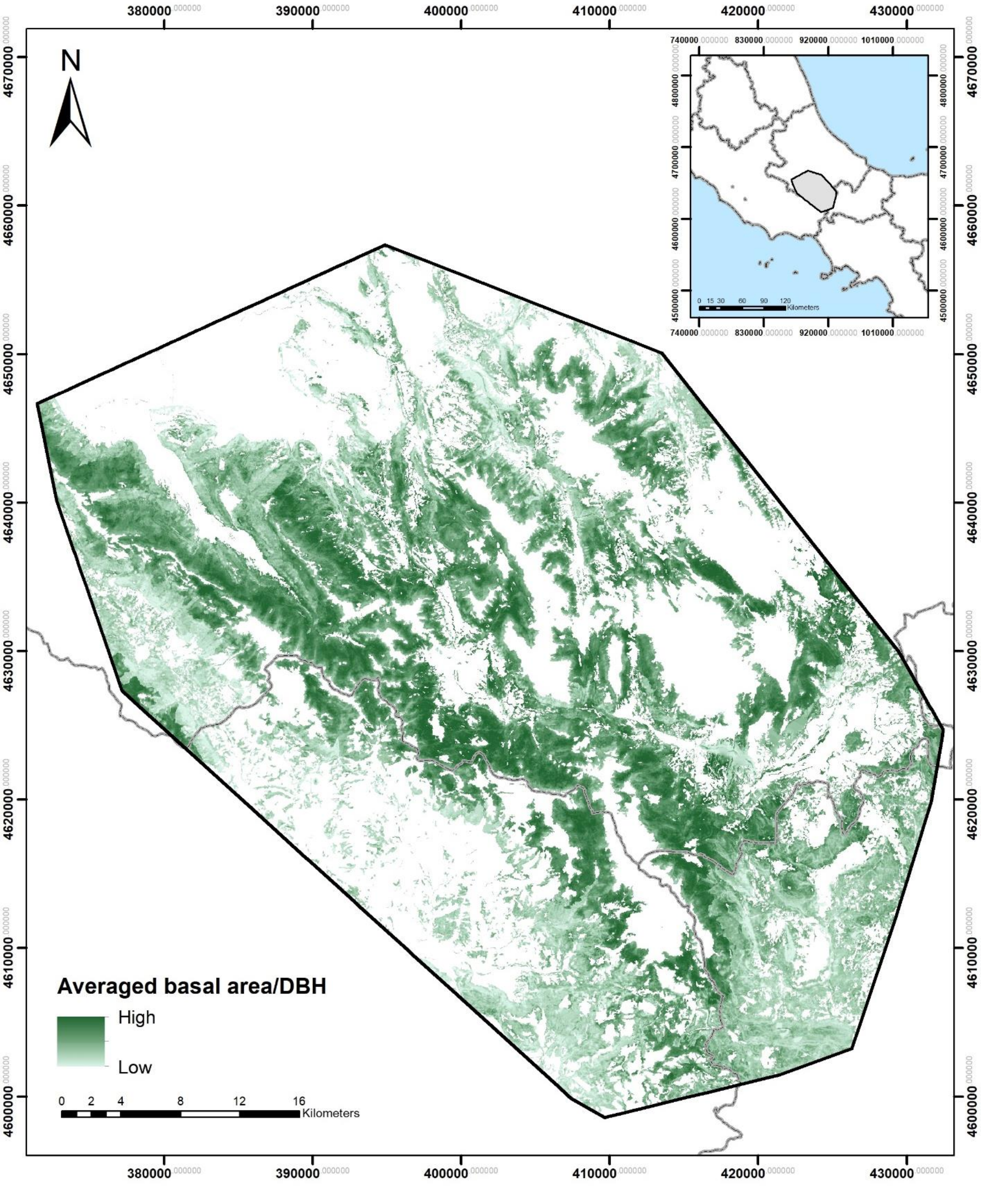

Figure 9. Response curves created by fitting an additive term in the linear regression (GAM; Wood 2011) between the values of (A) DBH and (B) tree density collected by Forestry Service on the field (expected values; y-axis) and derived by final averaged predicted value (predicted values; x-axis), combining both beech and oak forest strcuture maps. I also reported the root mean square error (RMSE) for each stand structure measure. Both expected and predicte values are extracted at the forest unit management scale of resoultion.

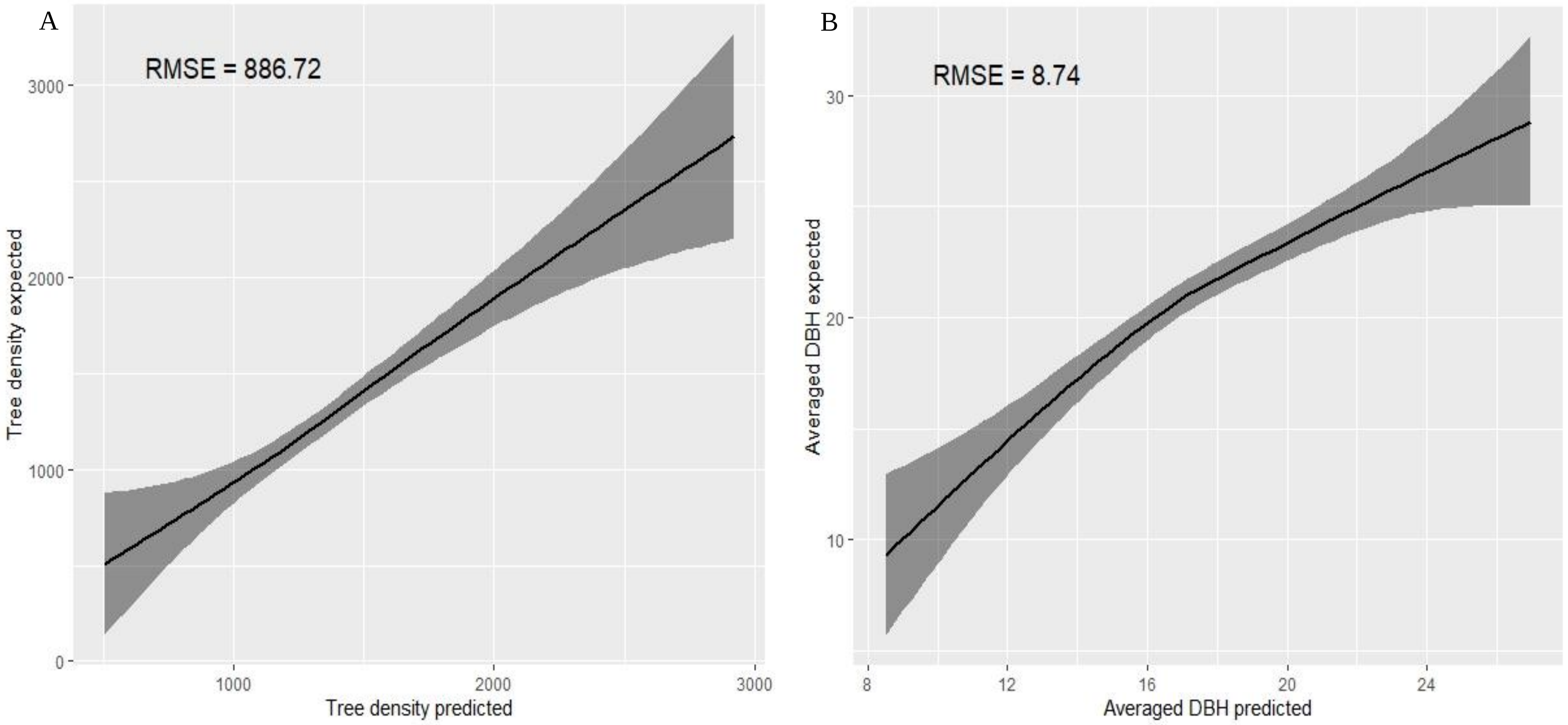

SUPPLEMENTARY MATERIAL

Forest inventory data collection

Comparing forest map accuracy with the local and NFIs data used in this analysis, I found that 168 inventory plots classified as beech forest (95.45%) occur correctly within beech forest class of the local forest map, of which 5 falling in oaks and 3 in hop-hornbeam forest; 87 plots classified as oak forest (88.76%) fall within oaks forest, with 6 falling in hop-hornbeam, 4 in beech and 1 in hygrophilous forest; 9 plots classified as hop-hornbeam forest (52.94%) fall within hop-hornbeam forest, with 7 falling in oaks and 1 in beech forest; only 1 of 3 plots classified as hygrophilous forest (33.33%) are in hygrophilous forest, with 2 fall within oaks forest. All inventory plots classified as coniferous forest (n=7) fall within coniferous forest class (100%).

Table S1. Multi-grain variables selection where I reported the grain size with the highest correlation score, one for each dominant tree species (beech and oak), stand attribute measure (basal area and tree density), vegetation index (NDVI and EVI), temporal window (May-June, May-July, June-July, and June-August), multi-scale approach (spatial-first and temporal-first approaches), and spatial grain (from 30 to 300 m, by 30 m).

Species	Forest structure attribute	Vegetation index	Temporal window	Statistic	Variable manipulation approach	Spatial grain (m)
Beech	Basal area	EVI	May-June	mean	"spatial-first"	210
Beech	Basal area	EVI	May-June	mean	"temporal-first"	300
Beech	Basal area	EVI	May-July	mean	"spatial-first"	210
Beech	Basal area	EVI	May-July	mean	"temporal-first"	300
Beech	Basal area	EVI	June-July	mean	"spatial-first"	240
Beech	Basal area	EVI	June-July	mean	"temporal-first"	300
Beech	Basal area	EVI	June-August	mean	"spatial-first"	270
Beech	Basal area	EVI	June-August	mean	"temporal-first"	300
Beech	Basal area	EVI	May-June	SD	"spatial-first"	300
Beech	Basal area	EVI	May-June	SD	"temporal-first"	300
Beech	Basal area	EVI	May-July	SD	"spatial-first"	300
Beech	Basal area	EVI	May-July	SD	"temporal-first"	300
Beech	Basal area	EVI	June-July	SD	"spatial-first"	300
Beech	Basal area	EVI	June-July	SD	"temporal-first"	60
Beech	Basal area	EVI	June-August	SD	"spatial-first"	300
Beech	Basal area	EVI	June-August	SD	"temporal-first"	300
Beech	Basal area	NDVI	May-June	mean	"spatial-first"	210
Beech	Basal area	NDVI	May-June	mean	"temporal-first"	300
Beech	Basal area	NDVI	May-July	mean	"spatial-first"	210
Beech	Basal area	NDVI	May-July	mean	"temporal-first"	300
Beech	Basal area	NDVI	June-July	mean	"spatial-first"	30
Beech	Basal area	NDVI	June-July	mean	"temporal-first"	300
Beech	Basal area	NDVI	June-August	mean	"spatial-first"	30
Beech	Basal area	NDVI	June-August	mean	"temporal-first"	30
Beech	Basal area	NDVI	May-June	SD	"spatial-first"	300
Beech	Basal area	NDVI	May-June	SD	"temporal-first"	30
Beech	Basal area	NDVI	May-July	SD	"spatial-first"	300
Beech	Basal area	NDVI	May-July	SD	"temporal-first"	30
Beech	Basal area	NDVI	June-July	SD	"spatial-first"	300
Beech	Basal area	NDVI	June-July	SD	"temporal-first"	30
Beech	Basal area	NDVI	June-August	SD	"spatial-first"	300
Beech	Basal area	NDVI	June-August	SD	"temporal-first"	180
Beech	Tree density	EVI	May-June	mean	"spatial-first"	240
Beech	Tree density	EVI	May-June	mean	"temporal-first"	60
Beech	Tree density	EVI	May-July	mean	"spatial-first"	210
Beech	Tree density	EVI	May-July	mean	"temporal-first"	30
Beech	Tree density	EVI	June-July	mean	"spatial-first"	60
Beech	Tree density	EVI	June-July	mean	"temporal-first"	60
Beech	Tree density	EVI	June-August	mean	"spatial-first"	60
Beech	Tree density	EVI	June-August	mean	"temporal-first"	60
Beech	Tree density	EVI	May-June	SD	"spatial-first"	210
Beech	Tree density	EVI	May-June	SD	"temporal-first"	30
Beech	Tree density	EVI	May-July	SD	"spatial-first"	210

Table S1. (continued) Multi-grain variables selection where I reported the grain size with the highest correlation score, one for each dominant tree species (beech and oak), stand attribute measure (basal area and tree density), vegetation index (NDVI and EVI), temporal window (May-June, May-July, June-July, and June-August), multi-scale approach (spatial-first and temporal-first approaches), and spatial grain (from 30 to 300 m, by 30 m).

Species	**Forest structure attribute**	**Vegetation index**	**Temporal window**	**Statistic**	**Variable manipulation approach**	**Spatial grain (m)**
Beech	Tree density	EVI	May-July	SD	"temporal-first"	60
Beech	Tree density	EVI	June-July	SD	"spatial-first"	210
Beech	Tree density	EVI	June-July	SD	"temporal-first"	30
Beech	Tree density	EVI	June-August	SD	"spatial-first"	90
Beech	Tree density	EVI	June-August	SD	"temporal-first"	270
Beech	Tree density	NDVI	May-June	mean	"spatial-first"	240
Beech	Tree density	NDVI	May-June	mean	"temporal-first"	60
Beech	Tree density	NDVI	May-July	mean	"spatial-first"	210
Beech	Tree density	NDVI	May-July	mean	"temporal-first"	60
Beech	Tree density	NDVI	June-July	mean	"spatial-first"	60
Beech	Tree density	NDVI	June-July	mean	"temporal-first"	60
Beech	Tree density	NDVI	June-August	mean	"spatial-first"	60
Beech	Tree density	NDVI	June-August	mean	"temporal-first"	60
Beech	Tree density	NDVI	May-June	SD	"spatial-first"	30
Beech	Tree density	NDVI	May-June	SD	"temporal-first"	30
Beech	Tree density	NDVI	May-July	SD	"spatial-first"	30
Beech	Tree density	NDVI	May-July	SD	"temporal-first"	60
Beech	Tree density	NDVI	June-July	SD	"spatial-first"	180
Beech	Tree density	NDVI	June-July	SD	"temporal-first"	210
Beech	Tree density	NDVI	June-August	SD	"spatial-first"	90
Beech	Tree density	NDVI	June-August	SD	"temporal-first"	240
Oak	Basal area	EVI	May-June	mean	"spatial-first"	180
Oak	Basal area	EVI	May-June	mean	"temporal-first"	270
Oak	Basal area	EVI	May-July	mean	"spatial-first"	60
Oak	Basal area	EVI	May-July	mean	"temporal-first"	240
Oak	Basal area	EVI	June-July	mean	"spatial-first"	30
Oak	Basal area	EVI	June-July	mean	"temporal-first"	30
Oak	Basal area	EVI	June-August	mean	"spatial-first"	30
Oak	Basal area	EVI	June-August	mean	"temporal-first"	30
Oak	Basal area	EVI	May-June	SD	"spatial-first"	300
Oak	Basal area	EVI	May-June	SD	"temporal-first"	270
Oak	Basal area	EVI	May-July	SD	"spatial-first"	300
Oak	Basal area	EVI	May-July	SD	"temporal-first"	240
Oak	Basal area	EVI	June-July	SD	"spatial-first"	300
Oak	Basal area	EVI	June-July	SD	"temporal-first"	30
Oak	Basal area	EVI	June-August	SD	"spatial-first"	300
Oak	Basal area	EVI	June-August	SD	"temporal-first"	60
Oak	Basal area	NDVI	May-June	mean	"spatial-first"	270
Oak	Basal area	NDVI	May-June	mean	"temporal-first"	30
Oak	Basal area	NDVI	May-July	mean	"spatial-first"	180
Oak	Basal area	NDVI	May-July	mean	"temporal-first"	30
Oak	Basal area	NDVI	June-July	mean	"spatial-first"	30
Oak	Basal area	NDVI	June-July	mean	"temporal-first"	30
Oak	Basal area	NDVI	June-August	mean	"spatial-first"	30
Oak	Basal area	NDVI	June-August	mean	"temporal-first"	30
Oak	Basal area	NDVI	May-June	SD	"spatial-first"	300

Table S1. (continued) Multi-grain variables selection where I reported the grain size with the highest correlation score, one for each dominant tree species (beech and oak), stand attribute measure (basal area and tree density), vegetation index (NDVI and EVI), temporal window (May-June, May-July, June-July, and June-August), multi-scale approach (spatial-first and temporal-first approaches), and spatial grain (from 30 to 300 m, by 30 m).

Species	Forest structure attribute	Vegetation index	Temporal window	Statistic	Variable manipulation approach	Spatial grain (m)
Oak	Basal area	NDVI	May-June	SD	"temporal-first"	210
Oak	Basal area	NDVI	May-July	SD	"spatial-first"	270
Oak	Basal area	NDVI	May-July	SD	"temporal-first"	210
Oak	Basal area	NDVI	June-July	SD	"spatial-first"	30
Oak	Basal area	NDVI	June-July	SD	"temporal-first"	30
Oak	Basal area	NDVI	June-August	SD	"spatial-first"	270
Oak	Basal area	NDVI	June-August	SD	"temporal-first"	30
Oak	Tree density	EVI	May-June	mean	"spatial-first"	30
Oak	Tree density	EVI	May-June	mean	"temporal-first"	30
Oak	Tree density	EVI	May-July	mean	"spatial-first"	30
Oak	Tree density	EVI	May-July	mean	"temporal-first"	30
Oak	Tree density	EVI	June-July	mean	"spatial-first"	30
Oak	Tree density	EVI	June-July	mean	"temporal-first"	30
Oak	Tree density	EVI	June-August	mean	"spatial-first"	30
Oak	Tree density	EVI	June-August	mean	"temporal-first"	30
Oak	Tree density	EVI	May-June	SD	"spatial-first"	180
Oak	Tree density	EVI	May-June	SD	"temporal-first"	300
Oak	Tree density	EVI	May-July	SD	"spatial-first"	300
Oak	Tree density	EVI	May-July	SD	"temporal-first"	300
Oak	Tree density	EVI	June-July	SD	"spatial-first"	30
Oak	Tree density	EVI	June-July	SD	"temporal-first"	240
Oak	Tree density	EVI	June-August	SD	"spatial-first"	30
Oak	Tree density	EVI	June-August	SD	"temporal-first"	240
Oak	Tree density	NDVI	May-June	mean	"spatial-first"	30
Oak	Tree density	NDVI	May-June	mean	"temporal-first"	30
Oak	Tree density	NDVI	May-July	mean	"spatial-first"	30
Oak	Tree density	NDVI	May-July	mean	"temporal-first"	30
Oak	Tree density	NDVI	June-July	mean	"spatial-first"	30
Oak	Tree density	NDVI	June-July	mean	"temporal-first"	30
Oak	Tree density	NDVI	June-August	mean	"spatial-first"	30
Oak	Tree density	NDVI	June-August	mean	"temporal-first"	30
Oak	Tree density	NDVI	May-June	SD	"spatial-first"	270
Oak	Tree density	NDVI	May-June	SD	"temporal-first"	300
Oak	Tree density	NDVI	May-July	SD	"spatial-first"	240
Oak	Tree density	NDVI	May-July	SD	"temporal-first"	300
Oak	Tree density	NDVI	June-July	SD	"spatial-first"	30
Oak	Tree density	NDVI	June-July	SD	"temporal-first"	210
Oak	Tree density	NDVI	June-August	SD	"spatial-first"	30
Oak	Tree density	NDVI	June-August	SD	"temporal-first"	240

Table S2. Pair-wise correlation (Pearson's *r*) between beech's basal area and variables selected by the optimized multi-grain variables selection. Savg-NDVI-30-JunAug = using the spatial-first approach, the mean value of NDVI is calculated within a circular buffer of 30 m, from June to August; Ssd-NDVI-300-MayJun = using the spatial-first approach, the standard deviation value of NDVI is calculated within a circular buffer of 300 m, from May to June; Savg-EVI-210-MayJuly = using the spatial-first approach, the mean value of EVI is calculated within a circular buffer of 210 m, from May to July; Savg-EVI-270-JunAug = using the spatial-first approach, the mean value of EVI is calculated within a circular buffer of 270 m, from June to August; Ssd-EVI-300-MayJun = using the spatial-first approach, the standard deviation value of EVI is calculated within a circular buffer of 300 m, from May to June; Ssd-EVI-30-JunAug = using the spatial-first approach, the standard deviation value of EVI is calculated within a circular buffer of 30 m, from June to August; DEM = elevation (m); Slp = terrain slope (°); DistFor = distance to forest edge; SolRad = solar radiation (W/m^2).

	Savg-NDVI-30-JunAug	Ssd-NDVI-300-MayJun	Savg-EVI-210-MayJuly	Savg-EVI-270-JunAug	Ssd-EVI-300-MayJun	Ssd-EVI-30-JunAug	DEM	Slp	DistFor	SolRad
Savg-NDVI-30-JunAug	-	-0.41	0.44	0.46	-0.21	-0.27	-0.16	0.08	-0.32	-0.16
Ssd-NDVI-300-MayJun		-	-0.61	-0.59	0.79	0.75	0.23	0.04	0.50	0.11
Savg-EVI-210-MayJuly			-	0.77	-0.29	-0.41	-0.37	0.00	-0.36	-0.11
Savg-EVI-270-JunAug				-	-0.32	-0.55	-0.26	0.06	-0.47	-0.12
Ssd-EVI-300-MayJun					-	0.74	0.01	0.13	0.30	-0.02
Ssd-EVI-30-JunAug						-	0.16	0.04	0.45	0.05
DEM							-	-0.06	0.51	0.42
Slp								-	-0.03	-0.62
DistFor									-	0.23
SolRad										-

Table S3. Pair-wise correlation (Pearson's *r*) between beech's tree density and variables selected by the optimized multi-grain variables selection. Tavg-EVI-60-MayJun = using the temporal-first approach, the mean value of EVI is calculated within a circular buffer of 60 m, from May to June; Savg-EVI-210-MayJuly = using the spatial-first approach, the mean value of EVI is calculated within a circular buffer of 210 m, from May to July; Tavg-EVI-60-JunJul = using the temporal-first approach, the mean value of EVI is calculated within a circular buffer of 60 m, from June to July; Ssd-EVI-210-JunJuly = using the temporal-first approach, the standard deviation value of EVI is calculated within a circular buffer of 210 m, from June to July; Savg-NDVI-60-JunJuly = using the spatial-first approach, the mean value of NDVI is calculated within a circular buffer of 60 m, from June to July; Ssd-NDVI-30-MayJuly = using the spatial-first approach, the standard deviation value of NDVI is calculated within a circular buffer of 30 m, from May to July; Ssd-NDVI-90-JunAug = using the spatial-first approach, the standard deviation value of NDVI is calculated within a circular buffer of 90 m, from June to August; DEM = elevation (m); Slp = terrain slope (°); DistFor = distance to forest edge; SolRad = solar radiation (W/m^2).

	Tavg-EVI-60-MayJun	Savg-EVI-210-MayJuly	Tavg-EVI-60-JunJul	Ssd-EVI-210-JunJuly	Savg-NDVI-60-JunJuly	Ssd-NDVI-30-MayJuly	Ssd-NDVI-90-JunAug	DEM	Slp	DistFor	SolRad
Tavg-EVI-60-MayJun	-	0.73	0.61	-0.26	0.43	-0.35	-0.29	-0.24	0.00	-0.17	-0.06
Savg-EVI-210-MayJuly		-	0.65	-0.45	0.52	-0.38	-0.47	-0.36	0.00	-0.36	-0.11
Tavg-EVI-60-JunJul			-	-0.27	0.66	-0.43	-0.41	-0.17	0.08	-0.26	-0.08
Ssd-EVI-210-JunJuly				-	-0.42	0.43	0.63	0.14	0.04	0.36	0.07
Savg-NDVI-60-JunJuly					-	-0.78	-0.72	-0.24	0.12	-0.38	-0.26
Ssd-NDVI-30-MayJuly						-	0.65	0.10	0.00	0.24	0.15
Ssd-NDVI-90-JunAug							-	0.24	-0.10	0.44	0.29
DEM								-	-0.06	0.51	0.43
Slp									-	-0.03	-0.68
DistFor										-	0.24
SolRad											-

Table S4. Pair-wise correlation (Pearson's *r*) between oak's basal area and variables selected by the optimized multi-grain variables selection. Ssd-EVI-300-MayJun = using the spatial-first approach, the standard deviation value of EVI is calculated within a circular buffer of 300 m, from May to June; Tsd-EVI-240-MayJun = using the temporal-first approach, the standard deviation value of EVI is calculated within a circular buffer of 240 m, from May to June; Ssd-EVI-300-JunJuly = using the spatial-first approach, the standard deviation value of EVI is calculated within a circular buffer of 300 m, from June to July; Tsd-EVI-30-JunJul = using the temporal-first approach, the standard deviation value of EVI is calculated within a circular buffer of 30 m, from June to July; Tsd-EVI-30-JunAug = using the temporal-first approach, the standard deviation value of EVI is calculated within a circular buffer of 30 m, from June to August; Tavg-NDVI-30-JunJul = using the temporal-first approach, the mean value of NDVI is calculated within a circular buffer of 30 m, from June to July; Ssd-NDVI-270-MayJuly = using the spatial-first approach, the standard deviation value of NDVI is calculated within a circular buffer of 270 m, from May to July; Ssd-NDVI-30-JunJuly = using the spatial-first approach, the standard deviation value of NDVI is calculated within a circular buffer of 30 m, from June to July; Tsd-NDVI-30-JunJul = using the temporal-first approach, the standard deviation value of NDVI is calculated within a circular buffer of 30 m, from June to July; Tsd-NDVI-30-JunAug = using the temporal-first approach, the standard deviation value of NDVI is calculated within a circular buffer of 30 m, from June to August; DEM = elevation (m); Slp = terrain slope (°); DistFor = distance to forest edge; SolRad = solar radiation (W/m^2).

	Ssd-EVI-300-MayJun	Tsd-EVI-240-MayJun	Ssd-EVI-300-JunJul	Tsd-EVI-30-JunJul	Tsd-EVI-30-JunAug	Tavg-NDVI-30-JunJul	Ssd-NDVI-270-MayJul	Ssd-NDVI-30-JunJul	Tsd-NDVI-30-JunJul	Tsd-NDVI-30-JunAug	DEM	Slp	DistFor	SolRad
Ssd-EVI-300-MayJun	-	-0.03	0.78	0.21	0.10	-0.03	0.72	0.17	-0.06	-0.04	-0.29	0.02	0.35	-0.11
Tsd-EVI-240-MayJun		-	-0.12	0.09	-0.05	0.12	-0.12	-0.10	0.14	0.13	0.55	-0.07	-0.14	0.30
Ssd-EVI-300-JunJuly			-	0.19	0.11	-0.15	0.77	0.28	-0.06	-0.08	-0.27	-0.10	0.51	0.00
Tsd-EVI-30-JunJul				-	0.73	-0.27	0.25	0.15	0.32	0.20	-0.08	-0.12	0.26	0.03
Tsd-EVI-30-JunAug					-	-0.18	0.15	0.13	0.13	0.26	-0.03	-0.16	0.17	0.05
Tavg-NDVI-30-JunJul						-	-0.42	-0.71	-0.33	-0.36	-0.11	0.14	-0.31	-0.08
Ssd-NDVI-270-MayJuly							-	0.44	0.14	0.17	-0.22	-0.14	0.49	0.02
Ssd-NDVI-30-JunJuly								-	0.09	0.17	0.08	-0.23	0.31	0.24
Tsd-NDVI-30-JunJul									-	0.78	0.13	0.01	0.03	-0.07
Tsd-NDVI-30-JunAug										-	0.19	-0.04	0.08	0.01
DEM											-	0.02	-0.11	0.42
Slp												-	-0.21	-0.65
DistFor													-	0.09
SolRad														-

Table S5. Pair-wise correlation (Pearson's *r*) between oak's tree density and variables selected by the optimized multi-grain variables selection. = using the spatial-first approach, the standard deviation value of EVI is calculated within a circular buffer of 300 m, from May to June; = using the temporal-first approach, the standard deviation value of EVI is calculated within a circular buffer of 240 m, from May to June; = using the spatial-first approach, the standard deviation value of EVI is calculated within a circular buffer of 300 m, from June to July; = using the temporal-first approach, the standard deviation value of EVI is calculated within a circular buffer of 30 m, from June to July; = using the temporal-first approach, the standard deviation value of EVI is calculated within a circular buffer of 30 m, from June to August; = using the temporal-first approach, the mean value of NDVI is calculated within a circular buffer of 30 m, from June to July; = using the spatial-first approach, the standard deviation value of NDVI is calculated within a circular buffer of 270 m, from May to July; = using the spatial-first approach, the standard deviation value of NDVI is calculated within a circular buffer of 30 m, from June to July; = using the temporal-first approach, the standard deviation value of NDVI is calculated within a circular buffer of 30 m, from June to July; = using the temporal-first approach, the standard deviation value of NDVI is calculated within a circular buffer of 30 m, from June to August; DEM = elevation (m); Slp = terrain slope (°); DistFor = distance to forest edge; SolRad = solar radiation (W/m^2).

	Ssd-EVI-180-MayJun	Tsd-EVI-240-JunJul	Tsd-EVI-240-JunAug	Savg-NDVI-30-MayJuly	Savg-NDVI-30-JunAug	Ssd-NDVI-240-MayJuly	Tsd-NDVI-300-MayJuly	Ssd-NDVI-30JunJuly	Tsd-NDVI-210-JunJul	Tsd-NDVI-240-JunAug	DEM	Slp	DistFor	SolRad
Ssd-EVI-180-MayJun	-	0.13	0.17	0.02	-0.01	0.65	0.01	0.20	-0.04	0.03	-0.16	-0.02	0.28	-0.08
Tsd-EVI-240-JunJul		-	0.75	-0.07	-0.11	0.16	0.04	0.05	0.48	0.22	0.02	-0.20	0.30	0.17
Tsd-EVI-240-JunAug			-	-0.02	-0.15	0.15	-0.10	0.17	0.23	0.35	-0.01	-0.32	0.34	0.26
Savg-NDVI-30-MayJuly				-	0.79	-0.36	-0.56	-0.59	-0.30	-0.32	-0.31	0.17	-0.18	-0.20
Savg-NDVI-30-JunAug					-	-0.43	-0.06	-0.70	-0.32	-0.43	-0.13	0.14	-0.28	-0.09
Ssd-NDVI-240-MayJuly						-	0.06	0.46	0.19	0.25	-0.20	-0.12	0.51	0.01
Tsd-NDVI-300-MayJuly							-	0.04	0.25	0.20	0.42	-0.04	-0.11	0.18
Ssd-NDVI-30JunJuly								-	0.11	0.25	0.08	-0.22	0.30	0.23
Tsd-NDVI-210-JunJul									-	0.71	0.18	-0.03	0.14	0.02
Tsd-NDVI-240-JunAug										-	0.17	-0.11	0.21	0.11
DEM											-	0.01	-0.11	0.42
Slp												-	-0.22	-0.65
DistFor													-	0.09
SolRad														-

Figure S1. Scatterplot of observed (x-axis) and predicted (y-axis) values of beech's basal area, one plot for each model algorithm models, generalized linear model (GAM), generalized additive model (GAM), generalized boosted regression model (GBM), random forest (RF), and for the ensemble model. I fitted a local polinomial regression (*loess* function in R software; solid lines in red) and its confidence interval at the 95% (IC95%; dotted red line) to visualize the observed-predicted relationship.

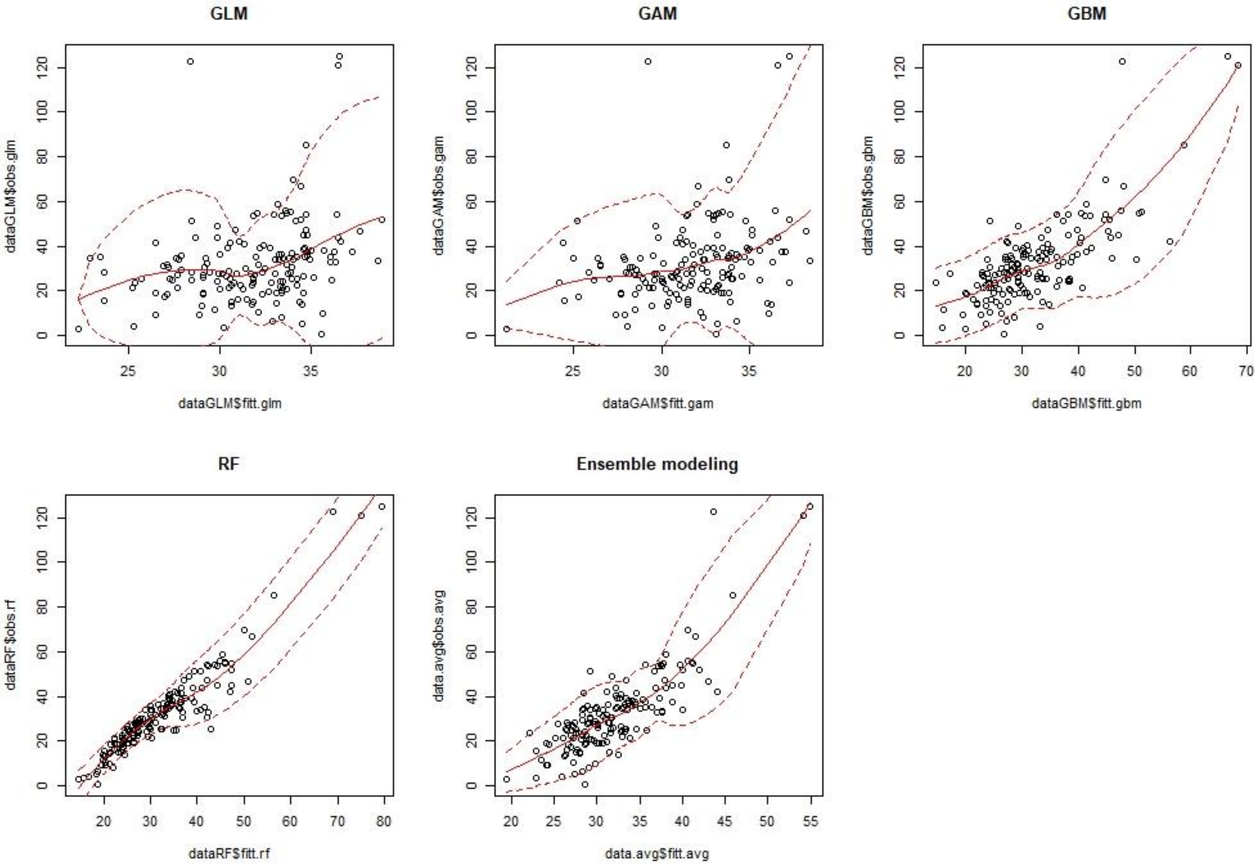

Figure S2. Scatterplot of observed (x-axis) and predicted (y-axis) values of beech's tree density, one plot for each model algorithm models, generalized linear model (GAM), generalized additive model (GAM), generalized boosted regression model (GBM), random forest (RF), and for the ensemble model. I fitted a local polinomial regression (*loess* function in R software; solid lines in red) and its confidence interval at the 95%ile (IC95%; dotted red line) to visualize the observed-predicted relationship.

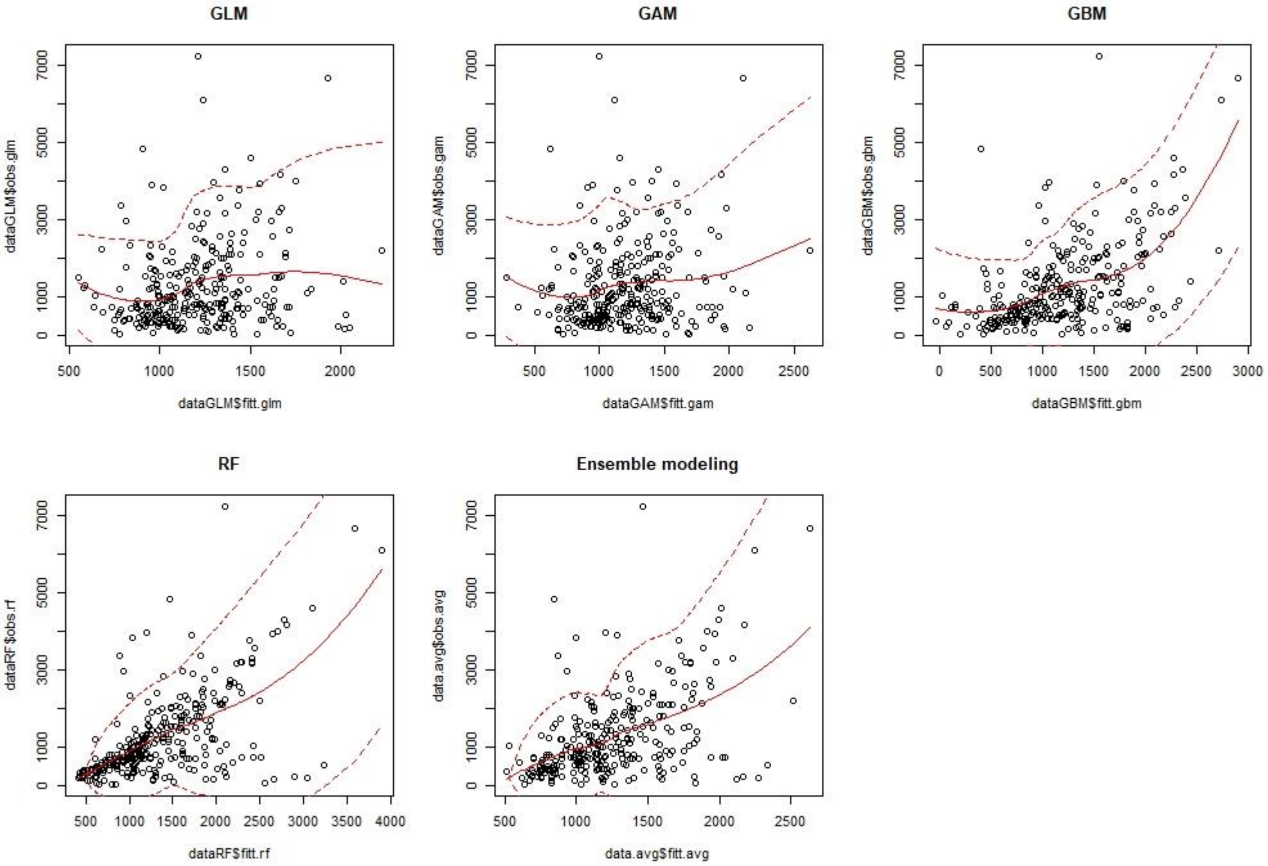

Figure S3. Scatterplot of observed (x-axis) and predicted (y-axis) values of oak’s basal area, one plot for each model algorithm models, generalized linear model (GAM), generalized additive model (GAM), generalized boosted regression model (GBM), random forest (RF), and for the ensemble model. I fitted a local polinomial regression (*loess* function in R software; solid lines in red) and its confidence interval at the 95%ile (IC95%; dotted red line) to visualize the observed-predicted relationship.

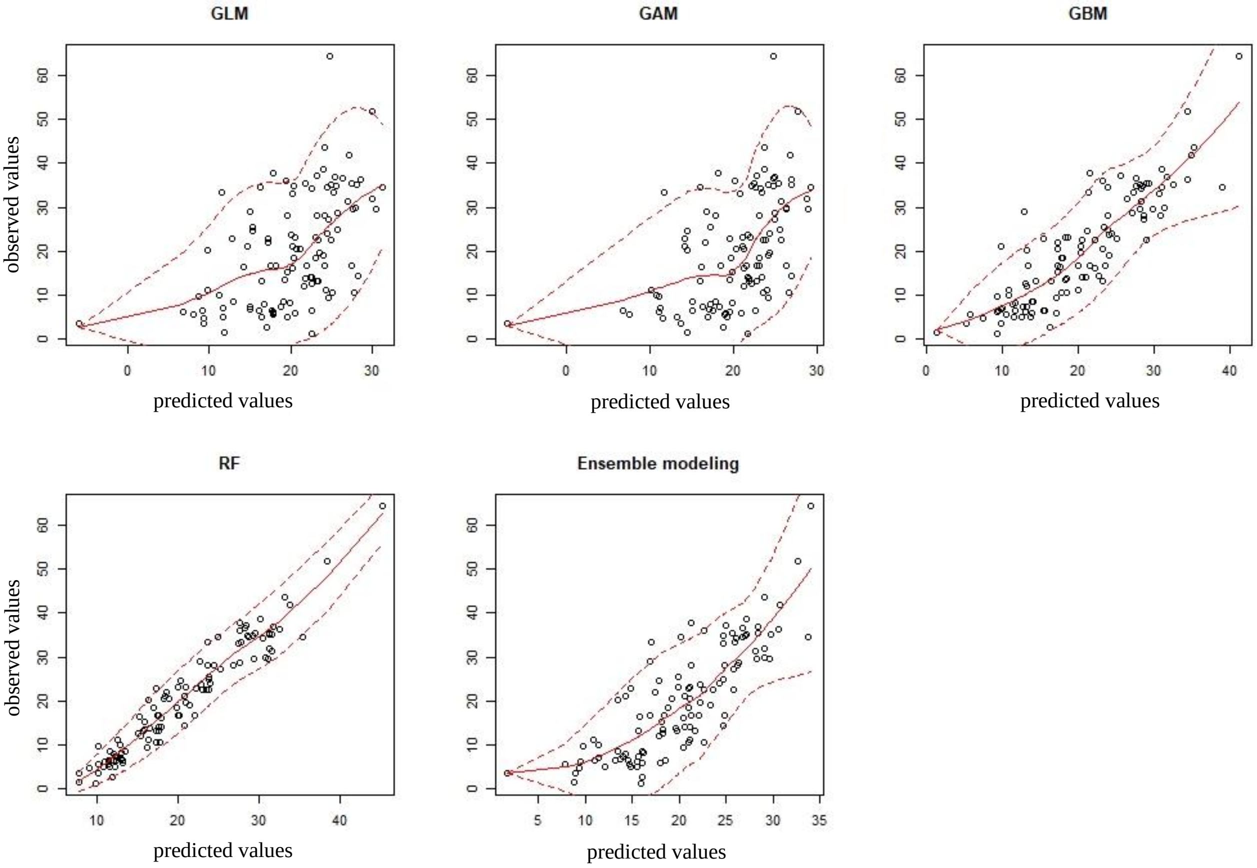

Figure S4. Scatterplot of observed (x-axis) and predicted (y-axis) values of oak's tree density, one plot for each model algorithm models, generalized linear model (GAM), generalized additive model (GAM), generalized boosted regression model (GBM), random forest (RF), and for the ensemble model. I fitted a local polinomial regression (*loess* function in R software; solid lines in red) and its confidence interval at the 95%ile (IC95%; dotted red line) to visualize the observed-predicted relationship.

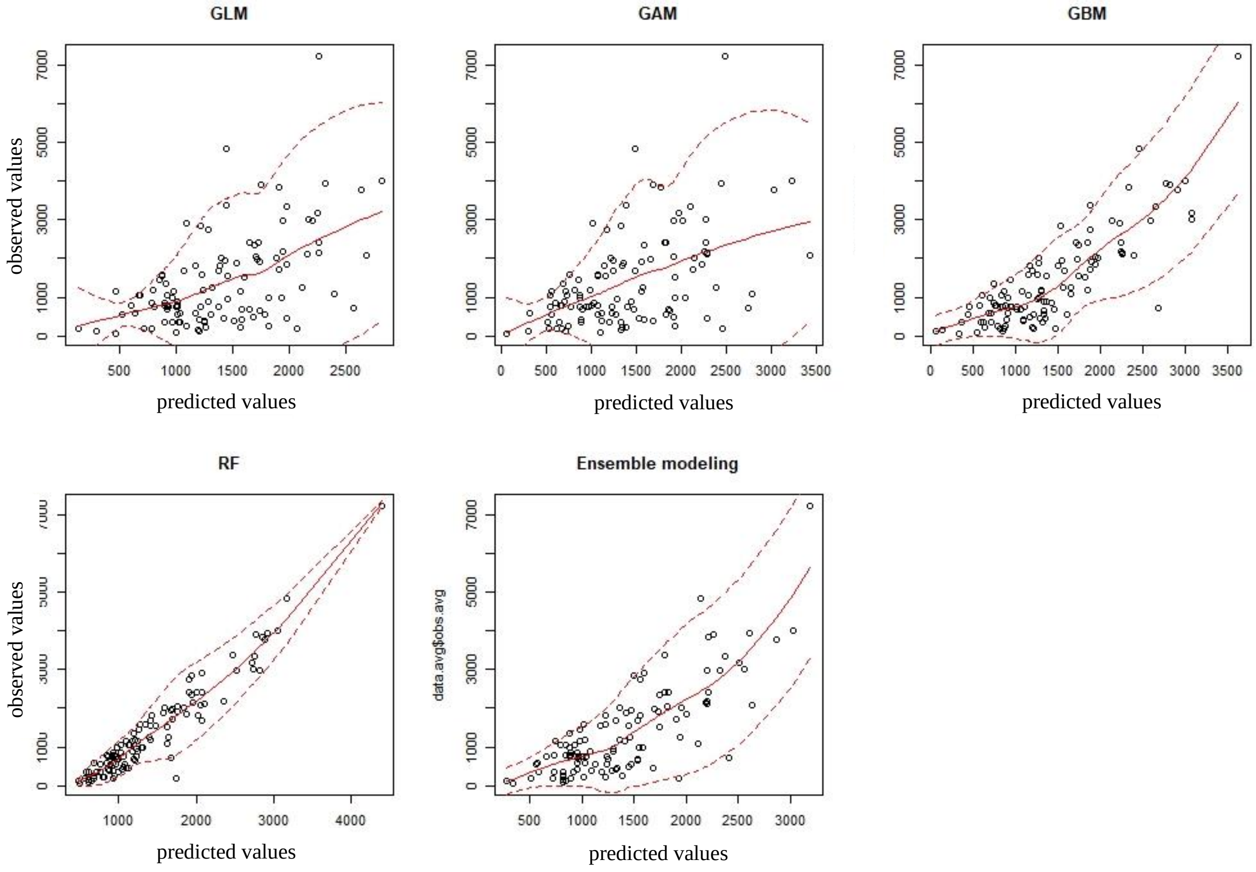

Figure S5. Continuous forest maps predicting beech's basal area over the study area developed from each model algorithm, and model ensamble (averaged models).

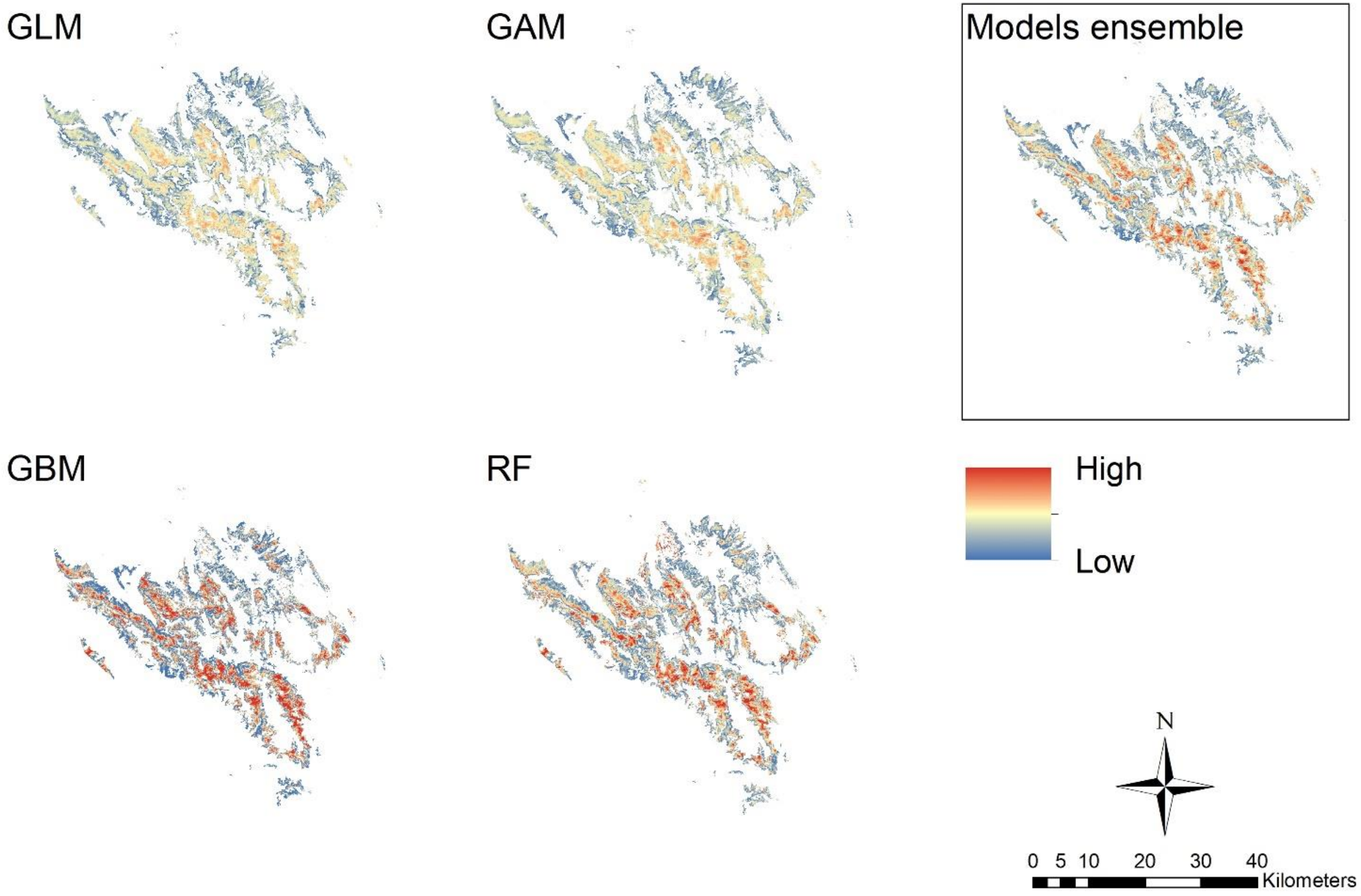

Figure S6. Continuous forest maps predicting beech’s tree density over the study area developed from each model algorithm, and model ensamble (averaged models).

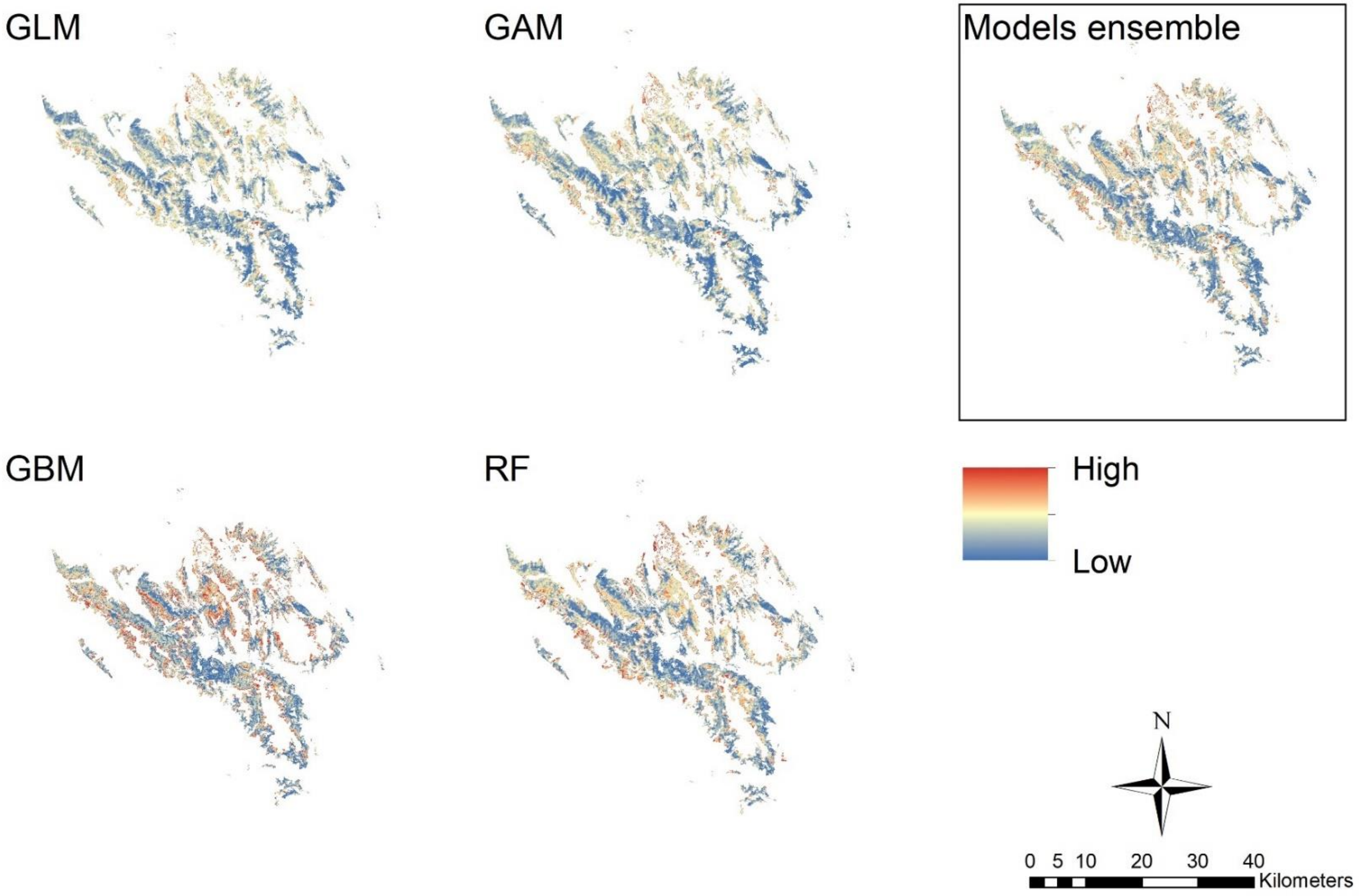

Figure S7. Continuous forest maps predicting oak's basal area over the study area developed from each model algorithm, and model ensamble (averaged models).

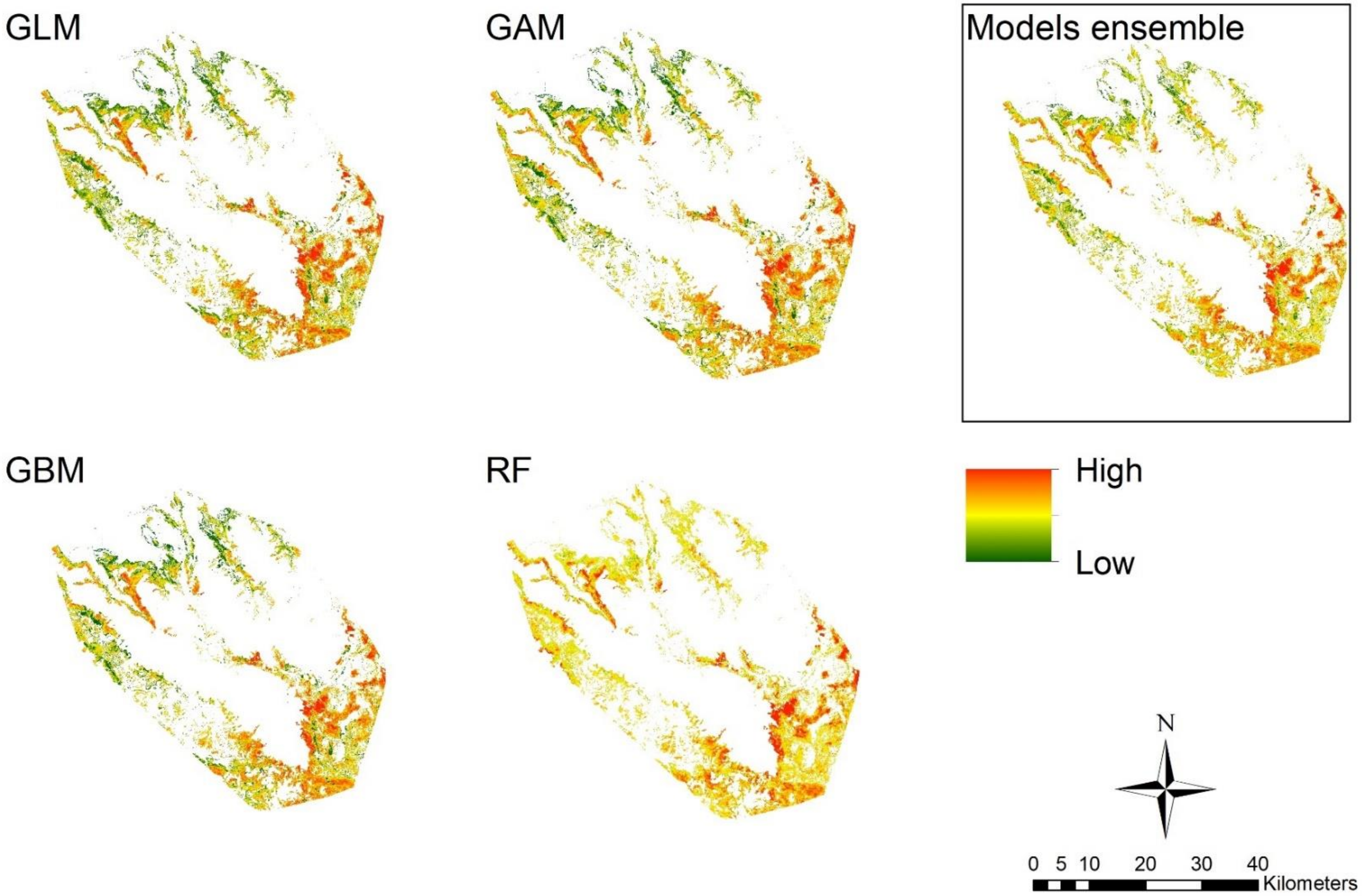

Figure S8. Continuous forest maps predicting oak's tree density over the study area developed from each model algorithm, and model ensamble (averaged models).

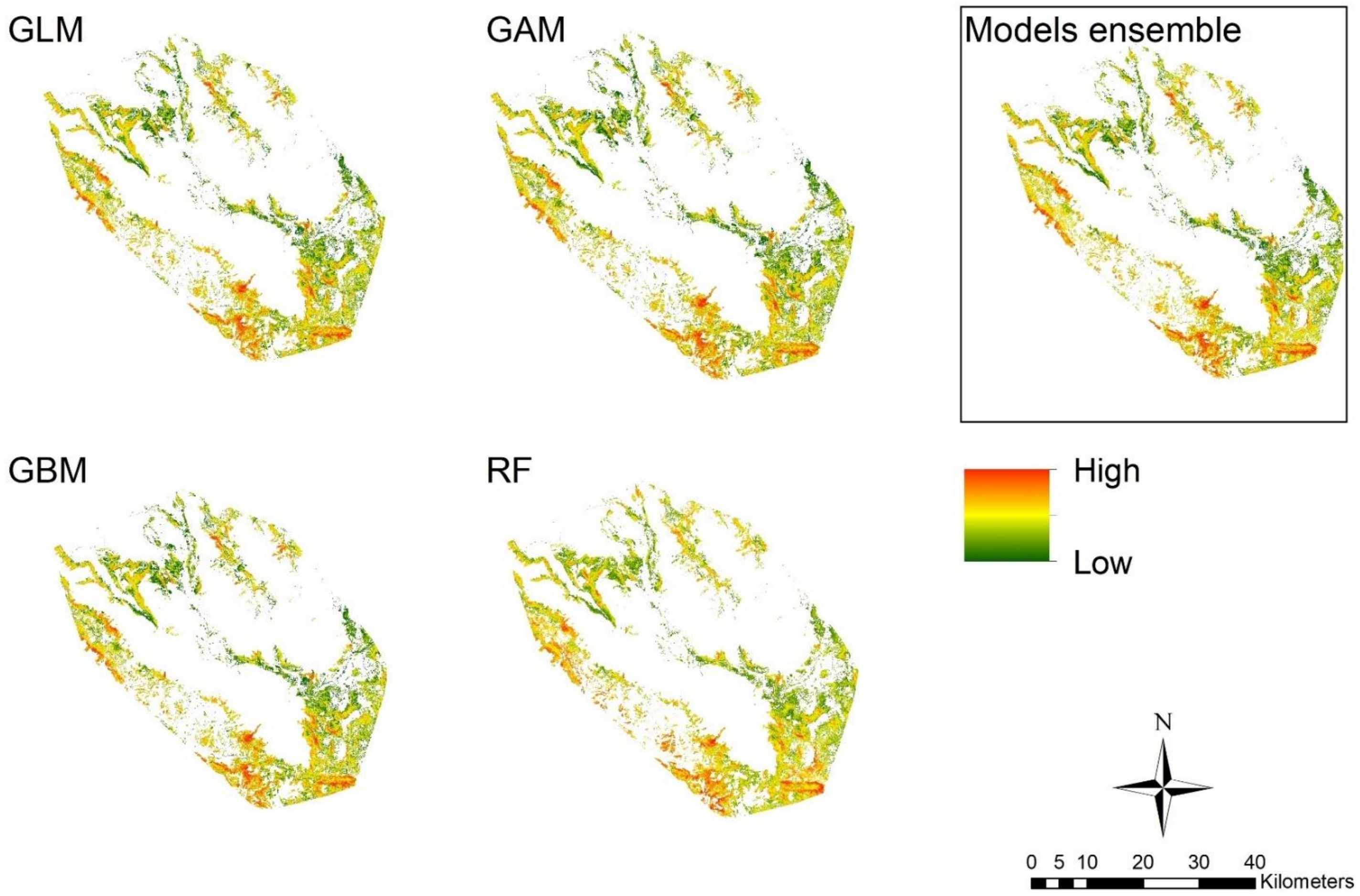

Chapter III

The importance of forest management strategies in wildlife conservation: Apennine brown bear’s habitat selection

Matteo Falco, Luigi Maiorano, and Paolo Ciucci

Sapienza University of Rome, Dept. of Biology and Biotechnology “Charles Darwin”, Viale dell’Università 32, Roma 00185, Italy

INTRODUCTION

Forest ecosystem provides numerous fundamental resources for such animals related to forest habitat to fulfil all their ecological biological requirements, like foraging, sheltering, denning, and breeding. However, not all forests are equivalent, and their spatial configuration and structure direct influence the availability of such resources. Forest succession can be affected by both intrinsic (e.g., growth, species competition, seed dispersal, and death) and external factors of natural (e.g., wind, and fire) or anthropogenic (e.g., trees harvesting, cattle pastures) source, which affect the structural composition and matrix-complexity of forest over time (Gustafson et al. 2000, Scheller et al. 2011, Wang et al. 2015). In terms of forest management regime (e.g., even-aged or uneven-aged, coppice or high-forest) and intensity of timbers harvested (e.g., volume, and harvesting rotation time), human sylvicultural actions are likely the most important factors altering the succession and productivity of the forest, also modifying the habitat suitability perceived by animals (Payer and Harrison 2003, Lõhmus 2005, Berger 2007, Jung et al. 2012). In fact, tridimensional composition of forest stands largely determines habitat quality for animals, because it may influence the availability and accessibility of resources such as rest sites (e.g., Goldstein et al. 2010), food (e.g., Hayes and Loeb 2007), exposure to predators (e.g., Baxter et al. 2006), and microclimatic conditions for thermoregulating (e.g., Chen et al. 1999). For instance, mature forests are characterized by larger trees and lower number of stems, and provide highest quantity of food (e.g., hard mast) compared to younger forest characterized instead of smaller trees and a higher number of stems; moreover, tree density can profoundly influence the capability animals' movement within forest according to the ecological needs, for instance, selecting closed forest with high tree density for sheltering from natural and anthropogenic disturbance, and forest with low tree density and canopy cover for moving and foraging across their territories (Caras and Korine 2009; Dewalt et al. 2003; Gouveia et al. 2014).

Usually, forest management regime and connected sylvicultural practices are planned according to economic perspective, with limited attention for animals' requirements living in the forest. In this context, forest management decisions should be taken considering not only economic but also wildlife conservation perspectives, for improving or, at least, preserving wildlife habitat suitability (Lindenmayer 2009). In this direction, understanding the effects of forest structure on animals' habitat selection patterns is essential to develop sustainable conservation and management strategies within modified forest landscapes (Chazdon et al. 2009, Gardner et al. 2009).

To reach this objective, habitat selection models are useful tools to assess environmental quality, and provide proactive conservation-oriented sylvicultural management actions (e.g., Roever et al. 2008a; Roever et al. 2008b). In habitat selection models, forest is commonly modeled as the percentage of forest cover within a certain area as continuous variable, or included as a categorical variable within a set of land use classes; however, in this way, any sort of information about tridimensional structure of the forest are ignored, assuming that resources within comparable forest cover patches have the same availability, accessibility, and selected with the same weight, clearly far from the truth. Nonetheless, accounting for tridimensional structural information in wildlife habitat selection models is particularly complex, because of the limited availability of spatial and continuous explicit measures of forest structure over large landscape, particularly in wilderness areas contest like protected areas. Usually, many studies investigated how animals selecting different even-age forest patches after clearcutting interventions, and researchers aimed to highlight different selection behaviors dependently to forest management interventions, comparing resource selection by animals in these sites before and after clearing interventions (e.g., Payer and Harrison 2003; Frank et al. 2015); in this way, I am able to investigate behavioral responses of habitat selection focused on few harvested forest patches, missing any information of the resource selection responses in the rest of wooded landscape in more wilderness contest (e.g., uneven-aged forest), where human sylvicultural interventions are totally absent or limited to few managed areas (e.g., protected areas). In this context, evaluating habitat selection using structural information is therefore fundamental for enhancing ecological and management proactive insight to preserve wildlife habitat quality.

One of the wildlife species mainly related to forest ecosystem with wide movement ranges and large spatial requirements is brown bear (*Ursus arctos*). Brown bear is one of the most iconic large carnivore species, able to provide several ecosystem services, like seed disperser (Hilderbrand et al. 1999, Schmitz et al. 2010), primary actor in the nutrient cycle (Ordiz et al. 2013, Mendia et al. 2019), and forest structure engineers (Zyśk-Gorczyńska et al. 2015). I focused on the last remnant and autochthonous Apennine population of brown bear (*Ursus arctos marsicanus*; Altobello 1921), living surrounded by a very high human-dominated landscape in central Italy, and isolated from other European bear populations for at least 1,500 years (Benazzo et al. 2017). In the previous study (Chapter 1), I focused on Apennine bear's habitat selection relating bear presence with the selection or avoidance of particular land use/cover classes, anthropogenic features (i.e., settlements and roads), and topographic characteristics, using different temporal (i.e., daytime, seasons) and spatial (i.e., multi-grain analysis; Laforge et al. 2015) scales at two orders of selection (second and third-order; Johnson 1980). Differently, in this work I aimed to evaluate habitat selection accounting for more explicit forest-related characteristics (i.e., spatial configuration and tridimensional structure of forest). Based on Global Positioning System (GPS) telemetry data recorded from 11 female bears, I assessed bear's habitat selection within a multi-scale resource selection function (RSF; Manly et al. 2002) design. Specifically, I am interested to understand how horizontal (i.e., shape and spatial configuration of opened and closed forest patches) and vertical (i.e., basal area, tree density, and canopy cover) spatial configuration of forest can affect resource selection by female bears, analyzing two order of selection (i.e., multi-order analysis; Johnson 1980) at different spatial (i.e., multi-grain analysis) and temporal (i.e., seasonal and circadian) scales. My specific aims are to (*i*) evaluate bears' use of space related to spatial configuration of forest interspersion with open areas, and tridimensional understory structure of forest at both home range (i.e., third-order of selection; Johnson 1980) and single forest-patch (i.e., fourth-order of selection; Johnson 1980) scales, and (*ii*) provide forest management insights for enhancing habitat quality for a long-term persistence of bears within Apennines. Similarly to the resource selection pattern evidenced in the Chapter 1, at the third order of selection my work hypotheses are that female bears select for safety areas characterized by forest patches with a high-aggregation, far from open areas, particularly during the period characterized by the highest human activities (i.e., daylight and summer season), with more heterogeneous behavioral patterns during the rest of the year (i.e., spring and autumn); at the fourth order of selection, I expect that female bears select for impervious forest patches (i.e., high tree density and canopy cover) for sheltering and resting, nonetheless preferring patches with larger trees (i.e., proxy for mature forest) with a highest hard mast productivity during the hyperphagic season (i.e., autumn).

METHODS

Study area and data collection

Study area (656.8 km^2) includes the range of reproductive Apennine female bears (Ciucci et al. 2017) and is defined as the area encompassed within the composite 100% Minimum Convex Polygon (100% MCP) calculated using all GPS-locations of female bears included in the analysis. Altitudes ranges from 145 to 2278 m. a. s. l. and is characterized by lower elevation areas with a moderate human population density and agricultural areas, and higher elevation surrounded by steep and wilderness areas covered by forests. Forest is mainly composed by beech (*Fagus sylvatica*) and oaks (*Quercus* spp.), and is interspersed with meadows and alpine prairies. Two of the four large carnivore species present in Europe, the wolf (*Canis lupus*) and the Apennine brown bear (*Ursus arctos marsicanus*), coexist in this area, as well as wild ungulates, like red deer (*Cervus elaphus*), roe deer (*Capreolus capreolus*), fallow deer (*Dama dama*), boar (*Sus scrofa*), and Apennine chamois (*Rupicapra pyrenaica ornata*).

I used GPS-locations acquired by 11 adult (≥ 4 years) female bears between 2005 and 2010, equipped with GPS-collars (i.e., Televilt Tellus GSM-VHF, and Vectronic GPS Plus), and collected during the active period, defined according to the median date of den exit and entrance (7 Mar–11 Dec, respectively; Ciucci et al. 2012). Collars deployed on bears were programmed to acquire one location every hour (i.e., 24 relocations/day) for ten days, followed by one location every 4-6 hours for the rest of the month. To enhance the quality of GPS locations (Lewis et al. 2007) for the analysis I retained all GPS locations acquired with (*i*) 3 satellites corresponding to HDOP < 8 (average location error = 23.3±33.8 m), and (*ii*) ≥ 4 satellites (Supplementary in Chapter 1). For the scope of the analysis, I grouped GPS-locations according to seasons. To account for seasonal variation in habitat selection within the home range (i.e., third-order of selection), I grouped GPS-locations according to the local seasonality in bear key foods (Ciucci et al. 2014): spring (March–May), early-summer (June–July), late-summer (August–September), and fall (October–denning date; 23 November is the median date of den entry of adult female bears in the study area). In case a bear had been tracked for more than one year, I did not include seasonal duplicates, selecting seasons with the highest number of acquired locations. The final dataset comprised a total of 9,380 GPS-locations for 11 female bears (14 bear-years; Supplementary Table S2 in Chapter 1).

Habitat variables

Home range scale

To account for resource selection by adult female bears at home range scale (third-order), I considered a set of land cover variables in a GIS environment (ArcMap v. 10.2; Environmental Systems Research Institute, ESRI, Redlands, CA, USA). I obtained land cover layers from the regional Corine Land Cover (CLC) V level and forest type vector maps, at 1:10,000 scale, from Regional administrations (http://geoportale.regione.abruzzo.it/; https://geoportale.regione.lazio.it/; http://www.geo.regione.molise.it/), and I integrated these layers with the forest tree cover density and grasslands layer products available by European Space Agency (ESA; Copernicus project: https://land.copernicus.eu/pan-european/high-resolution-layers/forests). I combined the original land cover categories into five classes: forests (including broadleaf and coniferous forest), open vegetated fields (including pastures, meadows, and alpine prairies), open areas with no vegetation (i.e., steep slopes, screes, cliffs, and rock fares), shrublands, and cultivated lands, hereafter 'semi-natural agriculture' because it is characterized by non-intensive agriculture and a high natural component. In addition, open fields areas are divided into 2 additional land cover classes: 'open areas', that include meadows and grasslands at middle and low altitude, and 'alpine prairies', that include high-mountain pastures; moreover, I used the tree cover density areas (i.e., values=0) to detect and include within the open natural areas variable forest-openness in the canopy (i.e., clearings; minimum map unit =

0.5 ha). To account for the importance of open areas in habitat selection by female bears in different period of the year, for each pixel of the study area I calculated the Euclidean distance from open areas, alpine prairies, and semi-natural agriculture (negative values inside the patch, and positive outside the patch) (Table 1); despite widely composed by a natural component, agricultural areas were included in these analyses to account for human component in the forest spatial configuration; for each pixel, I also calculated the cover percentage of open areas and alpine prairies, and the number of open natural patches within a circular buffer, calculated using different grain sizes (focal statistics tool in ArcMap, v. 10.1, ESRI; see multigrain analysis below) (Table 1). To investigate how spatial configuration of forest habitat, and its components affect habitat selection by female bears, I also introduced a set of variables that quantify the spatial configuration of the landscape, accounting for the shape of forest patches, and diversity of land use classes that characterized the environmental matrix. For this scope, using the Fragstat (v. 4.2; McGarigal and Marks 1995) software, and circular buffer at different grain sizes, I calculated 2 measures of landscape diversity, which consider the number of land use classes present within a buffer, like *SImpson Diversity Index* (SIDI) and *SHannon Diversity Index* (SHIDI), and 3 forest-class metric measures calculated at landscape scale, like *percentage of like adjacencies* (PLADJ; equals to an absolute measure of aggregation of the forest landcover class, expressed in percentage), *Normalized Landscape Shape Index* (nLSI; equals to the complexity of the forest patches' shape, i.e., perimeter-to area ratio, at landscape scale), and *edge density* (ED; equals to the sum of the lengths of all edge segments involving the corresponding forest land cover type, divided by the total landscape area) (Table 1).

Forest patch scale

To account for resource selection related to different forest structure at the scale of a single forest patch (fourth-order), I considered a set of forest structural variables that characterize the vertical and internal structure of the forest: tree density (i.e., N/ha; hereafter TD), sum of trees' basal area (i.e., m^2/ha; hereafter BA), averaged basal area of trees (i.e., m^2/ha; hereafter BAavg), and tree cover density (% of canopy cover; hereafter TCD) (Table 1). Excepted for TCD layer provided by the ESA

Copernicus project, I used spatially explicit forest structural maps derived by an ensemble modeling procedure where forest inventory stands information were predicted using remote sensing (i.e., Landsat vegetation indices) and other ancillary environmental data (for more details, see Chapter 2).

At both orders of selection, all variables were calculated with a common origin and 30x30 m cell size resolution, corresponding to the lower grid size resolution of the forest structural variables. Using the focal statistics tool in ArcMap (v. 10.2), for each variable included in the models I ran a map-algebra focal function over the entire study area, using a circular moving window of different radii to reflect alternative grain sizes in the multi-grain analysis.

Multi-grain Resource Selection Functions

Based on an use-availability design (Manly et al. 2002), I developed two multi-grain resource selection functions (MRSFs; Laforge et al. 2015), one contrasting habitat configuration features at bears' GPS locations with those within their corresponding seasonal home ranges (i.e., third-order selection; Johnson 1980), and one contrasting forest tridimensional features at bears' GPS locations within wooded areas with those within their corresponding seasonal home ranges (i.e., fourth-order selection; Johnson 1980). At both orders of selection, I fitted a mixed-effects logistic regression model (Generalized Linear Mixed Models, GLMMs) using the 'lme4' R package (Bates et al. 2015). I treated individual bears as random intercepts, to take into account differences in sample size among individuals and autocorrelation of data within individual bears (Gillies et al. 2006). I standardized all variables by subtracting the mean value from each observation and dividing by its standard deviation to allow comparison of covariates' effects (Zuur et al. *20*09). I then calibrated GLMMs including all combinations of variables (*dredge* function in 'MuMIn' R package; Barton 2018), and performed model selection using the sample-size corrected Akaike's Information Criterion (AIC_c; Burnham and Anderson 2002). I averaged estimates based on model weights ('MuMIn' R package; Barton 2018) limited to models whose AIC_c value was ≤ 2 from the most supported model (Burnham and Anderson 2002). Finally, I estimated unconditional standard errors and 95% confidence intervals for averaged coefficients, the latter considered significant when they did not include the 0 value. As few candidate models receive Akaike weights > 0, I did not incur the risk of spurious results from averaging parameter estimates of too many models with low weight (Grueber et al. 2011). Because analysis was based on a relatively small sample size, I accounted for overfitting problems (Anderson 2008) by considering models with low complexity and a limited number of covariates, and by reducing the number of models to be compared. In addition, the aim of these models was not to make predictions of habitat use by bears outside the study area, further reducing the negative effects of potential overfitting (Zellner et al. 2001, Anderson 2008).

To assess the calibration power of the final model (i.e., how much model predictions differed from a random expectation; Vaughan and Ormerod 2005), I used k-fold cross-validation (k=10) randomly splitting the dataset into 10 bins. By removing 1 bin at time, successively used as a validation set, I used the remaining data (training set) to estimate the MRSF coefficients, and I repeated the procedure for all the remaining bins. For each training set, instead of using fixed classes, I partitioned the predicted MRSF values into continuous bins calculated through a moving window of width W (W = 1/10 of the highest predicted value) (Hirzel et al. 2006). For each continuous bin, I first calculated the frequency of evaluation points falling in each class respect the total number of points (*predicted frequency*), and then the frequency of the predicted values of each class compared to the total amount of training points (*expected frequency*). Finally, I computed the Spearman rank correlation coefficient, also called "continuous Boyce index" (hereafter Boyce index, $B_{cont(W)}$; Hirzel et al. 2006), over the predicted-expected frequencies of all classes. The Boyce index ranges from -1 to 1, where positive values indicate both high predictive model's performance and deviation from randomness (i.e., values close to zero), while negative values indicate an incorrect model. The whole validation procedure was repeated for 100 times.

At the fourth-order of selection, I used multi-grain RSFs (MRSFs; Laforge et al. 2015) to account for differences in grain size for different variables; then, I evaluated the effect of changing the grain size of 1 focal variable at the time to determine its most parsimonious scale (i.e., single variable grain analysis; Laforge et al. 2015). At this scale of analysis, I therefore calculated forest structure variables by considering bear's movement scale of perception; hence, I defined a set of possible grain sizes (n=16) resulting from the Pareto curve fitted over the empirical bears' distance distribution (Zeller et al. 2014), calculated using the 'POT' R package (Ribatet and Dutang 2016). At the third-order of selection, I determined the spatial configuration of forest horizontal structure by considering bear's home range scale of perception, using the averaged radius (i.e., 3.61 Km) derived by averaging seasonal females' home ranges.

At both orders of selection, to investigate the circadian effects on seasonal habitat selection, I distinguished between daily and night GPS locations using the *solarpos* function ('maptools' R package; Bivand et al. 2016), performing different GLMM for both circadian period, using the same MRSF framework described below.

Optimized multi-grain analysis

To identify the optimal grain size for each environmental variable, I used the grain optimization procedure developed by Laforge et al. (2015). Within a resource selection function framework, this procedure involves assessing the most parsimonious grain size of a given variable by changing the grain size of one variable at the time, conditionally on the other covariates. Specifically, for one variable at the time, I compared the model with and without the focal variable measured at a given grain size using AIC_c; that is (Laforge et al. 2015):

$$\Delta AIC_c variable(x) = AIC_{c\ global\ model} - AIC_{c\ global\ model - variable(x)}$$

Using the 'MuMin' R package (Barton 2018), and by repeating the procedure above for different grain sizes, I then plotted ΔAIC_c versus grain size for each variable to identify the most parsimonious (i.e., minimum ΔAIC_c values) grain for a given variable (see Laforge et al. 2015 for more details). As this procedures potentially allows to detect different selection patterns for a given variable at different grain sizes (i.e., coefficients of different sign; Ciucci et al., 2018; Laforge et al., 2015), in these cases I included the variable twice in the in the final, multi-grain model using both grain sizes, provided these were not correlated (see below). To identify the values and range of grain sizes to be assessed for each variable, I followed Zeller et al. (2014) using the same procedure described in the Chapter 1. The entire grain-size optimization procedure was repeated to develop MRSF models both at the third and the fourth order of selection (Supplementary Fig. S1-S4).

Habitat selection within the home range scale (third-order selection)

Based on the use-available design (Manly et al. 2002), I followed a design III (Thomas and Taylor 2006) where both use (i.e., bear's GPS-locations) and availability (i.e., random sampled points) are quantified for individual bears within their home ranges. At the home range scale (i.e., third-order of selection; Johnson 1980), I contrasted habitat features at bear GPS-locations and seasonal home ranges. For each bear and season, I represented the use as GPS-locations and the availability as locations randomly sampled within the seasonal 100% MCP (10 points/km^2). I checked for collinearity among covariates for each grain size (i.e., $r<|0.7|$), and I discarded forest edge density, correlated with number of natural clearings and the forest aggregation index, normalized landscape shape index, correlated with the cover and number of natural open areas, and Shannon index, correlated with Simpson index (Supplementary Table S1). I also tested multicollinearity of selected variables (i.e., VIF<6; Supplementary Table S2), retaining a total of 7 uncorrelated variables in the final models (Table 2).

Habitat selection within the forest patch scale (fourth-order selection)

On single patch scale (i.e., fourth-order of selection; Johnson 1980), I contrasted forest structural characteristics at bear GPS-locations and forested areas within seasonal home ranges. I represented use as GPS-locations, and availability as locations randomly sampled within the seasonal 100% MCP, constraining points sampling (use and availability) only within forest patches, with use/availability ratio of 1:10. Again, I checked for pair-wise collinearity among covariates for each grain size, funding no correlated variables (i.e., $r>|0.7|$; Supplementary Tables S3-S6); then, I tested multicollinearity of selected variables (i.e., VIF<6; Supplementary Table S7), and I discarded sum of basal area because of its high multi-correlation with the other variables, retaining a total of 3 uncorrelated variables in the final models (Table 2).

RESULTS

Habitat selection within the home range scale

At the home range scale (third-order of selection), the saturated models give high predictive values ($B_{cont(W)}$) ranging from 0.85 (±0.11) to 0.91 (±0.11), respectively for early- and late-summer. At this scale of analysis, female bears response to open areas drastically change according to the type, and, secondary, according to season, and daytime (Table 3). Specifically, the probability of bear's presence increases in areas close to the cultivated lands in all seasons excepted in late-summer and independently by circadian effects (Table 3; Fig. 1); similarly, female bear select areas close to alpine prairies (or ecotone close to the forest edge) in all seasons, excepted in autumn and nightly hours, when I evidence an opposite resource selection trend (Table 3; Fig. 2); in spring and early-summer, bear selection for alpine prairies is mainly diurnal, while in late-summer where this positive selection is highlighted in both daily and nightly hours (Table 3; Fig. 2); nonetheless, in terms of covering extension, in early-summer a reducing cover of alpine prairies increase the probability of presence by female bears, independently by daytime (Table 3; Fig. 3). According to the medium and low open areas, female bears select further distances in all seasons, despite this response is greater during the day, and more relaxed during the night, excepted during late-summer (Table 3; Fig. 4). Moreover, in late-summer and autumn, female bears select areas characterized by a greater forest interspersion with open areas at medium and low elevation (i.e., number of open areas), independently by the circadian effect, while in early-summer, especially during the night, I observed an opposite trend in the resource selection response (Table 3; Fig. 5). In addition, female bears select areas characterized by a high cover type heterogeneity, in all seasons and independently by daytime, excepted during spring (Table 3; Fig. 6). Particularly in autumn, but also in early-summer and late-summer during daily hours, female bears select larger and more continuous forest patches, respect to the smaller and more fragmented (Table 3; Fig. 7).

Habitat selection within the forest patch

At the single forest patch scale (fourth-order of selection), the saturated models give high predictive values ($B_{cont(W)}$) ranging from 0.87 (±0.12) to 0.98 (±0.02), respectively for late-summer and spring. At this scale of analysis, female bears select forest patches with higher canopy cover in spring and autumn, while they select low canopy cover during the entire summer season (early- and late summer) (Table 4); however, this response is proportionally greater in oak dominated forest compared to the beech in all seasons, excepted for late-summer (Table 4; Fig. 8). Generally, female bears select oak forests compared to the beech dominated forests (Table 4), and this response is apparently strongest in early-summer, autumn and, limited to the nightly hours, also in spring and late-summer, when they prefer ecotonal areas close to the forest edge independently by daytime (Table 4; Fig. 9). Consistently in all seasons, female bears avoid forest characterized by trees with large basal area, response more pronounced in oak forest then beech forest (Table 4; Fig. 10), and select forest with a highest structural density, strongly influenced by circadian effect (i.e., positive selection of tree density during the day) excepted in spring (Table 4; Fig. 11); in fact, in early-summer and late-summer, I observed a significant inverted trend in the selection forest patch at low structural density by female bears during the nightly hours (Table 4; Fig. 11); moreover, the structural response is also affected by forest type, characterized by less pronounced positive-selection for high tree density in oak respect to the beech in early-summer, and more pronounced in late-summer and autumn (Table 4; Fig. 11).

DISCUSSION

At the home range scale (third-order of selection), the results confirmed the importance of forest like fundamental resource for this brown bear population, related to two main causes: (*i*) covering by anthropogenic disturbance, highlighted by the selection of continuous forest patch, especially during daily hours in summer (early-summer and late-summer), and (*ii*) foraging within the forest, highlighted by the increasingly selection for these continuous forested areas mainly in autumn, when there is the peak of hard mast production in the forests. Nonetheless, this study confirmed that brown bear is a species related to the forest ecosystem and not limited only to the forest. In this sense, bears select large and continuous forest patches interspersed with other land use type consistently in all seasons. In the study area, whereas bears show a negative selection for areas close to the natural open areas, they also highlight a positive selection for areas with a high number of open areas at medium and low elevation (open areas), excepted in spring and early-summer; on the other hand, female bear was attracted by open areas managed by human (agricultural areas) and alpine prairies, the latter with the important exception for the autumn season. The contribution of open areas (i.e., natural and artificial clearings) in bear's habitat suitability has been recognized in many studies (e.g., Frank et al. 2015; Lamb et al. 2017), and this selection pattern is connected to the great amount of food resources, such as ants, herbaceous vegetation and berries, that can be available in a short period of the year (Ciucci et al. 2014). In addition, it is important underline that agricultural areas enclosed in the study area include many abandoned crops and meadows once intensively cultivated, and now destinated to annual mowing, hence they almost never correspond to continuous and intensive form of agriculture. These areas can offer more productive trophic resources compared to the other grazing areas at medium and low elevation before the increasing of summer tourism; in fact, the absence of attraction for these areas in late-summer it could be connected to a high-level of anthropogenic disturbance at low elevation (Mancinelli et al. 2019) or presence of alternative food resources, like rhamnus berries which grows in high-altitude no-wooded areas, and they are largely consumed by bears exclusively between August and September (i.e., late-summer) (Ciucci et al. 2014). Circadian effects are not particularly relevant at the third order of selection, if not for: (a) an increased selection for sites further from natural open areas during daylight hours in spring and early summer (response which is released during the night), that can hide a selection for daybeds within forest, and (b) an increased selection during daylight hours of sites closer to alpine prairies during spring and early summer (response released during the night), and (c) selection for unfragmented and large forest patches which increases during daylight hours and wanes during the night in early and late-summer.

At the single forest patch scale (fourth-order of selection), more evident circadian effects highlight that oak forest selection respect to the beech forest is mainly nocturnal and never diurnal, and this may suggest a trophic rather than covering effect, probably linked to a higher diversity and availability of food; at the other hand, I cannot exclude an altitudinal effect for mediating the greater disturbance at low elevation (oak forest) by human activities. Forest selection for low canopy cover in early and late-summer, contrary to the other two seasons, may reflect a higher accessibility to more heliophiles source of food (e.g., ants, forbs, and grass) which are highly available only in this short period of the year far from wooded areas (Ciucci et al. 2014). In addition, the selection for high tree density structure is fundamentally diurnal in early-summer and late-summer, while during the night female bears show an opposite behavioral response (selection for lower tree density structure), suggesting that tree density have a sheltering role rather that trophic, especially for the entire summer period. Consistently in all seasons, female bears avoid mature forest whose trees tend to have higher basal areas; this response can be linked to a poor ground lighting and, consequently, poor productivity of the understory (low availability of food resources), or poor sheltering effect of these forest structure (areas with large trees and low tree density). Nonetheless, the first of the two hypotheses (foraging) can be supported by the fact that female bears with radio-collar included in the analysis were not monitored during high-productivity of beech’s hard mast (i.e., autumn 2007 and 2011). To solve the lack of food resource during the maximum period of foraging, bears could try to find alternative source of food selecting several forest structure (more heterogeneous), different from those commonly selected during high-productivity of beech nuts years, therefore preferring forest patches dominated by oak species which guarantee a low but safe and continuous nuts productivity over the years. According to the bears’ tracking period (i.e., 2005-2010), pronounced hard masting years occurred only during the autumn of 2007. However, calibrating the final models using only GPS-locations of bears collected in no-strong hard masting years, I am not be able to find any selection response for mature forest patches (i.e., high-productivity of hard mast), while I evidenced a more heterogeneous behavioral response in mixed forest structure selection, including younger successional stage (i.e., low hard mast productivity), supposing for increasing the amount of available food in the forest ecosystem. Nonetheless, further analysis was required to validate this hypothesis, for instance comparing habitat selection modeled using GPS-locations of bears collected during both strong and normal hard masting productivity years.

In conclusion, the affinity of brown bear for the forest ecosystem is highlighted by the selection for extensive and continuous forest patches in all seasons, despite interspersed with other land use types. Open areas, interspersed within forest, have a critical role for bears, particularly meadows and grasslands at medium and low elevation and alpine prairies located at higher elevation over the upper limit of forest tree-line. According to the forest areas, not all type and structure of forest have the same suitability value for bear; usually, excluding important seasonal and circadian variation, oak dominated forests are mainly selected compared to those dominated by beech, and mature forest (high average basal area and low tree density) are less selected respect to younger forests. The importance and direction of the effect of forest structure vary according to the seasons, type of forest (beech vs oak), and daytime, reflecting the result of a trade-off between sheltering value of forests and their trophic benefits. While further investigations are needed for highlighting on causal mechanisms of such kind of habitat relationship, perhaps at a higher level of ecological resolution, and with temporal range of reference that better capture the variability of forests' trophic productivity, it is reasonable to think that circadian variability I observed can suggest that the avoidance of anthropogenic disturbance in the study area can correspond to reduced foraging opportunities, balanced by bear with apparently modifications of the habitat use, at both third and fourth order of selection, between day and night.

Although the expansion of the range in Apennine bears has long been recognized as a fundamental conservation requirement (Boscagli 1987, Posillico et al. 2004, Ciucci and Boitani 2008), the lack of this expansion in Apennine bears can be related to the difference in spatial configuration of forested areas and tridimensional structure of understory outside the core range distribution (i.e., PNALM and external protected areas), factors not yet investigated outside the core distribution area. Despite I developed habitat selection by bear using a relative small sample size, composed by only GPS-locations of adult females, and collected only during low-level of hard mast productivity, this work pone the corner stone for future studies that must be conducted within and, mainly, outside the core range distribution of female bears to realize incisive conservation actions for the Apennine brown bear survival, in synergy with forestry management planning. To reach this challenging objective, future researches should be oriented to (*i*) collect a more representative GPS sample data, for instance expanding animal's sample period to multiple and successive years that include both low and high hard mast productivity periods, (*ii*) associate hard mast productivity to particular stand structure attribute(s) to give a realistic productivity measure of forest, at the single forest patch scale, and finally, with all these new information, (*iii*) relate the causal effect of the numerous bear's ecological needs (e.g., foraging, sheltering, covering, and breeding), which can directly influence its fitness and future viability in the central Apennines.

REFERENCES

Anderson, D. R. 2008. Model based inference in the life sciences: A primer on evidence. U. Springer, New York, New York, editor.

Barton, K. 2018. Package “MuMIn” Title Multi-Model Inference. Cran-R.

Bates, D., M. Mächler, B. Bolker, and S. Walker. 2015. Fitting linear mixed-effects models using lme4. Journal of Statistical Software 67:1–48.

Baxter, D. J. M., J. M. Psyllakis, M. P. Gillingham, and E. L. O’Brien. 2006. Behavioural response of bats to perceived predation risk while foraging. Ethology 112:977–983.

Benazzo, A., E. Trucchi, J. A. Cahill, P. M. Delser, S. Mona, M. Fumagalli, L. Bunnefeld, L. Cornetti, S. Ghirotto, M. Girardi, L. Ometto, A. Panziera, O. Rota-Stabelli, E. Zanetti, A. Karamanlidis, C. Groff, L. Paule, L. Gentile, C. Vilà, S. Vicario, L. Boitani, L. Orlando, S. Fuselli, C. Vernesi, B. Shapiro, P. Ciucci, and G. Bertorelle. 2017. Survival and divergence in a small group: The extraordinary genomic history of the endangered Apennine brown bear stragglers. Proceedings of the National Academy of Sciences of the United States of America 114:E9589–E9597.

Berger, J. 2007. Fear, human shields and the redistribution of prey and predators in protected areas. Biology Letters 3:620–623.

Bivand, R., N. Lewin-Koh, E. Pebesma, E. Archer, A. Baddeley, N. Bearman, H.-J. Bibiko, S. Brey, J. Callahan, G. Carrillo, S. Dray, D. Forrest, M. Friendly, P. Giraudoux, D. Golicher, V. G. Rubio, P. Hausmann, K. O. Hufthammer, T. Jagger, K. Johnson, S. Luque, D. MacQueen, A. Niccolai, E. Pebesma, O. P. Lamigueiro, T. Short, G. Snow, B. Stabler, M. Stokely, and R. Turner. 2016. Tools for reading and handling spatial objects: Package “maptools.” R Documentation.

Boscagli, G. 1987. Brown bear mortality in central Italy from 1970 to 1984. International Conference Research and Management 7:97–98.

Caras, T., and C. Korine. 2009. Effect of vegetation density on the use of trails by bats in a secondary tropical rain forest. Journal of Tropical Ecology 25:97–101.

Chazdon, R. L., C. A. Peres, D. Dent, D. Sheil, A. E. Lugo, D. Lamb, N. E. Stork, and S. E. Miller. 2009. The potential for species conservation in tropical secondary forests. Conservation Biology 23:1406–1417.

Chen, J., S. C. Saunders, K. D. Brosofske, G. D. Mroz, T. R. Crow, R. J. Naiman, J. F. Franklin, and B. L. Brookshire. 1999. Microclimate in forest ecosystem and landscape ecology: Variations in local climate can be used to monitor and compare the effects of different management regimes. BioScience 49:288–297.

Ciucci, P., T. Altea, A. Antonucci, L. Chiaverini, A. Di Croce, F. Mauro, P. Forconi, R. Latini, L. Maiorano, A. Monaco, P. Morini, F. Ricci, L. Sammarone, F. Striglioni, E. Tosoni, L. Carotenuto, I. Pizzol, M. C. Saltari, D. Serafini, M. Caporioni, L. Tarquini, S. Donfrancesco, I. Guj, A. Lecce, G. Di Clemente, and E. Peria. 2017. Distribution of the brown bear (*Ursus arctos marsicanus*) in the central Apennines, Italy, 2005–2014. Hystrix 28:1–6.

Ciucci, P., and L. Boitani. 2008. The Apennine brown bear: A critical review of its status and conservation problems. Ursus 19:130–145.

Ciucci, P., L. Boitani, M. Falco, and L. Maiorano. 2018. Hierarchical, multi-grain rendezvous site selection by wolves in southern Italy. The Journal of Wildlife Management 82:1049–1061.

Ciucci, P., E. Tosoni, G. Di Domenico, F. Quattrociocchi, and L. Boitani. 2014. Seasonal and annual variation in the food habits of Apennine brown bears, central Italy. Journal of Mammalogy 95:572–586.

Ciucci, P., E. Tosoni, L. Maiorano, L. Gentile, C. Sulli, and L. Boitani. 2012. Denning in the Apennine brown bear (*Ursus arctos marsicanus*) and potential conflict areas: Toward proactive conservation measures. VIII Congresso Italiano di Teriologia. Hystrix, It. J. Mamm. (N.S.) 64.

DeWalt, S. J., S. K. Maliakal, and J. S. Denslow. 2003. Changes in vegetation structure and composition along a tropical forest chronosequence: Implications for wildlife. Forest Ecology and Management 182:139–151.

Frank, S. C., S. M. J. G. Steyaert, J. E. Swenson, I. Storch, J. Kindberg, H. Barck, and A. Zedrosser. 2015. A “clearcut” case? Brown bear selection of coarse woody debris and carpenter ants on clearcuts. Forest Ecology and Management 348:164–173. .

Gardner, T. A., J. Barlow, R. Chazdon, R. M. Ewers, C. A. Harvey, C. A. Peres, and N. S. Sodhi. 2009. Prospects for tropical forest biodiversity in a human-modified world. Ecology Letters 12:561–582.

Gillies, C. S., M. Hebblewhite, S. E. Nielsen, M. A. Krawchuk, C. L. Aldridge, J. L. Frair, D. J. Saher, C. E. Stevens, and C. L. Jerde. 2006. Application of random effects to the study of resource selection by animals. Journal of Animal Ecology 75:887–898.

Goldstein, M. I., A. J. Poe, L. H. Suring, R. M. Nielson, and T. L. McDonald. 2010. Brown bear den habitat and winter recreation in South-Central Alaska. Journal of Wildlife Management 74:35–42.

Gouveia, S. F., F. Villalobos, R. Dobrovolski, R. Beltrão-Mendes, and S. F. Ferrari. 2014. Forest structure drives global diversity of primates. Journal of Animal Ecology 83:1523–1530.

Gustafson, E. J., S. R. Shifley, D. J. Mladenoff, K. K. Nimerfro, and H. S. He. 2000. Spatial simulation of forest succession and timber harvesting using LANDIS. Canadian Journal of Forest Research 30:32–43.

Hayes, J. P., and S. C. Loeb. 2007. The influences of forest management on bats in North America. Pages 207–236 in. Bats in Forests: Conservation and Management. eds M.J. L. John Hopkins University Press, Baltimore, MD.

Hilderbrand, G. V., T. A. Hanley, C. T. Robbins, and C. C. Schwartz. 1999. Role of brown bears (*Ursus arctos*) in the flow of marine nitrogen into a terrestrial ecosystem. Oecologia 121:546–550.

Hirzel, A. H., G. Le Lay, V. Helfer, C. Randin, and A. Guisan. 2006. Evaluating the ability of habitat suitability models to predict species presences. Ecological Modelling 199:142–152.

Johnson, D. H. 1980. The comparison of usage and availability measurements for evaluating resource preference. Ecology 61:65–71.

Jung, K., S. Kaiser, S. Böhm, J. Nieschulze, and E. K. V Kalko. 2012. Moving in three dimensions: Effects of structural complexity on occurrence and activity of insectivorous bats in managed forest stands. Journal of Applied Ecology 49:523–531.

Laforge, M. P., E. Vander Wal, R. K. Brook, E. M. Bayne, and P. D. McLoughlin. 2015. Process-focussed, multi-grain resource selection functions. Ecological Modelling 305:10–21.

Lamb, C. T., G. Mowat, B. N. McLellan, S. E. Nielsen, and S. Boutin. 2016. Forbidden fruit: human settlement and abundant fruit create an ecological trap for an apex omnivore. Journal of Animal Ecology 86:55–65.

Lewis, J. S., J. L. Rachlow, E. O. Garton, and L. A. Vierling. 2007. Effects of habitat on GPS collar performance: Using data screening to reduce location error. Journal of Applied Ecology 44:663–671.

Lindenmayer, D. B. 2009. Forest wildlife management and conservation. Annals of the New York Academy of Sciences 1162:284–310.

Lõhmus, A. 2005. Are timber harvesting and conservation of nest sites of forest-dwelling raptors always mutually exclusive? Animal Conservation 8:443–450.

Mancinelli, S., M. Falco, L. Boitani, and P. Ciucci. 2019. Social, behavioural and temporal components of wolf (*Canis lupus*) responses to anthropogenic landscape features in the central Apennines, Italy. Journal of Zoology 309:114–124.

Manly, B. F. J., L. Mcdonald, D. Thomas, T. L. McDonald, and W. P. Erickson. 2002. Resource selection by animals: Statistical design and analysis for field studies. 2nd ed. Volume 1. Kluwer Academic Publishers, Dordrecht, Netherlands. Merkle.

McGarigal, K., and B. J. Marks. 1995. FRAGSTATS: spatial pattern analysis program for quantifying landscape structure. General Technical Report - US Department of Agriculture, Forest Service.

Mendia, S. M., M. D. Johnson, and J. M. Higley. 2019. Ecosystem services and disservices of bear foraging on managed timberlands. Ecosphere 10:1–25.

Ordiz, A., R. Bischof, and J. E. Swenson. 2013. Saving large carnivores, but losing the apex predator? Biological Conservation 168:128–133.

Payer, D. C., and D. J. Harrison. 2003. Influence of forest structure on habitat use by American marten in an industrial forest. Forest Ecology and Management 179:145–156.

Posillico, M., A. Meriggi, E. Pagnin, S. Lovari, and L. Russo. 2004. A habitat model for brown bear conservation and land use planning in the central Apennines. Biological Conservation 118:141–150.

Ribatet, M., and C. Dutang. 2016. POT: Generalized pareto distribution and peaks over threshold.

Roever, C. L., M. S. Boyce, and G. B. Stenhouse. 2008a. Grizzly bears and forestry II: Grizzly bear habitat selection and conflicts with road placement. Forest Ecology and Management 256:1262–1269.

Roever, C. L., M. S. Boyce, and G. B. Stenhouse. 2008b. Grizzly bears and forestry I: Road vegetation and placement as an attractant to grizzly bears. Forest Ecology and Management 256:1253–1261.

Scheller, R. M., D. Hua, P. V. Bolstad, R. A. Birdsey, and D. J. Mladenoff. 2011. The effects of forest harvest intensity in combination with wind disturbance on carbon dynamics in Lake States Mesic Forests. Ecological Modelling 222:144–153.

Schmitz, O. J., D. Hawlena, and G. C. Trussell. 2010. Predator control of ecosystem nutrient dynamics. Ecology Letters 13:1199–1209.

Thomas, D. L., and E. J. Taylor. 2006. Study Designs and Tests for Comparing Resource Use and Availability. The Journal of Wildlife Management 54:322.

Vaughan, I. P., and S. J. Ormerod. 2005. The continuing challenges of testing species distribution models. Journal of Applied Ecology 42:720–730.

Wang, W. J., H. S. He, F. R. Thompson, J. S. Fraser, B. B. Hanberry, and W. D. Dijak. 2015. Importance of succession, harvest, and climate change in determining future composition in U.S. Central Hardwood Forests. Ecosphere 6:1–18.

Zeller, K. A., K. McGarigal, P. Beier, S. A. Cushman, T. W. Vickers, and W. M. Boyce. 2014. Sensitivity of landscape resistance estimates based on point selection functions to scale and behavioral state: Pumas as a case study. Landscape Ecology 29:541–557.

Zellner, A., H. A. Keuzenkamp, and M. McAleer. 2001. Simplicity, inference, and modeling. U. K. Cambridge University Press, Cambridge, editor.

Zuur, A. F., E. N. Ieno, N. J. Walker, A. A. Saveliev, G. M. Smith, Z. I. Walker, and S. Smith. 2009. Mixed effects models and extensions in ecology with R. Ecology. Springer-Verlag, New York, New York, USA.

Zyśk-Gorczyńska, E., Z. Jakubiec, and A. Wuczyński. 2015. Brown bears (*Ursus arctos*) as ecological engineers: The prospective role of trees damaged by bears in forest ecosystems. Canadian Journal of Zoology 93:133–141.

TABLES AND FIGURES

Table 1. Covariates contemplated to develop multi-grain resource selection functions to investigate third- and fourth-order habitat selection by Apennine brown bears in the Abruzzo, Lazio, and Molise National Park central Italy, 2005–2010. Because of collinearity, not all covariates were retained in the final models.

Variable				Study area [a]	
Type	**Description**	**Source**	**Code**	$\bar{\chi}$	**SD**
Home range (3rd order)	Distance to open areas (m) [b]	Regional CLC V level, Copernicus (ESA)	DisOpen	601.17	582.38
	Distance to alpine prairies (m) [c]	Regional CLC V level, Copernicus (ESA)	DisAlp	1530.83	1474.04
	Distance to cultivated lands (m)	Regional CLC V level, Copernicus (ESA)	DisAgri	2199.52	1549.06
	Open areas cover (%) [b]	Regional CLC V level, Copernicus (ESA)	OpenCov	0.10	0.08
	Alpine prairies cover (%) [c]	Regional CLC V level, Copernicus (ESA)	AlpCov	0.08	0.07
	Number of open areas (N/km^2)	Regional CLC V level, Copernicus (ESA)	OpenN	2.87	2.05
	Simpson's diversity index	FRAGSTAT measure	SIDI	0.45	0.12
	Shannon's diversity index [d]	FRAGSTAT measure	SHIDI	0.78	0.19
	Percentage of like adjacencies (%) [e]	FRAGSTAT measure	PLADJ	95.75	1.82
	Normalized landscape shape index [d]	FRAGSTAT measure	nLSI	0.10	0.05
	Edge density (m/ha) [d]	FRAGSTAT measure	ED	3.57	1.28
Forest-patch (4th order)	Tree canopy cover (%)	Copernicus (ESA)	TCD	88.14	18.64
	Tree density (N/ha)	Remote sensing data (see Chapter 2)	TD	1334.78	444.26
	Basal areas (m^2/ha)	Remote sensing data (see Chapter 2)	BA	64.68	28.77
	Averaged basal areas (m^2/ha)	Remote sensing data (see Chapter 2)	BAavg	0.02	0.01

[a]: study area is to the composite Minimum Convex Polygon (100%MCP) of bears' GPS-locations (third-order selection), and the forest areas within the MCP100% (fourth-order selection).

[b]: Open areas include meadows, pastures, and clearings (>0.5 ha) at low and middle elevation (about < 1700 m. a. l. s.).

[c]: Alpine prairies include alpine pastures, and open areas (>0.5 ha) at high elevation (about ≥ 1700 m. a. l. s.).

[d]: Not included in the final model due to collinearity with other variables.

[e]: calculated for the forest class.

Table 2. Most parsimonious AICc-selected, multi-grain, mixed effects logistic regression model to assess habitat selection by Apennine brown bears within their home ranges (third-order selection), and within single forest-patch (fourth-order selection). Habitat use has been investigated by means of GPS locations collected on 11 adult female bears in the Abruzzo, Lazio, and Molise National Park, central Italy (2005–2010). Model selection occurred through model dredging. Only candidate models with $\Delta AIC_c \leq 2$ are shown. K = number of model's parameters; logLik = loglikelihood; AIC_c = Akaike's Information Criterion adjusted for small sample size; ΔAIC_c = AIC_c difference between each candidate model and the most parsimonious model; w_i = Akaike weights.

Extent	Season	Model description	K	logLik	AIC$_c$	ΔAIC$_c$	w_i
Home range (3rd order)	Spring	DisAgri + DisAlp + DisOpen + PLADJ$_{3610}$ + SIDI$_{3610}$	7	-7122.38	14258.76	0.00	0.55
		DisAgri + DisAlp + DisOpen + OpenN$_{3610}$ + PLADJ$_{3610}$ + SIDI$_{3610}$	8	- 7121.59	14259.18	0.42	0.45
	Early-summer	DisAgri + DisAlp + DisOpen + AlpCov$_{3610}$ + OpenN$_{3610}$ + PLADJ$_{3610}$ + SIDI$_{3610}$	9	-7768.00	15554.01	0.00	1.00
	Late-summer	DisAlp + DisOpen + OpenN$_{3610}$ + PLADJ$_{3610}$ + SIDI$_{3610}$	7	-9104.11	18222.23	0.00	0.54
		DisAlp + DisOpen + AlpCov$_{3610}$ + OpenN$_{3610}$ + PLADJ$_{3610}$ + SIDI$_{3610}$	8	-9103.91	18223.82	1.59	0.25
		DisAgri + DisAlp + DisOpen + OpenN$_{3610}$ + PLADJ$_{3610}$ + SIDI$_{3610}$	8	-9104.06	18224.13	1.90	0.21
	Autumn	DisAgri + DisAlp + DisOpen + AlpCov$_{3610}$ + OpenN$_{3610}$ + PLADJ$_{3610}$ + SIDI$_{3610}$	9	-6847.60	13711.13	0.00	1.00
Forest-patch (4th order)	Spring	TCD$_{1531}$ * ForType + BAavg$_{666}$ * ForType + TD$_{47}$ * ForType + DisFor	10	-5992.80	12005.57	0.00	1.00
	Early-summer	TCD$_{1531}$ * ForType + BAavg$_{925}$ * ForType + TD$_{140}$ * ForType + DisFor	10	-6217.50	12455.13	0.00	1.00
	Late-summer	TCD$_{1531}$ * ForType + BAavg$_{236}$ * ForType + TD$_{61}$ * ForType + DisFor	10	-4945.40	9910.80	0.00	1.00
	Autumn	TCD$_{338}$ * ForType + BAavg$_{514}$ * ForType + TD$_{61}$ * ForType + DisFor	10	-5176.31	10372.62	0.00	0.6
		TCD$_{338}$ * ForType + BAavg$_{514}$ * ForType + TD$_{61}$ * ForType	9	-5177.71	10373.42	0.80	0.4

Table 3. Coefficients of multi-grain resource selection functions to investigate habitat selection by bears when selecting suitable-habitat patches within home ranges (third-order selection) according to seasons and daytime, in the Abruzzo-Lazio-Molise National Park, central Italy, 2005–2010.

Variable[a]	Spring								Early-summer								Late-summer								Autumn							
	Day				Night				Day				Night				Day				Night				Day				Night			
	β	SE	95% CI		β	SE	95% CI		β	SE	95% CI		β	SE	95% CI		β	SE	95% CI		β	SE	95% CI		β	SE	95% CI		β	SE	95% CI	
			Lower	Upper			Lower	Upper			Lower	Upper			Lower	Upper			Lower	Upper			Lower	Upper			Lower	Upper			Lower	Upper
(Intercept)	-2.34	0.06	-2.45	-2.23	-2.35	0.09	-2.53	-2.17	-2.38	0.06	-2.49	-2.27	-2.22	0.19	-2.59	-1.84	-2.38	0.08	-2.53	-2.22	-2.34	0.04	-2.42	-2.27	-2.36	0.09	-2.54	-2.18	-2.43	0.10	-2.62	-2.23
DisAgri	-0.41	0.05	-0.52	-0.31	-0.58	0.06	-0.69	-0.47	-0.46	0.05	-0.56	-0.36	-0.28	0.08	-0.43	-0.14	0.00	0.02	-0.05	0.04	0.00	0.02	-0.04	0.05	-0.29	0.06	-0.42	-0.16	-0.49	0.06	-0.61	-0.38
DisOpen	0.19	0.04	0.12	0.27	0.01	0.03	-0.05	0.08	0.38	0.04	0.31	0.46	0.05	0.05	-0.05	0.16	0.31	0.04	0.23	0.39	0.19	0.04	0.12	0.26	0.32	0.05	0.21	0.43	0.07	0.06	-0.05	0.19
DisAlp	-0.19	0.05	-0.30	-0.08	-0.05	0.06	-0.17	0.07	-0.29	0.05	-0.39	-0.20	-0.06	0.07	-0.19	0.08	-0.34	0.04	-0.42	-0.25	-0.20	0.04	-0.27	-0.12	-0.02	0.04	-0.11	0.06	0.19	0.04	0.11	0.27
OpenN	0.06	0.07	-0.07	0.20	-0.06	0.08	-0.21	0.10	-0.02	0.04	-0.11	0.07	-0.36	0.09	-0.53	-0.19	0.74	0.07	0.61	0.87	0.33	0.05	0.22	0.43	0.60	0.11	0.38	0.82	0.21	0.08	0.06	0.37
AlpCov									-0.48	0.07	-0.62	-0.34	-0.45	0.10	-0.64	-0.26	-0.04	0.06	-0.16	0.08	0.00	0.02	-0.04	0.04								
SIDI	0.02	0.06	-0.09	0.13	0.22	0.07	0.07	0.36	0.42	0.07	0.29	0.56	0.29	0.09	0.10	0.47	0.42	0.07	0.29	0.56	0.21	0.06	0.10	0.32	0.39	0.08	0.22	0.55	0.22	0.07	0.09	0.35
PLADJ	0.20	0.08	0.05	0.35	0.28	0.10	0.10	0.47	0.38	0.06	0.27	0.50	0.06	0.06	-0.06	0.17	0.58	0.08	0.43	0.73	0.03	0.05	-0.07	0.12	0.54	0.12	0.31	0.76	0.29	0.09	0.12	0.46

[a] DisAgri = distance to semi-natural agriculture; DisOpen = distance to open areas; DisAlp = distance to alpine prairies; OpenN = number of open areas; AlpCov = alpine prairies cover; SIDI = Simpson Diversity Index; PLADJ = forest aggregation index.

Table 4. Coefficients of averaged multi-grain resource selection functions to investigate habitat selection by bears when selecting suitable single forest patches within wooded areas (fourth-order selection) according to seasons and daytime, in the Abruzzo-Lazio-Molise National Park, central Italy, 2005–2010.

Variable[a]	Spring								Early-summer								Late-summer								Autumn							
	Day				Night				Day				Night				Day				Night				Day				Night			
	β	SE	95% CI		β	SE	95% CI		β	SE	95% CI		β	SE	95% CI		β	SE	95% CI		β	SE	95% CI		β	SE	95% CI		β	SE	95% CI	
			Lower	Upper			Lower	Upper			Lower	Upper			Lower	Upper			Lower	Upper			Lower	Upper			Lower	Upper			Lower	Upper
(Intercept)	-2.32	0.04	-2.40	-2.24	-2.49	0.08	-2.65	-2.33	-2.36	0.04	-2.44	-2.27	-2.48	0.07	-2.62	-2.34	-2.47	0.08	-2.62	-2.32	-2.57	0.07	-2.72	-2.43	-2.38	0.06	-2.50	-2.26	-2.66	0.09	-2.83	-2.49
TCD	0.27	0.05	0.17	0.37	0.28	0.07	0.16	0.41	-0.17	0.04	-0.25	-0.09	0.00	0.07	-0.13	0.14	-0.37	0.04	-0.46	-0.28	-0.41	0.06	-0.52	-0.30	0.29	0.07	0.16	0.42	0.03	0.05	-0.08	0.13
Oak	-0.20	0.15	-0.49	0.09	0.57	0.15	0.28	0.86	0.12	0.11	-0.09	0.33	0.64	0.14	0.38	0.91	-0.01	0.15	-0.31	0.29	0.48	0.12	0.24	0.72	-0.08	0.13	-0.33	0.18	0.64	0.11	0.43	0.86
BAavg	-0.29	0.06	-0.42	-0.17	-0.13	0.11	-0.34	0.09	-0.49	0.07	-0.62	-0.36	-0.41	0.10	-0.60	-0.22	-0.22	0.07	-0.36	-0.08					-0.51	0.09	-0.68	-0.33	-0.36	0.09	-0.53	-0.19
TD	0.28	0.05	0.18	0.37	0.23	0.07	0.09	0.37	0.34	0.05	0.24	0.44	-0.21	0.08	-0.37	-0.04	0.43	0.05	0.33	0.54	-0.13	0.06	-0.24	-0.02	0.25	0.07	0.12	0.38	0.09	0.08	-0.05	0.24
DisFor	-0.16	0.04	-0.23	-0.08	-0.33	0.05	-0.43	-0.22	0.03	0.04	-0.05	0.12	0.06	0.06	-0.06	0.19	-0.16	0.06	-0.27	-0.05	-0.39	0.07	-0.53	-0.25	-0.17	0.06	-0.29	-0.05	0.02	0.04	-0.06	0.10
TCD:Oak	-0.08	0.09	-0.25	0.10	-0.18	0.10	-0.37	0.01	-0.47	0.07	-0.61	-0.34	-0.62	0.10	-0.80	-0.43	-0.12	0.11	-0.33	0.10	0.16	0.11	-0.05	0.36	-0.22	0.10	-0.42	-0.03	0.03	0.07	-0.11	0.17
BAavg:Oak	0.11	0.12	-0.14	0.35	0.12	0.14	-0.16	0.40	0.46	0.11	0.24	0.67	0.47	0.14	0.19	0.75	0.45	0.16	0.14	0.76					0.13	0.14	-0.14	0.40	0.13	0.12	-0.11	0.36
TD:Oak	-0.04	0.08	-0.21	0.12	0.17	0.10	-0.02	0.37	0.10	0.07	-0.04	0.24	0.42	0.11	0.21	0.63	-0.27	0.12	-0.49	-0.04	0.00	0.09	-0.18	0.19	-0.28	0.10	-0.47	-0.08	-0.52	0.10	-0.72	-0.32

[a] TCD = canopy cover (most parsimonious grain size: spring, early- and late-summer = 1531 m, autumn = 338 m); Oak = oak dominated forest; BAavg = averaged basal area (spring = 666 m, early-summer = 925 m, late-summer = 236 m; autumn = 514 m); TD = tree density (spring and autumn = 47 m; early-summer = 140 m, late-summer = 61 m).

Figure 1. Circadian relative probability of bears establishing a home range (third-order of selection) as a function of distance from cultivated lands affecting habitat selection based on multi-grain resource selection functions in spring (A), early-summer (B), late-summer (C), and autumn (D). Colored areas (day = yellow; night = blue) represent predicted 95% confidence intervals. In all panels, the other predictors included in the models were set at their mean values. Data refer to 11 female bears in Abruzzo-Lazio-Molise National Park, central Italy (2005-2010). D=day; N=night.

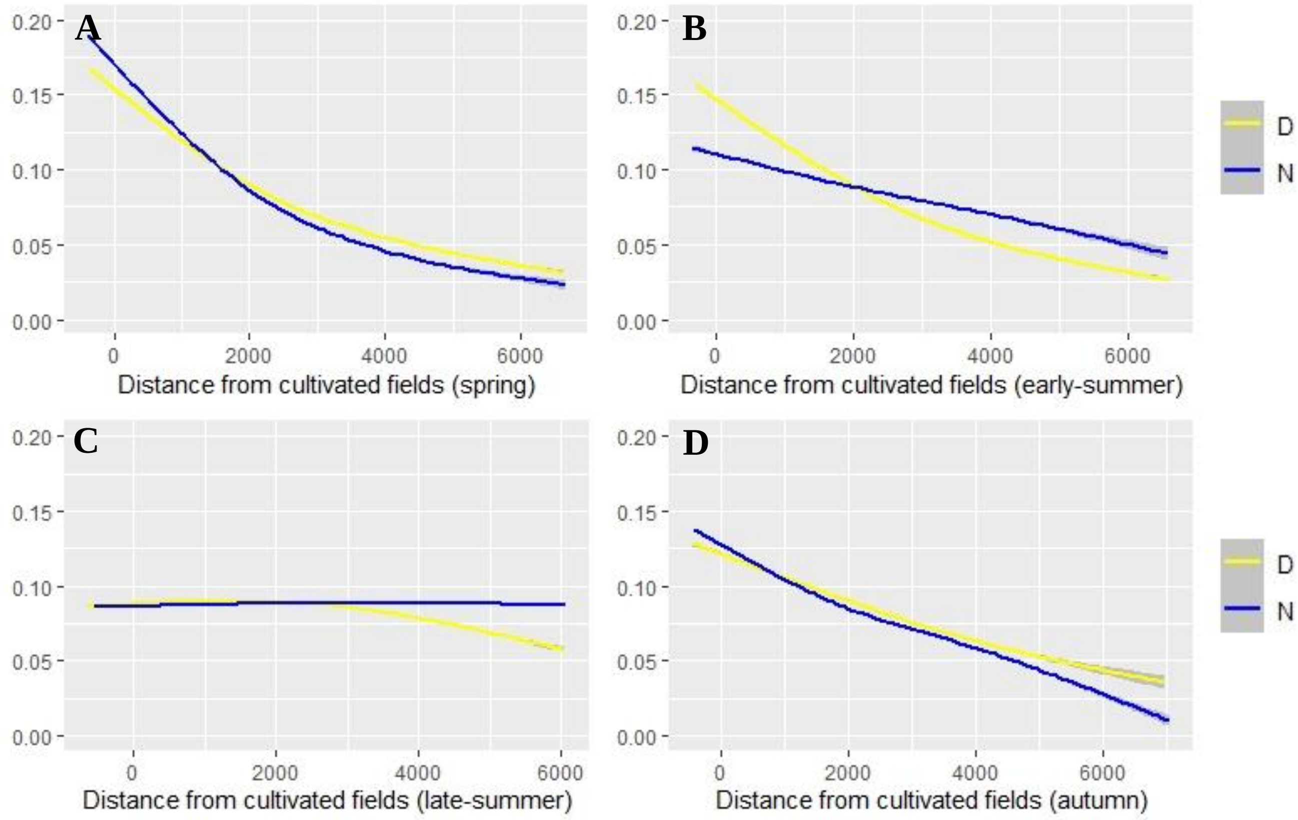

Figure 2. Circadian relative probability of bears establishing a home range (third-order of selection) as a function of distance from alpine prairies affecting habitat selection based on multi-grain resource selection functions in spring (A), early-summer (B), late-summer (C), and autumn (D). Colored areas (day = yellow; night = blue) represent predicted 95% confidence intervals. In all panels, the other predictors included in the models were set at their mean values. Data refer to 11 female bears in Abruzzo-Lazio-Molise National Park, central Italy (2005-2010). D=day; N=night.

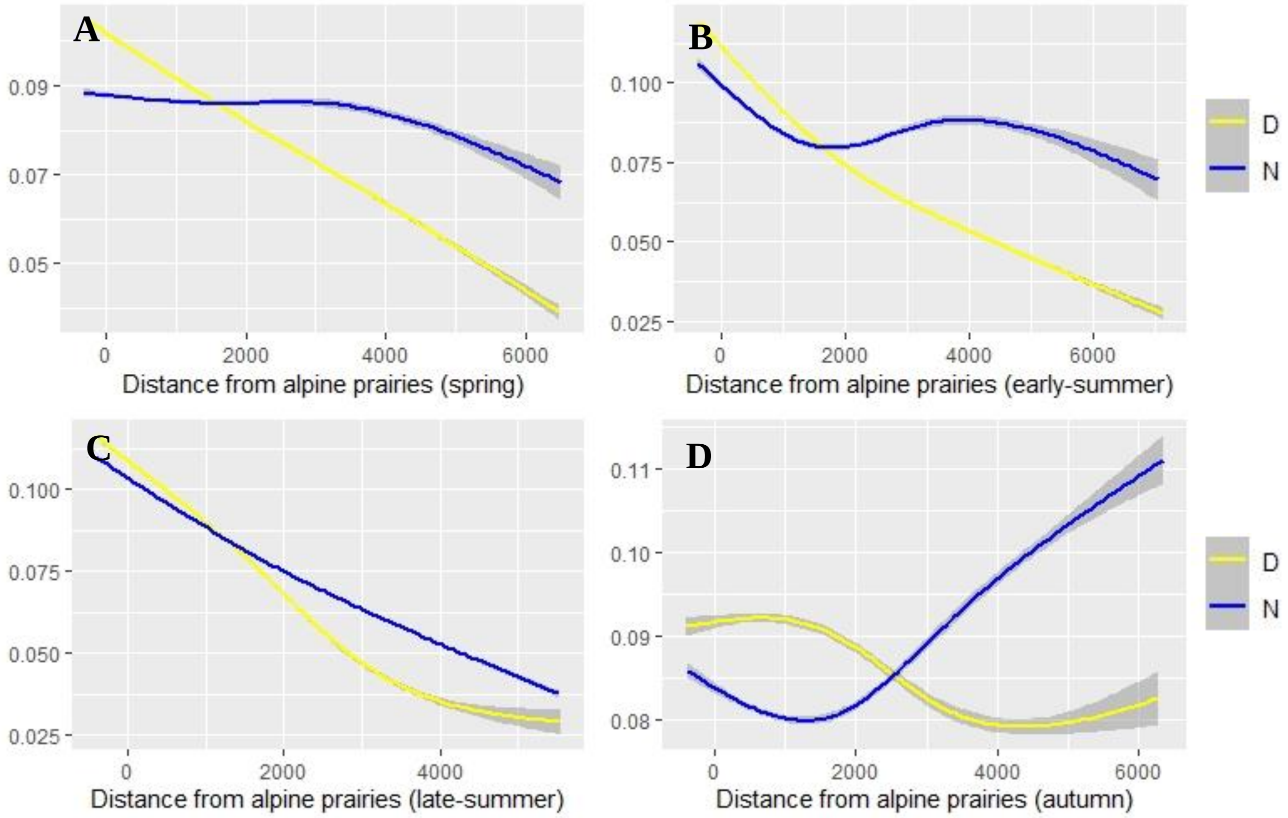

Figure 3. Circadian relative probability of bears establishing a home range (third-order of selection) as a function of alpine prairies cover affecting habitat selection based on multi-grain resource selection functions in early-summer (A), and late-summer (B). Colored areas (day = yellow; night = blue) represent predicted 95% confidence intervals. In all panels, the other predictors included in the models were set at their mean values. Data refer to 11 female bears in Abruzzo-Lazio-Molise National Park, central Italy (2005-2010). D=day; N=night.

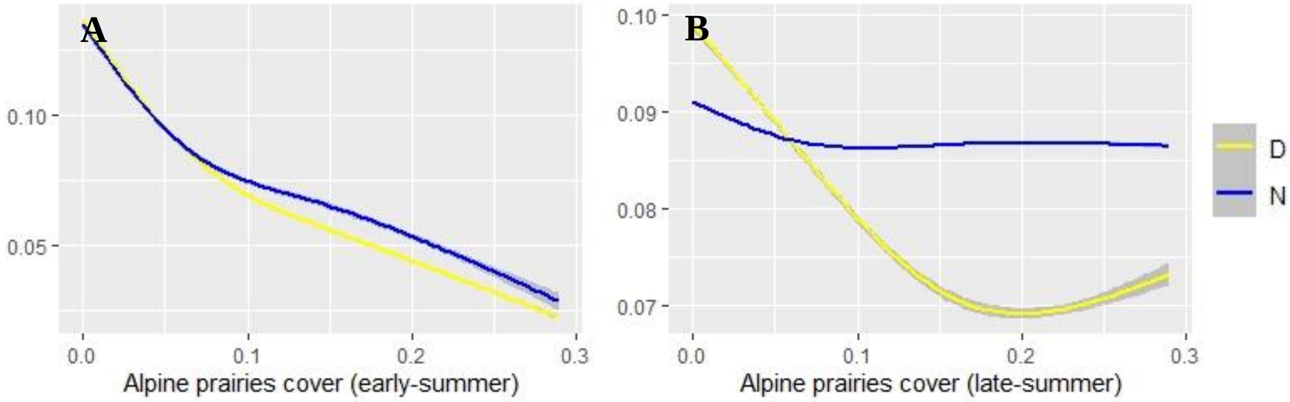

Figure 4. Circadian relative probability of bears establishing a home range (third-order of selection) as a function of distance from open areas affecting habitat selection based on multi-grain resource selection functions in spring (A), early-summer (B), late-summer (C), and autumn (D). Colored areas (day = yellow; night = blue) represent predicted 95% confidence intervals. In all panels, the other predictors included in the models were set at their mean values. Data refer to 11 female bears in Abruzzo-Lazio-Molise National Park, central Italy (2005-2010). D=day; N=night.

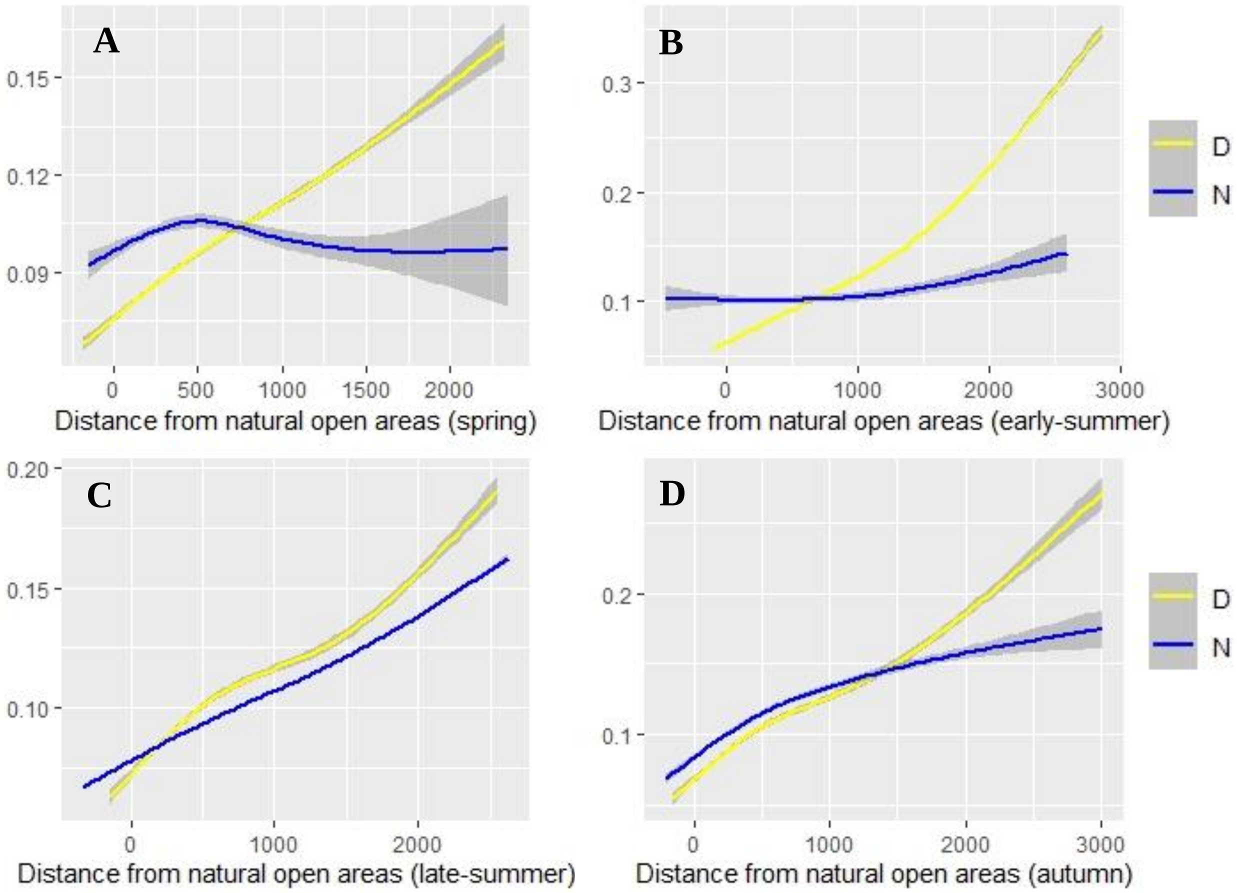

Figure 5. Circadian relative probability of bears establishing a home range (third-order of selection) as a function of number of open areas affecting habitat selection based on multi-grain resource selection functions in spring (A), early-summer (B), late-summer (C), and autumn (D). Colored areas (day = yellow; night = blue) represent predicted 95% confidence intervals. In all panels, the other predictors included in the models were set at their mean values. Data refer to 11 female bears in Abruzzo-Lazio-Molise National Park, central Italy (2005-2010). D=day; N=night.

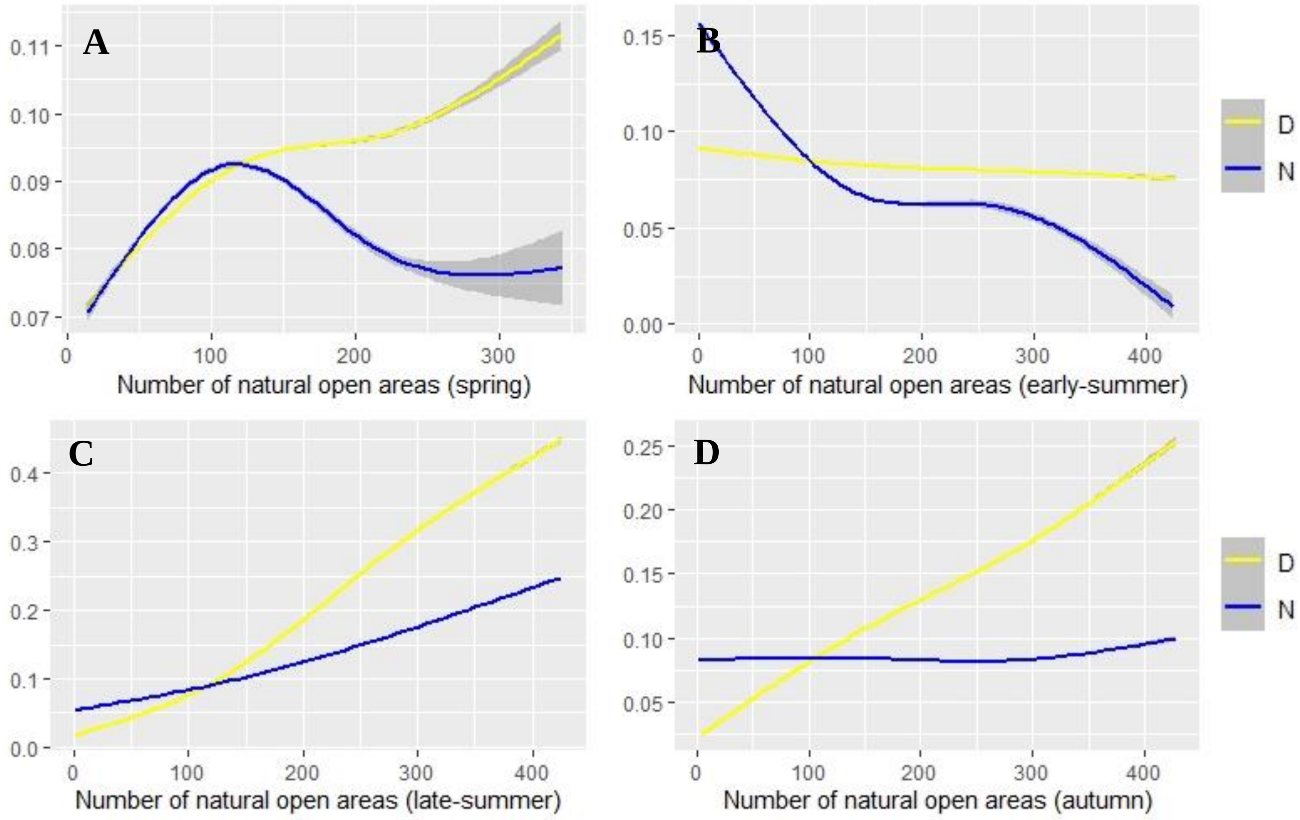

Figure 6. Circadian relative probability of bears establishing a home range (third-order of selection) as a function of Simpson's index (SIDI) affecting habitat selection based on multi-grain resource selection functions in spring (A), early-summer (B), late-summer (C), and autumn (D). Colored areas (day = yellow; night = blue) represent predicted 95% confidence intervals. In all panels, the other predictors included in the models were set at their mean values. Data refer to 11 female bears in Abruzzo-Lazio-Molise National Park, central Italy (2005-2010). D=day; N=night.

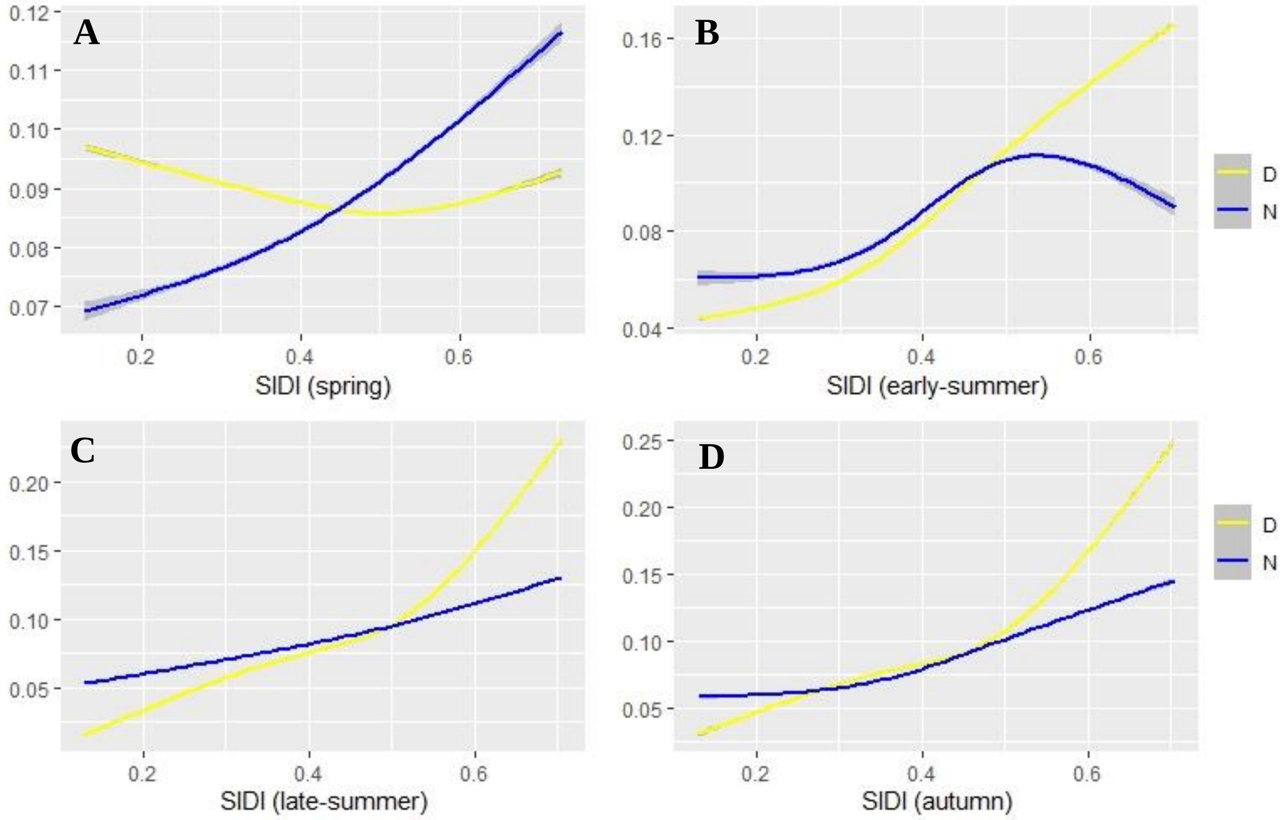

Figure 7. Circadian relative probability of bears establishing a home range (third-order of selection) as a function of forest aggregation (PLADJ) affecting habitat selection based on multi-grain resource selection functions in spring (A), early-summer (B), late-summer (C), and autumn (D). Colored areas (day = yellow; night = blue) represent predicted 95% confidence intervals. In all panels, the other predictors included in the models were set at their mean values. Data refer to 11 female bears in Abruzzo-Lazio-Molise National Park, central Italy (2005-2010). D=day; N=night.

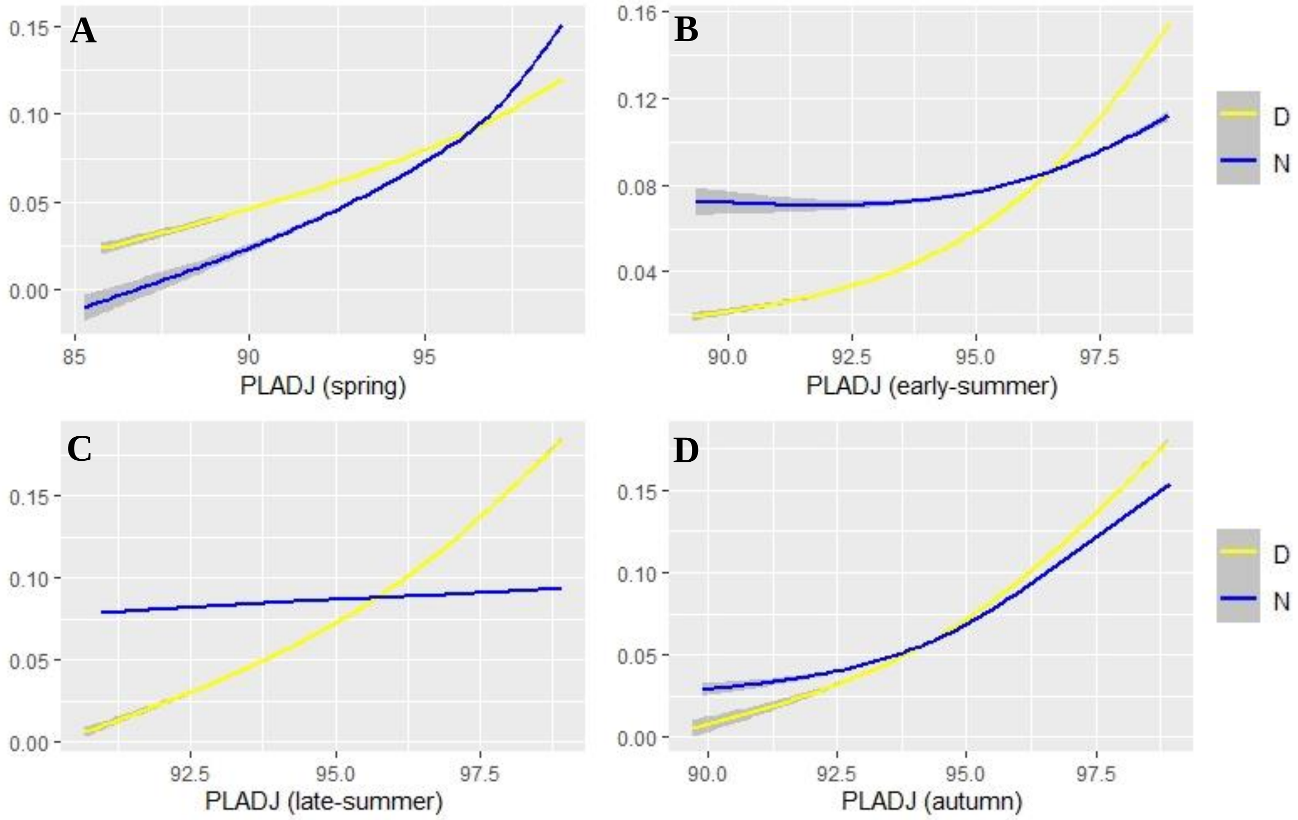

Figure 8. Circadian relative probability of bears selecting a forest patch within home range (fourth order of selection) as a function of tree canopy cover (%) in interaction with the dominant tree species (Fagg=beech; QuercFrax=oak) based on multi-grain resource selection functions in in spring (A), early-summer (B), late-summer (C), and autumn (D). Colored areas (day = yellow; night = blue) represent predicted 95% confidence intervals. In all panels, the other predictors included in the models were set at their mean values. Data refer to 11 female bears in Abruzzo-Lazio-Molise National Park, central Italy (2005-2010).

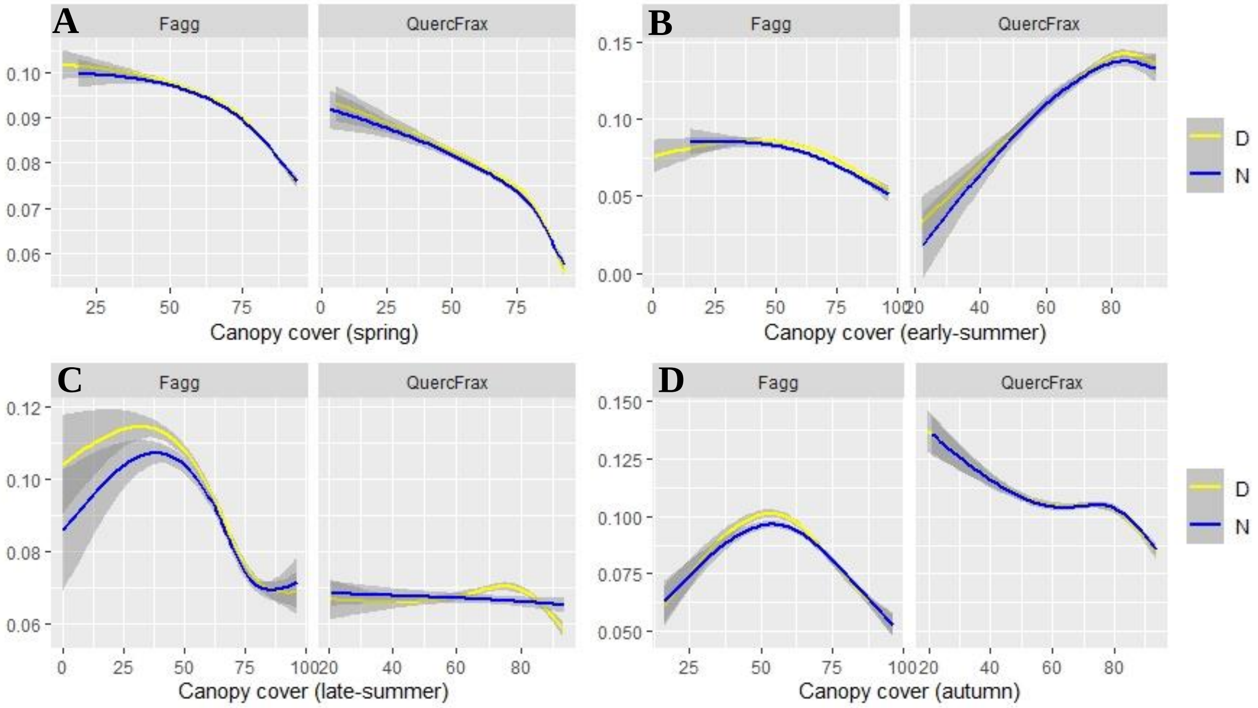

Figure 9. Circadian relative probability of bears selecting a forest patch within home range (fourth order of selection) as a function of distance from forest edge (m) based on multi-grain resource selection functions in in spring (A), early-summer (B), late-summer (C), and autumn (D). Colored areas (day = yellow; night = blue) represent predicted 95% confidence intervals. In all panels, the other predictors included in the models were set at their mean values. Data refer to 11 female bears in Abruzzo-Lazio-Molise National Park, central Italy (2005-2010).

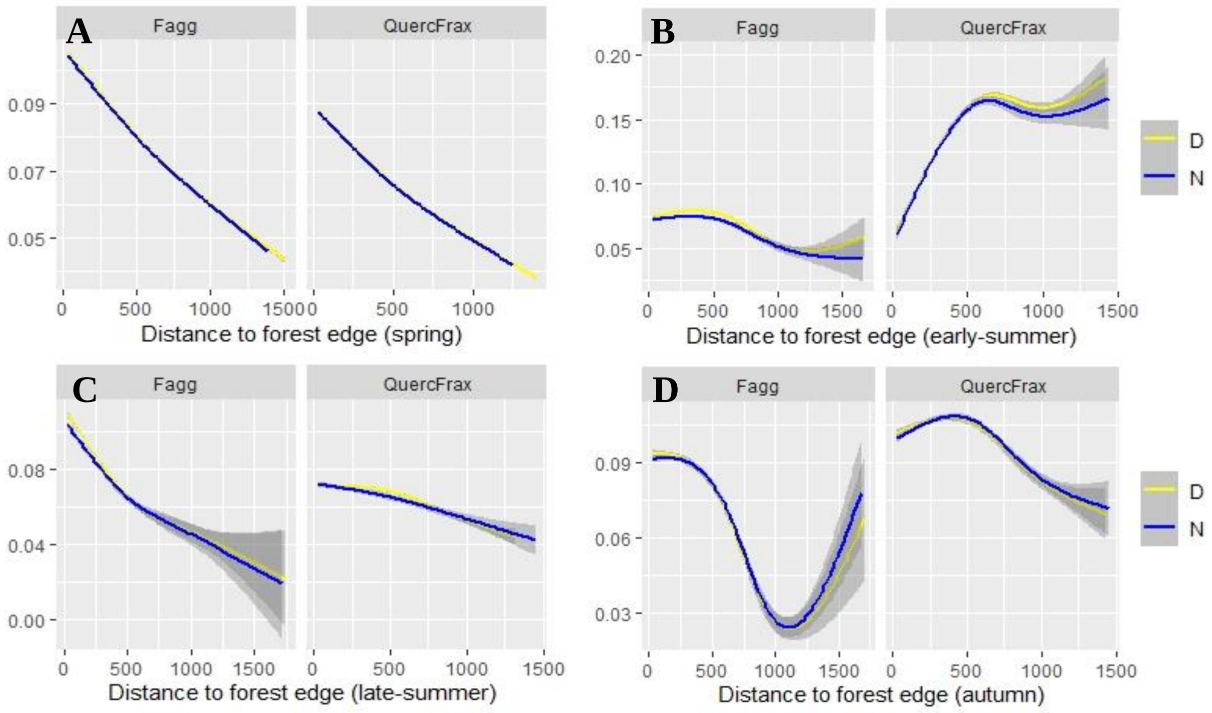

Figure 10. Circadian relative probability of bears selecting a forest patch within home range (fourth-order of selection) as a function of averaged basal area (m^2/ha) in interaction with the dominant tree species (Fagg=beech; QuercFrax=oak) based on multi-grain resource selection functions in in spring (A), early-summer (B), late-summer (C), and autumn (D). Colored areas (day = yellow; night = blue) represent predicted 95% confidence intervals. In all panels, the other predictors included in the models were set at their mean values. Data refer to 11 female bears in Abruzzo-Lazio-Molise National Park, central Italy (2005-2010).

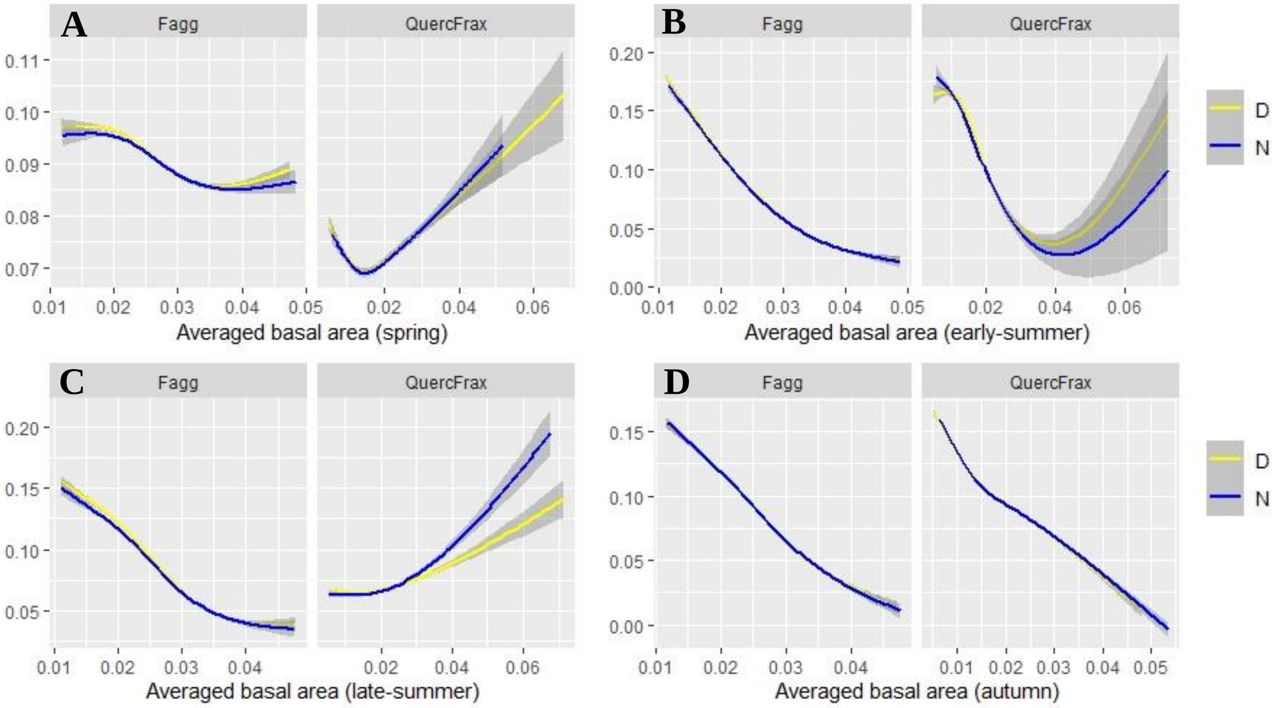

Figure 11. Circadian relative probability of bears selecting a forest patch within home range (fourth order of selection) as a function of tree density (N/ha) in interaction with the dominant tree species (Fagg=beech; QuercFrax=oak) based on multi-grain resource selection functions in in spring (A), early-summer (B), late-summer (C), and autumn (D). Colored areas (day = yellow; night = blue) represent predicted 95% confidence intervals. In all panels, the other predictors included in the models were set at their mean values. Data refer to 11 female bears in Abruzzo-Lazio-Molise National Park, central Italy (2005-2010).

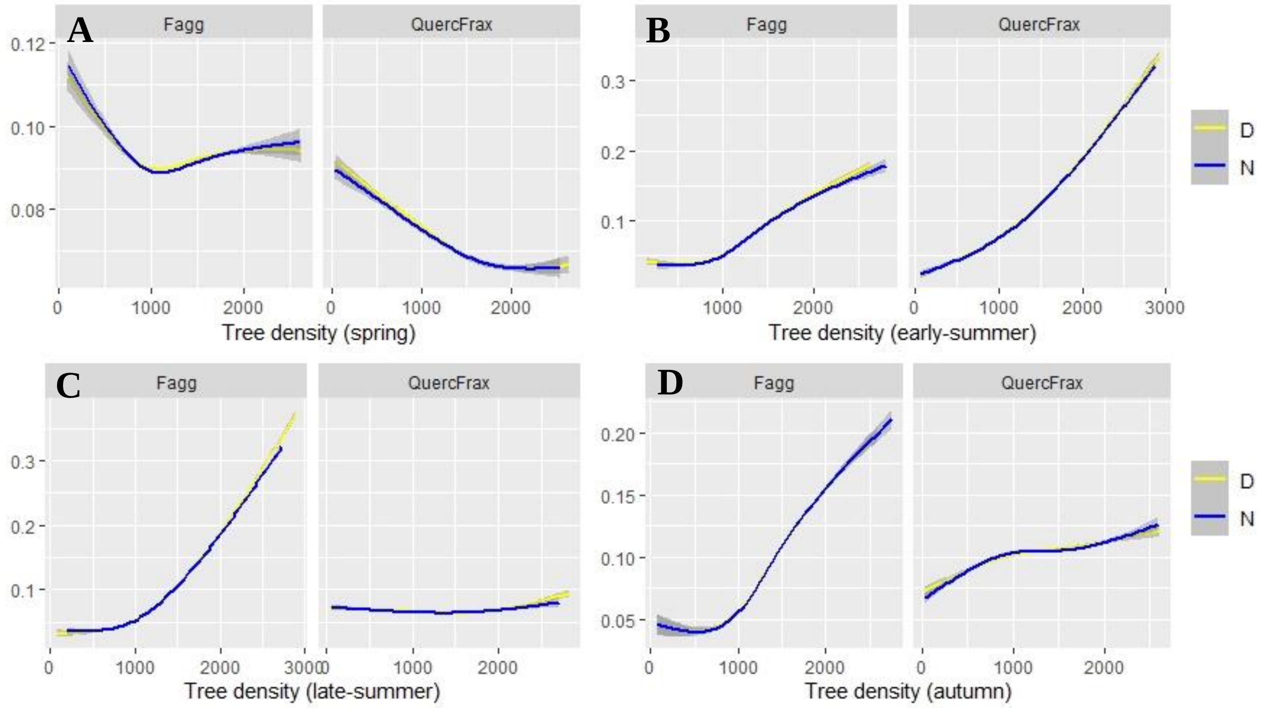

SUPPLEMENTARY MATERIAL

Table S1. Pair-wise correlation (Pearson's *r*) between variables at the third-order of selection calculated for each variable and reported as mean (white) and standard deviation (grey box) calculated at each season (spring, early-summer, late-summer, and autumn). I excluded from the analysis all variables with Pearson's *r*>0.7 (bold values). DisAgri = distance to cultivated lands; DisOpen = distance to open areas at low and medium elevation; DisAlp = distance to alpine prairies; AlpCov = alpine prairies cover; OpenCov = open areas cover at low and medium elevation; OpenN = number of open areas within circular buffer (see optimzed multigrain analysis); SIDI = Simpson's index; SHIDI = Shannon's index; PLADJ = meausur of forest aggregation; ED = edge density; nLSI = meausur of complexity of the forest patches' shape.

	DisAgri	DisOpen	DisAlp	AlpCov	OpenCov	OpenN	SIDI	SHIDI	PLADJ	ED	nLSI
DisAgri	1	0.57	-0.56	0.58	-0.61	-0.55	-0.10	-0.35	0.51	-0.55	-0.37
DisOpen	0.11	1	-0.36	0.60	-0.56	-0.54	0.13	-0.06	0.42	-0.57	-0.50
DisAlp	0.06	0.05	1	-0.62	0.31	0.52	-0.37	-0.18	-0.04	0.16	0.51
AlpCov	0.10	0.04	0.02	1	-0.51	-0.63	0.49	0.26	0.18	-0.46	**-0.76**
OpenCov	0.06	0.05	0.10	0.07	1	0.58	0.26	0.46	**-0.81**	**0.81**	0.38
OpenN	0.08	0.04	0.05	0.04	0.04	1	-0.27	-0.07	-0.48	**0.75**	**0.75**
SIDI	0.11	0.04	0.09	0.07	0.08	0.09	1	**0.95**	-0.55	0.17	-0.67
SHIDI	0.09	0.06	0.13	0.11	0.06	0.12	0.01	1	-0.68	0.35	-0.48
PLADJ	0.08	0.06	0.12	0.12	0.04	0.10	0.07	0.04	1	**-0.87**	-0.20
ED	0.08	0.06	0.10	0.10	0.01	0.08	0.12	0.09	0.03	1	0.54
nLSI	0.11	0.05	0.03	0.01	0.08	0.05	0.03	0.07	0.10	0.11	1

Table S2. Variance Inflation Factor (VIF) at the third-order of selection reported as mean (white) and standard deviation (grey box) calculated at each season (spring, early-summer, late-summer, and autumn). For each variable, VIF values are reported as mean and standard deviation calculated at each season. For variables names see Table S1.

	VIF			
	1^{st} round		**2^{nd} round**	
DisAgri	4.41	(±1.03)	3.20	(±0.66)
DisOpen	2.14	(±0.22)	2.03	(±0.23)
DisAlp	3.26	(±0.55)	2.25	(±0.23)
AlpCov	5.41	(±0.34)	3.90	(±0.39)
OpenCov	6.15	(±1.44)	-	-
OpenN	5.84	(±1.02)	3.43	(±0.24)
SIDI	71.75	(±12.41)	5.22	(±1.54)
SHIDI	49.96	(±10.95)	-	-
PLADJ	20.14	(±4.53)	4.86	(±0.72)
ED	20.15	(±4.21)	-	-
nLSI	16.59	(±2.97)	-	-

Table S3. Pair-wise correlation (Pearson's r) between variables at the fourth-order of selection during spring (March–May) calculated for each variable and reported as mean (white) and standard deviation (grey box) calculated at each grain size (i.e., from 47m to 1531m). TCD = canopy cover (%); BA = sum of basal areas (m^2/ha); TD = tree density (N/ha); BAavg = averaged basal area (m^2/ha), DisFor = distance from forest edge (m).

	TCD	BAavg	BA	TD	DisFor
TCD	-	0.29	0.61	0.35	0.51
BAavg	0.03	-	0.67	-0.41	0.12
BA	0.06	0.01	-	0.30	0.29
TD	0.12	0.18	0.21	-	0.19
DisFor	0.08	0.03	0.08	0.07	-

Table S4. Pair-wise correlation (Pearson's r) between variables at the fourth-order of selection during early-summer (June–July) calculated for each variable and reported as mean (white) and standard deviation (grey box) calculated at each grain size (i.e., from 47m to 1531m). For variables names see Table S3.

	TCD	BAavg	BA	TD	DisFor
TCD	-	0.23	0.55	0.31	0.49
BAavg	0.09	-	0.63	-0.48	0.05
BA	0.16	0.17	-	0.18	0.24
TD	0.13	0.16	0.18	-	0.23
DisFor	0.16	0.03	0.09	0.08	-

Table S5. Pair-wise correlation (Pearson's r) between variables at the fourth-order of selection during late-summer (June–July) calculated for each variable and reported as mean (white) and standard deviation (grey box) calculated at each grain size (i.e., from 47m to 1531m). For variables names see Table S3.

	TCD	BAavg	BA	TD	DisFor
TCD	-	0.33	0.67	0.38	0.53
BAavg	0.04	-	0.67	-0.38	0.13
BA	0.06	0.01	-	0.33	0.33
TD	0.15	0.20	0.23	-	0.23
DisFor	0.09	0.03	0.06	0.07	-

Table S6. Pair-wise correlation (Pearson's r) between variables at the fourth-order of selection during autumn (October-November 23) calculated for each variable and reported as mean (white) and standard deviation (grey box) calculated at each grain size (i.e., from 47m to 1531m). For variables names see Table S3.

	TCD	BAavg	BA	TD	DisFor
TCD	-	0.25	0.62	0.42	0.55
BAavg	0.03	-	0.63	-0.37	0.15
BA	0.06	0.00	-	0.39	0.33
TD	0.10	0.16	0.18	-	0.23
DisFor	0.09	0.02	0.05	0.06	-

Table S7. Variance Inflation Factor (VIF) at the fourth-order of selection reported on a seasonal basis. For each variable, VIF values are reported as mean and standard deviation calculated at each grain size (i.e., from 47m to 1531m). I excluded sum of basal area (BA) because high correlated with the rest of variables (VIF>6) For variables names see Table S3.

Variables	**VIF**							
	Spring		**Early-summer**		**Late-summer**		**Autumn**	
	1st round	**2nd round**	**1st round**	**2nd round**	**1st round**	**2nd round**	**1st round**	**2nd round**
TCD	2.17 (±0.39)	1.99 (±0.39)	2.18 (±0.37)	2.03 (±0.36)	2.52 (±0.53)	2.33 (±0.53)	2.31 (±0.41)	2.16 (±0.42)
BA	8.00 (±0.38)	- -	9.28 (±0.26)	- -	8.68 (±0.42)	- -	7.55 (±0.31)	- -
BAavg	8.45 (±3.07)	1.86 (±0.36)	7.94 (±1.78)	1.96 (±0.39)	9.76 (±3.36)	2.33 (±0.40)	8.82 (±3.10)	1.63 (±0.28)
TD	5.34 (±1.28)	1.93 (±0.24)	5.65 (±1.07)	2.06 (±0.28)	6.02 (±1.45)	1.93 (±0.23)	5.93 (±1.62)	1.86 (±0.18)
DisFor	1.40 (±0.15)	1.39 (±0.15)	1.46 (±0.19)	1.44 (±0.19)	1.46 (±0.19)	2.02 (±0.19)	1.51 (±0.20)	1.49 (±0.20)

Figure S1. Effect of adding a given variable to the quasi-global resource selection model (*sensu* Laforge et al. 2015) to assess to assess habitat selection at the third-order of selection by adult Apennine female bears (*n* = 11) during early-summer (June–July) in the Abruzzo-Lazio-Molise National Park (central Italy, 2005–2010). Effects assessed at incremental grain sizes, from 47 to 1,531 m, and are measured both in terms of AIC score (ΔAIC_c, top row) and model averaged coefficients (β ±95% confidence intervals; bottom row) across incremental grain sizes from 47–1,531 m. Following Laforge et al. (2015), I retained the grain size corresponding to the lowest ΔAIC_c for each variable: canopy cover, averaged basal area and tree density.

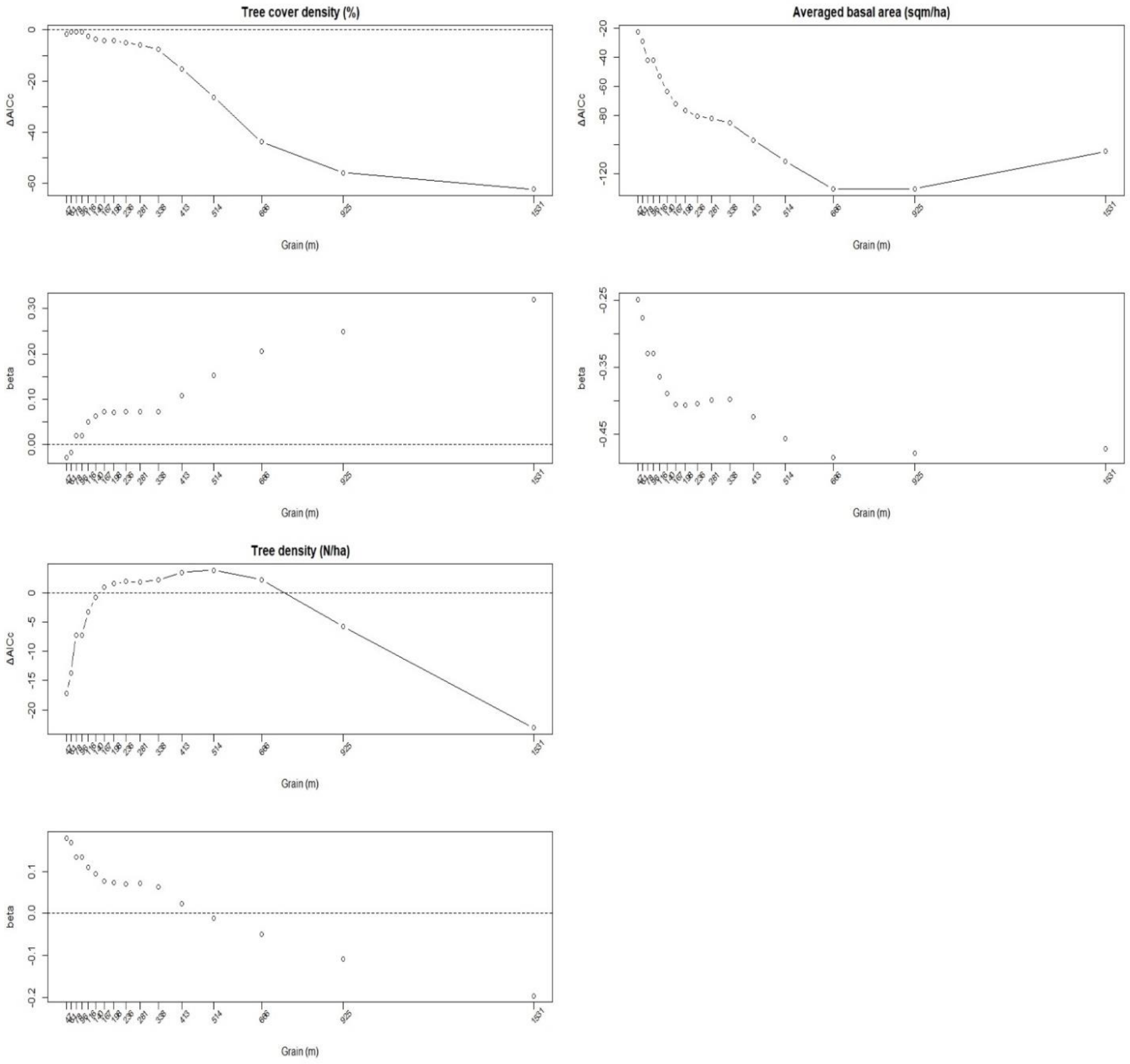

Figure S2. Effect of adding a given variable to the quasi-global resource selection model (*sensu* Laforge et al. 2015) to assess to assess habitat selection at the fourth-order of selection by adult Apennine female bears (*n* = 11) during early-summer (June–July) in the Abruzzo-Lazio-Molise National Park (central Italy, 2005–2010). Effects assessed at incremental grain sizes, from 47 to 1,531 m, and are measured both in terms of AIC score (ΔAIC_c, top row) and model averaged coefficients (β ±95% confidence intervals; bottom row) across incremental grain sizes from 47–1,531 m. Following Laforge et al. (2015), I retained the grain size corresponding to the lowest ΔAIC_c for each variable: canopy cover, averaged basal area and tree density.

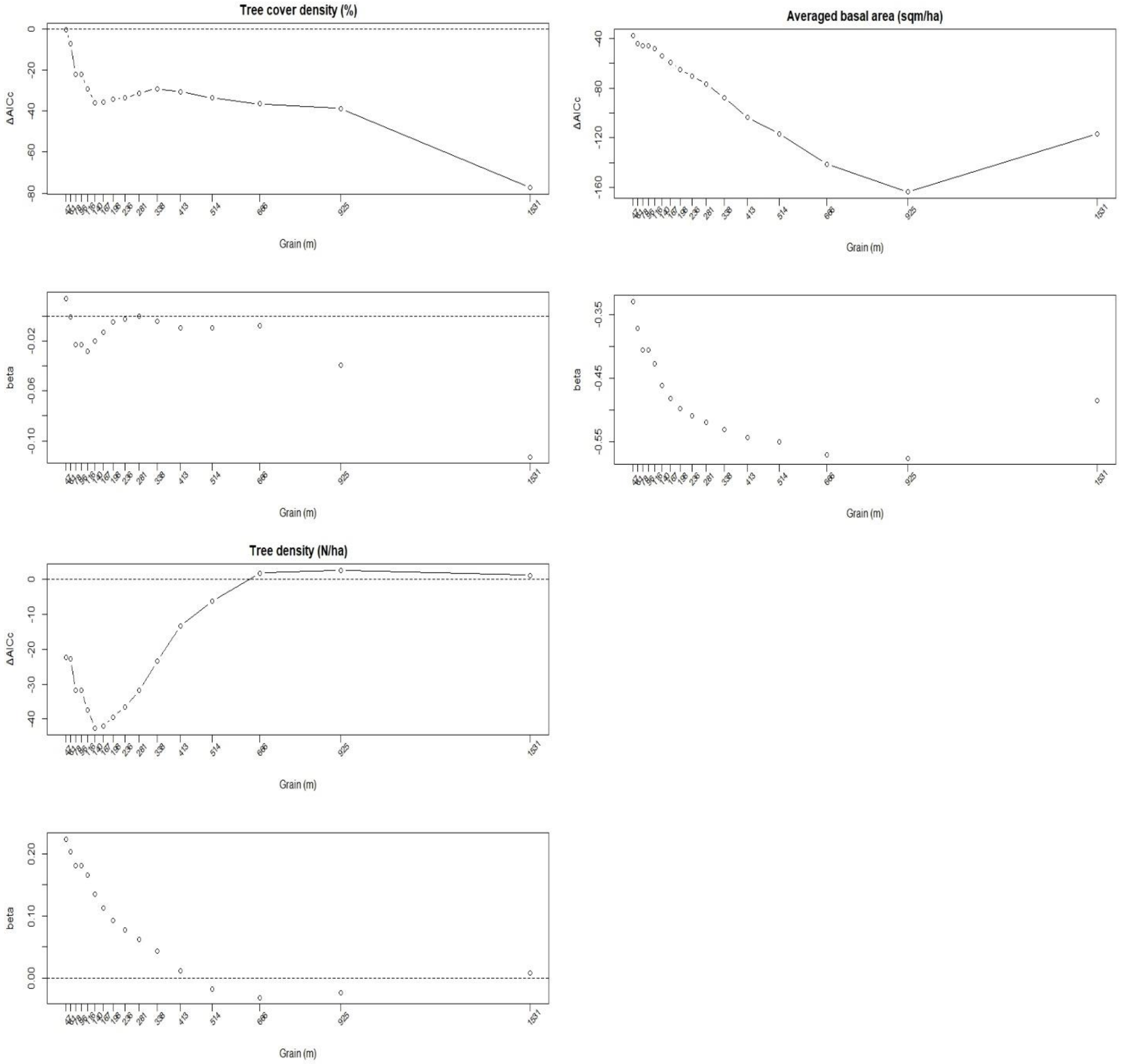

Figure S3. Effect of adding a given variable to the quasi-global resource selection model (*sensu* Laforge et al. 2015) to assess to assess habitat selection at the fourth-order of selection by adult Apennine female bears (n = 11) during late-summer (August–September) in the Abruzzo-Lazio-Molise National Park (central Italy, 2005–2010). Effects assessed at incremental grain sizes, from 47 to 1,531 m, and are measured both in terms of AIC score (ΔAIC_c, top row) and model averaged coefficients (β ±95% confidence intervals; bottom row) across incremental grain sizes from 47–1,531 m. Following Laforge et al. (2015), I retained the grain size corresponding to the lowest ΔAIC_c for each variable: canopy cover, averaged basal area and tree density.

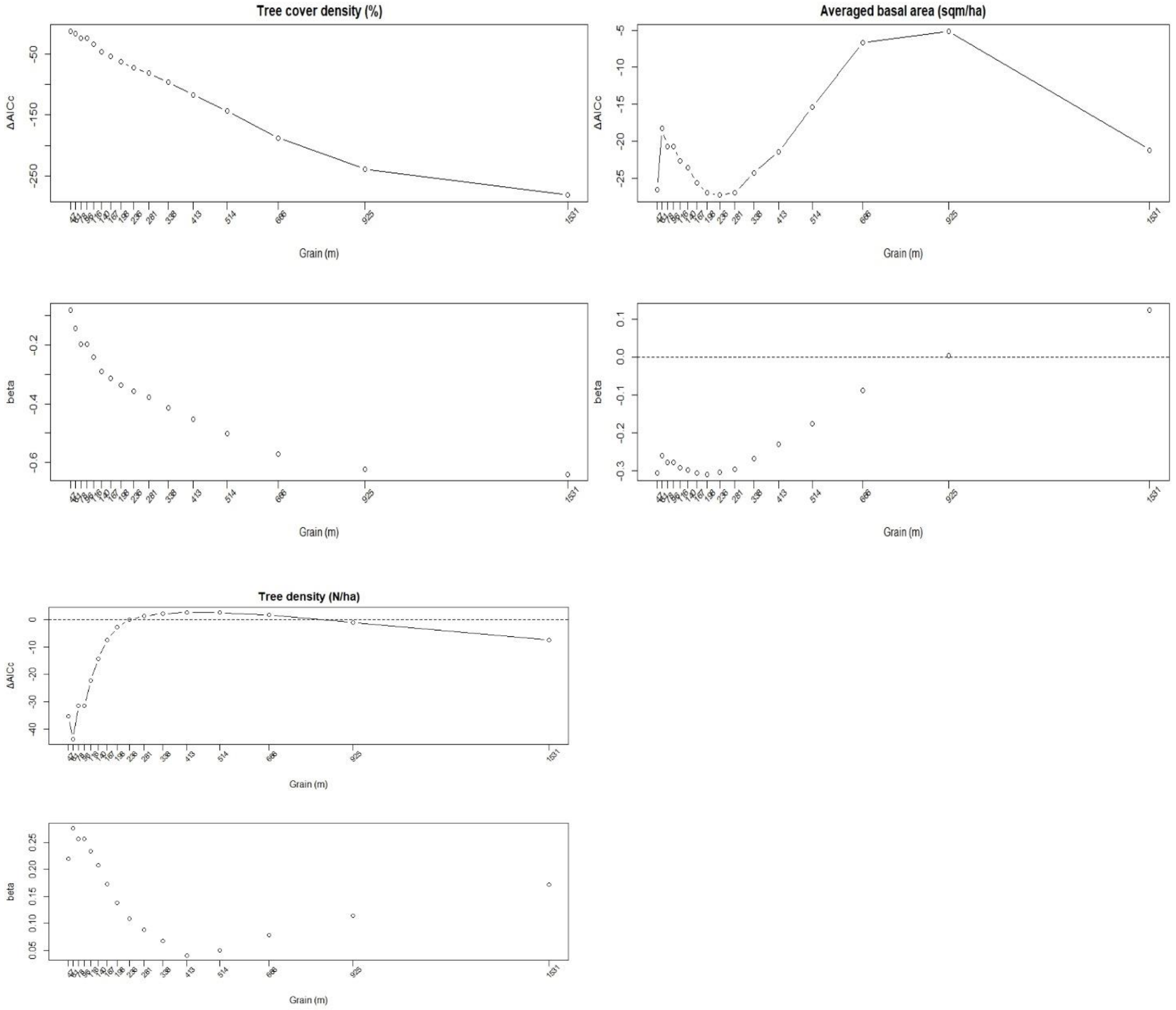

Figure S4. Effect of adding a given variable to the quasi-global resource selection model (*sensu* Laforge et al. 2015) to assess to assess habitat selection at the fourth-order of selection by adult Apennine female bears (n = 11) during autumn (October–November 23) in the Abruzzo-Lazio-Molise National Park (central Italy, 2005–2010). Effects assessed at incremental grain sizes, from 47 to 1,531 m, and are measured both in terms of AIC score (ΔAIC_c, top row) and model averaged coefficients (β ±95% confidence intervals; bottom row) across incremental grain sizes from 47–1,531 m. Following Laforge et al. (2015), I retained the grain size corresponding to the lowest ΔAIC_c for each variable: canopy cover, averaged basal area and tree density.

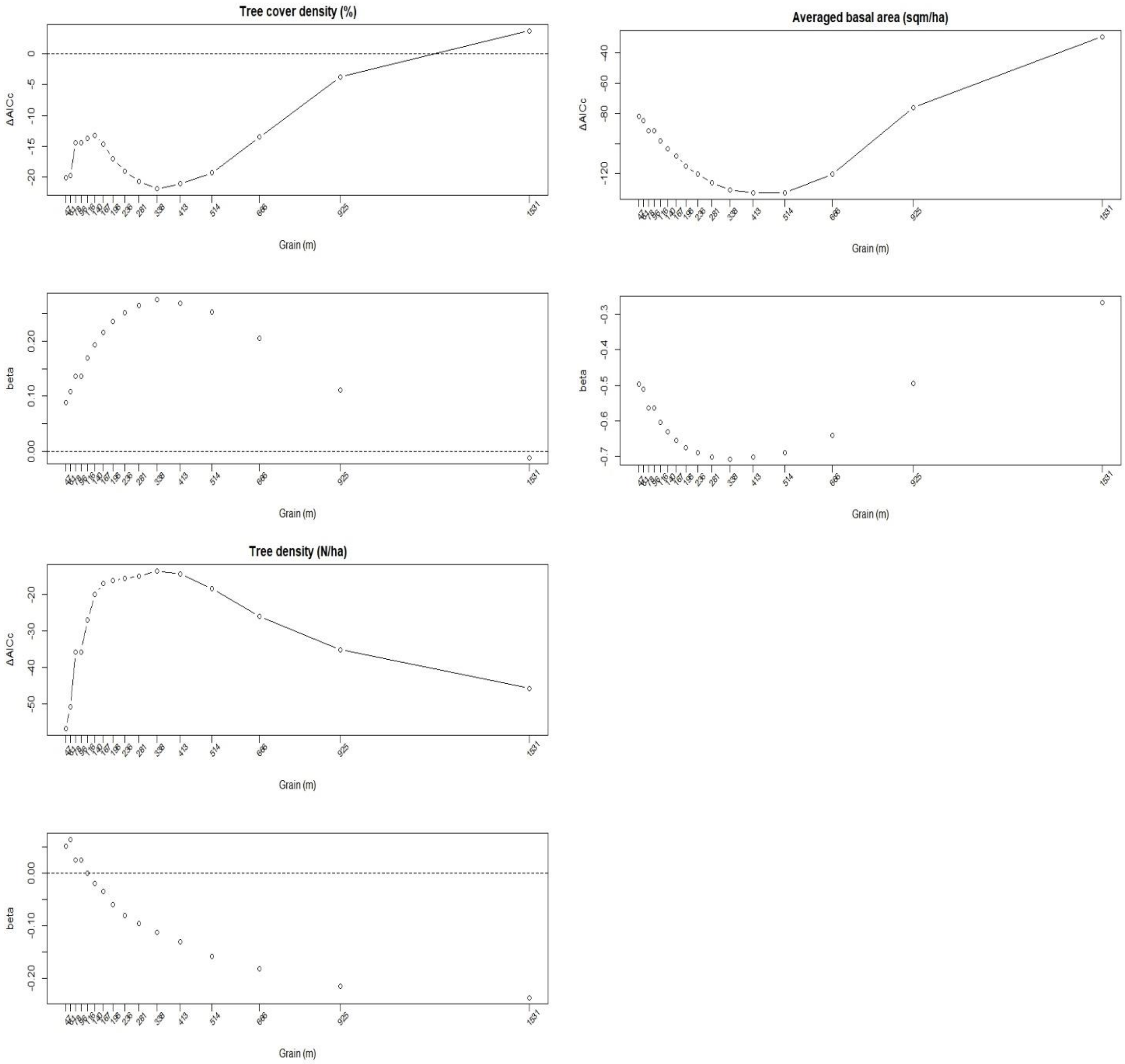

REFERENCES

Laforge, M. P., E. Vander Wal, R. K. Brook, E. M. Bayne, and P. D. McLoughlin. 2015. Process-focussed, multi-grain resource selection functions. Ecological Modelling 305:10–21.

Chapter IV

Forecasting habitat suitability for Apennine brown bear under climate change and alternative forest management scenarios

Matteo Falco[1], Luigi Maiorano[1], Luciano Sammarone[2,3], Carmelo Gentile[3], Mario Posillico[2], Olivier Bouriaud[4], Niklaus E. Zimmermann[5], and Paolo Ciucci[1]

[1] *Sapienza university of Rome. Dept. of Biology and Biotechnology "Charles Darwin", Viale dell'Università 32, Roma 00185, Italy*

[2] *Corpo Forestale dello Stato, Ufficio Territoriale Biodiversità, Via Sangro 45, 67031 Castel di Sangro (AQ), Italy*

[3] *Parco Nazionale d'Abruzzo, Lazio e Molise, Pescasseroli (AQ), Italy*

[4] *University Stefan cel Mare of Suceava, str. Universitatii nr. 13, 720229 Suceava, Romania*

[5] *Swiss Federal Research Institute WSL, Zürcherstr 111, Birmensdorf 8903, Switzerland*

INTRODUCTION

Forests provide fundamental resources for animal species living in forest ecosystems, and both their availability and quality are influenced by vegetation composition, tridimensional structure, and successional dynamic of the forest over the time. Wildlife resources associated to forest ecosystems are crucial to fulfill their primary biological requirements, including foods and refuge sites for thermoregulating, sheltering, and rearing offspring. Abundance, availability, and accessibility of these resources directly influence the survival of individuals, affecting their fitness at the individual and population levels. Notably, however, quality and abundance of these resources are not fixed over the time, but they vary as a function of ecological succession, land and resource use by humans, and forest adaptations to climate change, both in the short and in the long term.

Climate change may strongly influence species composition at large scales (Thuiller et al. 2008, Hickler et al. 2012). At the landscape scale, the topography, the site-specific growth conditions, and the spatial distribution of forest stands that has resulted from past and current forest management will also influence how forests respond to climate change (Farrell et al. 2000, Temperli et al. 2012); consequently, the combinations of these factors have a large impact on habitat suitability by animals living in forest ecosystems. Nonetheless, forest management planning by humans is commonly focused on commercial and economic perspectives, included within protected areas, with little attention to wildlife requirements (Shifley et al. 2006, Bouriaud et al. 2015). It is therefore important to recognize that silvicultural intervention, including no intervention, can deeply alter the rate of ecological succession of forests, potentially seriously impacting wildlife resources availability and habitat suitability. In fact, different stages of forest ecological succession affect its tridimensional structure and productivity (Bruelheide et al. 2011, Swanson et al. 2011, Gutiérrez and Huth 2012), and these factors can lead to top down effects across the trophic web, altering wildlife abundance of resources and habitat suitability (DeWalt et al. 2003, Casula et al. 2017), and having a large impact on biodiversity in forest ecosystem (Zellweger et al. 2016, Scolastri et al. 2017). In addition, whereas the increase or decrease of forest productivity in forest ecosystems can be reflected in the variety, quality, and abundance of trophic resources for wildlife during different period of the year (i.e., food seasonality), forest tridimensional structure, characterized by canopy cover, number and size of trees, plays an important role to fulfil ecological requirements like, for instance, the selection of sites and areas both in terms of covering (e.g., shelter, dens, and breeding sites) and thermoregulation (Ciarniello et al. 2005, Houle et al. 2009, van Beest et al. 2012). This is particularly true for animal species strictly related to forest ecosystems, like the brown bear (*Ursus arctos*), especially in human-dominated landscapes.

In Italy, the imperiled Apennine's population of brown bears is an ideal study case under many different aspects, going from the strict affinity between its functional biological requirements and forest ecosystems (Falcucci et al. 2009, Maiorano et al. 2019), to its conservation priority on national scale (Ciucci and Boitani 2008, Gervasi and Ciucci 2018). Most of the core distribution of Apennine brown bear is comprised within the Abruzzo-Lazio-Molise National Park (PNALM), which features relatively ideal habitat conditions for bears compared to other regions of Italy. About 45% of the current range of presence is covered by forests (Ciucci et al. 2017), and forests represent the 80% of critical areas of conservation identified on Apennine scale (Ciucci et al. 2016). In all previous studies (Chapters 1, 3), forests resulted the land use class strongly selected by bears, independently by season, daytime, and scale of analysis (i.e., orders of selection; Johnson 1980). More than 80% of food energy to Apennine bears is provided by forest resources, and in autumn more than 70% of the bear's diet come from beechnuts (Ciucci et al. 2014). In addition, forests provide a fundamental resource also as denning habitat: in the PNALM, all dens used by GPS-collared bears during the hibernation were selected within forests, and more than 75% of these sites were located in old-growth beech forests where the last harvest interventions date back to at least 80- 100 years ago (Ciucci et al. 2012).

In this study, I aimed to evaluate how alternative forest management scenarios in the PNALM are projected to affect habitat suitability for Apennine brown bears in the next 100 years. I simulated forest succession dynamics under climate change conditions using forest dynamic models at landscape scale (i.e., Program LandClim; Schumacher 2004, Schumacher and Bugmann 2006).

LandClim is a process-based forest model that considers competition-driven stand dynamics and climate sensitive processes such as species-specific recruitment, growth, and mortality. LandClim models allow for interactions between climate change and forest management to be examined at a landscape scale (Temperli et al. 2012, Elkin et al. 2013), providing spatially explicit stand structure information. Using the LandClim's harvest module, in all scenarios, I contemplated a set of forest harvesting schemes, reflecting both current and alternative silvicultural strategies . The current forest harvest regime has been designed and monitored by the Forest Service of the PNALM, which protects large forests in critical areas (i.e., "integral reserve areas") from timber harvesting, permitting it exclusively within few controlled areas (Fig. 1). In line with the forestry strategy adopted in many parts of Europe (Scolastri et al. 2017), and embraced by the PNALM harvesting policy, in these analysis I considered high-forest regime in forest dominated by beech, while I maintained coppice regime only in few portions of forest dominated by oak species detected by Park's Forest Service.

Combining several harvesting parameters in the corresponding LandClim module (e.g., type, quantity, and rotation time of tree species harvested), and presence/absence of local interventions on the forest edge to maintain the current spatial interspersion between forest patches and adjacent open areas, I simulated a total of 5 alternative forest harvesting scenarios. Specifically, my specific aims were to: (*i*) forecast and evaluate the potential changes in structure, species composition, and spatial distribution of the forest in the PNALM accounting for different forest management scenarios, under climate change conditions; (*ii*) calibrate forest dynamic simulation tool in a bear conservation perspective for quantifying changes in habitat suitability in next 100 years, (*iii*) quantify the effect of alternative forest management scenarios on brown bear's habitat suitability at the both home-range (third-order of selection; Johnson 1980) and single-forest patch (fourth-order of selection; Johnson 1980) scales of analysis to investigate which forest management strategy would better maintain (or enhance) habitat suitability for Apennine bears in the next 100 years. Despite in previous studies (Chap. 1, 3) I found both seasonal and circadian effects in habitat selection by Apennine bears, in this study I limited the projections to the overall habitat suitability by adult female bears during late hyperphagia (autumn), corresponding to the season in which I recorded the highest use of forest resources (i.e., hard mast).

METHODS

Study landscape

I simulated forest landscape dynamics of 50,686-ha landscape corresponding to the boundaries of the Abruzzo-Lazio-Molise National Park (PNALM), within central Apennines mountains, Italy (41° 48’N, 13° 47’E) (Fig. 1). Elevation ranges from 145 to 2278 meters above sea level (m. a. s. l.), and the mean tree line elevation in the central Apennine was 1,589 m. a. s. l., although considerable variability among peaks was found (from 863 to 2,049 m. a. s. l.) (Bonanomi et al. 2018). The climate in the area is Mediterranean mountain with dry summers and cold, snowy winters (Piovesan et al. 2003). The potential natural vegetation would be a mixed European beech (*Fagus sylvatica*) forest with oaks (*Quercus* spp.), hop-hornbeam (*Ostrya carpinofolia*; *Carpinus* spp.), the latter increasing in proportion at lower altitudes. Over tree line, higher altitudes are dominated by alpine pastures, shrubs (e.g., *Rhamnus* spp.), and no-vegetated rocks areas. Whereas broadleaf forests dominant the landscape, coniferous forest is exceedingly rare, and its presence is due to the past management actions, focused on Austrian pine (*Pinus nigra*) plantations. Assuming there are no changes in human settlements and agricultural covered areas in the future, I exclude from the LandClim simulations areas covered by cultivated lands, and human settlements.

LandClim functioning

LandClim design

LandClim is a spatially explicit, stochastic model developed starting from the well-established LANDIS model (He and Mladenoff 1999), and designed to study forest dynamics determined by a set of driving forces including large-scale natural disturbances, land-use, climatic parameters, soil properties, and topography (Schumacher 2004; Schumacher and Bugmann 2006). LandClim reflects processes at two spatial scales: (*i*) the patch scale (i.e., grid-cells of 30 x 30 m) and (*ii*) the landscape scale (i.e., large geographical areas up to several thousand hectares). At the patch scale, the processes that influence forest succession are simulated on an annual time-step. This includes the simulation of establishment, growth, reproduction, mortality, intra- and inter-specific competition. Similar to other forest models, LandClim does not simulate individual trees but rather uses a cohort approach, i.e. groups of trees of the same age and species (Bugmann 2001). At the landscape scale, LandClim simulates how these patch scale processes are influenced by large-scale natural disturbances (e.g., fires, windthrow, bark beetles), forest management, and the physical environment. Interactions between cells and landscape scale processes are implemented on a decadal time step. The model requires parameter sets describing autecological properties of tree species, physical site conditions, climate, and disturbance regimes (e.g., forest harvesting, wind, fire, and beetles). I used 23 tree species that mainly occur within the study area, parametrized for Central Europe (Schumacher 2004; Henne et al. 2011), and Mediterranean (Elkin et al. 2015) tree species, as defined and described by Schumacher (2004) (Table 1).

To reach the objectives of the study without increase the modeling complexity, I performed forest dynamic simulations using only the LandClim’s harvesting disturbance module. Finally, to account for stochasticity of the models, results reported in this work derived by the mean values of five simulation runs evaluated.

Defining forest current state

There are not many examples of landscape level modelling of forest succession under climate change in Europe, partly because it requires a detailed description of the current forest state. LandClim provides two alternative methods to produce an accurate current forest state (i.e., structure and tree species composition) of study landscape, namely ‘model initialization’, and ‘stand-alone method’. Using model initialization, the user have to calibrate thousands-years of forest ecological succession (about 2000 years) needed to reach the equilibrium between current climatic conditions, disturbance regime, and vegetation structure and composition (i.e., *pseudo-equilibrium*; Temperli et al. 2012); at the contrary, in the stand-alone method, for each pixel of the study landscape the user needed to create a file *a priori* that resume a detailed description of the all structural parameter of the cohorts which are normally produced by LandClim simulations. In this analysis, I used the stand-alone method, and I derived all necessary stand structure information combining both Regional forest type information with the forest structure maps (i.e., basal area, and tree density, and canopy cover), obtained by modeling remote sensing and forest inventory data within an ensemble modeling approach (Chapter 2). All missing structural information were derived by the available stand structural parameters (see Supplementary).

LandClim topographic and climatic input data

To simulate landscape vegetation dynamic, LandClim needed of both topographic and climatic information. I derived elevation, slope and aspect for every grid cell from a digital elevation model (DEM) with an original resolution of 10 m, upscaled to LandClim grid resolution (30 x 30 m) within geographic information system (GIS) environment (ArcMap v. 10.2; Environmental Systems Research Institute, ESRI, Redlands, CA, USA). Following Henne et al., (2011), I used the compound topographic index (CTI; calculated using the Spatial Analyst tools in ESRI ArcGIS 10.2), and elevation to calculate the available soil water content (AWC) values for each LandClim grid-cell. This measure is correlated to soil depth (Moore et al. 1993, Gessler et al. 2000), and it is necessary to LandClim for estimating the cell-specific drought index (DRI; Bugmann and Cramer, 1998; Schumacher et al., 2004), differently for each tree species. All topographic variables were calculated or re-sampled with a common origin and 30x30 m cell size resolution.

To simulate climate conditions, I needed of both past and future time series of mean temperatures and sum of precipitation at monthly resolution, and their altitudinal lapse rate (Schumacher and Bugmann 2006). To represent the future climate conditions, I used time series CHELSA data (Karger et al., 2017), derived from Global Climate Models (GCMs) and obtained from the World Climate Research Programme Coupled Model Intercomparison Project Phase 5 (CMIP5; Taylor et al. 2012) set of models. CHELSA time series monthly temperature and precipitation data were interpolated within the simulated area on 30x30 m grid using a downscaling procedure called Change Factor Methodology (CFM), sometimes referred as delta change factor methodology

(Anandhi et al. 2011). I performed downscaling procedure using time series climate data available from Italian meteorological base stations (1961–2009 time series data; http://www.scia.isprambiente.it/wwwrootscia/Home_new.html) that occurring within the study landscape. Specifically, monthly temperature was downscaled by applying the additive CFM (e.g., Hay et al. 2000; Kilsby et al. 2007; Akhtar et al. 2008), first calculating the arithmetic difference between the observed and CHELSA time series data, and then, adding this difference to future climate scenario; at the contrary, monthly precipitation was downscaled by applying the multiplicative CFM (e.g., Hay et al. 2000; Kilsby et al. 2007; Akhtar et al. 2008) in a similar way of additive CFM except that the ratio, rather than arithmetic difference, is calculated between the current climate baseline and future climate scenario, and then, multiplied to the future climate scenario. Finally, to derive the altitudinal lapse rate for the average temperature and precipitation, I used two close climate stations: Scanno (cod. 2841, elevation 1030 m. a. s. l.) and Pescasseroli (cod. 2891, elevation 1150 m. a. s. l.).

I simulated forest succession using the warmest GCM future climate change scenarios (Representative Concentration Pathways (RCPs), RCP 8.5), calculated with CESM1-BGC models (CMIP5; Knutti et al. 2013; Sanderson et al. 2015). A comparison of the monthly mean values of downscaled control simulation (control dataset 1961–2009) against observed climate data showed an equally similar pattern for temperature and precipitation, with a difference and a ratio respectively always under 1°C and < 1%.

Forest management scenarios

Forest harvesting strategies

To reach this objective, I defined 3 main forest harvesting management: (*i*) ‘*no-harvesting interventions’* scenario (*S0*; hereafter, ‘*baseline*’), in which landscape is managed like a unique entire integral reserved area (i.e., no-timber harvest); (*ii*) ‘*status-quo*’ scenario (*S1*), in which I accounted for the current silvicultural interventions; (*iii*) ‘*proactive practices for bear*’ (*S2*; hereafter, ‘*pro-bear*’), which is similar to *status-quo* scenario (*S1*) but introduces parameters of forest management regime used for timber harvesting in beech dominated forest that are expected to benefit productivity for bears. Each of the above forest management scenarios is characterized by different timber harvesting parameters, associated to the adopted forest management (coppice vs high forest), and dominant tree species (beech and oak forest) (Table 2). Specifically, in *S0* natural forest succession is not influenced by human harvesting, nor are open areas (i.e., hands off strategy); differently, in *S1* I simulated the current forest harvesting strategies delineated by the Forest service of the Park, and in *S2* I set some parameters of trees harvesting emerging from silvicultural indications for brown bear conservation (Rositi et al. 2019); in particular, beech trees are cut with increasing rotation time (from 40 to 20 years), decreasing harvesting volume for larger trees (DBH>40 cm), and increasing harvest rate for smaller trees (DBH=10-40 cm) (Table 2). The idea behind *S1* is to: (*i*) increase the space for largest beech's trees canopy, increasing the amount of solar radiation over the canopy, (*ii*) diversify the structural matrix of forest favoring the hard mast (seed) productivity of the beech's forest and understory productivity, and (*iii*) overall maximize the long-term habitat productivity for brown bear. Given the complexity in predicting oak's biological responses to different forest harvesting parameters compared to the beech, I maintained in the LandClim simulation analysis the oak's harvesting parameters currently adopted by the Forest Service of the Park in the study area, independently by scenarios (Table 2).

Forest-edge treatments

To account for the importance of spatial configuration of forest interspersion with open areas highlighted in the previous study (Chapter 3), limited to the fourth order of selection, I added both for *S1* and *S2* two forest-edge treatments, namely *S1a, S1b, S2a, S2b*: treatments denoted by *a* simulate the natural forest succession without any type of human interventions (e.g., excluding cattle browsing and local silvicultural practices); treatments denoted by *b* simulate instead the systematic intervention along forest edges to maintain the current forest-openness spatial configuration. Operatively, in the forest management scenarios comprising the first treatment (*S1a* and *S2a*), all pixels are included in the LandClim simulations, while in the scenarios comprising the second treatment (*S1b* and *S2b*) I included only the pixel classified as ‘forest’ land use class. In total I therefore simulated 5 forest management scenarios (*S0, S1a*, *S1b*, *S2a,* and *S2b*).

Climate change

In all scenarios, climate change is always accounted using the warmest climate change scenario (RCP 8.5) which corresponds to a global average temperature increase of 5 °C, and a strong decreasing of precipitation. I chose RCP 8.5 emission models to predict climate change for two main reasons: (*i*) the worst climate change scenario represents the most appropriate scenario in a conservation-oriented study focusing on an autochthonous brown bear subspecies at high-risk of extinction; (*ii*) RCP 8.5 emission scenario may in fact under-estimate or lead future concentrations of atmospheric carbon on the business-as-usual path (IPCC 2019).

Forecasting habitat suitability of brown bear

Creating future set of predictor variables

To compare changes in brown bear habitat quality over the time, I projected habitat suitability at the third and fourth Johnson’s order of selection for the next 100 years. For each scenario and order of selection, I used the coefficients estimated in habitat selection models (Chapter 3) in combination with the respective tridimensional structure, composition, and spatial configuration of forest predicted by LandClim’s after 100 years of simulations. To do this, contemplating the same set of covariates of the original habitat model, I calculate new values for those variables according to the 100-year LandClim’s projections: at the home range scale (third-order), the future spatial configuration of forest (i.e., forest aggregation index), open areas (i.e., number of open areas, distances from alpine pastures and open areas at lowest elevation), and the spatial configuration of the other land use classes (i.e., distances from agriculture, and Simpson’s diversity index); at the single-patch forest scale (fourth-order), the future forest structural maps like basal area (m^2/ha), tree density (N/ha), and tree canopy cover (%) (see Chapter 3). While LandClim provides for each pixel stand measures from which I can derive the tree density and average basal area (i.e., from the number of stems, and the sum of trees’ DBH), it does not provide a measure of canopy cover (CC). In this case, following Zhang et al. (2019), I derived canopy cover of trees using other correlated stand parameters predicted by LandClim, like the mean forest height (*MeanH*), leaf area index (*LAI*) and number of stems (*N*), using the following formula:

$$CC = (1.512 + (0.197 * MeanH) + (0.043 * N) - LAI)/1.828$$

For each order of selection, and forest dynamics scenario, I then used the inverse formula of the logit function (Manly et al. 2002) to combine beta coefficients of the previous habitat selection models with the new variables values, forecasting for each pixel of the study area the relative probability of bear presence.

Comparing alternative forest harvesting scenarios

For each order of selection, I divided the continuous projected forest habitat suitability values into two discrete probability classes (1=suitable; 0=unsuitable). To do this, I first used the habitat suitability values obtained from current bear habitat models and corresponding to the female bears' points of presence (i.e., GPS-locations) and absences (i.e., random points sampled within the PANLM), and then calculated the cut-off threshold that would maximize the sensitivity (i.e., proportion of bear presences correctly identified as 1s) and specificity (i.e., the proportion of bear absences correctly identified as 0s). Using then the binary (suitable, unsuitable) habitat suitability projections, I used the software FRAGSTATS 4.2 (McGarigal and Marks 1995) to quantify the overall suitable area and the degree of fragmentation of suitable habitat (Penteriani et al. 2019). I quantified suitable areas according to three measures: the total suitable area within the study area (TA); the mean patch size of suitable habitat (MPA; the average size of suitable areas in the landscape); and the largest patch index (LPI; the percentage of the suitable habitat encompassed by the largest patch). I also quantified habitat suitability fragmentation using the aggregation index (AI), which equals 0 when the suitable habitat is maximally disaggregated into single grid cell patches disconnected from all other patches, and increases to 1 as suitable habitat is increasingly aggregated into a single, compact patch. In addition, to account for the entire range of projected habitat suitability values, I also divided the projected habitat suitability values into ten discrete classes, dividing in deciles the range of values extracted from the current models by bear's presences; I therefore compared habitat suitability values for each suitable class among alternative forest management scenarios.

RESULTS

Changes in biomass and species composition

The development of the total forest biomass and its species composition over the 100-year simulation period varied greatly. In 100 years from now, the main portion of the forest biomass has shifted to highest elevation compared the current situation, followed by the same trend in species composition. For example, whereas at the 10-year simulation step the main portion of the beech's biomass occurred within 1200 – 1900 m. a. s. l. (i.e., the current altitudinal range), and the *beech* dominated over oaks, at the 100-year simulation step the main portion of the beech's biomass shift at 1500 – 2100 m. a. s. l., and beech lost their dominance in favor of oak forest, also dominating at lowest elevation (800 – 1600 m. a. s. l.). Also, coniferous forest showed an increase in biomass and altitudinal range throughout the projection time frame, over the upper tree line currently demarcated by alpine prairies.

In all scenarios, forest harvesting strategies have a little impact on forest composition and biomass compared to the changes related to climate change; in fact, both biomass and species composition were similar among the scenarios (Fig. 2-4), while I found marked differences when contemplating different forest edge treatments (Supplementary Fig. S1-S2); in particular, the forest-edge treatments (scenarios *S1b* and *S2b*) limited the natural shift of beech distribution over the current altitudinal range, drastically decreasing the portion covered by beech forest compared to the others scenarios which did not included these treatments (scenarios *S0*, *S1a*, *S2a*); conversely, in the latter scenarios alpine prairies were preserved by contrasting the natural forest closure (i.e., clearings within forest patches) and expansion over the current altitudinal range, allowing natural succession to take over forest edges.

Projections of bear habitat suitability under alternative forest harvesting regimes

Overall, I evidenced an increase of habitat suitability in all the scenarios I contemplated compared to the current levels of bear's habitat suitability, independently by the order of selection (Table 3), and this pattern is also confirmed by the distribution of projected suitable bins among current and alternatives scenarios (Tables 4-5); specifically, current habitat suitability showed the lowest values in all spatial metrics considered, excepted for MPA and, marginally, AI at the forest patch scale (Table 3). Nonetheless, comparing the alternative forest harvesting regimes changes in bear's habitat suitability differentially affected the two scales of habitat selection. At home range scale, according to *S0* the spatial configuration and fragmentation of projected suitable habitat had always higher values compared to *S1a* and *S2a*, in term of all the measures I considered (Table 3). This pattern was confirmed by the comparison of projected suitability classes among scenarios, where *S0* featured a greater increase in the areas of highest suitability (i.e., classes C6-10) and, correspondingly, the greatest decrease in areas of lowest suitability (i.e., classes C1-4; Table 4). At the forest patch scale, I found marked differences among projected suitability according to alternative forest management scenarios, and in particular regarding the treatment of forest edges (Table 3). Specifically, *S2a* showed the highest values in all spatial metrics, excepted MPA; accordingly, with the exception of MPA, both *S1b* and *S2b* yielded lower values of TA, LPI, and AI compared to *S0*, *S1a* and *S2a* (Table 3). These results were partially confirmed by the distribution of projected suitable bins among scenarios (Table 5).

DISCUSSION

There are not many examples of landscape level modelling of forest succession under climate change in Europe, partly because it requires a detailed description of the current forest state, climate, and spatially explicit management regimes. This case of study represents the first example in which I accounted for all these factors to evaluate the long-term and large-scale effects of forest management on habitat suitability for a large carnivore species strictly related to forest ecosystems. I also combined two modeling frameworks, those of forest dynamics and wildlife habitat selection models, the former rarely used in a conservation-oriented perspective. In this direction, Shifley et al. (2008) combined spatially explicit landscape simulations and habitat suitability models to compare the outcomes of seven forest management alternatives, with the aim to assess habitat quality for four species with diverse habitat requirements. Similarly, Di Febbraro et al. (2015) proposed a hybrid modelling framework based on the integration of the updated forest dynamic model (LANDIS-II; Thompson et al. 2016) with species distribution models (SDMs), comparing the impact of traditional and conservation-oriented forest management on vertebrates global distribution. However, these studies did not consider the effect of global climate change in modeling forest succession dynamics, while climate change has been widely shown to potentially affect the future distribution of many vertebrate and forest species (He et al. 2002, Scheller and Mladenoff 2005, Bu et al. 2008, Aragón et al. 2010, Maiorano et al. 2011, Ihlow et al. 2012).

In this study, I combined forest succession dynamics under climate change conditions, and habitat selection models to investigate the effects of alternative forest management strategies on brown bear's habitat suitability. In this framework, the main assumption is that the currently bear-habitat relationship remains unchanged in next 100 years, although changes in the forest dynamics over the time. Overall, I evidenced that bear's habitat suitability in the PNALM is projected to increase in next 100 years, independently by the forestry management regimes adopted and the scales of analysis (i.e., third and fourth order of selection; Johnson 1980). Specifically, these results highlighted that climate change is expected to deeply impact forest composition and distribution. At medium elevation, forest distribution and composition projected within the study area evidenced a conversion from beech-dominated to oak-dominated forests, while the beech range distribution shifted at higher elevation. This pattern can be explained by the lower drought tolerance and resistance of the beech compared to oaks, that has been accounted by the drought index LandClim setting. This accounts for the various morphological and physiological traits, like different hydraulic architecture and deeper rooting depth (Abrams 1990, Bréda et al. 2006) that favor oaks survival in warmest climate (Jump et al. 2006, Di Filippo et al. 2007, Piovesan et al. 2008). Change in species composition projected in next 100 years bears important consequences for the availability of hard mast to Apennine bears. In the study area (PNALM), bears consume a great amount of hard mast during the late hyperphagic season (autumn), of which two thirds are beechnuts (Ciucci et al. 2014). With the projected loss of beech-dominated forests, the issue is if bears can promptly adapt to find alternative good quality food sources. Food habits of bears vary according to latitude, season, and local conditions, all of which influence the availability of key foods for bears (Elgmork and Kaasa 1992, Hildebrand et al. 1999*b*, *a*). Whereas bears in northern regions are more carnivorous and consume less hard mast than southern populations (Elgmork and Kaasa 1992, Hildebrand et al. 1999*b*, *a*, Swenson et al. 2007), due possibly to the simpler ecological structure of northern ecosystems, bears in southern region eat the highest percentages of fleshy fruits and hard mast and the lowest percentages of vertebrates (Cicnjak et al. 1987, Clevenger et al. 1992, Naves et al. 2006, Paralikidis et al. 2010). For instance, in southern Europe, bears consume a great diversity of plant material in accordance with seasonal plant phenologies, with hard mast and fleshy fruits predominating in the diet during fall (Cicnjak et al. 1987, Clevenger et al. 1992, Naves et al. 2006, Paralikidis et al. 2010). Apennine bears also consumed insects (mostly ants) in early-summer and mammals, including wild ungulates in spring and early-summer, and livestock in early and late summer (Ciucci et al. 2014). Such protein- and lipid-rich foods in spring and summer are important for bears to build up lean body mass and to enhance structural growth in cubs and subadults (Hildebrand et al. 1999*b*). Ants contain up to 50% protein (Southwood 1973) and can be a source of essential amino acids (Eagle and Pelton 1983, Redford and Dorea 1994, Noyce et al. 1997). In addition, Ciucci et al. (2014) detected more moderate annual fluctuations in the consumption of acorns in autumn, with acorns providing 49.7% of dietary energy in the fall of 2006 (i.e., the year of beechnut failure) and 22% in the next spring. In this contest, the generalist behavior and high adaptability of Apennine bears to expect that the need of beechnuts must can be integrated by oak’s productivity (i.e., acorns) in autumnal season; however, further investigations must be conducted in order to cover all single aspects of the nutritional ecology of Apennine bears, deeply investigating forest ecosystem productivity relating population fitness with habitat carrying capacity. In this sense, the effects of climate change and forest management regimes over forest ecosystem resources (e.g., hard mast, fleshy fruit, berries, and ants) is another aspect to consider in future studies, as well as how climate change affect bear's physiology like, for instance, the effects on thermoregulation, the likely reduction of the denning period (or nondenning), and their impact on bears fitness. For instance, in the Southern Europe, brown bear denning period is already lowest (mean denning time 2.9 months; Huber and Roth 1997) compared to the Northern bear populations (>5 months; Manchi and Swenson 2005), and tracks and fresh scats are observed in all winter months, suggesting that many bears do not hibernate for the entire winter and that some may not hibernate at all (Huber and Roth 1997). This pattern could be increase in climate change condition, considering that nondenning brown bear have also been reported in the Southern Europe, like Spain (Naves and Palomero 1993), including central Italy (Roth et al. 1992).

At the home range scale, forest harvesting strategies (scenarios *S1* and *S2*) did not improve habitat suitability compared to the hands-off scenario (*S0*), while at the scale of forest patches habitat suitability was positively affected by silvicultural interventions, particularly in the *pro-bear* scenarios (*S2*). At the this scale of analysis, maintaining the current forest interspersion with open areas (*S1b* and *S2b*) was not projected to enhance habitat suitability, because this strategy tends to contrast the natural shifting of tree species at highest elevation as a consequence of climate change. This pattern was indicated by the lower projected suitability metrics (TA, LPI, and AI) reported for the scenarios *S1b* and *S2b* compared to *S1a* and *S1b*. The general projected increase of forested areas is in line with what already currently observed in the Italian forests (e.g., Falcucci et al. 2007; Camarretta et al. 2018). However, I caution with these results because (*i*) habitat selection models used for predicting habitat suitability by bears in the future are built using a relatively small sample size composed by only females (n=10 individual bears), and (*ii*) in these forest dynamic models I did not consider wildlife browsing pressure produced by the numerous ungulates living in the Park (e.g., roe deer and red deer), as I don't have detailed data in this regard. This aspect should be furthered investigated through the collection of more information about the intensity and locations of areas foraged by both wildlife and domestic herbivores.

To have a more realistic picture of the causal-effect relationship among alternatives forest management scenarios, wildlife habitat suitability, and climate change, as well as how this will impact Apennine bear conservation, further research will need to: (*i*) expand the study landscape to the entire central Apennines, (*ii*) quantify hard must productivity of the forest, finding the stand structure parameter(s) correlated with forest hard mast productivity, (*iii*) increase sample size of radio-collared bears, including both females and males, possibly with different age classes, and including years of both low and high productivity of hard mast, (*iv*) understand which factors drive the increase of habitat suitability in alternative forest harvesting scenarios according to the spatial configuration of forest interspersion with open areas, (*v*) collect data about natural (e.g., wind and fire) and anthropogenic (animal browsing) disturbance factors occurring in the study area, and (*vi*) provide more accurate stand structure input data for representing a more realistic picture of the current forest tridimensional structure (e.g., LIDAR images), and improving both forest dynamic simulations and habitat suitability models. While most of these aspects can be addressed by collecting new and detailed forestry and wildlife data, acquiring remote sensing images could be cost-expensive for a larger study area. Nevertheless, the benefits provided by these technologies would allow to obtain precious and high-quality data about the vegetation cover at a very-high spatial resolution (e.g., centimeters), which can drastically improve the accuracy of predictions outcomes, and finally provide more accurate conservation-oriented forest management indications.

REFERENCES

Abrams, M. D. 1990. Adaptations and responses to drought in *Quercus* species of North America. Tree Physiology 7:227–238.

Akhtar, M., N. Ahmad, and M. J. Booij. 2008. The impact of climate change on the water resources of Hindukush–Karakorum–Himalaya region under different glacier coverage scenarios. Journal of Hydrology 355:148–163.

Anandhi, A., A. Frei, D. C. Pierson, E. M. Schneiderman, M. S. Zion, D. Lounsbury, and A. H. Matonse. 2011. Examination of change factor methodologies for climate change impact assessment. 47:1–10.

Aragón, P., M. A. Rodríguez, M. A. Olalla-Tárraga, and J. M. Lobo. 2010. Predicted impact of climate change on threatened terrestrial vertebrates in central Spain highlights differences between endotherms and ectotherms. Animal Conservation 13:363–373.

van Beest, F. M., B. Van Moorter, and J. M. Milner. 2012. Temperature-mediated habitat use and selection by a heat-sensitive northern ungulate. Animal Behaviour 84:723–735.

Bonanomi, G., A. Rita, E. Allevato, G. Cesarano, L. Saulino, G. Di Pasquale, M. Allegrezza, S. Pesaresi, M. Borghetti, S. Rossi, and A. Saracino. 2018. Anthropogenic and environmental factors affect the tree line position of *Fagus sylvatica* along the Apennines (Italy). Journal of Biogeography 45:2595–2608.

Bouriaud, L., O. Bouriaud, C. Elkin, C. Temperli, C. Reyer, G. Duduman, I. Barnoaiea, L. Nichiforel, N. Zimmermann, and H. Bugmann. 2015. Age-class disequilibrium as an opportunity for adaptive forest management in the Carpathian Mountains, Romania. Regional Environmental Change 15:1557–1568.

Bréda, N., R. Huc, A. Granier, and E. Dreyer. 2006. Temperate forest trees and stands under severe drought: A review of ecophysiological responses, adaptation processes and long-term consequences. Annals of Forest Science 63:625–644.

Bruelheide, H., M. Böhnke, S. Both, T. Fang, T. Assmann, M. Baruffol, J. Bauhus, F. Buscot, X. Y. Chen, B. Y. Ding, W. Durka, A. Erfmeier, M. Fischer, C. Geißler, D. Guo, L. D. Guo, W. Härdtle, J. S. He, A. Hector, W. Kröber, P. Kühn, A. C. Lang, K. Nadrowski, K. Pei, M. Scherer-Lorenzen, X. Shi, T. Scholten, A. Schuldt, S. Trogisch, G. Von Oheimb, E. Welk, C. Wirth, Y. T. Wu, X. Yang, X. Zeng, S. Zhang, H. Zhou, K. Ma, and B. Schmid. 2011. Community assembly during secondary forest succession in a Chinese subtropical forest. Ecological Monographs 81:25–41.

Bu, R., H. S. He, Y. Hu, Y. Chang, and D. R. Larsen. 2008. Using the LANDIS model to evaluate forest harvesting and planting strategies under possible warming climates in Northeastern China. Forest Ecology and Management 254:407–419.

Bugmann, H. 2001. A review of forest gap models. Climatic Change 51:259–305.

Bugmann, H., and W. Cramer. 1998. Improving the behaviour of forest gap models along drought gradients. Forest Ecology and Management 103:247–263.

Camarretta, N., N. Puletti, U. Chiavetta, and P. Corona. 2018. Quantitative changes of forest landscapes over the last century across Italy. Plant Biosystems 152:1011–1019.

Casula, P., L. Luiselli, G. Milana, and G. Amori. 2017. Habitat structure and disturbance affect small mammal populations in Mediterranean forests. Basic and Applied Ecology 19:76–83.

Ciarniello, L. M., M. S. Boyce, D. C. Heard, and D. R. Seip. 2005. Denning behavior and den site selection of grizzly bears along the Parsnip River, British Columbia, Canada. Ursus 16:47–58.

Cicnjak, L., D. Huber, H. U. Roth, R. L. Ruff, and Z. Vinovrski. 1987. Food habits of brown bears in Plitvice Lakes National Park, Yugoslavia. International Conference on Bear Research and Management 7:221–226.

Ciucci, P., T. Altea, A. Antonucci, L. Chiaverini, A. Di Croce, F. Mauro, P. Forconi, R. Latini, L. Maiorano, A. Monaco, P. Morini, F. Ricci, L. Sammarone, F. Striglioni, E. Tosoni, L. Carotenuto, I. Pizzol, M. C. Saltari, D. Serafini, M. Caporioni, L. Tarquini, S. Donfrancesco, I. Guj, A. Lecce, G. Di Clemente, and E. Peria. 2017. Distribution of the brown bear (*Ursus arctos marsicanus*) in the central Apennines, Italy, 2005–2014. Hystrix 28:1–6.

Ciucci, P., and L. Boitani. 2008. The Apennine brown bear: A critical review of its status and conservation problems. Ursus 19:130–145.

Ciucci, P., L. Maiorano, L. Chiaverini, and M. Falco. 2016. Aggiornamento della cartografia di riferimento del PATOM su presenza e distribuzione potenziale dell'orso bruno marsicano nell'Appennino centrale. Relazione Tecnica. Unione Zoologica Italiana e Ministero per la tutela dell'Ambiente del Mare e del Territor. Roma.

Ciucci, P., E. Tosoni, G. Di Domenico, F. Quattrociocchi, and L. Boitani. 2014. Seasonal and annual variation in the food habits of Apennine brown bears, central Italy. Journal of Mammalogy 95:572–586.

Ciucci, P., E. Tosoni, L. Maiorano, L. Gentile, C. Sulli, and L. Boitani. 2012. Denning in the Apennine brown bear (*Ursus arctos marsicanus*) and potential conflict areas: Toward proactive conservation measures. VIII Congresso Italiano di Teriologia. Hystrix, It. J. Mamm. (N.S.) 64.

Clevenger, A. P., F. J. Purroy, and M. R. Pelton. 1992. Food habits of brown bears (*Ursus arctos*) in the Cantabrian Mountains, Spain. Journal of Mammalogy 73:415–421.

DeWalt, S. J., S. K. Maliakal, and J. S. Denslow. 2003. Changes in vegetation structure and composition along a tropical forest chronosequence: Implications for wildlife. Forest Ecology and Management 182:139–151.

Eagle, T. C., and M. R. Pelton. 1983. Seasonal nutrition of black bears in the Great Smoky Mountains National Park. International Conference on Bear Research and Management 5:94–101.

Elgmork, K., and J. Kaasa. 1992. Food habits and foraging of the brown bear *Ursus arctos* in central south Norway. Ecography 15:101–110.

Elkin, C., A. Giuggiola, A. Rigling, and H. Bugmann. 2015. Short- and long-term efficacy of forest thinning to mitigate drought impacts in mountain forests in the European Alps. Ecological Applications 25:1083–1098.

Elkin, C., A. G. Gutiérrez, S. Leuzinger, C. Manusch, C. Temperli, L. Rasche, and H. Bugmann. 2013. A 2 °C warmer world is not safe for ecosystem services in the European Alps. Global Change Biology 19:1827–1840.

Falcucci, A., P. Ciucci, L. Maiorano, L. Gentile, and L. Boitani. 2009. Assessing habitat quality for conservation using an integrated occurrence-mortality model. Journal of Applied Ecology 46:600–609.

Falcucci, A., L. Maiorano, and L. Boitani. 2007. Changes in land-use/land-cover patterns in Italy and their implications for biodiversity conservation. Landscape Ecology 22:617–631.

Farrell, E. P., E. Führer, D. Ryan, F. Andersson, R. Hüttl, and P. Piussi. 2000. European forest ecosystems: Building the future on the legacy of the past. Forest Ecology and Management 132:5–20.

Di Febbraro, M., F. Roscioni, L. Frate, M. L. Carranza, L. De Lisio, D. De Rosa, M. Marchetti, and A. Loy. 2015. Long-term effects of traditional and conservation-oriented forest management on the distribution of vertebrates in Mediterranean forests: A hierarchical hybrid modelling approach. Diversity and Distributions 21:1141–1154.

Di Filippo, A., F. Biondi, K. Čufar, M. De Luis, M. Grabner, M. Maugeri, E. Presutti Saba, B. Schirone, and G. Piovesan. 2007. Bioclimatology of beech (*Fagus sylvatica* L.) in the Eastern Alps: Spatial and altitudinal climatic signals identified through a tree-ring network. Journal of Biogeography 34:1873–1892.

Gervasi, V., and P. Ciucci. 2018. Demographic projections of the Apennine brown bear population *Ursus arctos marsicanus* (Mammalia: Ursidae) under alternative management scenarios. The European Zoological Journal 85:242–252.

Gessler, P. E., O. A. Chadwick, F. Chamran, L. Althouse, and K. Holmes. 2000. Modeling soil-landscape and ecosystem properties using terrain attributes. Soil Science Society of America Journal 64:2046–2056.

Gutiérrez, A. G., and A. Huth. 2012. Successional stages of primary temperate rainforests of Chiloé Island, Chile. Perspectives in Plant Ecology, Evolution and Systematics 14:243–256.

Hay, L. E., R. L. Wilby, and G. H. Leavesley. 2000. A comparison of delta change and downscaled GCM scenarios for three mountainous basins in the United States. Journal of the American Water Resources Association 36:387–397.

He, H. S., and D. J. Mladenoff. 1999. Spatially explicit and stochastic simulation of forest-landscape fire disturbance and succession. Ecology 80:81–99.

He, H. S., D. J. Mladenoff, and E. J. Gustafson. 2002. Study of landscape change under forest harvesting and climate warming-induced fire disturbance. Forest Ecology and Management 155:257–270.

Henne, P. D., C. M. Elkin, B. Reineking, H. Bugmann, and W. Tinner. 2011. Did soil development limit spruce (*Picea abies*) expansion in the Central Alps during the Holocene? Testing a palaeobotanical hypothesis with a dynamic landscape model. Journal of Biogeography 38:933–949.

Hickler, T., K. Vohland, J. Feehan, P. A. Miller, B. Smith, L. Costa, T. Giesecke, S. Fronzek, T. R. Carter, W. Cramer, I. Kühn, and M. T. Sykes. 2012. Projecting the future distribution of European potential natural vegetation zones with a generalized, tree species-based dynamic vegetation model. Global Ecology and Biogeography 21:50–63.

Hildebrand, G. V., M. E. Jacoby, C. C. Schwartz, S. M. Arthur, C. T. Robbins, T. A. Hanley, and C. Servheen. 1999a. The importance of meat, particularly salmon, to body size, population productivity, and conservation of North American brown bears. Canadian Journal of Zoology 77:132–138.

Hildebrand, G. V., S. G. Jenkins, C. C. Schwartz, T. A. Hanley, and C. T. Robbins. 1999b. Effect of seasonal differences in dietary meat intake on changes in body mass and composition in wild and captive brown bears. Canadian Journal of Zoology 77:1623–1630.

Houle, M., D. Fortin, C. Dussault, R. Courtois, and J. P. Ouellet. 2009. Cumulative effects of forestry on habitat use by gray wolf (*Canis lupus*) in the boreal forest. Landscape Ecology 25:419–433.

Huber, D., and H. D. Roth. 1997. Denning of brown bears in Croatia. Pages 79–83 in. Proc Int Conf Bear Res Manage 9.

Ihlow, F., J. Dambach, J. O. Engler, M. Flecks, T. Hartmann, S. Nekum, H. Rajaei, and D. Rödder. 2012. On the brink of extinction? How climate change may affect global chelonian species richness and distribution. Global Change Biology 18:1520–1530.

IPCC. 2019. The report on 1.5°C global warming-relevant aspects for climate services. Climate Services.

Johnson, D. H. 1980. The comparison of usage and availability measurements for evaluating resource preference. Ecology 61:65–71.

Jump, A. S., J. M. Hunt, and J. Peñuelas. 2006. Rapid climate change-related growth decline at the southern range edge of *Fagus sylvatica*. Global Change Biology 12:2163–2174.

Karger, D. N., O. Conrad, J. Böhner, T. Kawohl, H. Kreft, R. W. Soria-Auza, N. E. Zimmermann, H. P. Linder, and M. Kessler. 2017. Climatologies at high resolution for the earth's land surface areas. Scientific Data 4:1–20.

Kilsby, C. G., P. D. Jones, A. Burton, A. C. Ford, H. J. Fowler, C. Harpham, P. James, A. Smith, and R. L. Wilby. 2007. A daily weather generator for use in climate change studies. Environmental Modelling and Software 22:1705–1719.

Knutti, R., D. Masson, and A. Gettelman. 2013. Climate model genealogy: Generation CMIP5 and how I got there. Geophysical Research Letters 40:1194–1199.

Maiorano, L., L. Chiaverini, M. Falco, and P. Ciucci. 2019. Combining multi-state species distribution models, mortality estimates, and landscape connectivity to model potential species distribution for endangered species in human dominated landscapes. Biological Conservation 237:19–27.

Maiorano, L., A. Falcucci, N. E. Zimmermann, A. Psomas, J. Pottier, D. Baisero, C. Rondinini, A. Guisan, and L. Boitani. 2011. The future of terrestrial mammals in the Mediterranean basin under climate change. Philosophical Transactions of the Royal Society B: Biological Sciences 366:2681–2692.

Manchi, S., and J. E. Swenson. 2005. Denning behaviour of Scandinavian brown bears *Ursus arctos*. Wildlife Biology 11:123–132.

Manly, B. F. J., L. Mcdonald, D. Thomas, T. L. McDonald, and W. P. Erickson. 2002. Resource selection by animals: Statistical design and analysis for field studies. 2nd ed. Volume 1. Kluwer Academic Publishers, Dordrecht, Netherlands. Merkle.

McGarigal, K., and B. J. Marks. 1995. FRAGSTATS: spatial pattern analysis program for quantifying landscape structure. General Technical Report - US Department of Agriculture, Forest Service.

Moore, I. D., P. E. Gessler, G. A. Nielsen, and G. A. Peterson. 1993. Soil attribute prediction using terrain analysis. Soil Science Society of America Journal 57:443–452.

Naves, J., C. Fernández-Gil, C. Rodríguez, and M. Delibes. 2006. Brown bear food habits at the border of its range: A long-term study. Journal of Mammalogy 87:899–908.

Naves, J., and G. Palomero. 1993. Brown bear hibernation ecology in the Cantabrian Mountains. Pages 147–181 in. In: Naves J, Palomero G (eds) El oso pardo (*Ursus arctos*) en España. Instituto Nacional para la Conservacion de la Naturaleza, Madrid (in Spanish with English summary).

Noyce, K. V., P. B. Kannowski, and M. R. Riggs. 1997. Black bears as ant-eaters: seasonal associations between bear myrmecophagy and ant ecology in north-central Minnesota. Canadian Journal of Zoology 75:1671–1686.

Paralikidis, N. P., N. K. Papageorgiou, V. J. Kontsiotis, and A. C. Tsiompanoudis. 2010. The dietary habits of the brown bear (*Ursus arctos*) in western Greece. Mammalian Biology 75:29–35.

Penteriani, V., A. Zarzo-Arias, A. Novo-Fernández, G. Bombieri, and C. A. López-Sánchez. 2019. Responses of an endangered brown bear population to climate change based on predictable food resource and shelter alterations. Global Change Biology 25:1133–1151.

Piovesan, G., M. Bernabei, A. Di Filippo, M. Romagnoli, and B. Schirone. 2003. A long-term tree ring beech chronology from a high-elevation old-growth forest of Central Italy. Dendrochronologia 21:13–22.

Piovesan, G., F. Biondi, A. Di Filippo, A. Alessandrini, and M. Maugeri. 2008. Drought-driven growth reduction in old beech (*Fagus sylvatica* L.) forests of the central Apennines, Italy. Global Change Biology 14:1265–1281.

Redford, K. H., and J. G. Dorea. 1994. The nutritional value of invertebrates with emphasis on ants and termites as food for mammals. Journal of Zoology 203:385–395.

Rositi, A., C. Console, D. Di Santo, C. Gentile, L. Logiudice, M. Posillico, L. Sammarone, and P. Ciucci. 2019. Forest management guidelines to promote the conservation of Apennine brown bear in Italy. Forest@ - Rivista di Selvicoltura ed Ecologia Forestale 16:66–73.

Roth, H. U., G. Boscagli, and L. Gentile. 1992. Movements, activity and hibernation of brown bears in the Abruzzo National Park as revealed by radiotelemetry. In: Bourlière F (ed) Management and restoration of small and relictual bears populations. Museum d'Historie Naturelle, Grenoble, France.

Sanderson, B. M., R. Knutti, and P. Caldwell. 2015. A representative democracy to reduce interdependency in a multimodel ensemble. Journal of Climate 28:5171–5194.

Scheller, R. M., and D. J. Mladenoff. 2005. A spatially interactive simulation of climate change, harvesting, wind, and tree species migration and projected changes to forest composition and biomass in northern Wisconsin, USA. Global Change Biology 11:307–321.

Schumacher, S. 2004. The role of large scale disturbances and climate for the dynamics of forested landscapes in the European Alps. Dissertation. Swiss Federal Institute of Technology ETH Zurich, Switzerland.

Schumacher, S., and H. Bugmann. 2006. The relative importance of climatic effects, wildfires and management for future forest landscape dynamics in the Swiss Alps. Global Change Biology 12:1435–1450.

Schumacher, S., H. Bugmann, and D. J. Mladenoff. 2004. Improving the formulation of tree growth and succession in a spatially explicit landscape model. Ecological Modelling 180:175–194.

Scolastri, A., L. Cancellieri, M. Iocchi, and M. Cutini. 2017. Old coppice versus high forest: The impact of beech forest management on plant species diversity in central Apennines (Italy). Journal of Plant Ecology 10:271–280.

Shifley, S. R., F. R. Thompson, W. D. Dijak, and Z. Fan. 2008. Forecasting landscape-scale, cumulative effects of forest management on vegetation and wildlife habitat: A case study of issues, limitations, and opportunities. Forest Ecology and Management 254:474–483.

Shifley, S. R., F. R. Thompson, W. D. Dijak, M. A. Larson, and J. J. Millspaugh. 2006. Simulated effects of forest management alternatives on landscape structure and habitat suitability in the Midwestern United States. Forest Ecology and Management 229:361–377.

Southwood, T. R. E. 1973. The insect/plant relationship—An evolutionary perspective. L. Royal Entomological Society and U. Kingdom, editors.

Swanson, M. E., J. F. Franklin, R. L. Beschta, C. M. Crisafulli, D. A. DellaSala, R. L. Hutto, D. B. Lindenmayer, and F. J. Swanson. 2011. The forgotten stage of forest succession: Early-successional ecosystems on forest sites. Frontiers in Ecology and the Environment 9:117–125.

Swenson, J. E., M. Adamič, D. Huber, and S. Stokke. 2007. Brown bear body mass and growth in northern and southern Europe. Oecologia 153:37–47.

Taylor, K. E., R. J. Stouffer, and G. A. Meehl. 2012. An overview of CMIP5 and the experiment design. Bulletin of the American Meteorological Society 93:485–498.

Temperli, C., H. Bugmann, and C. Elkin. 2012. Adaptive management for competing forest goods and services under climate change. Ecological Applications 22:2065–2077.

Thompson, J. R., E. Simons-Legaard, K. Legaard, and J. B. Domingo. 2016. A LANDIS-II extension for incorporating land use and other disturbances. Environmental Modelling and Software 75:202–205.

Thuiller, W., C. Albert, M. B. Araújo, P. M. Berry, M. Cabeza, A. Guisan, T. Hickler, G. F. Midgley, J. Paterson, F. M. Schurr, M. T. Sykes, and N. E. Zimmermann. 2008. Predicting global change impacts on plant species' distributions: Future challenges. Perspectives in Plant Ecology, Evolution and Systematics 9:137–152.

Zellweger, F., A. Baltensweiler, C. Ginzler, T. Roth, V. Braunisch, H. Bugmann, and K. Bollmann. 2016. Environmental predictors of species richness in forest landscapes: Abiotic factors versus vegetation structure. Journal of Biogeography 43:1080–1090.

Zhang, D., J. Liu, W. Ni, G. Sun, Z. Zhang, Q. Liu, and Q. Wang. 2019. Estimation of forest leaf area index using height and canopy cover information extracted from unmanned aerial vehicle stereo imagery. IEEE Journal of Selected Topics in Applied Earth Observations and Remote Sensing 12:471–481.

TABLES AND FIGURES

Table 1. Species life history parameters used to simulate forest succession in all scenarios. *R*: maximum above-ground biomass growth; *K*: maximum aboveground tree biomass a species can potentially reach; *maxAge*: expected longevity; *matu*: maturity age for seed production; *ED*: effective seeding distance; *MD*: maximal seeding distance; *vegP*: probability of vegetative reproduction, and *sp _ag*: maximum age for vegetative reproduction.

Species	R_s **(*yr1*)**	**Ks (*t*)**	$maxAge_s$ **(*yr*)**	$matu_s$ **(*yr*)**	ED_S **(*m*)**	MD_s **(*m*)**	$vegP_s$ **(–)**	sp_ag_s **(*yr*)**
Acer campestre	0.08	1.5	170	40	60	200	1	50
Acer amons	0.06	0.7	150	40	60	200	1	50
Acer opalus	0.06	0.7	150	40	60	200	1	50
Acer pseudoplatanus	0.09	13.6	550	40	60	200	1	50
Carpinus betulus	0.1	4.6	220	30	55	180	1	30
Carpinus orientalis	0.1	4.6	220	30	55	180	1	30
Castanea sativa	0.05	41.0	1510	50	30	-1	1	50
Corylus sp.	0.1	4.6	220	30	55	180	1	30
Crataegus sp.	0.1	4.6	220	30	55	180	1	30
Fagus silvatica	0.1	28.0	430	60	30	-1	1	50
Fraxinus ornus	0.07	18.0	200	20	40	140	1	50
Ostrya carpinofolia	0.1	2.0	150	30	55	180	1	30
Pinus nigra	0.075	8.1	760	30	90	300	1	0
Pinus pinea	0.075	8.1	760	30	90	300	1	0
Populus nigra	0.12	3.8	140	20	240	800	1	50
Populus tremula	0.12	3.8	140	20	240	800	1	50
Prunus avium	0.1	4.6	220	30	55	180	1	30
Quercus cerris [a]	0.07	2.4	600	60	30	-1	1	75
Quercus frainetto	0.07	2.4	600	60	30	-1	1	75
Quercus ilex	0.03	8.9	600	20	30	1	1	75
Quercus pubescens	0.07	2.4	500	60	30	-1	1	50
Robinia pseudoacacia	0.1	2.0	150	30	55	180	1	30
Ulmus glabra	0.09	19.0	460	50	110	360	1	50

[a]: Species added by Elkin et al. (2015).

Table 1 (continued). Species life history parameters used to simulate forest succession in all scenarios. *E/D*: 1 denotes evergreen species; 2 deciduous species; *folType*: foliage type; *shdTol*: species shading tolerance (ordinal number between 1 and 5, 1 denotes least shade tolerant); *minDD*: minimum annual degree-day sum; *minT*: minimum temperature for establishment; *drTol*: drought tolerance of species.

Species	E/D_s (–)	$folType_s$ (–)	$shdTol_s$ (–)	$minDD_s$ (d)	$minT_s$ (°C)	$drTol_s$ (–)
Acer campestre	2	2	3	1062	-99	0.25
Acer amons	2	2	2	1554	-6	0.41
Acer opalus	2	2	2	1554	-6	0.41
Acer pseudoplatanus	2	3	4	898	-99	0.17
Carpinus betulus	2	3	4	898	-9	0.25
Carpinus orientalis	2	3	4	898	-9	0.25
Castanea sativa	2	3	3	1237	-99	0.33
Corylus sp.	2	3	4	898	-9	0.25
Crataegus sp.	2	3	4	898	-9	0.25
Fagus silvatica	2	3	5	723	-4	0.25
Fraxinus ornus	2	2	3	1639	0	0.36
Ostrya carpinofolia	2	2	4	937	-7	0.28
Pinus nigra	1	4	1	610	-99	0.32
Pinus pinea	1	4	1	610	-99	0.32
Populus nigra	2	2	2	610	-99	0.25
Populus tremula	2	2	2	610	-99	0.25
Prunus avium	2	3	4	898	-9	0.25
Quercus cerris [a]	2	3	2	1554	-1	0.28
Quercus frainetto	2	3	2	1554	-1	0.28
Quercus ilex	2	3	5	1773	1	0.32
Quercus pubescens	2	3	2	1011	-99	0.36
Robinia pseudoacacia	2	2	4	937	-7	0.28
Ulmus minor	2	3	4	1062	-16	0.165

[a]: Species added by Elkin et al. (2015).

Table 2. Forest harvesting strategies divided for each management scenarios: *status-quo* (*S1*) and *pro-bear* (*S2*). Each forest harvesting scenario differs for the possible range size of the tree harvested (DBH classes), forest regime (coppice or high forest), type of the silvicultural intervention, and priority of harvesting (density=highest tree density patches are cut first; biomass= highest biomass forest patches are cut first), and harvesting rotation time (period between one silvicultural intervention and the following).

Sceanario	**Dominant tree species**	**Regime**	**DBH classes (cm)**	**Type**	**Priority**	**Rotation time (years)**	**Harvested area (%)**
S1	Beech	High forest	10-20	Thinning	Density	40	40
			20-40	Thinning	Biomass	80	30
			> 40	Thinning	Biomass	120	90
	Oak	High forest	20-30	Thinning	Density	40	40
			30-40	Thinning	Biomass	80	30
			> 40	Thinning	Biomass	120	100
	Oak	Coppice	10-20	Thinning	Biomass	20	100
S2	Beech	High-forest	10-40	Thinning	Density	20	60
			> 40	Thinning	Density	20	12
	Oak	High forest	20-30	Thinning	Density	40	40
			30-40	Thinning	Biomass	80	30
			> 40	Thinning	Biomass	120	100
	Oak	Coppice	10-20	Thinning	Biomass	20	100

Table 3. Projections (100 years) of habitat suitability for adult female Apennine bears during autumn according to configuration (TA = total suitable areas, ha; LPI = largest patch index, %; MPA = mean patch area, ha) and landscape metric of aggregation (AI = aggregation index, %) at the third-order (home range) and fourth (forest patch) orders of selection.

Suitability metric	**Current**		***S0***		***S1a***		***S1b***		***S2a***		***S2b***	
	Home range	***Forest patch***	***Home range***	***Forest patch***	***Home range***	***Forest patch***	***Home range***	***Forest patch***	***Home range***	***Forest patch***	***Home range***	***Forest patch***
TA	23009.40	19342.80	34270.92	24899.58	30394.98	26091.18	-	20253.78	30760.38	26879.94	-	20953.08
LPI	37.65	17.00	56.09	52.46	47.84	63.92	-	37.02	49.48	66.54	-	38.01
MPA	852.20	30.65	2855.91	9.29	1599.74	10.14	-	10.35	2050.69	11.97	-	12.41
AI	99.13	92.11	99.46	91.55	99.34	91.07	-	88.78	99.45	91.78	-	89.70

Table 4. Bears habitat suitability projected over the next 100 years at the home range scale (third-order of selection) and classified into 10 bins (i.e., deciles: C1 = lowest value, C10 = highest value).

Suitability bins	**Scenarios**			
	Current	***S0***	***S1a***	***S2a***
	Area (%)	**Area (%)**	**Area (%)**	**Area (%)**
C1	26.42	15.31	21.48	21.89
C2	17.52	10.35	10.70	10.92
C3	15.14	10.54	11.47	9.46
C4	8.76	8.33	6.30	6.87
C5	8.47	9.12	7.20	7.667
C6	4.72	6.44	4.95	6.27
C7	3.54	5.99	4.52	4.98
C8	7.44	15.13	13.57	14.38
C9	7.97	17.85	19.15	16.91
C10	0.02	0.93	0.66	0.64

Table 5. Bears habitat suitability projected over the next 100 years at the forest patch scale (fourth-order of selection) and classified into 10 bins (i.e., deciles: C1 = lowest value, C10 = highest value).

Suitability bins	**Scenarios**					
	Current	***S0***	***S1a***	***S1b***	***S2a***	***S2b***
	Area (%)	**Area (%)**	**Area (%)**	**Area (%)**	**Area (%)**	**Area (%)**
C1	19.71	28.02	25.17	15.52	23.2	12.63
C2	15.5	3.83	1.97	0.81	1.77	0.86
C3	10.57	3.83	2.53	0.95	2.44	0.97
C4	10.26	4.15	3.14	0.87	3.28	0.88
C5	9.01	4.143	3.13	0.58	3.93	0.69
C6	12.18	7.03	6.12	0.83	7.03	2.29
C7	6.7	6.45	6.55	2.39	7.24	6.37
C8	5.34	12.32	13.55	16.71	13.6	19.58
C9	5.22	22.75	28.33	53.34	27.95	48.31
C10	5.51	7.48	9.52	7.99	9.57	7.46

Figure 1. Study area encompassed the Abruzzo-Lazio-Molise National Park (PNALM) and forest areas are represented by each forest management regime adopted by the Forestry Service of the Park: high-forest (green) and coppice (brown). Striped polygons show integral reserve areas manage by the Park Authorities in which timber harvesting is not permitted.

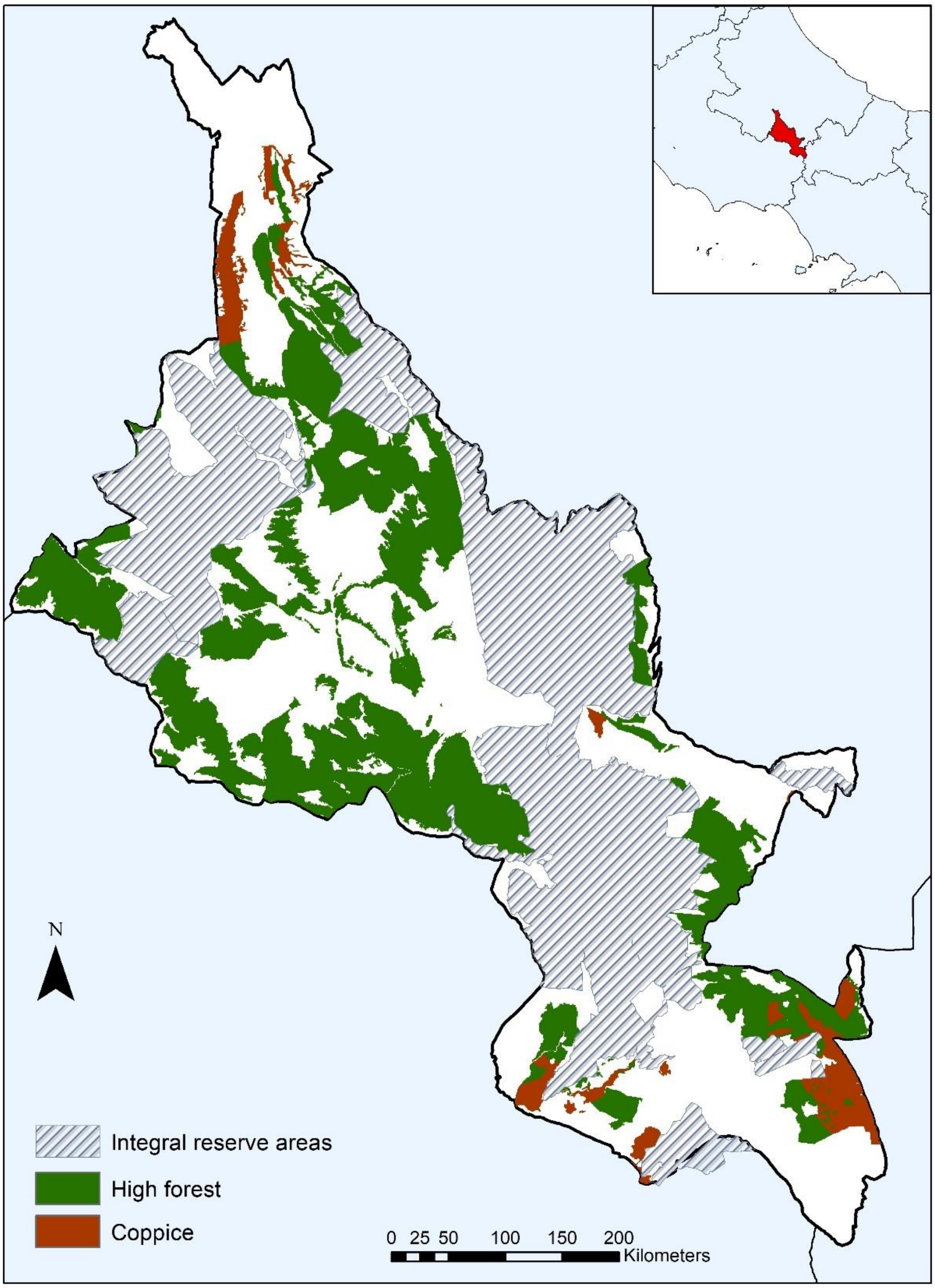

Figure 2. Tree species distribution measured as cumulative biomass (t/ha) over the study area after 10 (decade 1), 50 (decade 5), and 100-year simulation period (decade 10), at the *baseline* scenario (*S0*). For graphical reason, I show only the dominant tree species: fagusilv = *Fagus sylvatica*; fraxornu = *Fraxinus ornus*; ostrcarp = *ostrya carpinofolia*; pinunigr = *Pinus nigra*; pinupine = *P. pinea*; popunigr = *Populus nigra*; poputrem = *P. tremens*; quercerris = *Quercus cerris*; querfrai = *Q. frainetto*; querilex = *Q. ilex*; querpube = *Q. pubescens*.

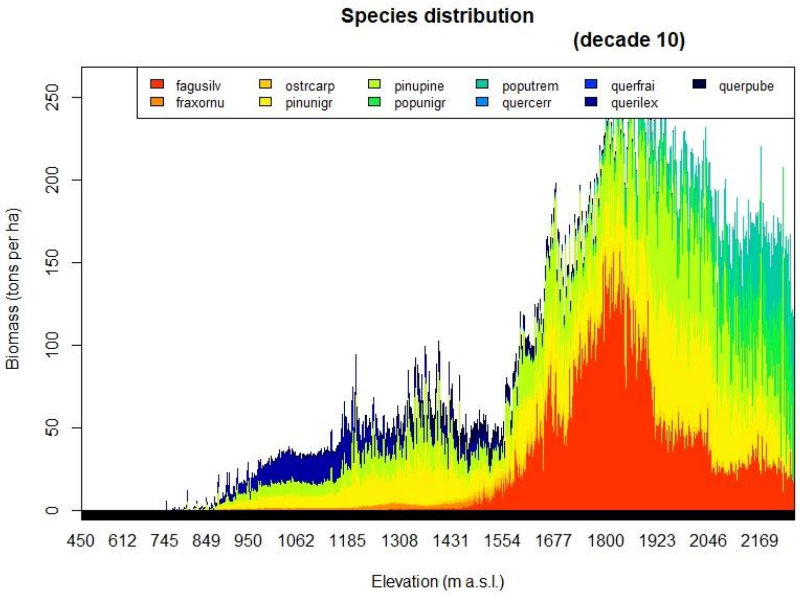
Species distribution
(decade 10)
fagusilv
fraxornu
ostrcarp
pinunigr
pinupine
popunigr
poputrem
quercerr
querfrai
querilex
querpube
Biomass (tons per ha)
0
50
100
150
200
250
450
612
745
849
950
1062
1185
1308
1431
1554
1677
1800
1923
2046
2169
Elevation (m a.s.l.)

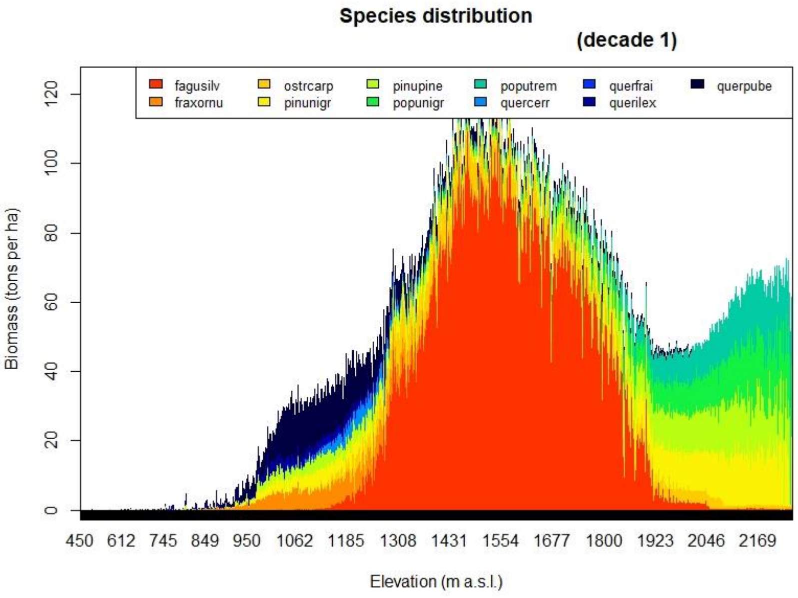
Species distribution
(decade 1)
fagusilv
fraxornu
ostrcarp
pinunigr
pinupine
popunigr
poputrem
quercerr
querfrai
querilex
querpube
Biomass (tons per ha)
0
20
40
60
80
100
120
450
612
745
849
950
1062
1185
1308
1431
1554
1677
1800
1923
2046
2169
Elevation (m a.s.l.)

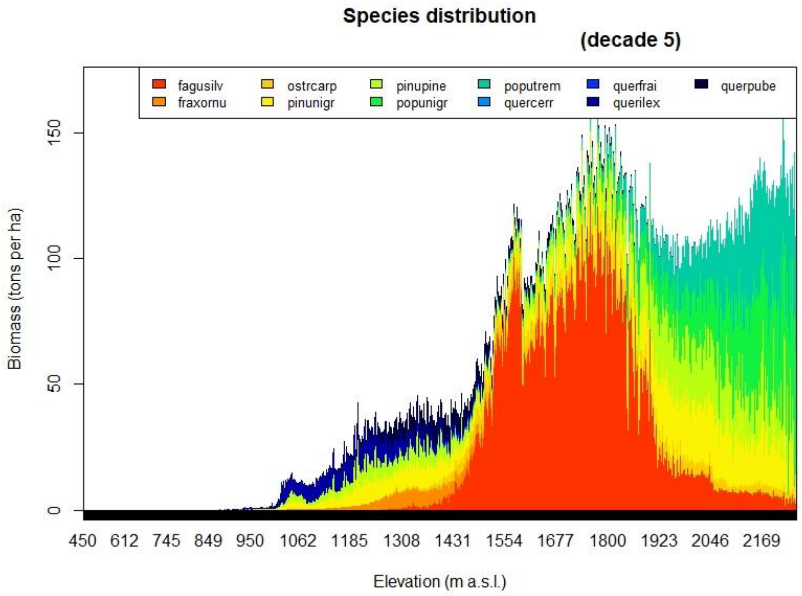
Species distribution
(decade 5)
fagusilv
fraxornu
ostrcarp
pinunigr
pinupine
popunigr
poputrem
quercerr
querfrai
querilex
querpube
Biomass (tons per ha)
0
50
100
150
450
612
745
849
950
1062
1185
1308
1431
1554
1677
1800
1923
2046
2169
Elevation (m a.s.l.)

Figure 3. Tree species distribution measured as cumulative biomass (t/ha) over the study area after 10 (decade 1), 50 (decade 5), and 100-year simulation period (decade 10), at the *status-quo* scenario (*S1*). See Figure 1 for tree species names.

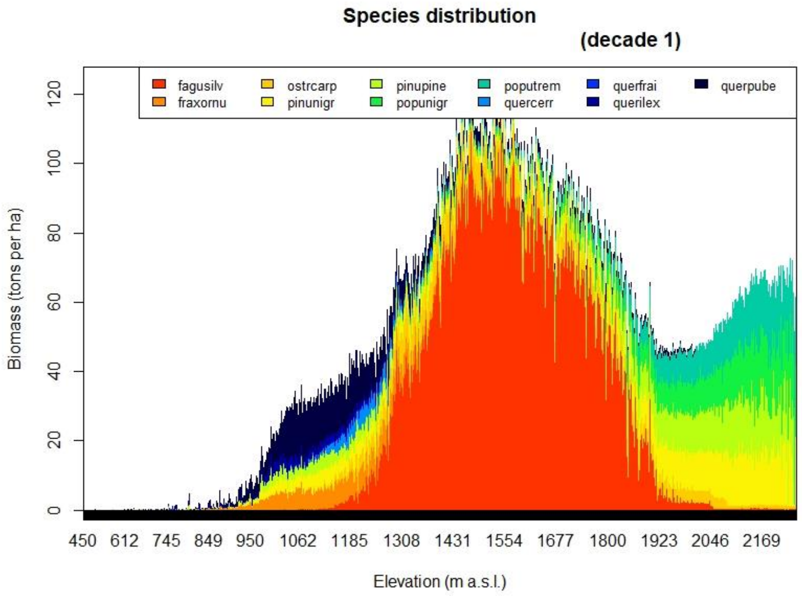
Species distribution
(decade 1)
fagusilv
fraxornu
ostrcarp
pinunigr
pinupine
popunigr
poputrem
quercerr
querfrai
querilex
querpube
Biomass (tons per ha)
0
20
40
60
80
100
120
450
612
745
849
950
1062
1185
1308
1431
1554
1677
1800
1923
2046
2169
Elevation (m a.s.l.)

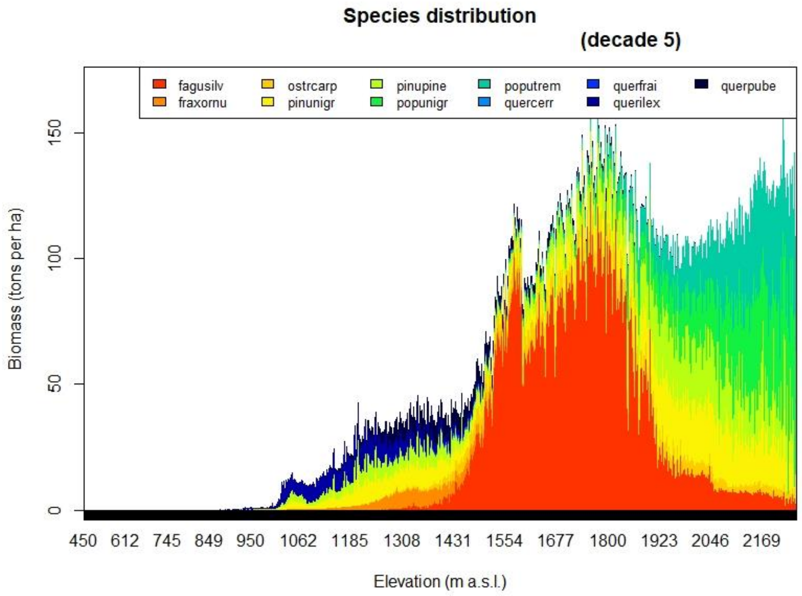
Species distribution
(decade 5)
fagusilv
fraxornu
ostrcarp
pinunigr
pinupine
popunigr
poputrem
quercerr
querfrai
querilex
querpube
Biomass (tons per ha)
0
50
100
150
450
612
745
849
950
1062
1185
1308
1431
1554
1677
1800
1923
2046
2169
Elevation (m a.s.l.)

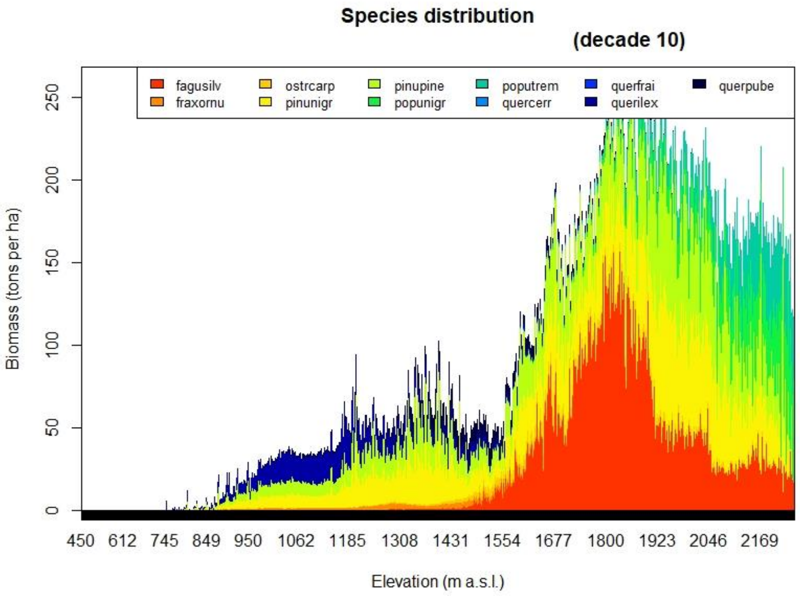
Species distribution
(decade 10)
fagusilv
fraxornu
ostrcarp
pinunigr
pinupine
popunigr
poputrem
quercerr
querfrai
querilex
querpube
Biomass (tons per ha)
0
50
100
150
200
250
450
612
745
849
950
1062
1185
1308
1431
1554
1677
1800
1923
2046
2169
Elevation (m a.s.l.)

Figure 4. Tree species distribution measured as cumulative biomass (t/ha) over the study area after 10 (decade 1), 50 (decade 5), and 100-year simulation period (decade 10), at the *pro-bear* scenario (*S2*). See Figure 1 for tree species names.

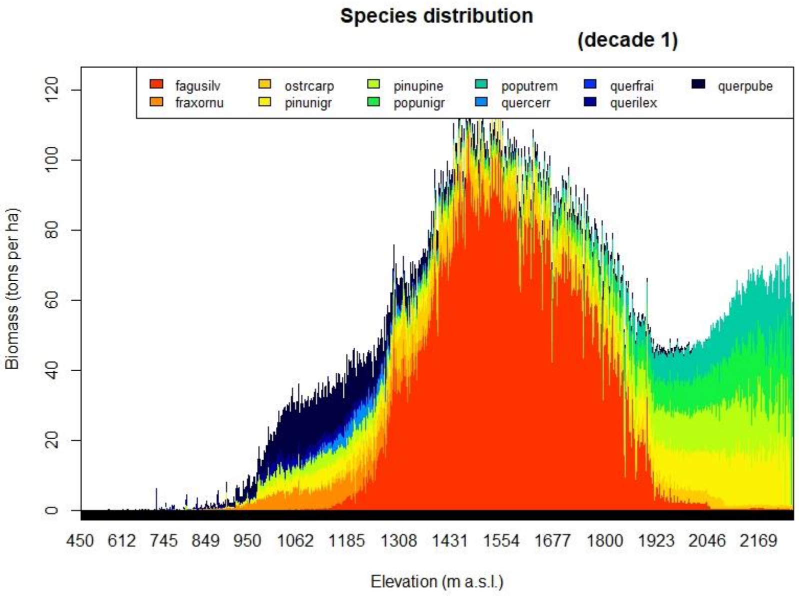
Species distribution
(decade 1)
fagusilv
fraxornu
ostrcarp
pinunigr
pinupine
popunigr
poputrem
quercerr
querfrai
querilex
querpube
Biomass (tons per ha)
0
20
40
60
80
100
120
450
612
745
849
950
1062
1185
1308
1431
1554
1677
1800
1923
2046
2169
Elevation (m a.s.l.)

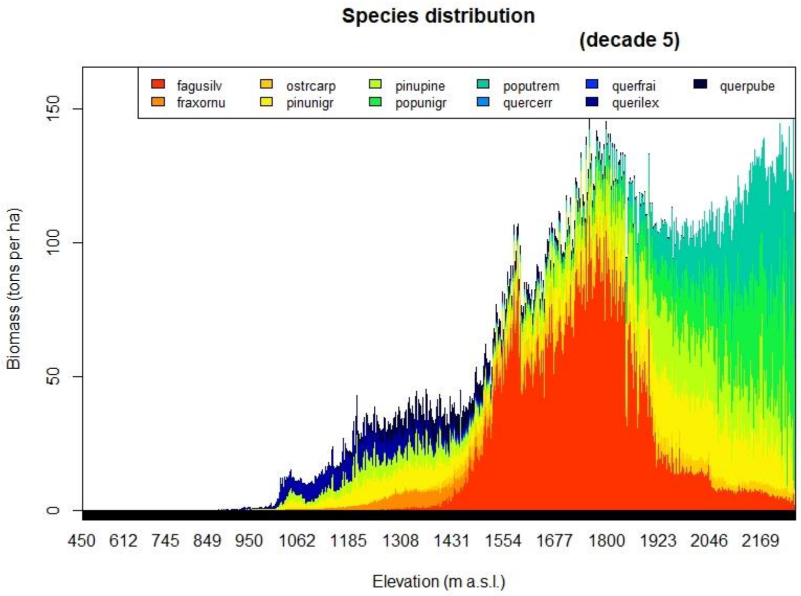
Species distribution
(decade 5)
fagusilv
fraxornu
ostrcarp
pinunigr
pinupine
popunigr
poputrem
quercerr
querfrai
querilex
querpube
Biomass (tons per ha)
0
50
100
150
450
612
745
849
950
1062
1185
1308
1431
1554
1677
1800
1923
2046
2169
Elevation (m a.s.l.)

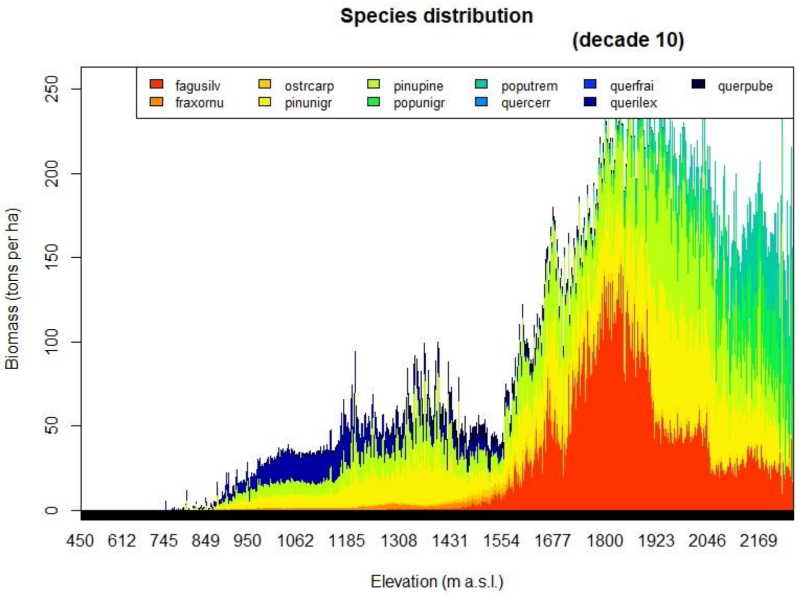
Species distribution
(decade 10)
fagusilv
fraxornu
ostrcarp
pinunigr
pinupine
popunigr
poputrem
quercerr
querfrai
querilex
querpube
Biomass (tons per ha)
0
50
100
150
200
250
450
612
745
849
950
1062
1185
1308
1431
1554
1677
1800
1923
2046
2169
Elevation (m a.s.l.)

SUPPLEMENTARY MATERIAL

Bioclimatic parameters

LandClim calculates bioclimatic metrics which are used to determine climatic limitations on vegetation growth. These metrics are based on monthly average temperature and precipitation sums occurring in the study area. The climatic parameters for every grid cell are adjusted for elevation using lapse rates, thus resulting in a landscape-wide input data set of weather conditions in any given simulation year. The main derived bioclimatic variables are the growing degree days (GDD) to represent temperature limitations, and the drought index (DRI) to represent water limitations on vegetation growth. In particular, LandClim calculates a water balance for each grid cell individually on a monthly basis which influences tree growth (via the drought reduction factor) (Schumacher 2004). The water balance is influenced by topographic and environmental factors (i.e. monthly temperature, precipitation sum, slope, and aspect). I used the 'original' water balance module (derived by Bugmann and Cramer 1998) that calculate water supply and demand at a monthly resolution. Water supply is controlled by incoming rainfall reaching the soil surface (i.e., monthly precipitation minus canopy interception), whereas demand is driven by evapotranspiration. For a complete description of more specific details about LandClim, the reader is referred to Schumacher (2004).

LandClim functioning: forest stand scale processes

LandClim distinguishes between three different types of stand-scale processes: (i) tree growth, (ii) tree mortality, and (iii) tree regeneration. These processes are simulated for each cohort, and tree growth is simulated via functions, which are based on a species-specific maximum growth rate (r_s; growth under optimum environmental conditions) and a species-specific maximum biomass (K_s; maximum biomass an individual tree of a certain species can reach). To account for the reduction of growth under non-optimum environmental conditions, reduction factors by light-, drought and temperature-limitation are considered in the growth formulation. Under non-optimal environmental conditions, a number of growth-limiting factors reduce the optimal growth rate. These factors include light limitation (*light_rf*), degree-day limitation (*DD_rf*)), and drought limitation(*drStr_rf*). These factors are implemented via Liebig's 'law of the minimum'. Thus, the realized growth rate ($r_i(t)$) is calculated as the optimum growth rate (r_s) reduced by the most limiting environmental factor (Eq. 1):

$$r_i(t) = r_s \cdot \min\,(light\_rf(t), DD\_rf(t), drSt\_rf(t))$$

In addition, the realized maximum biomass $K_i(t)$ is also limited by environmental conditions, which reduce the maximum biomass (K_s) by the minimum of growing degree-days or drought (Eq. 2):

$$K_i(t) = K_s \cdot \min\,(DD\_rf(t), drStr\_rf(t)) \tag{2}$$

Tree mortality can occur due to two factors, that are growth-dependent stress (*mStress*), and an intrinsic, age-related component (*mAge*). The stress-dependent mortality factor (*mStress*) assumes that only 1% of species would survive 10 years of consecutive stress. Growth-dependent stress (3) when one of the three growth response factors (Light, Degree Days, or Drought) drops below a threshold value (*thresholdGrowthRed*) and a minimum number of consecutive stress years (*minGrowthRF*) have accumulated. The counter for the number of slow-growth years is increased by one each time 'stress' occurs, and is set back to zero otherwise. The default values for the *thresholdGrowthRed* is 0.1 (90 % reduction of growth due to limiting environmental conditions), and 3 years for the minimum number of *minGrowthRF*. When these conditions are met, a stress-depended mortality probability is calculated as:

$$mStress = (1.0 - 0.01^{0.1}) \cdot (1 - \frac{minGrowthRF}{thresholdGrowthRed})$$

Intrinsic mortality (Eq. 3) is accounted for by a constant probability of death throughout the lifetime of the tree, assuming that 1% of trees belonging to particular species reach their maximum longevity (*maxAge*$_s$; Botkin, 1993, Bugmann, 1996):

$$mAge = 1 - e^{\frac{ln\,(0.01)}{maxAge_s}} \tag{4}$$

Finally, tree regeneration is simulated based on seed availability, environmental conditions and depends on the intensity of browsing and grazing. New tree cohorts are established once every ten years. However, the model checks the establishment potential for every year and calculates a decadal establishment probability. This ’establishment filter’ approach is widely applied in forest gap models (e.g., Bugmann 1994), for which a particular year is favorable for establishment only if the following criteria are met: (i) available light at forest floor is higher than a species-specific threshold value; (ii) winter temperature (mean temperature of the coldest month) is higher than a threshold minimum temperature; (iii) the sum of growing degree-days exceeds the minimum species-specific requirement; (iv) the drought index has to be lower than the species-specific maximum drought tolerance.

Creating the current state of forest

To create the current state of forest I needed of several structural information normally created by LandClim forest dynamic simulations at cohort level (i.e., group of stands with the same age and structure), like dominant species, age, biomass, stems, DBH and height. I used dominant species, DBH and stems spatially explicit information by forest structure models built in the Chapter 2, while I used allometric functions to derive height (Risch et al. 2005) and biomass (Schumacher 2004) from the DBH measure for each pixel of the study area. I used the *stand.generator* (i.e., function created by Bourioud 2020; not yet published) using R software to create virtual stands based on the current forest type, DBH distribution and species frequency parameters, included age class for each cohort.

Table S1. Table of studies using LandClim

Paper	Location	Study area (ha)	Focus of study
Schumacher et al. (2004)	Dischma valley (Switzerland)	1,700	Improving tree growth
Schumacher and Bugmann (2006)	Dischma valley	1,670	Fire regime, future climate
	Gantertal (Switzerland)	2,400	
Schumacher et al. (2006)	Lefthand Creek (Colorado Front Range, USA)	4,000	Fire
	Wild Basin (Colorado Front Range, USA)	8,000	
Colombaroli et al. (2010)	Rhone valley (tree line) (Switzerland)	80	Fire over last 12 000 years, Palaeoecology
Henne et al. (2011)	LakeGouillé Rion and Lake St Moritz (Switzerland)	2,800	Palaeoecology
Briner et al. (2012)	Saas Valley (Switzerland) EGS	n.a.	tree line
Elkin et al. (2012)	Dischma valley (Switzerland)	1,600	Growth model comparison, windthrow, fire
Temperli et al. (2012)	Black Forest (Germany)	2,000	Management regime
Temperli et al. (2013)	Black Forest (Germany)	2,000	Bark beetles, windthrow
Temperli and Bugmann (2013)	Black Forest (Germany)	2,000	EGS
Elkin et al. (2013)	Dischma Valley, Saas Valley (Switzerland)	1,700	EGS, Fire, windthrow
Henne et al. (2013)	Lago di Massacciucoli (Italy)	~2,800	Palaeoecology
Mette et al. (2013)	Franconian Plateau (Germany)	n.a.	Oak-Beech competition
Schwörer et al. (2014)	Lake Iffigsee (Switzerland)	n.a.	Treeline, Palaeoecology
Thrippleton et al. (2014)	Mt. Hauhungatahi (New Zealand)	n.a.	Disturbance, Palaeoecology
Temperli et al. (2015)	Northwestern Colorado (USA)	3,970	Bark beetles, fire
Bouriaud et al. (2015)	NE Romania	11,742.5	Adaptive forest management
Hengeveld et al. (2015)	Netherlands	n.a.	Forest management
Thrippleton et al. (2016)	Wilhelm valley (Switzerland)	1,218	Herbaceous understorey, Disturbance
	Feldberg (Germany)	1,700	
Schuler et al. (2017)	Dischma (Switzerland)	1,600	EGS
	Feldberg (Germany)	1,700	
(Thrippleton et al. 2017)	Valais (Switzerland)	1,700	Water competition herbs, trees
Thrippleton et al. (2018)	Jura (Switzerland)	1,700	Disturbance, Browsing
	Dischma (Switzerland)	1,600	
	Valais (Switzerland)	1,700	
	Feldberg (Germany)	1,700	
Huber et al. (2017)	Valais (Switzerland)	1,700	EGS, Model coupling

Snell et al. (2017)	Jura (Switzerland)	111	Pasture woodland
Zlatanov et al. (2017)	Western Rhodopes (Bulgaria)	736	EGS
Snell et al. (2018)	Valais (Switzerland)	1,700	Climate uncertainty
Fronzek et al. (2018)	Lisbon District (Portugal)	n.a.	Climate response surfaces
Current study	Abruzzo-Lazio-Molise National Park (central-Apennines mountains, Italy)	50,686	Climate change response, harvesting, conservation of brown bears

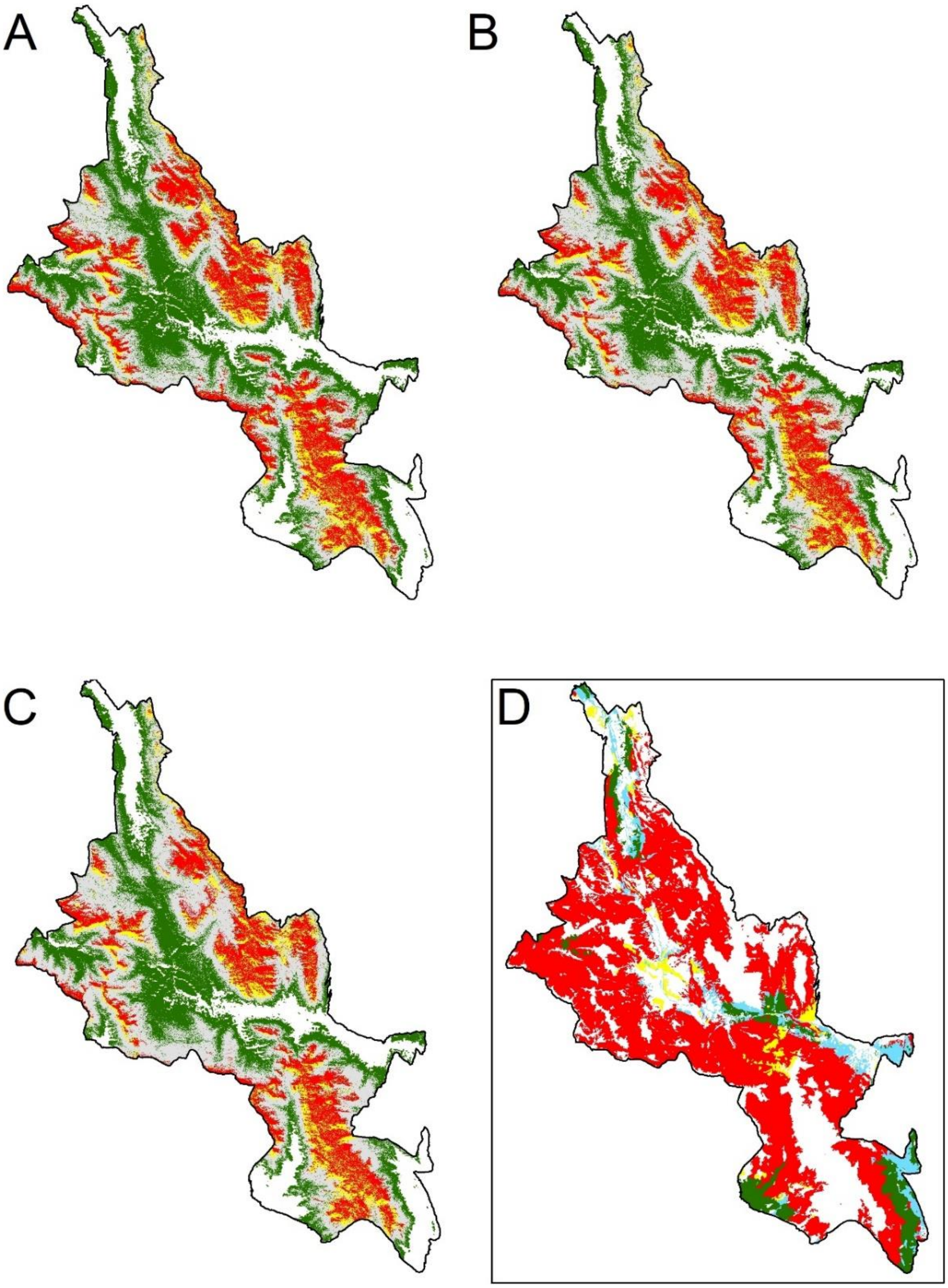

Figure S1. Dominant tree species distribution in the study area (PNALM) for each alternative forest management scenario without forest-edge treatments, *S0* (A), *S1a* (B), *S2a* (C), and current situation (D). Red color = beech forest; green = oak; grey = other deciduous species (e.g., *Castanea sativa*); yellow = coniferous forest; azure = hop-hornbeam.

Figure S2. Dominant tree species distribution in the study area (PNALM) for each alternative forest management scenario with forest-edge treatments, *S0* (A), *S1b* (B), *S2b* (C), and current situation (D). Red color = beech forest; green = oak; grey = other deciduous species (e.g., *Castanea sativa*); yellow = coniferous forest; azure = hop-hornbeam.

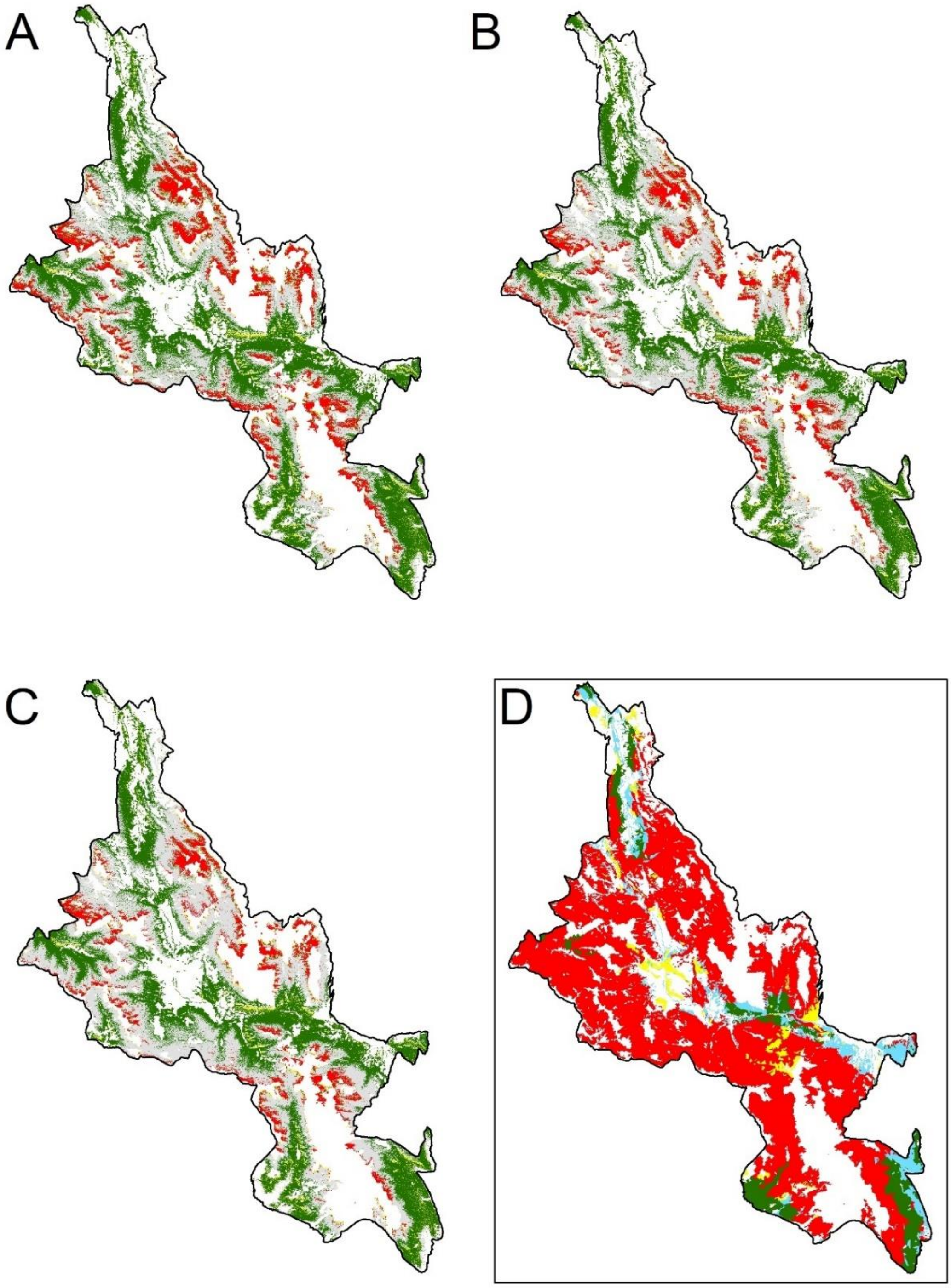

Figure S3. Binary bear's habitat suitability maps derived by continuous probability models at the home range scale (third-order selection). I used the cut-off threshold that maximizes the sensitivity (proportion of bear localities correctly identified as 1 s) and specificity (i.e., the proportion of bear absences correctly identified as 0 s).

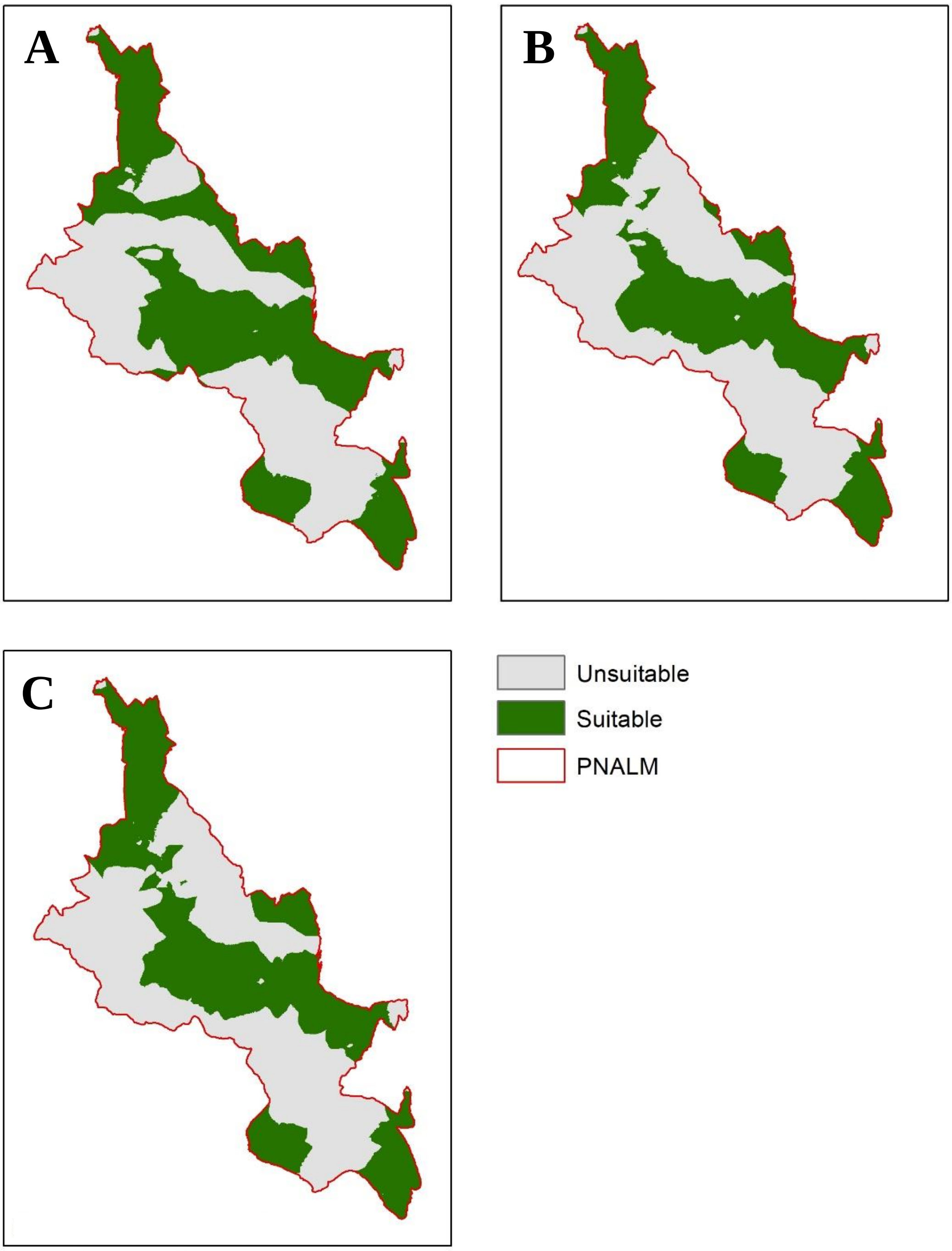

Figure S4. Binary bear's habitat suitability maps derived by continuous probability models at the single forest-patch scale (fourth-order selection) in the next 100 years, using the *baseline* scenario (*S0*; A), *status-quo* scenario without open areas treatment (*S1a*; B), *pro-bear* scenario without open areas treatment (*S2a*; C), *status-quo* scenario with open areas treatment (*S1b*; D), *pro-bear* scenario with open areas treatment (*S2b*; E). I used the cut-off threshold that maximizes the sensitivity (proportion of bear localities correctly identified as 1 s) and specificity (i.e., the proportion of bear absences correctly identified as 0 s).

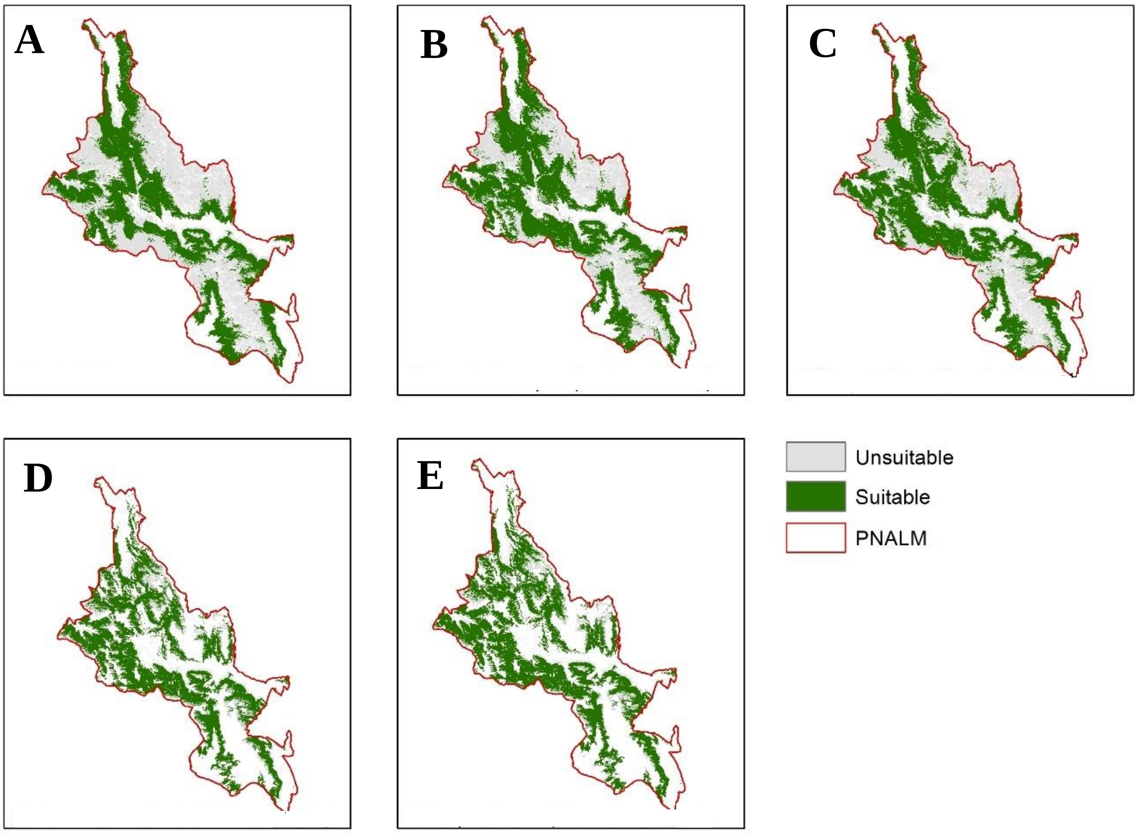

REFERENCES

Bouriaud, L., O. Bouriaud, C. Elkin, C. Temperli, C. Reyer, G. Duduman, I. Barnoaiea, L. Nichiforel, N. Zimmermann, and H. Bugmann. 2015. Age-class disequilibrium as an opportunity for adaptive forest management in the Carpathian Mountains, Romania. Regional Environmental Change 15:1557–1568.

Briner, S., C. Elkin, R. Huber, and A. Grêt-Regamey. 2012. Assessing the impacts of economic and climate changes on land-use in mountain regions: A spatial dynamic modeling approach. Agriculture, Ecosystems and Environment 149:50–63.

Bugmann, H. 1994. On the ecology of mountainous forests in a changing climate: A simulation study. Dissertation. Swiss Federal Institute of Technology ETH Zurich.

Bugmann, H., and W. Cramer. 1998. Improving the behaviour of forest gap models along drought gradients. Forest Ecology and Management 103:247–263.

Colombaroli, D., P. D. Henne, P. Kaltenrieder, E. Gobet, and W. Tinner. 2010. Species responses to fire, climate and human impact at tree line in the Alps as evidenced by palaeo-environmental records and a dynamic simulation model. Journal of Ecology 98:1346–1357.

Elkin, C., A. G. Gutiérrez, S. Leuzinger, C. Manusch, C. Temperli, L. Rasche, and H. Bugmann. 2013. A 2 °C warmer world is not safe for ecosystem services in the European Alps. Global Change Biology 19:1827–1840.

Elkin, C., B. Reineking, C. Bigler, and H. Bugmann. 2012. Do small-grain processes matter for landscape scale questions? Sensitivity of a forest landscape model to the formulation of tree growth rate. Landscape Ecology 27:697–711.

Fronzek, S., T. R. Carter, N. Pirttioja, R. Alkemade, E. Audsley, H. Bugmann, M. Flörke, I. Holman, Y. Honda, A. Ito, V. Janes-Bassett, V. Lafond, R. Leemans, M. Mokrech, S. Nunez, D. Sandars, R. Snell, K. Takahashi, A. Tanaka, F. Wimmer, and M. Yoshikawa. 2019. Determining sectoral and regional sensitivity to climate and socio-economic change in Europe using impact response surfaces. Regional Environmental Change 19:679–693.

Hengeveld, G. M., M. Didion, S. Clerkx, C. Elkin, G. J. Nabuurs, and M. J. Schelhaas. 2015. The landscape-level effect of individual-owner adaptation to climate change in Dutch forests. Regional Environmental Change 15:1515–1529.

Henne, P. D., C. Elkin, D. Colombaroli, S. Samartin, H. Bugmann, O. Heiri, and W. Tinner. 2013. Impacts of changing climate and land use on vegetation dynamics in a Mediterranean ecosystem: Insights from paleoecology and dynamic modeling. Landscape Ecology 28:819–833.

Henne, P. D., C. M. Elkin, B. Reineking, H. Bugmann, and W. Tinner. 2011. Did soil development limit spruce (*Picea abies*) expansion in the Central Alps during the Holocene? Testing a palaeobotanical hypothesis with a dynamic landscape model. Journal of Biogeography 38:933–949.

Huber, R., R. Snell, F. Monin, H. Brunner Sibyl, D. Schmatz, and R. Finger. 2017. Interaction effects of targeted agri-environmental payments on non-marketed goods and services under climate change in a mountain region. Land Use Policy 66:49–60.

Mayers, M., M. Jansen Bishop, D. Walerius, K. Conway, M. Usseglio, S. Hasty, and S. Allison. 2019. Improving your spectacle patients' in-practice experience with contact lenses during frame selection. Contact Lens and Anterior Eye 42:406–410.

Mette, T., K. Dolos, C. Meinardus, A. Bräuning, B. Reineking, M. Blaschke, H. Pretzsch, C. Beierkuhnlein, A. Gohlke, and C. Wellstein. 2013. Climatic turning point for beech and oak under climate change in Central Europe. Ecosphere 4:1–19.

Schuler, L. J., H. Bugmann, and R. S. Snell. 2017. From monocultures to mixed-species forests: Is tree diversity key for providing ecosystem services at the landscape scale? Landscape Ecology 32:1499–1516.

Schumacher, S. 2004. The role of large scale disturbances and climate for the dynamics of forested landscpaes in the European Alps. Dissertation. Swiss Federal Institute of Technology ETH Zurich, Switzerland.

Schumacher, S., and H. Bugmann. 2006. The relative importance of climatic effects, wildfires and management for future forest landscape dynamics in the Swiss Alps. Global Change Biology 12:1435–1450.

Schumacher, S., H. Bugmann, and D. J. Mladenoff. 2004. Improving the formulation of tree growth and succession in a spatially explicit landscape model. Ecological Modelling 180:175–194.

Schumacher, S., B. Reineking, J. Sibold, and H. Bugmann. 2006. Modeling the impact of climate and vegetation on fire regimes in mountain landscapes. Landscape Ecology 21:539–554.

Snell, R. S., C. Elkin, S. Kotlarski, and H. Bugmann. 2018. Importance of climate uncertainty for projections of forest ecosystem services. Regional Environmental Change 18:2145–2159.

Snell, R. S., A. Peringer, and H. Bugmann. 2017. Integrating models across temporal and spatial scales to simulate landscape patterns and dynamics in mountain pasture-woodlands. Landscape Ecology 32:1079–1096.

Temperli, C., H. Bugmann, and C. Elkin. 2012. Adaptive management for competing forest goods and services under climate change. Ecological Applications 22:2065–2077.

Temperli, C., T. T. Veblen, S. J. Hart, D. Kulakowski, and A. J. Tepley. 2015. Interactions among spruce beetle disturbance, climate change and forest dynamics captured by a forest landscape model. Ecosphere 6:1–20.

Temperli, C., J. Zell, H. Bugmann, and C. Elkin. 2013. Sensitivity of ecosystem goods and services projections of a forest landscape model to initialization data. Landscape Ecology 28:1337–1352.

Thrippleton, T., H. Bugmann, M. Folini, and R. S. Snell. 2018. Overstorey–understorey interactions intensify after drought-induced forest die-off: Long-term effects for forest structure and composition. Ecosystems 21:723–739.

Thrippleton, T., H. Bugmann, K. Kramer-Priewasser, and R. S. Snell. 2016. Herbaceous understorey: An overlooked player in forest landscape dynamics? Ecosystems 19:1240–1254. Springer US.

Thrippleton, T., H. Bugmann, and R. S. Snell. 2017. Herbaceous competition and browsing may induce arrested succession in central European forests. Journal of Ecology 106:1120–1132. Springer US.

Thrippleton, T., K. Dolos, G. L. W. Perry, J. Groeneveld, and B. Reineking. 2014. Simulating long-term vegetation dynamics using a forest landscape model: The post-Taupo succession on Mt Hauhungatahi, North Island, New Zealand. New Zealand Journal of Ecology 38:26–38.

Zlatanov, T., C. Elkin, F. Irauschek, and M. J. Lexer. 2017. Impact of climate change on vulnerability of forests and ecosystem service supply in Western Rhodopes Mountains. Regional Environmental Change 17:79–91.

Conclusions

In this thesis, I investigated all environmental and ecological drivers can affect resource selection by bears, accounting for the hierarchical nature of resource selection and behavioral responses related to seasonal and circadian effects. This study represents an important step forward able to fill the ecological gap concerning the current relationship between Apennine bears and forest ecosystem components, included human presence. These new ecological information will be essential to address conservation-oriented management efforts for the preservation of habitat quality for protecting this imperiled and autochthonous brown bear population. In addition, investigating bears' habitat selection for forest structure, and forest spatial configuration, I had the opportunity to learn and use cutting-edge tools and modeling framework to forecast bear's habitat suitability under climate change and alternative forest harvesting scenarios in the next 100 years. Although it needed of further investigations with new data (e.g., forest productivity, increased bears' sample size including years of both low and high productivity of hard mast) and technologies (e.g., LIDAR images) to improve the accuracy of predictions outcomes, this pilot study represents the first effort aimed to picture a more realistic portrait of the causal-effect relationship among alternatives forest management strategies, wildlife habitat suitability, and climate change.

1. Which environmental and ecological drivers affect resource selection by bears?

Habitat selection by female brown bears revealed a hierarchical and scale-sensitive process, according to the spatial (i.e., extent and grain) and temporal (i.e., seasons and circadian effect) scale investigated. Overall, female bears' habitat choices reflect several adaptations to minimize chances of disturbance by humans (e.g., roads and settlements), optimizing the use of resources available within the study area to fulfil their biological requirements, according to the ecological domain investigated. For instance, whereas at the landscape scale bear's avoidance of human settlements, cultivated lands, and paved roads reflects their tendency to reduce risk associated to human disturbance, at home range scale bears evidenced relevant seasonal and circadian effects in habitat selection. Specifically, when bears decide to establish their home ranges, they prefer remote and naturally areas with less human features (e.g., territory with few human settlements and paved roads, but with more unpaved roads), rather than more anthropized areas and located at lower altitudes (e.g., territory with more human settlements and paved roads, compared to unpaved roads). At the third order of selection, temporal scales (i.e., daylight and seasonality) have a primary role in habitat selection responses: according to the hazard arising encounters with humans, females used home range portions mainly covered by forest, with steeper slope and far from unpaved roads during the day, independently by seasons. These circadian patterns are in concordance with the findings reported in others European brown bear's populations, such as Scandinavian (Moe et al. 2007) and Balkan (Kaczensky et al. 2006) ones, where bears' resting was mainly restricted to the daylights hours, and their activity was limited to crepuscular and nocturnal hours. As anthropogenic and orographic resource selection can change depending on the scale investigated, forests remain a fundamental positive-selected resource independently from the domain of scales. In conclusion, bear's habitat selection unveiled changes in perceived costs and benefits, thereby revealing trade-offs in multiple scales resource selection decisions (e.g., Thompson and McGarigal 2002; Leblond et al. 2011). Interpreting multi-scale bear's decisions, it could better appreciate how scale affected their resource selection pointing out that risks related to human disturbance exceed rewards when bears establish their home ranges, or select suitable patches within home range during periods of intense human activity.

2. *How does forest structure affect habitat selection by bears?*

At the home range scale (third-order of selection), the results confirmed the importance of forest like fundamental resource for this brown bear population, related to two main causes: (*i*) covering by anthropogenic disturbance, highlighted by the selection of continuous forest patch, especially during daily hours in summer (early-summer and late-summer), and (*ii*) foraging within the forest, highlighted by the increasingly selection for these continuous forested areas mainly in autumn, when there is the peak of hard mast production in the forests. The contribute of natural open areas in bear's habitat suitability has been recognized in many studies (e.g., Frank et al. 2015; Lamb et al. 2017), and this pattern is connected to the great amount of food resources, such as ants, herbaceous vegetation and berries, that are available in these areas within a short period of the year (Ciucci et al. 2014). Similar to autumn season, the end of the summer is critical for bears because the early-hyperphagic period (June-August) coincides with the peak of tourism and related human activities. According to results of the Chapter I, at home range scale (third-order) human component emerged as one of the main driving factors for females' resources selection, reflected by the strong avoidance of cultivated lands, exclusively in late-summer. At the forest patch scale (fourth-order of selection), more evident circadian effects highlighted that oak forest selection (compared to the beech forest) is mainly nocturnal and never diurnal, and this pattern may suggest a trophic rather than covering effect, probably linked to a higher diversity and availability of food; at the other hand, I cannot exclude an altitudinal effect for mediating the greater disturbance at low elevation (oak forest) by human activities. However, the most unexpected result is the avoidance for oldest trees (i.e., higher averaged basal area) during bear's hyperphagic period, when bear's diet is characterized by a consumption for the 64% of hard mast (Ciucci et al. 2014). This pattern can be in part explained by considering the hard mast productivity cycle of Apennine deciduous forest. The availability of beech's (and in part of oak's) hard mast is not fixed and constantly among years, but they are characterized by few years with a noticeable masting productivity (i.e., approximatively every 4 years) following by years of low masting productivity.

3. *How natural succession and human-driven habitat changes will affect habitat suitability for bears in the future?*

Overall, in this study area (i.e., Abruzzo, Lazio, and Molise National Park, PNALM) for both order of selection (third and fourth), I evidenced an increase of habitat suitability projected in all scenarios contemplated, compared to the current bear's habitat suitability. Specifically, comparing the alternatives forest strategies simulated, at the home range scale forest harvesting strategies (scenarios *S1* and *S2*) did not improve habitat suitability compared to the hands-off scenario (scenario *S0*), while at the scale of forest patches habitat suitability was positively affected by silvicultural interventions, particularly in the *pro-bear* scenarios (scenario *S2*). At the this scale of analysis, maintaining the current forest interspersion with open areas (scenarios *S1b* and *S2b*) was not projected to enhance habitat suitability, because this strategy tends to contrast the natural shifting of tree species, especially beech, at highest elevation as a consequence of climate change. In addition, change in species composition in next 100 years bears important consequences for the availability of hard mast to Apennine bears: in the PNALM bears consume a great amount of hard mast during the late hyperphagic season, of which two thirds are beech nuts (Ciucci et al. 2014), and the partial substitution of beech dominated forest to oak domination during the next 100 years will represent an important issue for bear's and all other wildlife species foraging within forest. With the projected loss of beech-dominated forests, the issue is if bears can quickly adapt to find alternative good quality food sources. In this sense, we expect that the generalist behavior of bear and its high adaptability can balance its need for hard must in autumn given the increasing acorns productivity of oak forests; however, further investigations must be conducted in order to cover all single aspects of the nutritional ecology of Apennine bears, deeply investigating habitat forest productivity in relation to fitness, and population performance.

REFERENCES

Ciucci, P., E. Tosoni, G. Di Domenico, F. Quattrociocchi, and L. Boitani. 2014. Seasonal and annual variation in the food habits of Apennine brown bears, central Italy. Journal of Mammalogy 95:572–586.

Frank, S. C., S. M. J. G. Steyaert, J. E. Swenson, I. Storch, J. Kindberg, H. Barck, and A. Zedrosser. 2015. A “clearcut” case? Brown bear selection of coarse woody debris and carpenter ants on clearcuts. Forest Ecology and Management 348:164–173. .

Kaczensky, P., D. Huber, F. Knauer, H. Roth, A. Wagner, and J. Kusak. 2006. Activity patterns of brown bears (*Ursus arctos*) in Slovenia and Croatia. Journal of Zoology 269:474–485.

Lamb, C. T., G. Mowat, B. N. McLellan, S. E. Nielsen, and S. Boutin. 2016. Forbidden fruit: human settlement and abundant fruit create an ecological trap for an apex omnivore. Journal of Animal Ecology 86:55–65.

Leblond, M., J. Frair, D. Fortin, C. Dussault, J. P. Ouellet, and R. Courtois. 2011. Assessing the influence of resource covariates at multiple spatial scales: An application to forest-dwelling caribou faced with intensive human activity. Landscape Ecology 26:1433–1446.

Moe, T. F., J. Kindberg, I. Jansson, and J. E. Swenson. 2007. Importance of diel behaviour when studying habitat selection: Examples from female Scandinavian brown bears (*Ursus arctos*). Canadian Journal of Zoology 85:518–525.

Thompson, C. M., and K. McGarigal. 2002. The influence of research scale on bald eagle habitat selection along the lower Hudson River, New York (USA). Landscape Ecology 17:569–586.